University of Massachusetts Amherst

ScholarWorks@UMass Amherst

March 2016

Design of ROMP-based Protein Mimics for siRNA Delivery

Brittany M. deRonde
University of Massachusetts - Amherst

Recommended Citation

DESIGN OF ROMP-BASED PROTEIN MIMICS FOR SIRNA DELIVERY

A Dissertation Presented

by

Brittany Morgan deRonde

Submitted to the Graduate School of the
University of Massachusetts Amherst in partial fulfillment
of the requirements for the degree of

DOCTOR OF PHILOSOPHY

February 2016

Department of Polymer Science and Engineering

DESIGN OF ROMP-BASED PROTEIN MIMICS FOR SIRNA DELIVERY

A Dissertation Presented

by

BRITTANY MORGAN DERONDE

Approved as to style and content by:

_____
Gregory N. Tew, Chair

_____
Scott C. Garman, Member

_____
David Hoagland, Member

_____
Lisa M. Minter, Member

_____
David Hoagland
Department of Polymer Science and Engineering

DEDICATION
To my loving family.

ACKNOWLEDGMENTS

To start, I would like to thank my advisor, Prof. Greg Tew, for pushing me to be a better scientist, to stand up for my scientific ideas, and to fight for opportunities that I want. Training in his lab will no doubt prepare me for future scientific opportunities. To my committee member, Prof. Lisa Minter, I will be forever grateful that she opened her lab to me and allowed me to work with her students to learn cell culture and perform my own transfection experiments. To my committee members, Prof. Scott Garman and Prof. David Hoagland, I truly appreciated all of the valuable feedback on scientific experiments and career advice you provided. In addition, to Prof. Garman, it was great having your as a professor for the Drug Design course. Your outlook on science was a motivating factor for me selecting you as an outside committee member. Ron

I would also like to sincerely thank the entire Tew Group, both past and present members: Jing, Ke, Yan, Abhi, Fede, Bob, Semra, Raj, Hitesh, Ozgul, Jun, Yongping, Mike L., Melissa, Cathy, Katie, Joel, Madhura, Ilker, Coralie, Nick, Kelly, and Mike K. Their continued guidance, support, and friendship helped me navigate through my PhD. I am truly thankful to have had Ke, Fede, and Hitesh mentors to to teach me to problem solve and think more critically about my science. To especially Feda, Hitesh, Melissa, Mike, Cathy, Katie, and Madhura, your incredible friendships meant the world to me and I will never forget all the great memories we shared. I was also fortunate to have a talented group of undergraduates working with me: Leah, Tammy, Salimar, Angie, and Orett. In particular, my first undergraduate, Leah, it has been a great two

years working with you in the lab and watching you develop into a talented young scientist. Last, but certainly not least, to Trouble, the group's administrative assistant and "mom", without whom our group would truly fall apart. Words cannot express how grateful I am to have had you around to help with day-to-day group business and for being a shoulder to cry on when trying to schedule important meetings.

Additionally, I would like to thank the Osborne and Minter Groups, both past and present members: Becky, Gaby, Jyothi, Anushka, Tina, Karthik, Furkan, Joe, Ankita, Manit, Wes, and Pavitra. Thank you so much for adopting me as one your lab members and for making me feel at home in ISB. To Joe and Furkan, thank you not only for your friendship, and for making me laugh when my experiments seemed like lost causes.

To the PSE staff: Lisa G., Maria, Jessica, Lisa M., Ann, Andre, Jack. Thank you for making daily life at Conte much more manageable.

To all UMass staff who maintain instruments that were used my thesis work, especially Weiguo (NMR), Steve (GPC / MS), and Amy (Flow Cytometry).

To the GPC Facility, particularly Steve, Justin, Katrina, Rachel, Katie, Cristiam, and Nick. Thank you for keeping the GPCs running and for dealing with all the crazy issues that come with the responsibilities of day to day maintenance and repair. Rachel, thank you for being my repair partner and making the instrument downtime more bearable.

To the Class of 2010, thank you so much for your friendship and support throughout my time in PSE. The fond memories together will remain with me always. To my closest classmates Dan, Jon, Nick, Kyle, Angela, Rachel, Anesia, and Hsin-Wei, you all have truly become some of my best friends and I will sincerely miss our potlucks, gym outings, movie nights, holiday parties, and random dinner/dessert outings. From classes, to cumes, to qualifying exams, and defenses you were there and

supportive the entire time. Although graduate school was stressful, the memories we shared made this experience some of the best times of my life.

To my PhD roommates Angela (+CJ), Anesia, and Sarah, it was nice after rough days in Conte to come home to caring friends. I will truly miss post-work day talks and late night study sessions.

In relation to PSE Softball, I would like to acknowledge the Spare Parts, the Persistent Radicals, the Free Radicals, Entropic Thunder, and the Renegades. It was a ton of fun playing softball and helping to co-manage the teams. It was also great to have an excuse to take break from research to go outside and enjoy the summer weather.

To Prof. Kathryn Uhrich, my undergraduate research advisor, thank you for being a wonderful mentor and for always pushing me to be a better scientist.

To my Associate Alumnae of Douglass College (AADC) family, thank you for supporting throughout my higher education. Not only did the scholarships they provided ensure I could afford to take classes and present my research at conferences, but also their career development and women in science opportunities completely prepared me for graduate school and life as a working profession.

Last, but certainly not least, my family. Thank you to all of you who have supported me on this long journey! I am looking forward to moving back to NJ, where I will be closer to you all and can attend more family functions. To my grandmother and parents, thank you for helping me, supporting me, keeping me going throughout this entire process, not allowing me to quit, and for making me the person who I am today. Thank you also to my sisters Kaila, Aimee and Ashleigh and my little niece Hailee. You truly are my very best friends and I am eternally grateful for the confidence

you had in me and for your continued support. With you all (and our text message thread) I would not have made it to where I am today.

ABSTRACT

DESIGN OF ROMP-BASED PROTEIN MIMICS FOR SIRNA DELIVERY

February 2016

BRITTANY MORGAN DERONDE, B.A., DOUGLASS COLLEGE, RUTGERS UNIVERSITY

M.S., UNIVERSITY OF MASSACHUSETTS AMHERST

Ph.D., UNIVERSITY OF MASSACHUSETTS AMHERST

Directed by: Professor Gregory N. Tew

Designing delivery agents for therapeutics is an ongoing challenge. As treatments and desired cargoes become more complex, the need for improved delivery vehicles becomes critical. Excellent delivery vehicles must ensure the stability of the cargo, maintain the cargo's solubility, and promote efficient delivery and release. In order to address these issues, many research groups have looked to nature for design inspiration. Proteins, such as HIV-1 TAT and Antennapedia homeodomain protein, are capable of crossing cellular membranes. However, due to the complexities of their structures, they are synthetically challenging to reproduce in the laboratory setting. Being able to incorporate the key features of these proteins that enable cell entry into simpler scaffolds opens up a wide range of opportunities for the development of new delivery reagents with improved performance.

Herein we report the development of guanidinium-rich polymeric protein mimics using a ring-opening metathesis polymerization (ROMP)-based scaffold capable of interacting with cell membranes and facilitating the internalization of small interfering ribonucleic acids (siRNAs). These materials are referred to interchangeably as cell-penetrating peptide mimics (CPPMs) or protein transduction domain mimics (PTDMs), and derive inspiration from proteins and peptides with cellular internalization capabilities,

capturing key features of these materials necessary for intracellular delivery, including cationic charge content in the form of guanidinium moieties and a segregated, hydrophobic component. This thesis documents the development of design principles for PTDMs with optimal membrane interactions and siRNA internalization and delivery.

Chapter 2 documents the development of homopolymer CPPMs that contain aromatic rings with varying π-electronics. This study demonstrated that a wide range of functional groups could be incorporated into CPPMs without negatively impacting their ability to interact with cellular membranes. It is also suggested that other design parameters, such as cationic charge content and overall hydrophobic content, play more dominant roles in membrane interactions. This finding ultimately influenced the PTDM optimization performed in later chapters.

Chapter 3 documents the development of homopolymer and block copolymer PTDMs with varying numbers of guanidinium moieties that were tested to assess the affect cationic charge content and the addition of a segregated, hydrophobic block had on siRNA delivery. This study demonstrated that there was a critical charge content necessary for internalization and established the importance of incorporating a hydrophobic block into PTDM structures. Furthermore, this platform demonstrated that bioactive siRNA could successfully be delivered into cells and affect the target gene.

Chapter 4 documents the exploration of hydrophobic block incorporated into copolymer PTDMs in order to determine how the length of the hydrophobic block of the PTDMs as well as the hydrophobic block composition of the PTDMs impacted siRNA internalization. This study demonstrated that there was a critical hydrophobic content necessary for efficient siRNA internalization and that incorporation of additional hydrophobicity did not guarantee improved efficiencies.

TABLE OF CONTENTS

LIST OF TABLES

CHAPTER 1

INTRODUCTION

1.1 Introduction

Proteins are large, complex biomolecules that perform numerous biological functions.[1] They contain both secondary and tertiary structure, which helps them arrange and fold into specific and functional conformations. While nature has developed efficient ways to generate correctly folded and functional proteins, it is substantially more difficult to recreate these structures synthetically. Many research groups have successfully developed peptidomimetics that mimic conformations of short peptide sequences, but to date, mimicking larger protein surfaces or entire protein functions represent more significant challenges.[2] The field of proteomimetics looks to specifically address these challenges by moving away from naturally occurring amino acids and developing non-peptidic materials that can capture key secondary structures found in proteins.[2]

An elegant example of synthetic protein mimic development is from Andrew Hamilton and coworkers in which they were able to mimic part of the protein helix from the myosin light chain kinase using a terphenyl scaffold.[3] These synthetic mimics operate on the premise that the critical residues needed for efficient protein-protein interactions lie along one face of the α-helix.[3,4] Using this scaffold, they were also able to assess binding affinities for calmodulin, which is a calcium-binding messenger that aids in cell signaling.[3] Specifically, they were able to prove that the synthetic α-helix had similar binding properties to the myosin light chain kinase, thus demonstrating the

protein mimicking capacity of these materials.[3]   Other excellent work has also been published in this field.[5-8]

In addition, many researchers have explored foldamers, which are chains of molecules that can fold into organized structures, such as α-helices and β-sheets, in solution.[9-22] Foldamers differ from other proteomimetics in that they require non-covalent interactions for folding, such as hydrogen bonding, π-interactions, electrostatic interactions, van der Waal's interactions, and solvophobic effects with non-adjacent surfaces.[9,10,12,15,16,18,20,21] These molecules have been used to mimic the folding of proteins, polysaccharides, and nucleic acids.[9,10,12,15,16,18,20,21]   One specific subset of foldamers, referred to as abiotic foldamers, aim to capture key features of proteins, such as secondary structure, with non-natural materials.[9-17,19-22]

While mimicking protein secondary structure is an impressive feat and can aid the future development of entirely synthetic protein mimics, it remains difficult to generate these scaffolds and to predict the proper folding or assembly processes. Protein mimics that capture key features using simpler scaffolds without secondary structures can more easily be attained with tunable, synthetic platforms.[23,24]   One prominent example involves mimicking antimicrobial peptides (AMPs). AMPs are potent antibacterial agents that are part of the innate immune systems for many organisms.[25-28] Magainin 2, which is one of the many AMPs currently found in nature, and other similar antimicrobial agents have been shown to be effective against both Gram positive and Gram negative bacteria.[25-27,29,30]   These peptides have facially amphiphilic topologies, enabling segregation of hydrophilic (cationic) and hydrophobic residues for improved membrane activity and antimicrobial properties.[25,31]   Much effort has been devoted to understanding these peptides and the mechanisms by which they kill bacteria, both experimentally and computationally.[25,32-49] Despite the level of controversy surrounding their mode of action, hydrophobic and electrostatic interactions between these peptides

and the bacterial cell wall play prominent roles in pore formation, which ultimately leads to bacterial cell death.[44,45]

Given the rise in antibacterial resistance, researchers have turned to AMPs as a source of inspiration. Incorporating key features of these peptides into synthetic scaffolds offer more structural options for tuning chemical compositions for improved performance.[15,25,45,50-54] These molecules are often referred to as synthetic mimics of antimicrobial peptides (SMAMPs). One example from DeGrado and coworkers demonstrated the use of β-peptides, which mimic the α-helical structures and amphiphilicity of many AMPs.[55] Although many of these molecules contained α-helical structures, linear β-peptides made by Gellman and coworkers and β- and Y-peptides made by Seebach and coworkers demonstrated that α-helical structures were not necessary for potent antimicrobial properties.[56,57] These studies paved the way for the development of synthetic mimics with completely abiotic scaffolds. Such molecules, designed by Tew and coworkers, used facially amphiphilic triaryl scaffolds in which the hydrophobic content and cationic charge content (ammonium or guanidinium groups) could be tuned for improved antimicrobial properties and selectivities.[58-61] By converting AMP designs to simple, synthetic scaffolds, production time and costs are considerably reduced.[51] In addition, peptide *in vivo* limitations, such as proteolysis, tissue distribution, and toxicity, are overcome and robust *in vivo* antibacterial activity against drug-resistant infections has been demonstrated, specifically with a compound in phase II clinical trials.[51] An important new development was the demonstration that polymers could be designed with AMP-like biological activity.[15,17,23,50,53,54,62-72] Unlike proteins and peptides, which typically have a single, exact molar mass, synthetic polymers, even when termed monodisperse, are characterized by a distribution of molecular weights. Although it is unclear how antimicrobial activity trends with dispersity, this opens a wider range of

molecules and chemistries that can be used for the development of synthetic antimicrobial mimics.

By using the same process that gave rise to SMAMPs, researchers have used proteins and peptide sequences as inspiration for the design of the next generation of delivery reagents (Figure 1.1.1).[23]
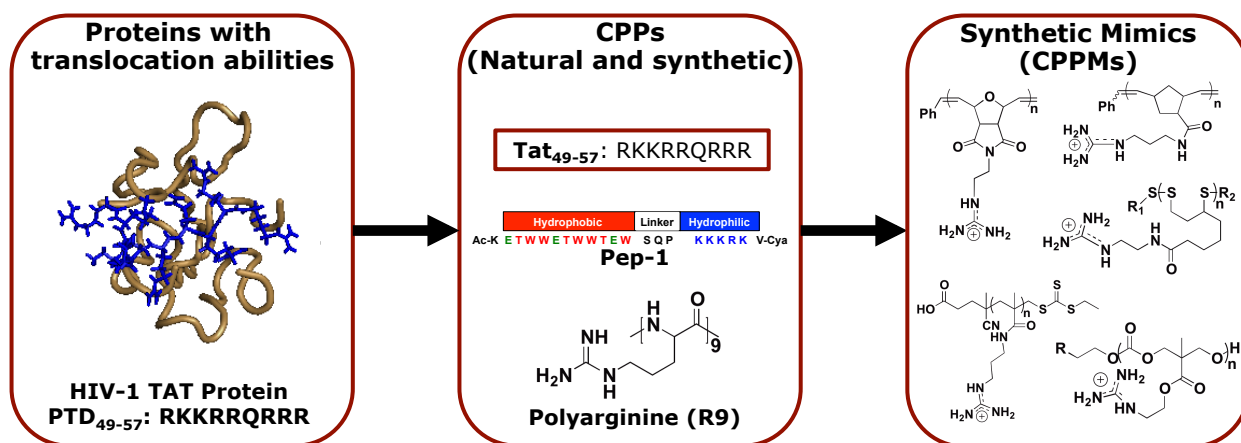
Figure 1.1. The progression from proteins and peptides to guanidinium-rich CPPMs.

This is an area of particular interest since delivery of therapeutic agents is an ongoing challenge. Although there is an increasing demand for new treatments and treatment options, the field lacks a clear understanding of how to efficiently and reliably deliver bioactive molecules across cellular membranes, especially as therapies move increasingly toward more complex biologics.[73-79] Nature, however, is already capable of designing proteins that can perform these functions. One example is HIV-1 TAT (trans-activator of transcription) protein, which is responsible for the spread of the virus[80,81] This protein, along with others, contains a region referred to as a protein transduction domain (PTD) that is responsible for their abilities to enter cells.[82-84] The study of TAT and other PTDs have subsequently led to the development of cell-penetrating peptides (CPPs), which are peptides that are capable of delivering cargo, such as small molecules, siRNA, pDNA, antibodies, and proteins, into cells *via* covalent or non-

covalent interactions.[85-90] Two examples of such molecules include TAT$_{49-57}$, which is a guanidinium-rich sequence, and Pep-1, which has a segregated architecture similar to a block copolymer.[83,84,90-92] While both peptides are cation-rich, Pep-1 also incorporates a hydrophobic segment that is thought to further aid in cellular uptake.

Despite the development of CPPs such as Pep-1, which is now commercially available through Active Motif as Chariot™, moving away from the peptide scaffold offers distinct advantages. Most peptides are prepared by solid phase synthesis, which is both costly and time-consuming because amino acids need to be sequentially added using a series of deprotection, addition, wash, and protection steps. Switching to a completely abiotic backbone allows delivery agents to be made cheaper and potentially in larger quantities. In addition, a non-peptide-based system offers many more structural options in terms of chemical compositions and molecular arrangements because it is not restricted to the incorporation of natural amino acids.[23] This expanded chemistry toolset is expected to generate more efficient structures than their natural peptide analogs.[23]

This chapter documents the early development of cell-penetrating peptide mimics (CPPMs), in particular ones based on polymeric scaffolds. A number of recent reports suggest this area will develop similarly to SMAMPs and will provide new tools for biology and perhaps new delivery opportunities for society.[23,24] A summary of the early CPP work is highlighted followed by an overview of polymeric CPPMs developed to date.

1.2   Cell-penetrating Peptides (CPPs)

CPPs are a class of peptides that can facilitate the delivery of various cargoes into cells.[85-90] These peptides are generally 7-30 amino acid residues in length and cation-rich, usually containing multiple arginine and/or lysine residues.[85] In general, CPPs can be broken down into three broad categories: protein-derived, chimera-derived,

and synthetic. These classes of peptides are summarized in the following subsections

and in Table 1.1.[85]

Table 1.1. Summary of Cell Penetrating Peptides (CPPs) color-coded based on classification into three categories: protein-derived (top, pink), chimera (middle, blue), and synthetic (bottom, yellow).

Peptide	Sequence	Derivation	Total # of charged residues	Cargo	Alternative Classification
HIV-1 TAT$_{49-57}$ [74,93]	RKKRRQRRR	Human Immunodeficiency Virus	8	protein, peptides, siRNA	Non-amphipathic
Penetratin[94]	RQIKIWFQNRRMKWKK	*Drosophila* homeoprotein antennapedia	7	protein, PNA, siRNA	Secondary amphipathic
pVEC[95]	LLIILRRRIRKQAHAHSK	Murine VE-cadherin	6	protein, peptides	Secondary amphipathic
VP22[96]	NAKTRRHERRRKLAIER	Herpes simplex virus	8	protein	Secondary amphipathic
Pep-1[90-92,97]	KETWWETWWTEWSQPKKKRKV	NLS from SV40 T-antigen and a Tryptophan-rich domain	5	protein, peptides	Primary amphipathic
MPG[91,98,99]	GALFLGFLGAAGSTMGAWSQPKKKRKV	Hydrophbic domain from fusion sequence of HIV gp41 and NLS of SV40 T-antigen	5	siRNA, plasmids	Primary amphipathic
Transportan (TP10) [100,101]	AGYLLGKINLKALAALAKKIL	Galanin and mastoparan	4	protein, PNA, siRNA	Primary amphipathic
M918[102]	MVTVLFRRLRIRRACGPPRVRV	Tumor suppressor protein p14ARF	7	Proteins, PNA	Secondary amphipathic
YTA2[103]	YTAIAWVKAFIRKLRK	MMP cleavage site	5	small molecules	Secondary amphipathic
YTA4[103]	IAWVKAFIRKLRKGPLG	MMP cleavage site	5	small molecules	Secondary amphipathic
MAP[104,105]	KLALKLALKALKAALKLA	Synthetic	5	small molecules, plasmids	Secondary amphipathic
Polyarginine[83,84,89,106]	R$_{5-15}$	HIV-1 TAT	5-15	protein, peptides, siRNA	Non-amphipathic
CADY[107,108]	GLWRALWRLLRSLWRLLWRA	Derived from PPTG1 peptide	5	protein, peptides, siRNA	Secondary amphipathic

1.2.1 Protein-derived CPPs

Protein-derived CPPs are based on known sequences from naturally occurring proteins.[85] The specific sequences used for these CPPs are generally derived from the protein transduction domains (PTDs) of these molecules. Disruptions in these sequences often lead to partial or complete uptake inhibition.[82,84,109] Two examples of protein-derived CPPs are TAT_{49-57} and the Antennapedia homeodomain protein derivative Penetratin. These proteins are modeled in Figure 1.2 with their PTDs highlighted in blue.

A.

HIV-1 TAT Protein
PTD_{49-57}: RKKRRQRRR

B.

Antennapedia Homeodomain Protein
PTD_{43-58}: RQIKIWFQWRRMKWKK
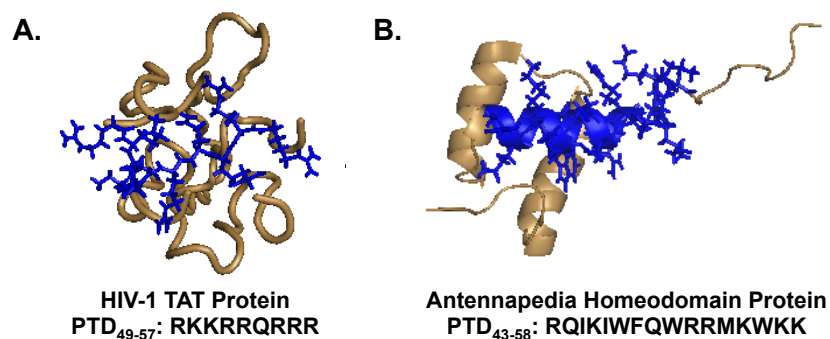
Figure 1.2. Models of HIV-1 TAT and antennapedia homeodomain protein with their protein transduction domains modeled in blue.

In 1988, Green and Loewenstein, as well as Frankel and Pabo, independently reported that HIV-1 TAT had the unique ability to translocate into and out of cells.[80,81] Then, in 1994, Fawell *et al.* tested the delivery efficiencies of two truncated HIV-1 TAT sequences: TAT_{1-72} and TAT_{38-72}.[110] The former was examined because it was thought to be involved in protein binding and cellular uptake and the latter was examined because it lacked the cysteine-rich region (residues 22-37).[110] Both sequences were able to deliver proteins, demonstrating that the entire protein sequence was not required for efficient delivery.[110] This study also compared these sequences to shorter peptides, Tat_{37-58} and Tat_{47-58}, which were also able to deliver proteins to cells.[110] Following this

study, in 1997, Vives *et al.* studied four HIV-1 TAT-derived sequences to test the effects of altering the α-helical and basic regions on cellular uptake.[82] Uptake data illustrated that the α-helix was not required for cellular uptake but that there could be no interruptions in the basic domain.[82]

In 2000, Wender *et al.* also studied the TAT peptide, as well as polyarginine. They confirmed that the basic region, amino acids 49-57, must be completely preserved in order for it to maintain its function.[82,84] Truncating the sequence or substituting individual amino acids with alanine residues all resulted in a reduction in uptake efficiency. By studying Tat_{49-57} sequences that were synthesized with D-amino acids and/or in reverse, they also illustrated that backbone chirality, hydrogen bonding, and overall peptide backbone were not critical for efficacy.[84]

Similar studies were also performed for the antennapedia homeodomain protein. This protein contains approximately 60 amino acids, which fold to give three α-helices, and is a transcription factor that aids in DNA binding in *Drosophila*.[111] In 1991, it was discovered that this antennapedia homeodomain protein could translocate into cells and that the third α-helix was important for the its cellular uptake ability.[111] Similar studies to those performed on HIV-1 TAT, demonstrated that the entire protein sequence was not required for cellular uptake, just the 3rd α-helix and that backbone chirality, hydrogen bonding, and peptide secondary structure were also not required for uptake.[109,112] This sequence of amino acids required for uptake has since been referred to as Penetratin.[109] Other CPPs inspired by proteins include pVEC and VP22.[95,96]

Through studying HIV-1 TAT, antennapedia homeodomain protein, and their structural derivatives, it became apparent that full protein sequences, protein secondary structures, and peptide-based backbones are not necessarily required for efficient

cellular uptake but that the cationic charge content was absolutely critical.[82-84,94,109,110,112] These results opened up the possibility of designing synthetic mimics.

1.2.2   Chimera-derived CPPs

As an alternative to shortened TAT sequences and overcoming some of the limitations of the full TAT-protein, amphiphilic peptides with improved stability were developed based on a chimeric scaffold.[90]   Chimera-derived CPPs are fusions of two or more naturally occurring protein or peptide sequences.[85]   Most often, they are the combination of sequences that enable specific protein functions, such as nuclear localization sequences (NLSs) and signaling sequences.[85]   One of the first chimera-derived CPPs reported in the literature was Transportan (AGYLLGKINLKALAALAKKIL-NH_2), which was a fusion of the neuropeptide galanin1-13 and the wasp venom peptide mastoparan.[100,101,113,114]

One of the most popular examples of a chimera-derived CPP is Pep-1. [90-92] This peptide has a block copolymer-like structure with a tryptophan-rich hydrophobic domain that is segregated from a lysine-rich hydrophilic domain by a linker and is based on the NLS of the simian virus 40 (SV-40) large T antigen, as well as on the reverse transcriptase of HIV.[90-92]   Pep-1 is considered to be a primary amphipathic peptide because the hydrophilic/hydrophobic segregation is not dependent on the secondary structure of the peptide.[90-92]   Although stability is often an issue with peptide-based carriers, Pep-1 has an acetylated N-terminus and a cystamide C-terminus to improve shelf life.   Since the development of Pep-1, structural variations have been made to enhance delivery of proteins, peptides, and peptide nucleic acids.[91]   In addition, Divita and coworkers have developed MPG for nucleic acid delivery, which is structurally similar CPP with a primary amphipathic and alpha-helical structure.[91,98,99]   This CPP is commercially available as DeliverX™ through Panomics.[91,98,99]

In addition to their amphiphilicity, what set Transportan, Pep-1, and MPG apart from others CPPs is their ability to deliver cargo using non-covalent attachment.[90-92,99-101,113,114] Many CPPs, such TAT$_{49-57}$ and Penetratin, require covalent attachment for efficient cargo delivery.[81,82,110-112] By developing a non-covalent system, the carrier can simply be mixed with its cargo to form a transient complex that can dissociate upon entry into cells. Although this presents *in vivo* limitations because of the high risk of non-specific binding, it could mean less complex synthetic procedures and fewer experiments to ensure activity is not lost upon chemical conjugation.

1.2.3 Synthetic CPPs

Synthetic CPPs are based on a peptide backbone but are not derived from naturally occurring protein or peptide sequences.[85] CPPs that fall into this category include polyarginine; Amphiphatic Model Peptide (MAP), which is a lysine-rich secondary amphiphatic peptide; and CADY, which is arginine-rich and self-assembles to yield a facially amphiphilic structure.[104,115] While polyarginine does not require secondary structure or self assembly for delivery, the delivery activities of MAP and CADY are highly dependent on their secondary structures.[104,115] Disruptions in the helices or self assembly lead to diminished delivery efficiencies.[104,115] The primary focus in this discussion will be polyarginine due to its importance in the development of synthetic guanidinium-rich molecular transporters.

"Polyarginine" and "oligoarginine" broadly define a series of peptide sequences that only contain arginine residues and, depending on length, may be synthetically easier to prepare than TAT$_{49-57}$.[80-82,84,110] As part of Wender *et al*'s study in 2000, polyarginine (lengths = five to nine resides) was shown to outperform TAT$_{49-57}$, with longer sequences performing better than shorter ones.[84] Polyarginine sequences were also compared to their D enantiomers and their corresponding peptoids.[84] Both sets led

to better cellular uptake. This indicated that cellular uptake was not dependent on hydrogen bonding present in the peptide backbone and that the peptide backbone may not be necessary.[84] Another study from Mitchell *et al.* in 2000 showed that guanidinium groups led to superior uptake efficiencies compared to other possible cationic residues.[83] They also demonstrated that cellular uptake increased as the number of arginine residues increased up to 15 and that further increases in arginine content led to decreased cellular uptake.[83] This suggested that there is a critical number of arginine residues required for efficient uptake/delivery.

Unlike other hydrophobic-containing CPPs such as Pep-1, MPG, MAP, and CADY, which contain hydrophobic components to aid in cellular uptake, polyarginine is purely hydrophilic. To further explore polyarginine's internalization efficiencies, Matile and coworkers studied the effect counter ions have on cellular uptake.[106] In 2005, they reported that pairing polyarginine with bulky, aromatic activators, such as pyrenebutyrate, led to better peptide activity. This study suggested that there was some intrinsic benefit to having a hydrophobic component in addition to cationic charge as opposed to just having cationic charge.[106]

Through systematic studies with polyarginine and other synthetic peptides, it became clear that efficient delivery could be achieved without restricting structures to naturally occurring sequences.[83,84,106] Not only did structure-activity relationships (SARs) reveal that these molecules could be optimized for more efficient delivery through altering molecular weights and/or structural compositions, but also that the peptide backbone was not necessarily essential for successful delivery. This set the stage for the development of tunable delivery vehicles based on novel, abiotic scaffolds.

1.2.4 Alternative Classification of CPPs

As an alternative to the aforementioned CPP classification system, CPPs can be classified based on their distribution of hydrophilic/cationic amino acids and hydrophobic amino acids.[116] These categories include primary amphipathic, secondary amphipathic, and non-amphipathic CPPs.[116,117] A summary of CPPs that fall into these categories can be found in the last column of **Table 1**. For primary amphipathic peptides, segregation of cationic and hydrophobic amino acids is based on the sequential order of amino acids. Examples of these peptides include Pep-1, MPG, and Transportan.[90-92,98-100] Secondary amphipathic peptides, such as penetratin, MAP, pVEC, and M918, achieve the segregation of cationic and hydrophobic amino acids through their secondary structures, which enable them to either form α-helices or β-sheets.[95,102,104,105,109,118] Lastly, non-amphipathic peptides contain mostly cationic residues, with no cationic/hydrophobic amino acid segregation including polyarginine and TAT_{49-57}.[82-84,89,110]

1.3 Survey of Cell-penetrating Peptide Mimics

Although a large body of work focused on the development of peptide and peptidomimetic scaffolds for intracellular delivery,[79,83,84,119-127] moving away from naturally occurring amino acid residues and peptide backbones offers many advantages. Solid phase peptide synthesis can be avoided, which saves both time and money in producing the desired delivery vehicles. Additionally, a non-peptidic system, such as a polymeric scaffold, permits the use of different chemistries and allows the chemical compositions and polymer architectures to be tailored for efficient cargo delivery.[23] As a direct result of the easily tunable scaffolds, these materials are expected to be more potent and provide new models for fundamental studies. One prominent example of this is Tew and

workers oxanorbornene-based mimics of R_9 referred to as GMe_9 and dG_9.[128] These polymeric-based mimics both contain nine repeat units, but dG_9 has double the guanidine density (18 charges) than GMe_9 (9 charges).[128] Both of these mimics perform better than R9, with dG_9 outperforming GMe_9, suggesting that higher guanidinium density yields better cellular uptake.[128] Branched peptide scaffolds have been developed[127], which increase the guanidinium density. These molecules have similar uptake efficiencies to their linear analogs; however, they are synthetically more difficult to access and develop, making it harder to tune uptake and delivery efficiencies.[127] Figure 1.3 charts the development and progress of guanidinium-rich molecular transporters. While this review highlights the use of guanidinium-rich, polymeric materials, other scaffolds have been developed and extensively studied, including guanidinioglycosides, dendrimers/branched materials, and carbohydrates.[129-137]
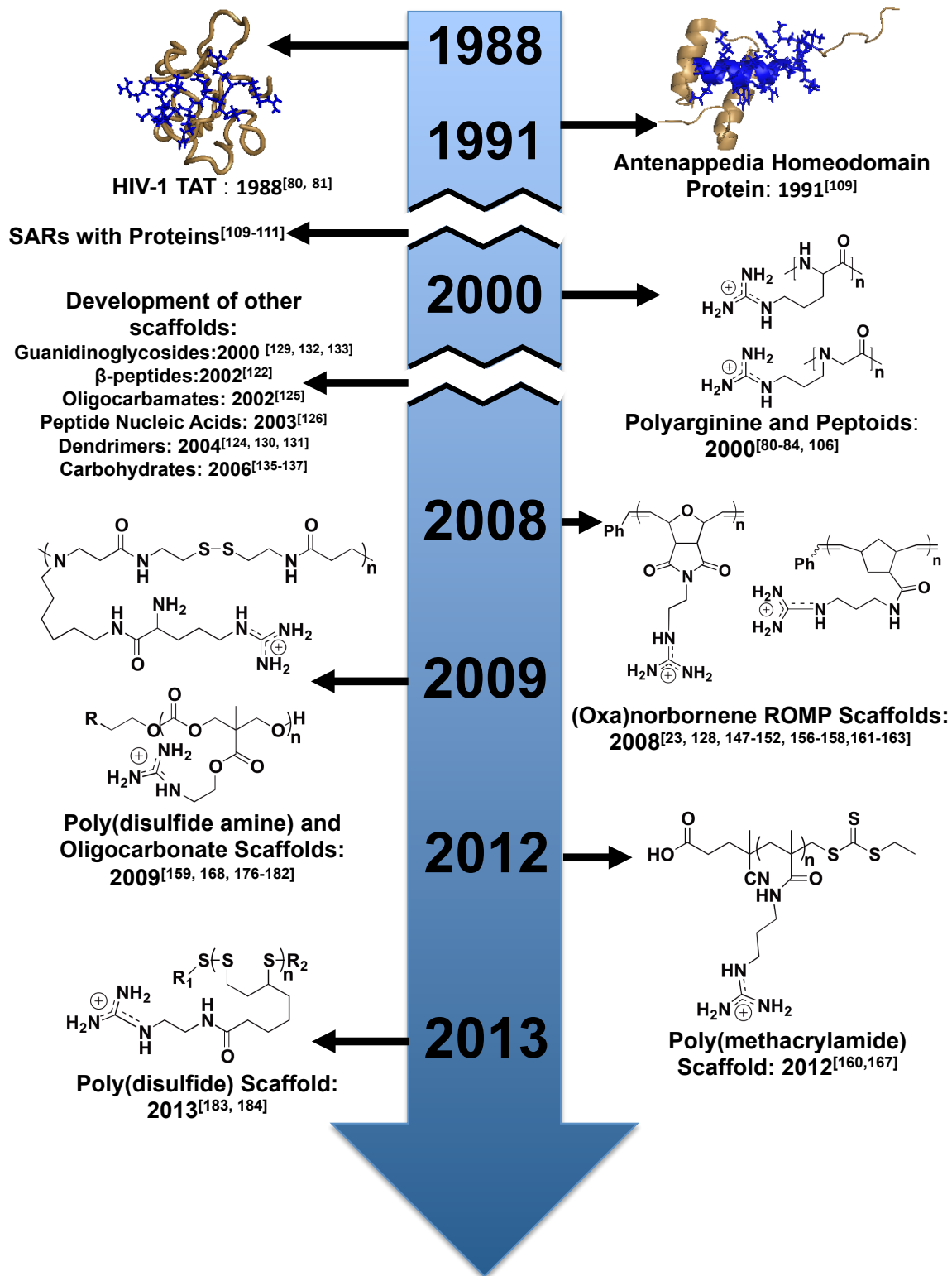
Figure 1.3. Development timeline for key guanidinium-rich CPPM scaffolds.

1.3.1   Ring-opening Metathesis Polymerization-based Scaffold

In 2008, Tew and coworkers, as well as Kiessling and coworkers independently demonstrated that they could use ring-opening metathesis polymerization-based scaffolds to design materials with CPP-like activity.   Tew and coworkers employ oxanorbornene-based systems for the design of their materials and Kiessling and coworkers primarily employ a norbornene-based system.   Both groups selected ROMP because it offers fast, efficient, and functional group tolerant polymerizations.[138-146] These polymerizations are often living, allowing for good control over molecular weights and polydispersities and allowing for the formation of more advanced architectures, such as block copolymers.[23,129,147,148]   Both groups' work is summarized below.

1.3.1.1   Oxanorbornene-based CPPMs

The first ROMP-based CPPM developed by Tew and coworkers was polyguanidinium oxanorbornene (PGON).[149,150]   This molecule (**Figure 4)** was originally designed as an alternative to their amine-based antimicrobial agents.[149]   Although it had good antimicrobial activity against *E. coli* and *S. aureus* and was non-hemolytic, PGON was also not membrane-disruptive, suggesting it could also be used as a molecular transporter.[149]   Preliminary dye release experiments using model vesicle systems confirmed that PGON (degree of polymerization (DP) = 5-41) was able to induce dye release in a non-linear, molecular weight-dependent fashion, further indicating it was membrane active and potentially a molecular transporter.[150]

In an effort to improve PGON's activity, hydrophobic monomers, which contained alkyl chains ranging from methyl to dodecyl, were copolymerized with guanidinium-rich monomers to obtain a new series of CPPMs (Figure 1.3.2).   Inspiration for this came from a Matile and coworkers study, which showed that hydrophobic counterion activators improve cellular uptake of polyarginine.[106]   The goal was to develop CPPMs that were

"self-activating", meaning they did not need external activators for improved efficiency.[151] CPPM activity improved with increasing alkyl chain length up until the incorporation of the butyl chain (Figure 1.4)[151] Beyond this, CPPM insolubility led to a reduction in polymer activity.[151] All CPPMs, however, performed better than PGON, indicating the importance of incorporating hydrophobic moieties.[149-151]
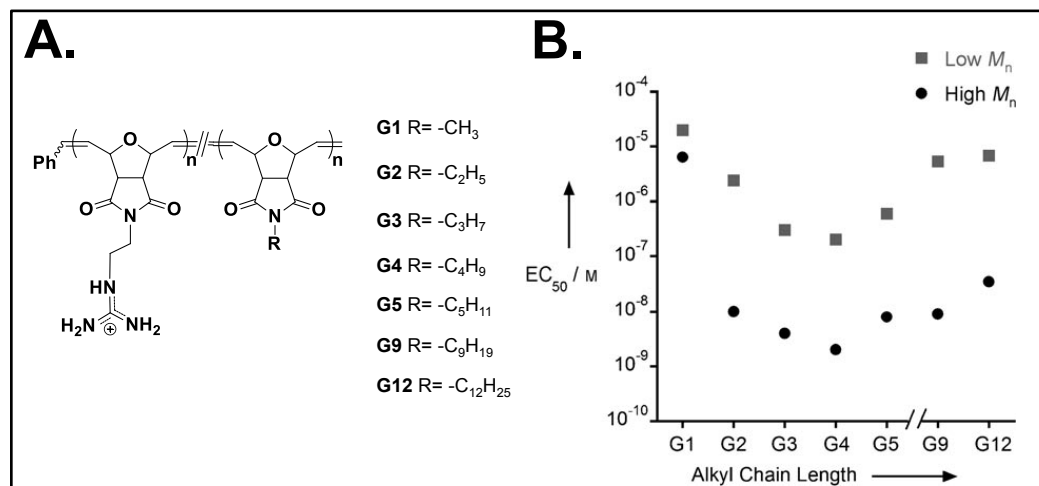
Figure 1.4. Oxanorbornene-based "self-activating" CPPMs. A) Molecular structures and B) Plot of EC_{50} vs. alkyl chain length.

As a follow up to this study, CPPMs were designed to assess the role of aromaticity.[152] Aromatic groups were selected because they are common structural features in CPPs, such as Pep-1 and Penetratin, and because some of the best CPP activators contain aromatic groups.[90-92,106,109,112] Also, many cellular components contain aromatic groups, such as transmembrane proteins, which use aromatic amino acids to stabilize the interface between the hydrophilic and hydrophobic portions of the protein.[153,154] In addition, it has been shown that the flat, rigid shape of aromatic rings along with their quadrupole moments can aid in membrane interactions.[155] The CPPMs containing phenyl rings were the most active in the series, thus indicating the importance of aromaticity for CPPM activity.[152] Further studies looked to probe the role of π-electronics in these phenyl ring systems through the incorporation of electron-donating

16

and electron-withdrawing groups. All CPPMs, regardless of the electron rich or electron poor ring, maintained similar membrane activities.[156] This demonstrated both the limits of the structural tuning that could be performed in this system and the number of structural options available without loss of membrane activity.[156]

Tew and coworkers also designed CPPMs based on di-armed oxanorbornene monomers. This system added more synthetic versatility as each monomer contains two functionalities that can be independently tuned.[23] Homopolymers containing one guanidine group and one hydrophobic group (aliphatic, aromatic, electron rich / electron poor aromatic systems) per monomer were designed as a direct comparison to their imide counterparts. These polymers had similar activities compared to the imide system.[151,156] In addition, further studies were aimed at understanding the role of functional group segregation. The results indicated improved delivery efficiencies of a block copolymer scaffold without loss of activity in the presence of serum compared to its homopolymer counterparts (Figure 1.5).[157] This block copolymer was designed to capture the guanidinium-rich nature of TAT_{49-57} and the amphiphilicity of Pep-1.[82-84,90-92] Follow-up studies explored the functional group distribution using constitutional macromolecular isomers, which are polymers of the same degree of polymerization but different arrangements of their pendent groups, ranging from completely segregated to completely mixed.[158] These arrangements were accessed through block (completely segregated), gradient (partially segregated), and homopolymerizations (mixed distribution).[158] Although studies indicated that the homopolymers enabled the best cellular uptake of the polymers, it is likely that block copolymers will deliver cargo more efficiently, as suggested by the literature.[148,157,159,160]

While early studies with PGON strictly applied model vesicle systems to assess membrane activity, di-armed homopolymers were chosen to assess the effect of guanidinium density on cellular uptake in three different cell lines: HEK293T, CHO, and

Jurkat T cells.[128] Although these polymers could enter all cell types with low cell death, uptake efficiencies were highly cell line-dependent.[128]   In all cases, these CPPMs outperformed polyarginine (R9).[128]   These studies were extended to explore constitutional macromolecular isomers, wherein cellular uptake was the best for the homopolymer tested and uptake efficiencies were found to be cell-type dependent. To further these studies by probing the effect of architecture when delivering biologically relevant cargo, a block copolymer was synthesized containing a 1:1 (n=m=5) ratio of hydrophobic to cationic monomers (Figure 1.5).[157,161]
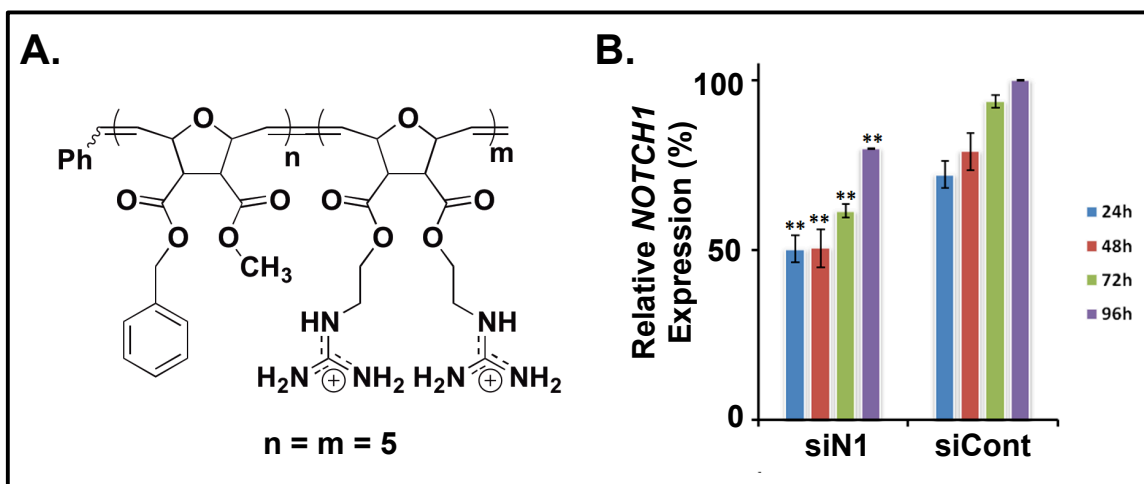
Figure 1.5. Delivery of siRNA to *NOTCH1* into human peripheral blood mononuclear cells (PBMCs). A. Block copolymer structure used for delivery. B. Percent relative protein expression as a function of time for PBMCs that received siRNA to *NOTCH1* (siN1) and PBMCs that received a scrambled, negative control (siCont).

This block copolymer was shown to deliver FITC-tagged siRNA and bioactive siRNA to *NOTCH1* in Jurkat T cells and human peripheral blood mononuclear cells (hPBMCs), respectively, with > 90% viability.[157]   Delivery efficiencies were not altered by the presence of serum proteins in the media.   The *NOTCH1* knockdown results were noteworthy because 50% knockdown of an active gene was reported (Figure 1.3.3).[157] This siRNA study represents proof of concept work that explored the delivery capabilities of this type of CPPM.   Additional SARs studies contained in this thesis aimed to

determine design princples for efficient siRNA delivery using these molecular transporters. These studies will also be expanded in order to develop design parameters for other biologically relevant cargo.[23]

1.3.1.2 Norbornene-based CPPMs

Kiessling and coworkers developed a norbornene-based scaffold.[147,148] Single-armed norbornene monomers for these materials initially contained succinimidyl ester moieties, which provided handles for post-polymerization functionalization. Polymeric materials could be reacted with N-(3-aminopropyl)guanidine in the presence of N-methyl morpholine to achieve near complete replacement of the succinimidyl ester pendent groups. This scaffold is based on previously published work.[162] The guanidinium-rich scaffold builds on this initial work by terminating the polymers with an enol-ether, which allows for dye-labeling the polymer chains for easy tracking of the materials during cellular experiments.[147] Uptake of these labeled molecules in HeLa cells was monitored using fluorescence imaging and results indicated that the polymer was trapped in endosomes, as noticed by punctated fluorescence, with some polymer dispersed in the cytosol.[147] Greater than 95% viability was observed for all polymer concentrations tested (up to 5µM).[147]

Given that after post-polymerization functionalization only homopolymer and random copolymer architectures can be accessed, follow-up work looked at the formation of block copolymers.[147,148] Two monomers were developed that could be modified post-polymerization by chemospecific methods, one succinimidyl ester-containing monomer and one alpha chloroacetamide-containing monomer.[148] These monomers were polymerized sequentially in order to yield a block copolymer template. Based on the different chemistries involved, this template could be modified post-polymerization using separate reactions to yield segregation of attached functional

19

groups.[148] High degrees of conversion were demonstrated for both starting functional groups.[148] Internalization of dye labeled block copolymers was demonstrated using HeLa cells, with cellular uptake following similar patterns to their previously reported homopolymer counterparts.[148]

More recently, Kiessling and coworkers developed a completely degradable ROMP scaffold using oxazinone-based monomers.[163] The authors demonstrated that a wide range of functional groups could be incorporated into these scaffolds, making them potential candidates for drug delivery and biomaterials applications.[163-166]

1.3.2   Polymethacrylamides

In 2012, McCormick and coworkers reported the synthesis of guanidinium-rich polymethacrylamides using aqueous reversible addition fragmentation chain transfer (aRAFT).[160] This synthetic method was advantageous for the synthesis of materials because polymerizations by this method are well-controlled and the guanidinium-containing monomers could be polymerized without protecting groups.[160] Homopolymers were synthesized using a N-[3-(dimethylaminopropyl) methacrylamide monomer and copolymers were synthesized using a N-[3-(dimethylaminopropyl) methacrylamide and N-[2-(hydroxypropyl) methacrylamide monomer.[160] Similar to polymers generated by the Tew and Wender groups, both sets of polymers were readily able to enter KB cells, with block copolymers out performing their homopolymer counterparts.[148,157,159,160] The authors note that the good control over the polymerization technique could enable this platform to be used for bioactive cargo delivery.[160] More recently, Peneva and coworkers developed a series of guanidinium-rich, statistical copolymers using aRAFT as potential siRNA delivery reagents.[167] Binding strength and competitive binding were studied but, to date, no cellular uptake or viability results have been reported.[167]

1.3.3 Oligocarbonates

Wender, Hedrick, Waymouth and coworkers developed a series of CPPMs based on oligocarbonate polymers.[159,168] Molecules were synthesized using metal-free, ring-opening polymerization of cyclic carbonates.[159,168] Initiators for these materials were designed such that the drug molecule or molecular probe to be delivered could be attached at the beginning of the polymerization to allow for simpler conjugation to various cargoes.[168] These molecules were shown to be biodegradable under physiological conditions, with half-lives around eight hours. Cellular uptake in Jurkat T cells revealed that these polymers entered in a charge-dependent manner, with longer polymers outperforming their shorter counterparts. To assess whether a biologically active cargo could be delivered, proof-of-concept experiments were performed in which luciferin was successfully delivered and shown to luminesce in HepG2 cells.

In a follow-up study, Wender, Hedrick, Waymouth and coworkers showed that they could tune their oligocarbonate structures through the incorporation of hydrophobic moieties for more efficient siRNA complexation and release.[159] Experiments with a dual-functional reporter HaCaT cell line that expressed both enhanced green fluorescent protein (EGFP) and Tomato fluorescent protein (tdTOM) was utilized to show specificity of knockdown.[159] Delivery of siRNA to tdTOM was shown to yield efficient reduction in tdTOM protein levels but to have a negligible effect on EGFP protein levels, thus demonstrating good knockdown specificity.[159] Polymers were shown to perform better in serum free media (86% knockdown) than in serum-containing media (64%).[159] Oligomers that incorporate longer alkyl chains (up to dodecyl) were also shown to out perform their counterparts that contained shorter alkyl chains.[159] Shorter oligomer lengths were also shown to out perform their longer counterparts.[159] Cell viability studies

using the 3-(4, 5-dimethylthiazolyl-2)-2, 5-diphenyltetrazolium bromide (MTT) assay demonstrated that the most active polymers showed significant toxicity at the higher concentrations tested (100 nM) but could be greatly improved by cutting the polymer concentrations in half (50 nM).[159] Lastly, it was demonstrated that knockdown efficiencies and complex sizes could be tuned by mixing different oligomers.[159] Overall Wender, Hedrick, Waymouth and coworkers developed a versatile, biodegradable platform for efficient delivery of biologically active siRNA. This platform has since been expanded by Wender *et al.* to include glycerol-based monomers to allow for better control over oligocarbonate/siRNA complex stability.[169]

1.3.4   Poly(disulfide)s

Poly(disulfide)s are polymers that contain at least one disulfide bond in the polymer repeat unit structure.[170] These materials are different from proteins and vulcanized rubber, which both utilize disulfide bonds for crosslinking.[170] Poly(disulfide)s can serve as efficient delivery reagents for nucleic acids and proteins, releasing their cargo through reductive de-polymerization in the presence of glutathione. Initially poly(amido amines) (PAAs) containing disulfide bonds were explored. These materials were synthesized by reacting cationic and/or hydrophobic monomers with cystaminebisacrylamide using Michael addition.[171,172] This platform is functional group tolerant, allowing for the incorporation of a wide range of functionalities, which enabled fine-tuning of PAA structures for efficient uptake and delivery.[173-175] Kim and coworkers, utilized a similar platform to design poly(disulfide amines) and their guanidinium-rich counterparts, which are often referred to as arginine-grafted bioreducible polymers (ABPs) and guanidinylated bioreducible polymers (GBPs).[176-182] The ABPs and GBPs molecules led to higher transfection efficiencies when compared to their amine

counterparts.[177,179-182] ABPs have been explored for RNAi applications related to anti-angiogenesis gene therapy of tumors as well as *ex vivo* pDNA delivery vehicles for treatment of ischemic heart diseases.[177,179-182]

While most poly(disulfide) delivery reagents utilize non-covalent delivery strategies, Matile and coworkers developed an efficient method of generating cell penetrating poly(disulfide)s that are covalently attached to their cargo utilizing surface-initiated ring-opening disulfide-exchange polymerization.[183,184] Many probes, drugs, and bioactive cargoes contain or can be easily made to contain thiol moieties, which makes them convenient initiating species for this polymerization method. Molecule formation and subsequent depolymerization in the presence of dithiothreitol (DTT) were monitored using dye-loaded vesicles.[183,184] Fast, efficient delivery (5 minutes), and subsequent fast depolymerization rates to release cargo into the cytosol (1 minute) were demonstrated in HeLa cells.[184] Low toxicities were demonstrated for all molecules tested up to 10µM.[184] Molecular uptake mechanism was independent of the cargo but could be altered based on the hydrophobic/cationic content of the materials.[183] The authors also suggested a thiol/counterion-mediated uptake mechanism to explain cell entry and how chemical compositions of the delivery vehicles change their ability to enter cells efficiently.[184]

1.4 Biophysical Characterization of CPP(M)s/PTD(M)s

Biophysical assays using model membranes can assess internalization and membrane interactions of CPPs/PTDs and their synthetic mimics.[106,149-152,170,183,185-189] These methods represent simpler systems than cells and remove complexities of active transport, such as endocytosis, and receptor-mediated uptake and focus primarily on mimicking direct translocation and membrane interactions. Commonly, large unilamellar vesicles (LUVs) that are swelled with dyes, such are carboxyfluorescein, are used to

evaluate membrane leakage.[106,149-152,156,170,183,185-189]   Carboxyfluorescein is self-quenched at high concentrations and its release from model membranes can be monitored using either a fluorimeter, or in the case of a more high-throughput screening method, a fluorescence plate reader.[156]   Dye leakage as a function of polymer concentration can be monitored, and data points can be fit to the Hill Equation to determine EC_{50} values, which are the effective concentration at which 50% of the dye is released.[106,149-152,156,185-190]   These values can be compared across many peptide systems to assess their membrane activities. Lipid compositions of these membranes can be tuned to assess how the incorporation of different lipids and/or the overall charge of the vesicles impacts membrane activity.[152,156] Tew and coworkers,[150-152,156] Matile and coworkers,[106,150,170,183,188,189] and Almeida and coworkers[185,186] used similar assays as a way to study the way molecules interact with model membranes. In addition to these authors, other researchers, including Pooga and coworkers, developed more advanced lipid systems.[191] Using chemical formulations, cells can be induced to produce small vesicles by budding off parts of their membranes. These systems more closely resemble actual lipid membrane compositions because they often include membrane proteins and cell surface receptors.[191]

1.5   Modes of Internalization for CPP(M)s

The mechanisms of CPP(M) uptake remains highly debated in the literature.[79,116,119,123] Early studies suggested direct translocation as the primary mode of internalization, which refers to molecules crossing membranes and directly entering the cytosol.[192-194]   However, many of these observations were shown to be erroneous, primarily due to cell fixation, which permeabilizes cell membranes and allows extracellular cargo to be internalized.[192-194] Additional modes of uptake have been

considered, including engulfment of particular molecules by the cell's membrane through forms of endocytosis, such as Clathrin-mediated endocytosis, caveolae-mediated endocytosis, macropinocytosis, and receptor-mediated endocytosis.[116,119,123,194] Glycosaminoglycans and lipid compositions are also thought to play a role in uptake mechanism.[119] Complicating matters even further, experimental conditions including, but not limited to, composition, cargo, concentration, and cell types as well as incubation temperatures and times may play distinct roles in modes of internalization.[79,116,119,123]

Extensive effort has been made to understand the primary modes of internalization. One common way to do so is to inhibit certain entry methods and to compare uptake and delivery efficiencies to those cells under normal conditions.[195-197] A summary of common methods can be found in Table 1.2. It is important to keep in mind that inhibiting specific modes of uptake may actually cause the cell to up-regulate other modes of entry or lead to off-target effects.[195-197] It is also important to note that CPPs likely enter cells through multiple methods at the same time, with the different possible modes of cellular uptake being highly cell-type dependent.[116,198,199]

Table 1.2. Summary of Inhibitors, the pathways they affect, and the blocking mechanisms.

Inhibitor	Affected Pathways	Blocking Mechanism
Lowered Temperature (4°C)[200]	Energy dependent	Reduces cell metabolism, inhibiting energy-dependent pathways
Sodium azide and 2-deoxy-D-glucose[201]	Energy dependent	Depletes ATP
Cytochalasin D[119]	Macropinocytosis	Promotes disassembly of the actin cytoskeleton and blocks actin polymerization
Wortmannin[202]	Macropinocytosis and Clathrin-mediated endocytosis	Inhibitor of phosphatidylinositol 3-kinase inhibitor
5-(N-ethyl-N-isopropylamiloride)[119]	Macropinocytosis	Inhibitor of sodium-proton pump exchange
Chloroquine[203,204]	Endosomal Escape	Promoted endosomal escape
Nocodazole[205,206]	Macropinocytosis	Blocks actin polymerization and disrupts actin cytoskeleton
Chlorpromazine and sucrose[207]	Clathrin-mediated endocytosis	Depletes clathrin and AP2 adapter protein complex
Dynasore[208]	Clathrin-mediated endocytosis	Dynamin inhibitor
Methyl-β-Cyclodextrin[209]	Clathrin-independent endocytosis	Cholesterol extraction from membrane

In addition, colocalization studies, which look at where polymer/cargo complexes end up in cells, and biophysical methods, which look at interactions between polymer/cargo complexes with lipid membranes, have also been utilized to elucidate uptake mechanism.[106,151,152,185,186,188,189,210-214] To date, no one method has been shown to clearly document all possible and prominent methods of internalization.[79,116] Often many methods need to be taken together in order to begin to understand what is happening in the cellular environment. This challenging problem is an area of active research.

1.6   Methods of Bioactive Cargo delivery, with a Focus on T Cells

Delivery of therapeutic agents is an ongoing challenge for the biomedical community.[73-79,215] Many methods have been developed in efforts to help efficiently and

reliably deliver bioactive molecules across cellular membranes. Although CPP(M)s fall under the category of transfection/transduction, this method as well as other methods of delivery are summarized in this section, along with their major advantages and disadvantages, to have a more complete view of the delivery options available to the field.

1.6.1 Electroporation

Electroporation is a method of delivery that applies a short, high voltage pulse to cell membranes as a way to transiently permeabilize them.[216,217] This technique was initially developed for gene delivery. Voltages for this process typically range from 0.2-1V, depending on the resting transmembrane potential of the cell type.[216,217] The longer the pulse applied to the cells, the more pores that form in the membrane.[216,217] While it only takes a couple seconds for pores to form, the resealing of the membrane can take several minutes, which provides time for charged cargo to enter the permeabilized cell. The major drawback of this method is the high cell death (50-60% viability often reported) due to high voltages and membrane resealing time.[216-219] Although long-term stability results show improved viability, initial viability after treatment often remains low.[218,219]

1.6.2 Viral Vectors

Viral vectors harness the ability of viruses to infect host cells.[85] In their design, the genes that allow them to replicate or cause toxicity are removed but the ones that allow for capsid formation and the incorporation into the host genome remain to facilitate stable expression of a desired addition to the infected cell type.[85] The protein coating of the virus capsid can also be varied in order to allow for a wider range of cells to be transduced.[85] Three different types of viral vectors used for these applications include

adenoviral vectors, retroviral vectors, and lentiviral vectors.[85] Adenoviral vectors have

been used *in vitro* for vaccine development and gene delivery.[85] These vectors suffer

from major drawbacks, which include the inability for its DNA to incorporate into the host

genome and immune responses that are mounted by the host in response to the

presence of the adenoviral vectors.[85,216] For this method to be improved, adenoviral

vectors that humans are not immune to would need to be identified.

Retroviral vectors contain reverse transcriptase, which enables incorporation of

the desired gene into the host cell;[85] however, the major drawback of this method is that

it requires that the cells be dividing in order to for genome incorporation to occur.[85,216]

Without the breakdown of the nuclear membrane, which occurs during cell division,

incorporation cannot be achieved.[85,216] There have also been reports of this method

leading to instances of malignancies as a result of genetic incorporation near proto-

oncogenes and alterations to the genome that may change copy number or delete the

tumor suppressor genes.[216] Lentiviral vectors, which are a subclass of retroviral vectors,

offer the advantage that they can infect and integrate their genetic material into non-

dividing cells.[216] Most often, HIV-based vectors are selected. Despite the advantage

offered by this system, there is still the chance that malignant transformations can

occur.[85,216] The safety of these vectors needs to be evaluated on a case-by-case basis.

1.6.3 Microinjection

The process of microinjection involves gripping individual cells with a capillary

holder and using a micro-needle to deliver cargo into the cell.[220] This method offers

many advantages, including that the exact amount of cargo injected into the cells is

known, that it is not cell-type dependent, and that it can allow for quantitative delivery

directly to the nucleus.[220] Despite these advantages, this method suffers from major

drawbacks. For this method, cells need to be injected individually, which is both time

consuming and limits the numbers of cells that can be treated.[220] The low cell numbers, in turn, makes extensive exploration of treatments difficult.[220] Lastly, this method often has a steep learning curve and takes a long time to master.[220]

1.6.4   Lipofection

Lipofection is a method of delivering cargo into cells using liposomes.[221] Most often, cationic lipids are used to complex with anionic cargo to form liposomes, which in turn can fuse with the phospholipid bilayer of cells to deliver its cargo into the cytosol.[221] This method is advantageous because it is compatible with many cell types and generally has good efficiencies and low toxicities.[221] The major drawback of this method is that this method has poor efficiencies in the presence of serum proteins.[221]

1.6.5   Delivery Using Transfection/Transduction Reagents

This method of delivery uses a carrier molecule to associate with a desired cargo to help facilitate the cargo's cellular internalization. Delivery reagents of this sort can either be peptides[90,92,107,110,113,115], lipids[222,223], or polymers[157,159,168-170,176,179,183,224] and they often associate with cargo by covalent or non-covalent interactions. Methods of association with the cargo with the carrier molecule will be discussed in the next section. The ratio of delivery reagent to cargo ratio must also be determined for each new delivery reagent, cargo, and cell type used for experiments. These materials hold much promise in the realm of biological cargo delivery due to the fact that they are often less toxic and lead to fewer mutagenic effects than other methods previously discussed.[75,225-227] Despite these advantages, some reagents still suffer from poor efficiencies in certain cell types, particularly immune cells.[75,225-227] This thesis will primarily focus on the development of polymeric-based transfection reagents and how the structures of these

materials impact their internalization efficiencies. Development of design principles for these materials will help guide the further development of efficient delivery reagents.

1.6.6 Association of Carrier Molecule with Cargo

For transfection experiments, the cargo of interest can be associated to the carrier molecule using covalent linkages or non-covalent interactions. When using covalent attachment, chemical reactions are generally used to form either degradable or non-degradable linkages between the carrier molecule and the cargo.[110,228-232] Although this method is advantageous, particularly for *in vivo* applications, because the covalent attachment ensures the cargo is always associated with the carrier molecule, the formation and presence of these linkages can lead to other complications.[110,228-232] Chemically modifying cargo presents the risks of either denaturing the cargo or adding the linkage to an area of the cargo that may impact its biological function.[230] Additionally, complex conjugation steps need to be preformed for each unique cargo to be delivered, which can be costly.[228] CPPs such as TAT[110], penetratin[109], and polyarginine[89] have all been shown to deliver covalently attached cargo.

An alternative to the covalent attachment method is the association of cargo using non-covalent interactions. Most often, this involves the use of electrostatic or hydrophobic interactions to associate the carrier molecule with the cargo. This method is advantageous because the conditions for complex formation are more mild and because it opens up the opportunity to use one carrier molecule for multiple different cargoes. The major drawback of this method, however, is the susceptibility for these complexes to exchange out their cargo for something else in the surrounding medium.[216,233] This presents a major limitation for *in vivo* application, but may be avoided for *ex vivo* and *in vitro* experiments. CPPs such as Pep-1 and MPG have been

used for the non-covalent delivery of proteins and siRNA, respectively.[90,99] Non-covalent attachment has also been a common method used with polymeric deliver reagents.[233]

1.6.7   Cargo Selection

When selecting a delivery reagent, it is very important to take into consideration the cargo being selected. Although proteins, siRNA, pDNA, and small molecules may fall under the general umbrella of "bioactive cargo", often times they require delivery reagents to be tailored for specific delivery of one type of cargo.[234] For example, even though siRNA and pDNA are both negatively charged and comprised of nucleic acids, separate delivery reagents are often required given the different issues associated with delivery of each cargo.[234]   siRNA is much smaller, only consisting of 18-21 base pairs, and reagents needs to address issues with siRNA easily being exchanged out of a complex for other, larger, negatively charged molecules in the delivery medium and with the fact that it ribonucleic acids are not as stable as deoxyribonucleic acids and are therefore more easily degraded.[234] In comparison, pDNA consists of thousands of base pairs and the primary delivery concern condensing the DNA and masking the negative charge.[234]   It is not uncommon for companies to offer different variations of delivery reagents that are tailored to specific cargo. For this thesis, siRNA was specifically selected as the cargo of choice for structure activity relationship studies.

1.7   siRNA and RNAi

In 1998, Andrew Fire and Craig Mello published their discovery of RNA interference (RNAi), a process that has been shown to temporarily reduce gene expression following the destruction of mRNA.[235] This process continues to be an important tool to probe molecular pathways and treat diseases.[153,236-239] Small interfering RNA (siRNA), which represents one RNAi approach, must be present in the cytosol so

that the siRNA guide strand can be incorporated into the RISC complex and degrade its complementary mRNA. This leads to transient, sequence-specific, post-transcriptional gene knockdown,[240-242] which is advantageous for discrete biological and clinical applications.[153,236-239] Although in some cases siRNA is endogenously produced, for most desired applications, it must be exogenously produced and then introduced into cells.[243] siRNA's net negative charge and susceptibility to degradation by RNases pose challenges for cellular internalization.[216] Additional challenges associated with siRNA are related to off-target effects related to sequence overlaps within the biological system or due to concentration-dependent effects.[244-248] Developing delivery strategies that meet the requirements of siRNA internalization while minimizing off-target affects is growing area of research and holds great promise for advancing our understanding of cellular processes and for developing new disease treatments.

1.8 T Cells and Their Delivery Challenges

Although there are many challenges associated with intracellular delivery, delivery to T cells poses added difficulties.[216] T cells are key components of the immune system. They orchestrate essential functions during the immune response to pathogens, chronic inflammation, and autoimmune disorders.[249] *In vivo* delivery to this subset of cells poses both the problems of targets T cells and crossing cellular membranes.[216] While monoclonal antibodies specific to T cell receptors have been tethered to biomolecules to provide targeting capabilities, it does not address the issues with cellular internalization or cargo stability.[216] These are particularly problems for cargoes such as siRNA, which can be easily degraded while traveling through the bloodstream without proper protection. [216] Although these challenges can largely be avoided using *ex vivo* delivery, which involves extracting cells from a patient, treating

them *in vitro*, and then re-introducing them into the patient, T cells, particularly primary T cells, are considered "hard-to-transfect." [216]   Only select commercial delivery reagents are able to facilitate cargo internalization in T cells lines and even fewer are able to delivery to primary T cells. Although electroporation and viral vectors have sometimes been used in place of a reliable transfection reagent, these methods often lead to high cell death, immunogenicity effects, or require T cell activation prior to, or concurrently, with delivery. [216]   The need for reliable T cell delivery vehicles is high. Successful delivery reagents for these subsets of cells would provide avenues for exploring molecular pathways and for developing new disease treatments.

1.9   Thesis Overview

Herein we document efforts to tune polymer-based protein mimic structures for improved internalization and delivery of siRNA. Ring-opening metathesis polymerization (ROMP) was utilized for the synthesis of these molecules since it is a fast, efficient, and functional group-tolerant method that also allows for relatively precise control over molecular weights and polydispersities.[138-146] Also, since ROMP is a living polymerization, it allows for the formation of more advanced architectures, such as block copolymers.[138-146] Structure activity relationships (SARs) using model membranes and cells were used to probe how polymer composition, molecular weight, and architecture impact polymer activity and siRNA internalization and delivery efficiencies. By understanding the essential design principles necessary for siRNA internalization and delivery, the next generation of efficient CPPMs/PTDMs can be optimized for specific applications.

Chapter 2 explores how π-elections of aromatic systems incorporated into our CPPM/PTDM systems impacts their resulting membrane interactions. Following this, chapters 3 and 4 document the development of design principles for the development of

our ROMP-based PTDMs. Chapter 3 specifically establishes that there is a critical

cationic charge content necessary for efficient siRNA delivery and that the addition of a

hydrophobic block lead to improved efficiencies compared to their corresponding

homopolymer counterparts with the same cationic charge content. Building on this,

Chapter 4 explores the role hydrophobicity plays in siRNA delivery efficiencies,

establishing a critical hydrophobic window for which there is optimal siRNA

internalization. The thesis then concludes with Chapters 5 and 6, which address

potential future directions for this work and summarize materials and methods,

respectively.

1.10 References

(1)   Jeffrey, G. A.; Saenger, W. Hydrogen Bonding in Biological Structures; Springer-Verlag: Berlin, 1991.

(2)   Fletcher, S.; Hamilton, A. D. Curr Opin Chem Biol 2005, 9, 632-638.

(3)   Orner, B. P.; Ernst, J. T.; Hamilton, A. D. J Am Chem Soc 2001, 123, 5382-5383.

(4)   Fairlie, D. P.; West, M. L.; Wong, A. K. Curr Med Chem 1998, 5, 29-62.

(5)   Weiser, P. T.; Chang, C. Y.; McDonnell, D. P.; Hanson, R. N. Bioorg Med Chem 2014, 22, 917-926.

(6)   Jayatunga, M. K.; Thompson, S.; Hamilton, A. D. Bioorg Med Chem Lett 2014, 24, 717-724.

(7)   Barnard, A.; Long, K.; Yeo, D. J.; Miles, J. A.; Azzarito, V.; Burslem, G. M.; Prabhakaran, P.; T, A. E.; Wilson, A. J. Org Biomol Chem 2014, 12, 6794-6799.

(8)   Barnard, A.; Long, K.; Martin, H. L.; Miles, J. A.; Edwards, T. A.; Tomlinson, D. C.; Macdonald, A.; Wilson, A. J. Angew Chem Int Ed Engl 2015, 54, 2960-2965.

(9)   Gellman, S. H. Acc Chem Res 1998, 31, 173-180.

(10)   Hill, D. J.; Mio, M. J.; Prince, R. B.; Hughes, T. S.; Moore, J. S. Chem Rev 2001, 101, 3893-4012.

(11)   Ernst, J. T.; Bercerril, J.; Park, H. S.; Yin, H.; Hamilton, A. D. Angew Chem Int Ed Engl 2003, 42, 535-539.

(12)   Saraogi, I.; Hamilton, A. D. Chem Soc Rev 2009, 38, 1726-1743.

(13)   Jones, T. V.; Blatchly, R. A.; Tew, G. N. Org Lett 2003, 5, 3297-3299.

(14)   Gabriel, G. J.; Tew, G. N. Org Biomol Chem 2008, 6, 417-423.

(15)   Tew, G. N.; Scott, R. W.; Klein, M. L.; Degrado, W. F. Acc Chem Res 2010, 43, 30-39.

(16)   Stigers, K. D.; Soth, M. J.; Nowick, J. S. Curr Opin Chem Biol 1999, 3, 714-723.

(17)   Slutsky, M. M.; Phillip, J. S.; Tew, G. N. N J Chem 2008, 32, 670-675.

(18)   Martinek, T. A.; Fulop, F. Chem Soc Rev 2012, 41, 687-702.

(19)   Jones, T. V.; Slutsky, M. M.; Tew, G. N. N J Chem 2008, 32, 676-679.

(20)   Horne, W. S.; Gellman, S. H. Acc Chem Res 2008, 41, 1399-1408.

(21)   Goodman, C. M.; Choi, S.; Shandler, S.; DeGrado, W. F. Nat Chem Biol 2007, 3, 252-262.

(22)   Arnt, L.; Tew, G. N. Macromolecules 2004, 37, 1283-1288.

(23)   Sgolastra, F.; deRonde, B. M.; Sarapas, J. M.; Som, A.; Tew, G. N. Acc Chem Res 2013.

(24)   Stanzl, E. G.; Trantow, B. M.; Vargas, J. R.; Wender, P. A. Acc Chem Res 2013, 46, 2944-2954.

(25)   Brogden, K. A. Nat Rev Microbiol 2005, 3, 238-250.

(26)   Zasloff, M. Nature 2002, 415, 389-395.

(27)   Hancock, R. E.; Diamond, G. Trends Microbiol 2000, 8, 402-410.

(28)   Benko-Iseppon, A. M.; Galdino, S. L.; Calsa, T., Jr.; Kido, E. A.; Tossi, A.; Belarmino, L. C.; Crovella, S. Curr Protein Pept Sci 2010, 11, 181-188.

(29)   Hancock, R. E.; Sahl, H. G. Nat Biotechnol 2006, 24, 1551-1557.

(30)   Wilmes, M.; Sahl, H. G. Int J Med Microbiol 2014, 304, 93-99.

(31)   Som, A.; Vemparala, S.; Ivanov, I.; Tew, G. N. Biopolymers 2008, 90, 83-93.

(32)   Yang, L.; Gordon, V. D.; Trinkle, D. R.; Schmidt, N. W.; Davis, M. A.; DeVries, C.; Som, A.; Cronan, J. E., Jr.; Tew, G. N.; Wong, G. C. Proc Natl Acad Sci U S A 2008, 105, 20595-20600.

(33)   Vriens, K.; Cammue, B. P.; Thevissen, K. Molecules 2014, 19, 12280-12303.

(34)   Shai, Y.; Makovitzky, A.; Avrahami, D. Curr Protein Pept Sci 2006, 7, 479-486.

(35)   Shai, Y. Biopolymers 2002, 66, 236-248.

(36)   Schmidt, N. W.; Tai, K. P.; Kamdar, K.; Mishra, A.; Lai, G. H.; Zhao, K.; Ouellette, A. J.; Wong, G. C. J Biol Chem 2012, 287, 21866-21872.

(37)   Schmidt, N. W.; Mishra, A.; Lai, G. H.; Davis, M.; Sanders, L. K.; Tran, D.; Garcia, A.; Tai, K. P.; McCray, P. B.; Ouellette, A. J.; Selsted, M. E.; Wong, G. C. J Am Chem Soc 2011, 133, 6720-6727.

(38)   Oliveira, M. D.; Franco, O. L.; Nascimento, J. M.; de Melo, C. P.; Andrade, C. A. Curr Protein Pept Sci 2013, 14, 543-555.

(39)   Li, W.; Tailhades, J.; O'Brien-Simpson, N. M.; Separovic, F.; Otvos, L., Jr.; Hossain, M. A.; Wade, J. D. Amino Acids 2014, 46, 2287-2294.

(40)   Lemeshko, V. V. Arch Biochem Biophys 2014, 545, 167-178.

(41)   Harrison, P. L.; Abdel-Rahman, M. A.; Miller, K.; Strong, P. N. Toxicon 2014, 88, 115-137.

(42)   Hancock, R. E.; Rozek, A. FEMS Microbiol Lett 2002, 206, 143-149.

(43)   Bolintineanu, D. S.; Kaznessis, Y. N. Peptides 2011, 32, 188-201.

(44)   Devine, D. A.; Hancock, R. E. Curr Pharm Des 2002, 8, 703-714.

(45)   Yeaman, M. R.; Yount, N. Y. Pharmacol Rev 2003, 55, 27-55.

(46)   Polyansky, A. A.; Chugunov, A. O.; Vassilevski, A. A.; Grishin, E. V.; Efremov, R. G. Curr Protein Pept Sci 2012, 13, 644-657.

(47)   Mangoni, M. L.; Shai, Y. Cell Mol Life Sci 2011, 68, 2267-2280.

(48)   Nguyen, L. T.; Haney, E. F.; Vogel, H. J. Trends Biotechnol 2011, 29, 464-472.

(49)   Scocchi, M.; Tossi, A.; Gennaro, R. Cell Mol Life Sci 2011, 68, 2317-2330.

(50)   Takahashi, H.; Palermo, E. F.; Yasuhara, K.; Caputo, G. A.; Kuroda, K. Macromol Biosci 2013, 13, 1285-1299.

(51)   Scott, R. W.; DeGrado, W. F.; Tew, G. N. Curr Opin Biotechnol 2008, 19, 620-627.

(52)   Rotem, S.; Mor, A. Biochim Biophys Acta 2009, 1788, 1582-1592.

(53)   Kuroda, K.; Caputo, G. A. Wiley Interdiscip Rev Nanomed Nanobiotechnol 2013, 5, 49-66.

(54)   Gabriel, G. J.; Som, A.; Madkour, A. E.; Eren, T.; Tew, G. N. Mater Sci Eng R Rep 2007, 57, 28-64.

(55)   Hamuro, Y.; Schneider, J. P.; DeGrado, W. F. J Am Chem Soc 1999, 121, 12200-12201.

(56)   Seebach, D.; Beck, A. K.; Bierbaum, D. J. Chem Biodivers 2004, 1, 1111-1239.

(57)   Porter, E. A.; Weisblum, B.; Gellman, S. H. J Am Chem Soc 2002, 124, 7324-7330.

(58)   Thaker, H. D.; Cankaya, A.; Scott, R. W.; Tew, G. N. ACS Med Chem Lett 2013, 4, 481-485.

(59)   Thaker, H. D.; Sgolastra, F.; Clements, D.; Scott, R. W.; Tew, G. N. J Med Chem 2011, 54, 2241-2254.

(60)   Thaker, H. D.; Som, A.; Ayaz, F.; Lui, D. H.; Pan, W. X.; Scott, R. W.; Anguita, J.; Tew, G. N. J Am Chem Soc 2012, 134, 11088-11091.

(61)   Som, A.; Navasa, N.; Percher, A.; Scott, R. W.; Tew, G. N.; Anguita, J. Clin Vaccine Immunol 2012, 19, 1784-1791.

(62)   Lienkamp, K.; Madkour, A. E.; Musante, A.; Nelson, C. F.; Nusslein, K.; Tew, G. N. J Am Chem Soc 2008, 130, 9836-9843.

(63)   Al-Badri, Z. M.; Som, A.; Lyon, S.; Nelson, C. F.; Nusslein, K.; Tew, G. N. Biomacromolecules 2008, 9, 2805-2810.

(64)   Arnt, L.; Nusslein, K.; Tew, G. N. J Polym Sci A1 2004, 42, 3860-3864.

(65)   Colak, S.; Nelson, C. F.; Nusslein, K.; Tew, G. N. Biomacromolecules 2009, 10, 353-359.

(66)   Ilker, M. F.; Nusslein, K.; Tew, G. N.; Coughlin, E. B. J Am Chem Soc 2004, 126, 15870-15875.

(67)   Lienkamp, K.; Kumar, K. N.; Som, A.; Nusslein, K.; Tew, G. N. Chem Eur J 2009, 15, 11710-11714.

(68)   Lienkamp, K.; Madkour, A. E.; Kumar, K. N.; Nusslein, K.; Tew, G. N. Chem Eur J 2009, 15, 11715-11722.

(69)   Madkour, A. E.; Dabkowski, J. M.; Nusslein, K.; Tew, G. N. Langmuir 2009, 25, 1060-1067.

(70)   Rennie, J.; Arnt, L.; Tang, H.; Nusslein, K.; Tew, G. N. J Ind Microbiol Biotechnol 2005, 32, 296-300.

(71)   Ishitsuka, Y.; Arnt, L.; Majewski, J.; Frey, S.; Ratajczek, M.; Kjaer, K.; Tew, G. N.; Lee, K. Y. J Am Chem Soc 2006, 128, 13123-13129.

(72)   Arnt, L.; Tew, G. N. J Am Chem Soc 2002, 124, 7664-7665.

(73)   Park, T. G.; Jeong, J. H.; Kim, S. W. Adv Drug Deliv Rev 2006, 58, 467-486.

(74)   Snyder, E. L.; Dowdy, S. F. Pharm Res 2004, 21, 389-393.

(75)   Thomas, M.; Klibanov, A. M. Appl Microbiol Biotechnol 2003, 62, 27-34.

(76)   Whitehead, K. A.; Langer, R.; Anderson, D. G. Nat Rev Drug Discov 2009, 8, 129-138.

(77)   Deshayes, S.; Morris, M. C.; Divita, G.; Heitz, F. Cell Mol Life Sci 2005, 62, 1839-1849.

(78)   Fonseca, S. B.; Pereira, M. P.; Kelley, S. O. Adv Drug Deliv Rev 2009, 61, 953-964.

(79)   Heitz, F.; Morris, M. C.; Divita, G. Brit J Pharmacol 2009, 157, 195-206.

(80)   Green, M.; Loewenstein, P. M. Cell 1988, 55, 1179-1188.

(81)   Frankel, A. D.; Pabo, C. O. Cell 1988, 55, 1189-1193.

(82)   Vives, E.; Brodin, P.; Lebleu, B. J Biol Chem 1997, 272, 16010-16017.

(83)   Mitchell, D. J.; Kim, D. T.; Steinman, L.; Fathman, C. G.; Rothbard, J. B. J Pept Res 2000, 56, 318-325.

(84)   Wender, P. A.; Mitchell, D. J.; Pattabiraman, K.; Pelkey, E. T.; Steinman, L.; Rothbard, J. B. Proc Natl Acad Sci U S A 2000, 97, 13003-13008.

(85)   Lindgren, M.; Langel, U. Cell-Penetrating Peptides: Methods and Protocols 2011, 683, 3-19.

(86)   Siprashvili, Z.; Reuter, J. A.; Khavari, P. A. Mol Ther 2004, 9, 721-728.

(87)   Opalinska, J. B.; Gewirtz, A. M. Nat Rev Drug Discov 2002, 1, 503-514.

(88)   Patel, L. N.; Zaro, J. L.; Shen, W. C. Pharm Res 2007, 24, 1977-1992.

(89)   Futaki, S.; Suzuki, T.; Ohashi, W.; Yagami, T.; Tanaka, S.; Ueda, K.; Sugiura, Y. J Biol Chem 2001, 276, 5836-5840.

(90)   Morris, M. C.; Depollier, J.; Mery, J.; Heitz, F.; Divita, G. Nat Biotechnol 2001, 19, 1173-1176.

(91)   Morris, M. C.; Deshayes, S.; Heitz, F.; Divita, G. Biol Cell 2008, 100, 201-217.

(92)   Morris, M. C.; Vidal, P.; Chaloin, L.; Heitz, F.; Divita, G. Nucleic Acids Res 1997, 25, 2730-2736.

(93)   Schwarze, S. R.; Ho, A.; Vocero-Akbani, A.; Dowdy, S. F. Science 1999, 285, 1569-1572.

(94)   Joliot, A.; Prochiantz, A. Nat Cell Biol 2004, 6, 189-196.

(95)   Elmquist, A.; Lindgren, M.; Bartfai, T.; Langel, U. Exp Cell Res 2001, 269, 237-244.

(96)   Elliott, G.; O'Hare, P. Cell 1997, 88, 223-233.

(97)   Gros, E.; Deshayes, S.; Morris, M. C.; Aldrian-Herrada, G.; Depollier, J.; Heitz, F.; Divita, G. Biochim Biophys Acta 2006, 1758, 384-393.

(98)   Simeoni, F.; Arvai, A.; Bello, P.; Gondeau, C.; Hopfner, K. P.; Neyroz, P.; Heitz, F.; Tainer, J.; Divita, G. Biochemistry 2005, 44, 11997-12008.

(99)   Simeoni, F.; Morris, M. C.; Heitz, F.; Divita, G. Nucleic Acids Res 2003, 31, 2717-2724.

(100)   Pooga, M.; Hallbrink, M.; Zorko, M.; Langel, U. FASEB J 1998, 12, 67-77.

(101)   Soomets, U.; Lindgren, M.; Gallet, X.; Hallbrink, M.; Elmquist, A.; Balaspiri, L.; Zorko, M.; Pooga, M.; Brasseur, R.; Langel, U. BBA-Biomembranes 2000, 1467, 165-176.

(102)   El-Andaloussi, S.; Johansson, H. J.; Holm, T.; Langel, U. Mol Ther 2007, 15, 1820-1826.

(103)   Lindgren, M.; Rosenthal-Aizman, K.; Saar, K.; Eiriksdottir, E.; Jiang, Y.; Sassian, M.; Ostlund, P.; Hallbrink, M.; Langel, U. Biochem Pharmacol 2006, 71, 416-425.

(104)   Oehlke, J.; Scheller, A.; Wiesner, B.; Krause, E.; Beyermann, M.; Klauschenz, E.; Melzig, M.; Bienert, M. BBA-Biomembranes 1998, 1414, 127-139.

(105)   Wolf, Y.; Pritz, S.; Abes, S.; Bienert, M.; Lebleu, B.; Oehlke, J. Biochemistry 2006, 45, 14944-14954.

(106)   Nishihara, M.; Perret, F.; Takeuchi, T.; Futaki, S.; Lazar, A. N.; Coleman, A. W.; Sakai, N.; Matile, S. Org Biomol Chem 2005, 3, 1659-1669.

(107)   Crombez, L.; Aldrian-Herrada, G.; Konate, K.; Nguyen, Q. N.; McMaster, G. K.; Brasseur, R.; Heitz, F.; Divita, G. Mol Ther 2009, 17, 95-103.

(108)   Kurzawa, L.; Pellerano, M.; Morris, M. C. Biochim Biophys Acta 2010, 1798, 2274-2285.

(109)   Derossi, D.; Joliot, A. H.; Chassaing, G.; Prochiantz, A. J Biol Chem 1994, 269, 10444-10450.

(110)   Fawell, S.; Seery, J.; Daikh, Y.; Moore, C.; Chen, L. L.; Pepinsky, B.; Barsoum, J. Proc Natl Acad Sci U S A 1994, 91, 664-668.

(111)   Joliot, A.; Pernelle, C.; Deagostinibazin, H.; Prochiantz, A. Proc. Natl. Acad. Sci. U. S. A. 1991, 88, 1864-1868.

(112)   Derossi, D.; Chassaing, G.; Prochiantz, A. Trends Cell Biol 1998, 8, 84-87.

(113)   Deshayes, S.; Morris, M.; Heitz, F.; Divita, G. Adv Drug Deliv Rev 2008, 60, 537-547.

(114)   Lindgren, M.; Hallbrink, M.; Elmquist, A.; Soomets, U.; Gallet, X.; Brasseur, R.; Zorko, M.; Langel, U. Eur J Neurosci 2000, 12, 48-48.

(115)   Crombez, L.; Morris, M. C.; Deshayes, S.; Heitz, F.; Divita, G. Curr Pharm Des 2008, 14, 3656-3665.

(116)   Madani, F.; Lindberg, S.; Langel, U.; Futaki, S.; Graslund, A. J Biophys 2011, 2011, 414729.

(117)   Ziegler, A. Adv Drug Deliv Rev 2008, 60, 580-597.

(118)   Wolff, J. A.; Malone, R. W.; Williams, P.; Chong, W.; Acsadi, G.; Jani, A.; Felgner, P. L. Science 1990, 247, 1465-1468.

(119)   Copolovici, D. M.; Langel, K.; Eriste, E.; Langel, U. ACS Nano 2014, 8, 1972-1994.

(120)   Fillon, Y. A.; Anderson, J. P.; Chmielewski, J. J Am Chem Soc 2005, 127, 11798-11803.

(121)   Rothbard, J. B.; Kreider, E.; Vandeusen, C. L.; Wright, L.; Wylie, B. L.; Wender, P. A. J Med Chem 2002, 45, 3612-3618.

(122)   Umezawa, N.; Gelman, M. A.; Haigis, M. C.; Raines, R. T.; Gellman, S. H. J Am Chem Soc 2002, 124, 368-369.

(123)   Wender, P. A.; Galliher, W. C.; Goun, E. A.; Jones, L. R.; Pillow, T. H. Adv Drug Deliv Rev 2008, 60, 452-472.

(124)   Wender, P. A.; Kreider, E.; Pelkey, E. T.; Rothbard, J.; Vandeusen, C. L. Org Lett 2005, 7, 4815-4818.

(125)   Wender, P. A.; Rothbard, J. B.; Jessop, T. C.; Kreider, E. L.; Wylie, B. L. J Am Chem Soc 2002, 124, 13382-13383.

(126)   Zhou, P.; Wang, M.; Du, L.; Fisher, G. W.; Waggoner, A.; Ly, D. H. J Am Chem Soc 2003, 125, 6878-6879.

(127)   Futaki, S.; Nakase, I.; Suzuki, T.; Youjun, Z.; Sugiura, Y. Biochemistry 2002, 41, 7925-7930.

(128)   Tezgel, A. O.; Telfer, J. C.; Tew, G. N. Biomacromolecules 2011, 12, 3078-3083.

(129)   Baker, T. J.; Luedtke, N. W.; Tor, Y.; Goodman, M. J Org Chem 2000, 65, 9054-9058.

(130)   Chung, H. H.; Harms, G.; Seong, C. M.; Choi, B. H.; Min, C.; Taulane, J. P.; Goodman, M. Biopolymers 2004, 76, 83-96.

(131)   Huang, K.; Voss, B.; Kumar, D.; Hamm, H. E.; Harth, E. Bioconjug Chem 2007, 18, 403-409.

(132)   Luedtke, N. W.; Baker, T. J.; Goodman, M.; Tor, Y. J Am Chem Soc 2000, 122, 12035-12036.

(133)   Luedtke, N. W.; Carmichael, P.; Tor, Y. J Am Chem Soc 2003, 125, 12374-12375.

(134)   Moazed, D.; Noller, H. F. Nature 1987, 327, 389-394.

(135)   Maiti, K. K.; Jeon, O. Y.; Lee, W. S.; Chung, S. K. Chemistry 2007, 13, 762-775.

(136)   Maiti, K. K.; Jeon, O. Y.; Lee, W. S.; Kim, D. C.; Kim, K. T.; Takeuchi, T.; Futaki, S.; Chung, S. K. Angew Chem Int Ed Engl 2006, 45, 2907-2912.

(137)   Maiti, K. K.; Lee, W. S.; Takeuchi, T.; Watkins, C.; Fretz, M.; Kim, D. C.; Futaki, S.; Jones, A.; Kim, K. T.; Chung, S. K. Angew Chem Int Ed Engl 2007, 46, 5880-5884.

(138)   Bielawski, C. W.; Benitez, D.; Grubbs, R. H. J Am Chem Soc 2003, 125, 8424-8425.

(139)   Bielawski, C. W.; Grubbs, R. H. Angew Chem Int Ed Engl 2000, 39, 2903-2906.

(140)   Bielawski, C. W.; Grubbs, R. H. Prog. Polym. Sci. 2007, 32, 1-29.

(141)   Cannizzo, L. F.; Grubbs, R. H. Macromolecules, 21, 1961-1967.

(142)   Love, J. A.; Morgan, J. P.; Trnka, T. M.; Grubbs, R. H. Angew Chem Int Ed Engl 2002, 41, 4035-4037.

(143)   Schrock, R. R.; Hoveyda, A. H. Angew Chem Int Ed Engl 2003, 42, 4592-4633.

(144)   Schwab, P.; France, M. B.; Ziller, J. W.; Grubbs, R. H. Angew Chem Int Ed Engl 1995, 34, 2039-2041.

(145)   Singh, R.; Czekelius, C.; Schrock, R. R. Macromolecules 2006, 39, 1316-1317.

(146)   Trnka, T. M.; Grubbs, R. H. Acc Chem Res 2001, 34, 18-29.

(147)   Kolonko, E. M.; Kiessling, L. L. J Am Chem Soc 2008, 130, 5626-+.

(148)   Kolonko, E. M.; Pontrello, J. K.; Mangold, S. L.; Kiessling, L. L. J Am Chem Soc 2009, 131, 7327-7333.

(149)   Gabriel, G. J.; Madkour, A. E.; Dabkowski, J. M.; Nelson, C. F.; Nusslein, K.; Tew, G. N. Biomacromolecules 2008, 9, 2980-2983.

(150)   Hennig, A.; Gabriel, G. J.; Tew, G. N.; Matile, S. J Am Chem Soc 2008, 130, 10338-10344.

(151)   Som, A.; Tezgel, A. O.; Gabriel, G. J.; Tew, G. N. Angew Chem Int Ed Engl 2011, 50, 6147-6150.

(152)   Som, A.; Reuter, A.; Tew, G. N. Angew Chem Int Ed Engl 2012, 51, 980-983.

(153)   de Planque, M. R.; Bonev, B. B.; Demmers, J. A.; Greathouse, D. V.; Koeppe, R. E., 2nd; Separovic, F.; Watts, A.; Killian, J. A. Biochemistry 2003, 42, 5341-5348.

(154)   Yau, W. M.; Wimley, W. C.; Gawrisch, K.; White, S. H. Biochemistry 1998, 37, 14713-14718.

(155)   White, S. H.; Wimley, W. C. Annu Rev Biophys Biomol Struct 1999, 28, 319-365.

(156)   deRonde, B. M.; Birke, A.; Tew, G. N. Chem Eur J 2015, 21, 3013-3019.

(157)   Tezgel, A. O.; Gonzalez-Perez, G.; Telfer, J. C.; Osborne, B. A.; Minter, L. M.; Tew, G. N. Mol Ther 2013, 21, 201-209.

(158)   Sgolastra, F.; Minter, L. M.; Osborne, B. A.; Tew, G. N. Biomacromolecules 2014, 15, 812-820.

(159)   Geihe, E. I.; Cooley, C. B.; Simon, J. R.; Kiesewetter, M. K.; Edward, J. A.; Hickerson, R. P.; Kaspar, R. L.; Hedrick, J. L.; Waymouth, R. M.; Wender, P. A. Proc Natl Acad Sci U S A 2012, 109, 13171-13176.

(160)	Treat, N. J.; Smith, D.; Teng, C.; Flores, J. D.; Abel, B. A.; York, A. W.; Huang, F.; McCormick, C. L. ACS Macro Lett 2012, 1, 100-104.

(161)	Tezgel, A. O.; Jacobs, P.; Telfer, J. C.; Tew, G. N. Submitted 2015.

(162)	Strong, L. E.; Kiessling, L. L. J Am Chem Soc 1999, 121, 6193-6196.

(163)	Fishman, J. M.; Kiessling, L. L. Angew Chem Int Ed Engl 2013, 52, 5061-5064.

(164)	Smith, D.; Pentzer, E. B.; Nguyen, S. T. Polym Rev 2007, 47, 419-459.

(165)	Shoichet, M. S. Macromolecules 2010, 43, 581-591.

(166)	Liechty, W. B.; Kryscio, D. R.; Slaughter, B. V.; Peppas, N. A. Annu Rev Chem Biomol 2010, 1, 149-173.

(167)	Tabujew, I.; Freidel, C.; Krieg, B.; Helm, M.; Koynov, K.; Mullen, K.; Peneva, K. Macromol Rapid Commun 2014, 35, 1191-1197.

(168)	Cooley, C. B.; Trantow, B. M.; Nederberg, F.; Kiesewetter, M. K.; Hedrick, J. L.; Waymouth, R. M.; Wender, P. A. J Am Chem Soc 2009, 131, 16401-16403.

(169)	Wender, P. A.; Huttner, M. A.; Staveness, D.; Vargas, J. R.; Xu, A. F. Mol Pharm 2015, 12, 742-750.

(170)	Bang, E. K.; Lista, M.; Sforazzini, G.; Sakai, N.; Matile, S. Chem Sci 2012, 3, 1752-1763.

(171)	Hartmann, L.; Hafele, S.; Peschka-Suss, R.; Antonietti, M.; Borner, H. G. Macromolecules 2007, 40, 7771-7776.

(172)	Hartmann, L.; Krause, E.; Antonietti, M.; Borner, H. G. Biomacromolecules 2006, 7, 1239-1244.

(173)	Lin, C.; Blaauboer, C. J.; Timoneda, M. M.; Lok, M. C.; van Steenbergen, M.; Hennink, W. E.; Zhong, Z.; Feijen, J.; Engbersen, J. F. J Control Release 2008, 126, 166-174.

(174)	Lin, C.; Zhong, Z.; Lok, M. C.; Jiang, X.; Hennink, W. E.; Feijen, J.; Engbersen, J. F. J Control Release 2007, 123, 67-75.

(175)	Lin, C.; Zhong, Z.; Lok, M. C.; Jiang, X.; Hennink, W. E.; Feijen, J.; Engbersen, J. F. Bioconjug Chem 2007, 18, 138-145.

(176)	Kim, S. H.; Jeong, J. H.; Ou, M.; Yockman, J. W.; Kim, S. W.; Bull, D. A. Biomaterials 2008, 29, 4439-4446.

(177)	Kim, T. I.; Kim, S. W. React Funct Polym 2011, 71, 344-349.

(178)	Ou, M.; Wang, X. L.; Xu, R.; Chang, C. W.; Bull, D. A.; Kim, S. W. Bioconjug Chem 2008, 19, 626-633.

(179)	Kim, S. H.; Jeong, J. H.; Kim, T. I.; Kim, S. W.; Bull, D. A. Mol Pharm 2009, 6, 718-726.

(180)	Kim, T. I.; Lee, M.; Kim, S. W. Biomaterials 2010, 31, 1798-1804.

(181)	Kim, T. I.; Ou, M.; Lee, M.; Kim, S. W. Biomaterials 2009, 30, 658-664.

(182)	Ou, M.; Kim, T. I.; Yockman, J. W.; Borden, B. A.; Bull, D. A.; Kim, S. W. J Control Release 2010, 142, 61-69.

(183)	Bang, E. K.; Gasparini, G.; Molinard, G.; Roux, A.; Sakai, N.; Matile, S. J Am Chem Soc 2013, 135, 2088-2091.

(184)	Gasparini, G.; Bang, E. K.; Molinard, G.; Tulumello, D. V.; Ward, S.; Kelley, S. O.; Roux, A.; Sakai, N.; Matile, S. J Am Chem Soc 2014, 136, 6069-6074.

(185)	Almeida, P. F.; Pokorny, A. Biochemistry 2009, 48, 8083-8093.

(186)	Almeida, P. F.; Pokorny, A. Methods Mol Biol 2010, 618, 155-169.

(187)	Katayama, S.; Hirose, H.; Takayama, K.; Nakase, I.; Futaki, S. J Control Release 2011, 149, 29-35.

(188)	Sakai, N.; Matile, S. J Am Chem Soc 2003, 125, 14348-14356.

(189)	Sakai, N.; Takeuchi, T.; Futaki, S.; Matile, S. Chembiochem 2005, 6, 114-122.

(190)   Takeuchi, T.; Kosuge, M.; Tadokoro, A.; Sugiura, Y.; Nishi, M.; Kawata, M.; Sakai, N.; Matile, S.; Futaki, S. ACS Chem Biol 2006, 1, 299-303.

(191)   Pae, J.; Saalik, P.; Liivamagi, L.; Lubenets, D.; Arukuusk, P.; Langel, U.; Pooga, M. J Control Release 2014, 192, 103-113.

(192)   Lundberg, M.; Wikstrom, S.; Johansson, M. Mol Ther 2003, 8, 143-150.

(193)   Richard, J. P.; Melikov, K.; Vives, E.; Ramos, C.; Verbeure, B.; Gait, M. J.; Chernomordik, L. V.; Lebleu, B. J Biol Chem 2003, 278, 585-590.

(194)   Trabulo, S.; Cardoso, A. L.; Mano, M.; Pedroso de Lima, M. Pharmaceuticals 2010, 3, 961-993.

(195)   Ivanov, A. I. Methods Mol Biol 2008, 440, 15-33.

(196)   Ivanov, A. I. Methods Mol Biol 2014, 1174, 3-18.

(197)   Vercauteren, D.; Vandenbroucke, R. E.; Jones, A. T.; Rejman, J.; Demeester, J.; De Smedt, S. C.; Sanders, N. N.; Braeckmans, K. Mol Ther 2010, 18, 561-569.

(198)   Maiolo, J. R.; Ferrer, M.; Ottinger, E. A. Biochim Biophys Acta 2005, 1712, 161-172.

(199)   Manceur, A.; Wu, A.; Audet, J. Anal Biochem 2007, 364, 51-59.

(200)   Silverstein, S. C.; Steinman, R. M.; Cohn, Z. A. Annu Rev Biochem 1977, 46, 669-722.

(201)   Schmid, S. L.; Carter, L. L. J Cell Biol 1990, 111, 2307-2318.

(202)   Wymann, M. P.; Bulgarelli-Leva, G.; Zvelebil, M. J.; Pirola, L.; Vanhaesebroeck, B.; Waterfield, M. D.; Panayotou, G. Mol Cell Biol 1996, 16, 1722-1733.

(203)   Ohkuma, S.; Poole, B. Proc Natl Acad Sci U S A 1978, 75, 3327-3331.

(204)   Wibo, M.; Poole, B. J Cell Biol 1974, 63, 430-440.

(205)   Samson, F.; Donoso, J. A.; Heller-Bettinger, I.; Watson, D.; Himes, R. H. J Pharmacol Exp Ther 1979, 208, 411-417.

(206)   Vasquez, R. J.; Howell, B.; Yvon, A. M.; Wadsworth, P.; Cassimeris, L. Mol Biol Cell 1997, 8, 973-985.

(207)   Wang, L. H.; Rothberg, K. G.; Anderson, R. G. J Cell Biol 1993, 123, 1107-1117.

(208)   Macia, E.; Ehrlich, M.; Massol, R.; Boucrot, E.; Brunner, C.; Kirchhausen, T. Dev Cell 2006, 10, 839-850.

(209)   Rodal, S. K.; Skretting, G.; Garred, O.; Vilhardt, F.; van Deurs, B.; Sandvig, K. Mol Biol Cell 1999, 10, 961-974.

(210)   Sandgren, S.; Cheng, F.; Belting, M. J Biol Chem 2002, 277, 38877-38883.

(211)   Schmidt, N. W.; Lis, M.; Zhao, K.; Lai, G. H.; Alexandrova, A. N.; Tew, G. N.; Wong, G. C. J Am Chem Soc 2012, 134, 19207-19216.

(212)   Sieczkarski, S. B.; Whittaker, G. R. J Gen Virol 2002, 83, 1535-1545.

(213)   Perret, F.; Nishihara, M.; Takeuchi, T.; Futaki, S.; Lazar, A. N.; Coleman, A. W.; Sakai, N.; Matile, S. J Am Chem Soc 2005, 127, 1114-1115.

(214)   Sakai, N.; Futaki, S.; Matile, S. Soft Matter 2006, 2, 636-641.

(215)   Lorenzer, C.; Dirin, M.; Winkler, A. M.; Baumann, V.; Winkler, J. J Control Release 2015, 203, 1-15.

(216)   Freeley, M.; Long, A. Biochem J 2013, 455, 133-147.

(217)   Gehl, J. Acta Physiol Scand 2003, 177, 437-447.

(218)   Freeley, M.; Long, A. J Immunol Methods 2013, 396, 116-127.

(219)   McManus, M. T.; Haines, B. B.; Dillon, C. P.; Whitehurst, C. E.; van Parijs, L.; Chen, J.; Sharp, P. A. J Immunol 2002, 169, 5754-5760.

(220)   .

(221)   Felgner, P. L.; Gadek, T. R.; Holm, M.; Roman, R.; Chan, H. W.; Wenz, M.; Northrop, J. P.; Ringold, G. M.; Danielsen, M. Proc Natl Acad Sci U S A 1987, 84, 7413-7417.

(222)   Dalby, B.; Cates, S.; Harris, A.; Ohki, E. C.; Tilkins, M. L.; Price, P. J.; Ciccarone, V. C. Methods 2004, 33, 95-103.

(223)   Iczkowski, K. A.; Omara-Opyene, A. L.; Klosel, R. Mol Biotechnol 2004, 28, 97-103.

(224)   deRonde, B. M.; Torres, J. A.; Minter, L. M.; Tew, G. N. Biomacromolecules 2015, 16, 3172–3179.

(225)   Goffinet, C.; Keppler, O. T. Faseb Journal 2006, 20, 500-+.

(226)   Marodon, G.; Mouly, E.; Blair, E. J.; Frisen, C.; Lemoine, F. M.; Klatzmann, D. Blood 2003, 101, 3416-3423.

(227)   Zhang, Y. F.; Lu, H. Z.; LiWang, P.; Sili, U.; Templeton, N. S. Mol Ther 2003, 8, 629-636.

(228)   Becker-Hapak, M.; McAllister, S. S.; Dowdy, S. F. Methods 2001, 24, 247-256.

(229)   Gait, M. J. Cell Mol Life Sci 2003, 60, 844-853.

(230)   Juliano, R.; Alam, M. R.; Dixit, V.; Kang, H. Nucleic Acids Res 2008, 36, 4158-4171.

(231)   Moulton, H. M.; Moulton, J. D. Drug Discov Today 2004, 9, 870.

(232)   Zatsepin, T. S.; Turner, J. J.; Oretskaya, T. S.; Gait, M. J. Curr Pharm Des 2005, 11, 3639-3654.

(233)   deRonde, B. M.; Tew, G. N. Biopolymers 2015, 104, 265-280.

(234)   Scholz, C.; Wagner, E. *J Control Rel* 2012, **161**, 554-565.

(235)   Fire, A.; Xu, S.; Montgomery, M. K.; Kostas, S. A.; Driver, S. E.; Mello, C. C. *Nature* 1998, **391**, 806-811.

(236)   Kim, J.; Lee, S. H.; Choe, J.; Park, T. G. *J Gene Med* 2009, **11**, 804-812.

(237)   Mello, C. C.; Conte, D. *Nature* 2004, **431**, 338-342.

(238)   Vicentini, F. T. M. D.; Borgheti-Cardoso, L. N.; Depieri, L. V.; Mano, D. D.; Abelha, T. F.; Petrilli, R.; Bentley, M. V. L. B. *Pharm Res* 2013, **30**, 915-931.

(239)   Whitehead, K. A.; Langer, R.; Anderson, D. G. *Nat Rev Drug Discov* 2009, **8**, 129-138.

(240)   Carthew, R. W. *Curr Opin Cell Biol* 2001, **13**, 244-248.

(241)   Elbashir, S. M.; Harborth, J.; Lendeckel, W.; Yalcin, A.; Weber, K.; Tuschl, T. *Nature* 2001, **411**, 494-498.

(242)   Meister, G.; Tuschl, T. *Nature* 2004, **431**, 343-349.

(243)   Hammond, S. M.; Bernstein, E.; Beach, D.; Hannon, G. J. *Nature* 2000, **404**, 293-296.

(244)   Fedorov, Y.; Anderson, E. M.; Birmingham, A.; Reynolds, A.; Karpilow, J.; Robinson, K.; Leake, D.; Marshall, W. S.; Khvorova, A. *RNA* 2006, **12**, 1188-1196.

(245)   Jackson, A. L.; Burchard, J.; Schelter, J.; Chau, B. N.; Cleary, M.; Lim, L.; Linsley, P. S. *RNA* 2006, **12**, 1179-1187.

(246)   Jackson, A. L.; Linsley, P. S. *Nat Rev Drug Discov* 2010, **9**, 57-67.

(247)   Persengiev, S. P.; Zhu, X.; Green, M. R. *RNA* 2004, **10**, 12-18.

(248)   Semizarov, D.; Frost, L.; Sarthy, A.; Kroeger, P.; Halbert, D. N.; Fesik, S. W. *Proc. Natl. Acad. Sci. U. S. A.* 2003, **100**, 6347-6352.

(249)   Mantei, A.; Rutz, S.; Janke, M.; Kirchhoff, D.; Jung, U.; Patzel, V.; Vogel, U.; Rudel, T.; Andreou, I.; Weber, M.; Scheffold, A. *Eur J Immunol* 2008, **38**, 2616-262.

CHAPTER 2

**DESIGN OF AROMATIC-CONTAINING CELL-PENETRATING PEPTIDE
MIMICS WITH STRUCTURALLY MODIFIED π-ELECTRONICS**

2.1 Introduction

Cell-penetrating peptides (CPPs) and their synthetic mimics (CPPMs) represent a

unique class of molecules that is capable of crossing biological membranes.[1-10] The

peptides are generally short, cationic sequences rich in arginine and/or lysine residues,

with some containing hydrophobic residues such as leucine, phenylalanine, or

tryptophan.[2,7,9,10] They derive inspiration from proteins with translocation abilities, such

as HIV-1 Tat and Antennapedia Homeodomain protein.[11-13] It has been shown that the

cation-rich domains of these proteins, referred to as protein transduction domains

(PTDs), are primarily responsible for their uptake abilities.[11,14-16] Many studies have

highlighted the ability of CPP(M)s to facilitate the intracellular delivery of various cargo,

including, but not limited to, small molecules, siRNA, pDNA, and proteins *via* covalent or

non-covalent interactions.[2,3,5,7-10,17-22] Although their mechanism of uptake is debated in

the literature, various forms of endocytosis, macropinocytosis, protein-dependent

translocation, and energy-independent translocation are involved in the internalization

process.[23-28]

In efforts to elucidate the mechanisms of CPP(M) uptake and assess the

structural components of CPP(M)s necessary for uptake, model vesicle membrane

studies have frequently been used.[29-33] Vesicle experiments represent a simpler system

for evaluating energy-independent methods of transduction than using cells, where it is

difficult to decouple various methods of cellular uptake. Previously, Matile and

coworkers have used model vesicle systems to show that polyarginine, a widely used

CPP, requires hydrophobic counterions to efficiently cross lipid membranes.[30,34-37] For

these studies, lipids were swollen in a solution of carboxyfluorescein, which is a hydrophilic, anionic dye that self-quenches at high concentrations, and dye release was monitored as a function of peptide concentration. Changes in peptide activity were assessed by calculating the effective concentrations to release 50% of the dye (EC_{50}). Similar assays were also been used by Almeida and coworkers to explore CPP internalization mechanisms.[38,39] The hydrophobic counterions selected for Matile and coworkers' studies were said to help mask the overall cationic charge of the peptides to aid in transduction, a process referred to as activation.[30,34-37] Although these studies showed that bulky aromatic activators, such as pyrene butyrate, outperformed aliphatic activators, the roles of hydrophobicity and aromaticity were not fully understood.

Motivated by these studies, our lab previously developed a series of oxanorbornene imide-based CPPMs to assess the effect of hydrophobicity on CPPM activity.[32,33] Instead of using external activators, the hydrophobic components were chemically incorporated into the polymeric structures to yield self-activating polymers.[32,33] These polymers were correctly predicted to outperform their counterparts that only contained cationic residues.[29,32,33] Initially, various aliphatic chains were incorporated into the CPPMs to assess the effect of chain length on activity.[33] These results were evaluated by assessing differences in reported EC_{50} values from vesicle dye release assays.[35] Although polymer activity improved by increasing the alkyl chain lengths from one carbon to four carbons, longer alkyl chains were less water soluble and thus led to poorer performance.[33]

Another series of polymers was designed to evaluate the impact of various aromatic, cyclic non-aromatic, and alkyl hydrophobic moieties of similar hydrophobicity on polymer activity.[32] This was done to gain a better understanding of the interplay between hydrophobicity and aromaticity. Aromaticity was the cornerstone of that report because of the significant role it plays in protein-membrane interactions. The aromatic

amino acids tyrosine and tryptophan are present as part of aromatic belts that flank either end of transmembrane proteins.[40,41] These residues sit at the interface between the hydrophobic core of the proteins and the more hydrophilic external environment to enhance stability at those regions.[40,41] Although not typically present in aromatic belts, phenylalanine has also been shown to aid in anchoring proteins in the membrane.[42,43] All three of these aromatic amino acids have been shown to provide favorable energies of insertion into membranes.[42,43] It was further reasoned that aromatic moieties are ideal for incorporation into CPPMs because such residues are found in many CPPs such as Penetratin, Pep-1, and MPG and have been shown in some cases to be critical for uptake.[5,44-47] Experiments in which aromatic residues in Tat and Penetratin were replaced with non-aromatic hydrophobic residues led to a reduction in cellular interalization efficiencies.[5,44-47]

Using HPLC retention times to assess relative hydrophobicity of the polymer side chains[48,49], these values were compared to the polymer EC_{50} values to illustrate that the effects of hydrophobicity and aromaticity could be distinguished. Through these studies, it was suggested that aromatic hydrophobic moieties were superior activators.[32] Similar results were obtained by Matile and coworkers when they monitored dye release of polyarginine with various external activators.[37]

Given these observations and the different electronic properties of tyrosine, phenylalanine, and tryptophan (Figure 2.1) the role of aromaticity in CPP(M) activity was studied by exploring the effect that changes in quadrupole moments have on these systems.
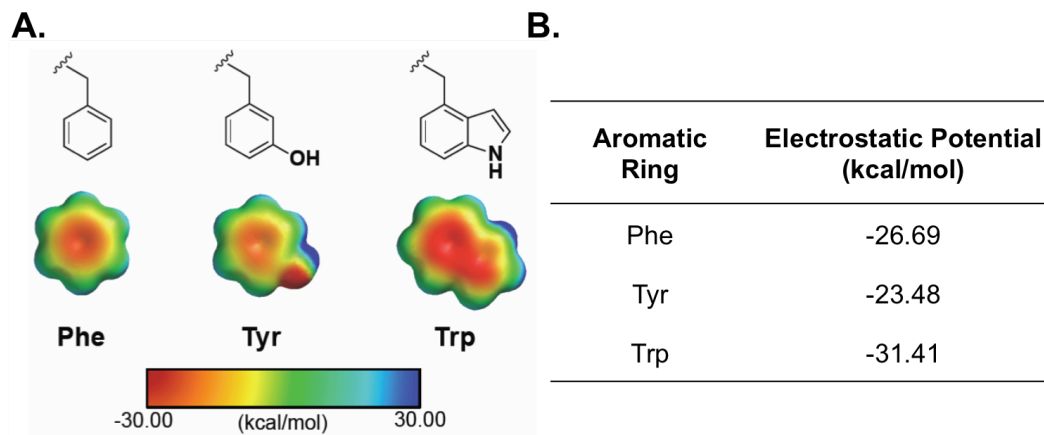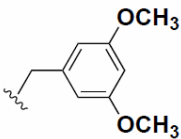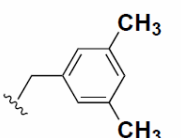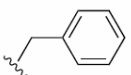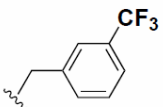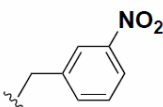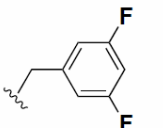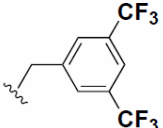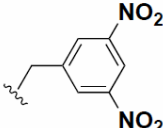
Figure 2.1. Electrostatic potential maps and values for modeled aromatic rings in amino acids phenylalanine, tyrosine, and tryptophan. A) Electrostatic potential. The range for electrostatic potential was set between -30.00 and 30.00 kcal/mol. The color scale bar reflects this range with red representing electron-rich surfaces and blue representing electron-poor surfaces. All surfaces were calculated at the HF level using the 3-21G* basis set. B) Electrostatic potential values in kcal/mol taken from the center of the aromatic ring system.

The flat, planar structures of these aromatic rings and their associated quadrupole moments are thought to enable various π-interactions, such as π-π, π-cation, π-anion, and π-polar interactions within the cellular environment that can aid in membrane interactions.[42,50-55] Since the quadrupole moment collects the electron density on the face of these planar, aromatic rings, it was hypothesized that by strengthening or weakening this phenomenon, the corresponding π-membrane interactions would provide additional handles for tuning of CPPM activity. Specifically, this was attempted by incorporating electron donating and electron withdrawing groups into the aromatic systems as a way to alter the electron density of the ring system. Although nature offers an electrostatic potential range for its aromatic amino acids between -31.41 kcal/mol (Trp) and -23.48 (Tyr) kcal/mol, by using synthetic systems, it was possible to examine a much wider electrostatic potential window of -29.69 kcal/mol (Figure 2.2, **R**= b = CH_3) to +15.57 kcal/mol (Figure 2.4, **R'**= c = NO_2). All values are summarized in Table 2.1.

Table 2.1. Summary of electrostatic potential values for modeled aromatic rings incorporated into CPPM starting materials and polymers

Aromatic Ring	Electrostatic Potential (kcal/mol)
a =	-18.10
b =	-29.69
c =	-26.69
d =	-13.15
e =	-4.66
f =	-5.99
g =	0.37
h =	15.57

As part of this study, π-rich and π-poor CPPMs were designed and synthesized based on both the diester and imide ROMP scaffolds. CPPMs based on the diester system were synthesized since the dual-functional monomers offer greater potential for polymeric structure variations. Also, CPPMs based on the imide scaffold were synthesized as a direct comparison to polymers from previous hydrophobicity structure activity relationships (SARs) with model membranes.[32,33] These CPPMs were designed to contain π-rich and π-poor aromatic functionalities in order to assess the role of π-interactions in tuning membrane activity.

2.2   Monomer Synthesis

Diester monomers were synthesized using a two-step process, as depicted in Figure 2.2.1.   These procedures were adapted from previously described methods with modifications.[17,56] In brief, oxanorbornene anhydride (**1**) was ring-opened using various aromatic alcohols (**a-h**) and DMAP to yield the half-ester intermediates.
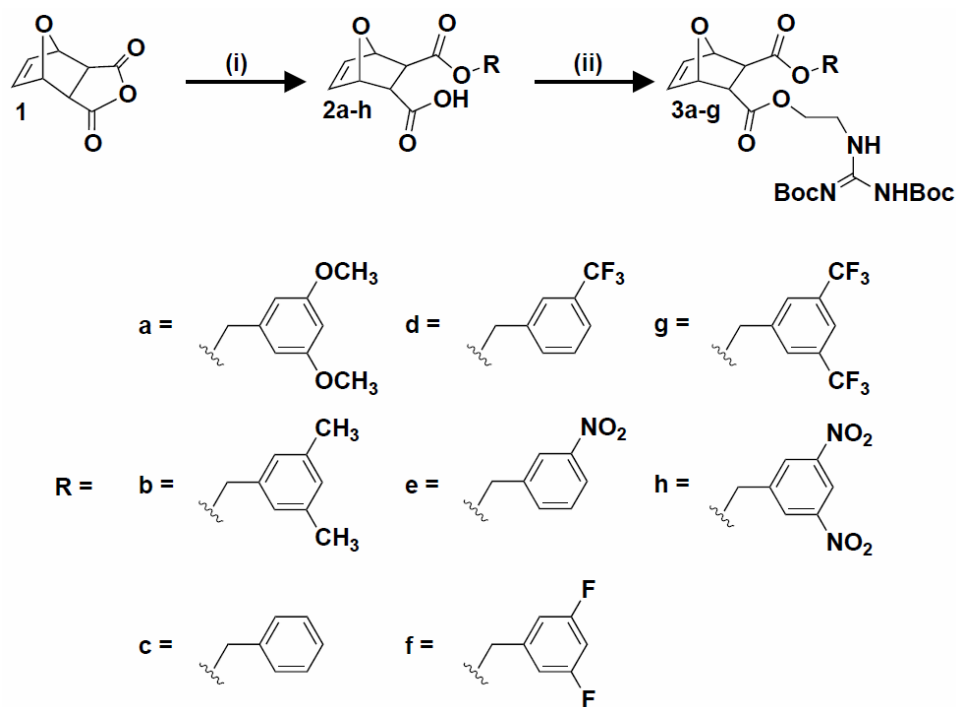
Figure 2.2 Synthesis of diester monomers containing π-rich and π-poor aromatic rings. i)R-OH, DMAP, CH₂Cl₂,, RT, overnight; ii) 1,3-di-boc-2-(2-hydroxyethyl)guanidine, EDC, DMAP, CH₂Cl₂, 0°C to RT, overnight.

Half-esters **2a-f** were then further reacted with 1,3-di-boc-2-(2-hydroxyethyl)guanidine using EDC coupling conditions to yield monomers **3a-f**. Half-esters **2g-h** were not used for monomer synthesis because they proved to be unstable in solution at room temperature. As shown in Figure 2.3**A**, half-esters **2g-h** underwent a spontaneous retro-Diels-Alder reaction to yield **4g-h** and furan (**5**). This was demonstrated by isolating the retro-Diels-Alder product, **4g**, using column chromatography and verifying its chemical composition using ^{1}H NMR, ^{13}C NMR, and mass spectrometry (MS). Retro-Diels-Alder product **4h** proved more difficult to isolate because of additional nitro-based impurities.

However, peaks for the retro-Diels-Alder product were observed in the ^{1}H NMR of **2h**. Since **2a-f** did not appear to undergo the retro-Diels-Alder reaction, it was hypothesized

that this reaction was affected by the electron withdrawing substituents attached to the aromatic rings. To investigate this, all π-poor aromatic rings were modeled using Spartan molecular modeling software as shown in Figure 2.3**A**. The most electron poor (most blue in color) aromatic rings were the rings associated with the unstable half esters. From this and a study by Nanjappan and Czarnik, it was concluded that electron-withdrawing groups destabilized Diels-Alder adducts and accelerated the retro-Diels-Alder reaction.[57]
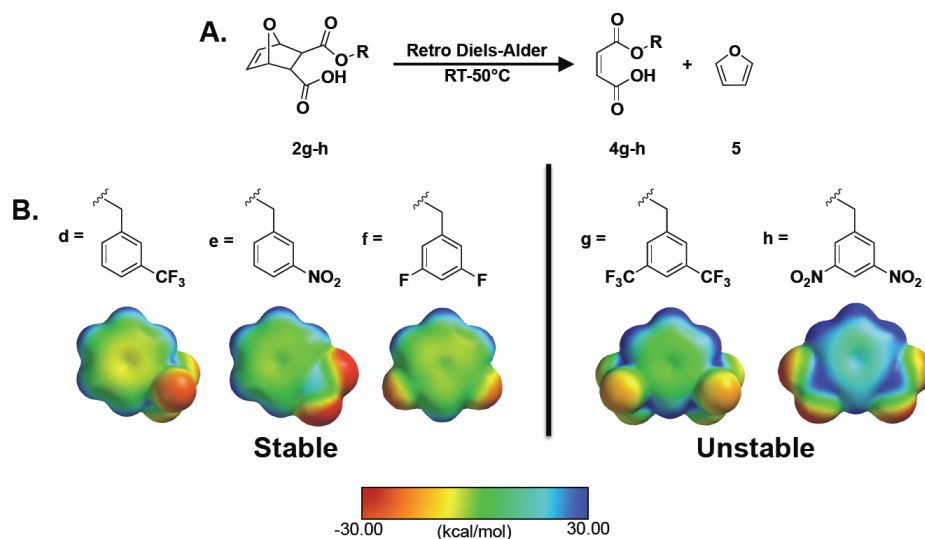
Figure 2.3. Stability of π-poor monomers. A) Retro-Diels-Alder reaction that occurs for monomers **4g-h**. B) Stable and unstable π-poor monomer aromatic groups with their corresponding electrostatic potential maps. The range for electrostatic potential was set between -30.00 and 30.00 kcal/mol. The color scale bar reflects this range with red representing electron rich surfaces and blue representing electron poor surfaces. Surfaces were calculated at the HF level using the 3-21G* basis set.

2g-h were not pursued for monomer formation because the retro-Diels-Alder impurities **4g-h** have the same reactive functional groups (-COOH, C=C) as **2a-f**. All stable half-esters and monomers were characterized by ^{1}H NMR, ^{13}C NMR, and MS. In terms of electrostatic potential values, the six stable monomers covered an electrostatic potential range from -4.66 kcal/mol (**Scheme 1**, **R**= e= NO_2) to +29.69 kcal/mol (**Scheme 1,** R=

b= CH₃).   Electrostatic potential values are summarized in Table 2.1.   All

characterization data is provided in the supporting information.
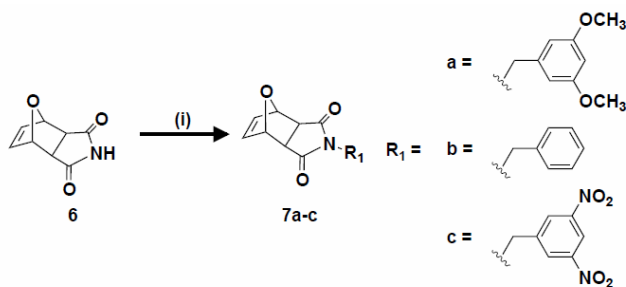
Figure 2.4 Synthesis of imide monomers containing π-rich and π-poor aromatic rings. i) R_1-OH, PPh₃, DIAD, THF, RT, 18 hr.

Imide monomers were synthesized using a one-step process adapted from Som

et al., as illustrated in Figure 2.4.[32,33]   Unlike the diester system, there were no issues

with stability for the imide system and no retro-Diels-Alder products were observed.   All

monomers were characterized by ^{1}H NMR, ^{13}C NMR, and MS.   In terms of electrostatic

potential values for the aromatic groups incorporated, all stable monomers covered an

electrostatic potential range from -18.10 kcal/mol (Figure 2.4, R_1 = a = OCH₃) to 15.57

kcal/mol (Figure 2.4, R_1 = c = NO₂).   These monomers expand the negative end of the

electrostatic potential range so that in total the monomer design spans -29.69 to +15.57

kcal/mol as summarized in Table 2.1.

2.3   Polymer Synthesis

Polymers were synthesized using ROMP with Grubbs 3rd generation catalyst, as

illustrated in Figure 2.5, Figure 2.6, and Figure 2.7.
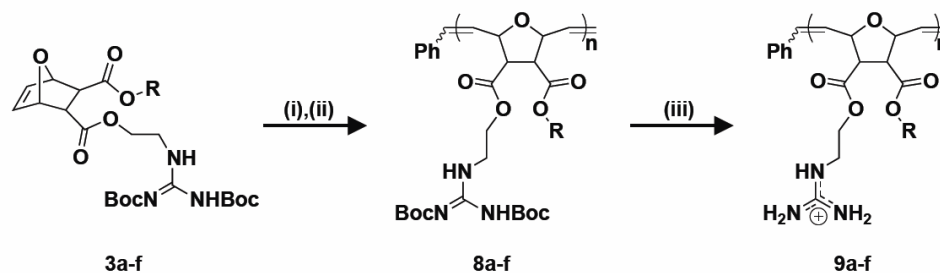
Figure 2.5 Synthesis of diester homopolymers containing π-rich and π-poor aromatic rings. i) Dichloro-di(3-bromopyridino)-*N,N'*-Dimesitylenoimidazolino-Ru=CHPh (G3) catalyst, CH$_2$Cl$_2$, RT, 45 min; ii) Ethyl vinyl ether, RT, overnight; iii) TFA/CH$_2$Cl$_2$ (1:1), RT, overnight. Products 9a-f further purified by dialysis with molecular weight cut-off : 2,000 g/mol. All polymers were synthesized with n=20. R was defined in **Figure 2.2**.
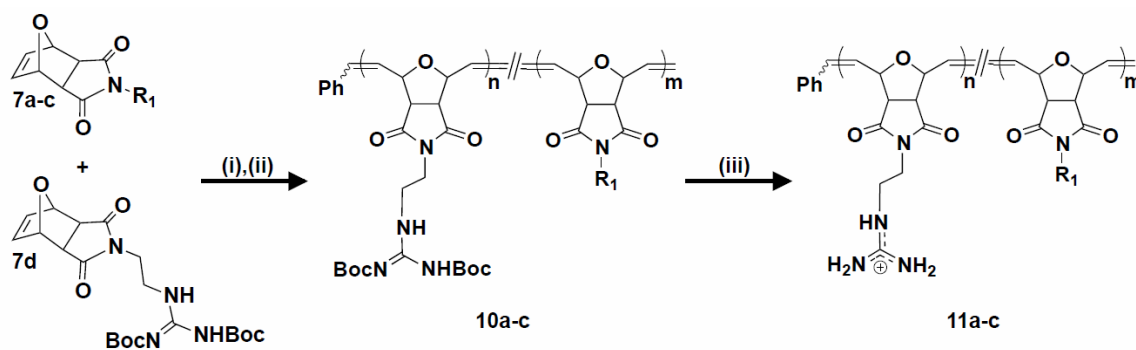
Figure 2.6. Synthesis of imide random copolymers containing π-rich and π-poor aromatic rings. i) Dichloro-di(3-bromopyridino)-*N,N'*-Dimesitylenoimidazolino- Ru=CHPh (G3) catalyst, CH$_2$Cl$_2$, RT, 45 min; ii) Ethyl vinyl ether, RT, overnight; iii) TFA/CH$_2$Cl$_2$ (1:1), RT, overnight. All polymers were synthesized with n=20 and m=20. R$_1$ was defined in **Figure 2.4**.
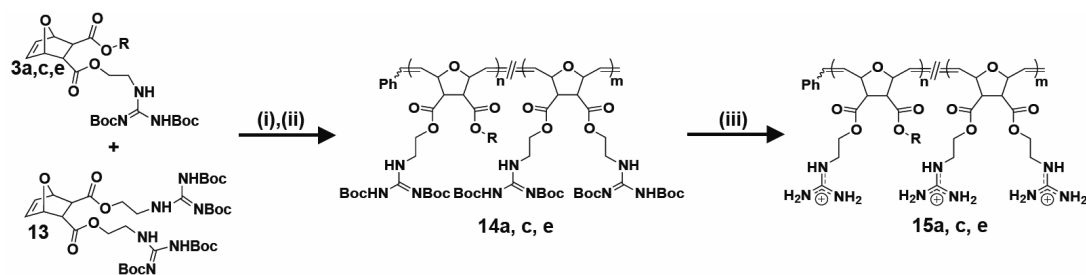
Figure 2.7. Synthesis of diester random copolymers containing π-rich and π-poor aromatic rings. i) Dichloro-di(3-bromopyridino)-*N,N'*-Dimesitylenoimidazolino- Ru=CHPh (G3) catalyst, CH_2Cl_2, RT, 45 min; ii) Ethyl vinyl ether, RT, overnight; iii) TFA/CH_2Cl_2 (1:1), RT, overnight. Products 15a,c,e further purified by dialysis with molecular weigth cut-off: 1,000 g/mol. All polymers were synthesized with n=8 and m=12. R was defined in **Figure 2.2.**

All boc-protected polymers (8a-f, 10a-c, 13a,c,e) were characterized by ^{1}H NMR to assess chemical composition and gel permeation chromatography (GPC) to assess relative molecular weights. Molecular weight data is summarized in Table 2.2 and representative chromatograms are in Figure 2.8, Figure 2.9, and Figure 2.10.

Table 2.2. Molecular weight characterization of π-rich and π-poor CPPMs.

A. Diester Homopolymers			B. Imide and Diester Random Copolymers			
CPPM	M_n[a] (Da)	Đ	CPPM	n:m	M_n[a] (Da)	Đ
8a	11,600	1.05	11a	56:44	16,200	1.06
8b	11,200	1.05	11b	55:45	13,700	1.07
8c	11,300	1.05	11c	58:42	17,000	1.06
8d	12,600	1.05	14a	38:62	10,600	1.10
8e	11,400	1.05	14b	40:60	12,100	1.08
8f	11,500	1.05	14c	39:61	10,700	1.14

[a]Number average molecular weight (M_n) and polydispersity indices (Đ=M_w/M_n) determined by GPC using polymethyl methacrylate (PMMA) standards for diester polymers and polystyrene standards for the imide polymers using tetrahydrofuran (THF) as the eluent and toluene as the flow marker. [b]Ratio of residues, where n represents the percentage of hydrophobic residues and m represents the percentage of guanidine-containing residues.
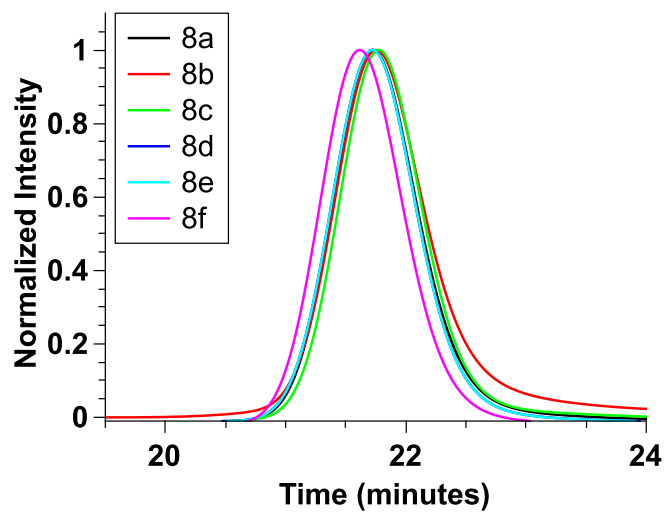
Figure 2.8. THF GPC chromatograms for boc-protected diester homopolymer CPPMs **8a-f**.
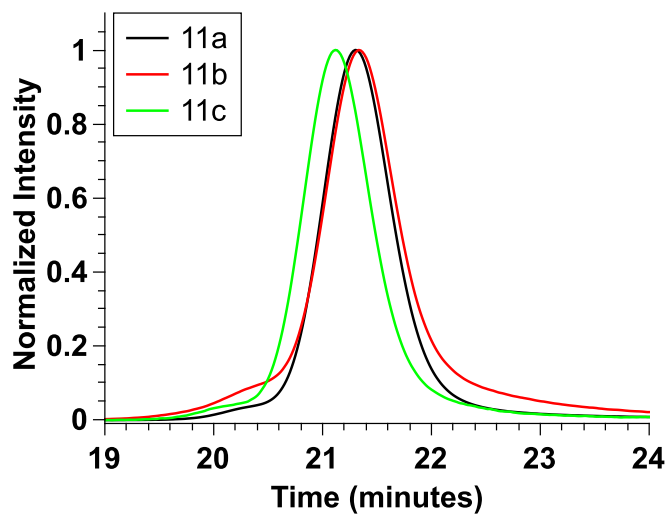
Figure 2.9. THF GPC chromatograms for boc-protected imide random copolymer CPPMs 11a-c.
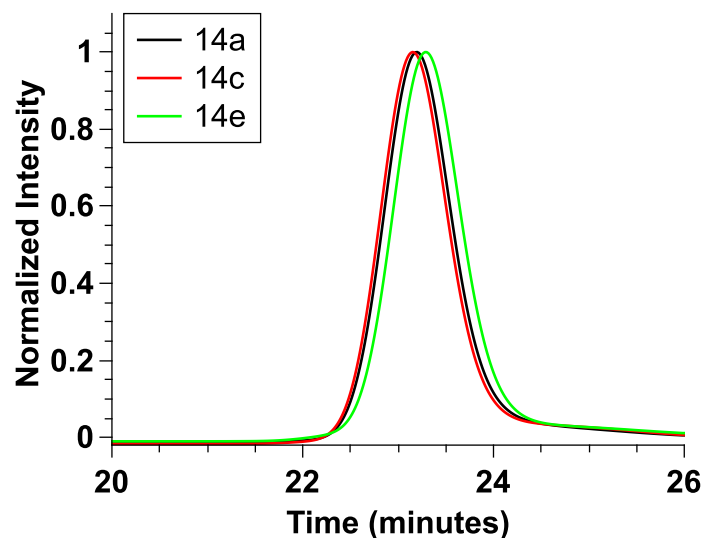
Figure 2.10. THF GPC chromatograms for boc-protected diester random copolymer CPPMs 14a, c, e.

Polymers were subsequently deprotected using trifluoroacetic acid (TFA) and CH_2Cl_2 (1:1) overnight.[17,32,33,56] TFA was removed by azeotropic distillation with methanol. Diester polymers were dialyzed for three days in water using membranes with a molecular weight cut-off of 2,000 g/mol for homopolymers and 1,000 g/mol for random copolymers. All polymers were then dissolved in water and lyophilized to yield dry **9a-f, 12a-c,** and **15a,c,e**.

2.4 Dye Release Assays

All polymers were tested using a vesicle dye release assay to assess relative polymer activity using a fluorescence plate reader.[29,31-33] This assay is summarized in cartoon form in **Figure 2.11**. This high throughput screening method enabled the testing of all samples in a 12-well plate at the same time. Carboxyfluorescein (CF) filled phosphatidylcholine (PC) or PC/phosphatidylserine (PS) vesicles were prepared as described in the supporting information and then used for these experiments.

For this dye release assay, the baseline fluorescence (F_0) of Tris saline buffer with carboxyfluorescein filled vesicles was determined. Then, polymer solutions (in DMSO) of varying concentrations were added to the vesicle-containing solutions. After
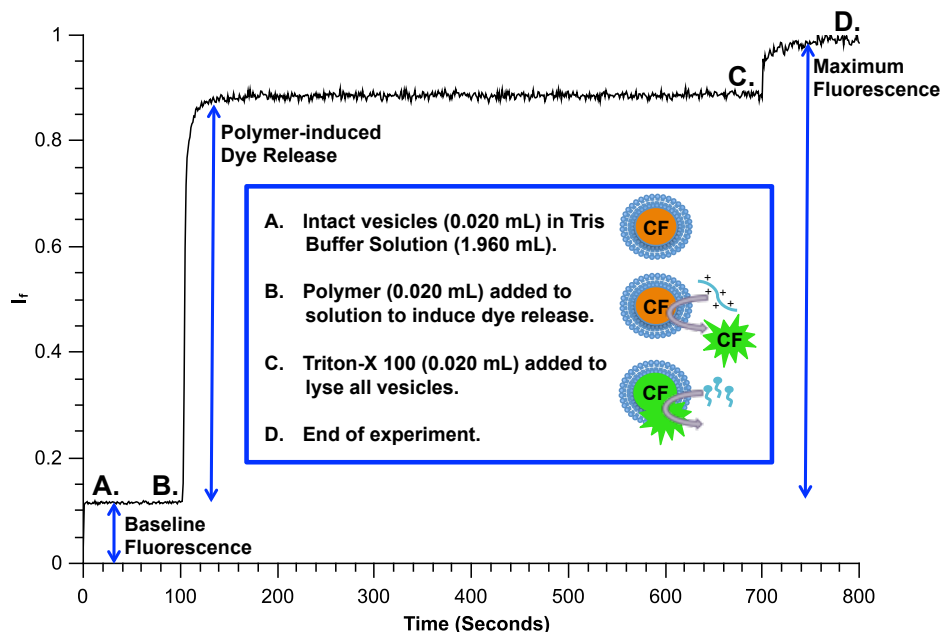
Figure 2.11. Cartoon depiction of the dye release assays performed.

10 minutes, the fluorescence intensity ($F_{f,0}$) was measured again. Triton X-100 (5% in DMSO) was then added to each experimental solution to lyse the vesicles and release all of the dye. The final fluorescence measurement (F_t) was taken after five minutes. The results were normalized according to the baseline and Triton controls to yield fractional dye release (I_f) according to **Equation 1.**

$I_f = (F_{f,0} - F_0) / (F_t - F_0)$

Equation 1

For Hill analysis, I_f was plotted against polymer concentration, c, and fit to the Hill equation, **Equation 2**, to give the EC_{50}, where $I_{f,0}$ and $I_{f,max}$ are the minimum and maximum value of I_f obtained for each well, respectively.

$$I_f = I_{f,0} + (I_{f,max} - I_{f,0}) / [(1 + c / EC_{50})^n]$$

Equation 2

The first set of polymers tested were **9a-f** and **12a-c**, since both sets of polymers had comparable hydrophobic and hydrophilic contents (roughly 1:1) but different backbone compositions. Overlays of all diester homopolymer CPPMs are shown in Figure 2.12 and overlays of all imide random copolymer CPPMs are shown in Figure 2.13. A summary of the EC_{50}, $I_{f,max}$, and n values obtained from testing **9a-f** and **12a-c** with PC vesicles are displayed in Table 2.3.
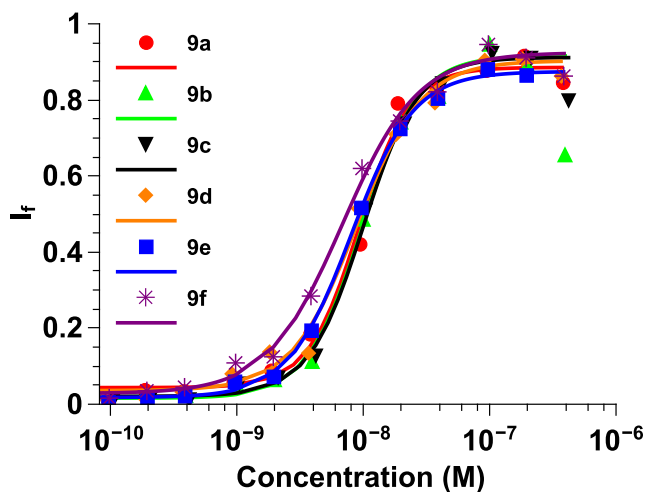
Figure 2.12. Overlay of hill plots for diester homopolymer CPPMs **9a-f** (red, green, black, orange, blue, and purple, respectively) using 100 nm PC large unilamellar vesicles swelled with carboxyfluorescein. Data was fit to the Hill Equation and I_f represents the fraction of dye released.

57
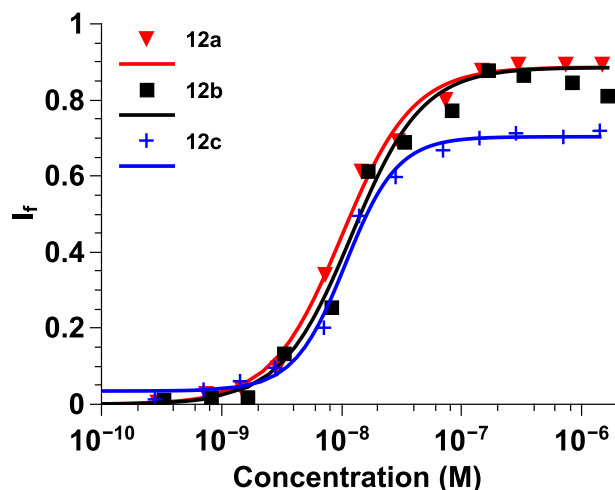
Figure 2.13. Overlay of hill plots for imide random copolymer CPPMs **12a-c** (red, black, and blue, respectively) using 100 nm PC large unilamellar vesicles swelled with carboxyfluorescein. Data was fit to the Hill Equation and I_f represents the fraction of dye released.

For comparison, representative overlays of π-rich and π-poor polymers from both sets of polymers are shown in Figure 2.14. All EC_{50} values were similar (7-12 nM) and, with the exception of the lower $I_{f,max}$ for **12c**, the Hill plots were also almost identical. Only EC_{50} values that differ over several orders of magnitiude represent significant changes, as observed in previous studies where the aliphatic hydrophobic group incorporated was changed from a methyl group (EC_{50} = 6.4 µM) to a butyl group (EC_{50} = 0.003 µM).[33]

Table 2.3. EC_{50}, Y_{max}, and Hill coefficient n values for diester homopolymer and imide random copolymer-based CPPM activity using 100 nm PC large unilamellar vesicles swelled with carboxyfluorescein.

CPPM	EC_{50}[a] (nM)	Y_{max}[b]	n [c]
9a	8.27 ± 0.84	0.89 ± 0.00	2.01 ± 0.04
9b	7.36 ± 1.87	0.92 ± 0.02	1.59 ± 0.04
9c	9.07 ± 0.79	0.90 ± 0.01	1.93 ± 0.02
9d	7.48 ± 0.50	0.91 ± 0.01	1.43 ± 0.01
9e	9.93 ± 0.50	0.92 ± 0.02	1.50 ± 0.06
9f	8.63 ± 0.52	0.85 ± 0.02	1.79 ± 0.01
12a	10.09 ± 1.96	0.87 ± 0.01	1.59 ± 0.07
12b	11.85 ± 0.19	0.84 ± 0.05	1.63 ± 0.14
12c	10.64 ± 0.21	0.72 ± 0.02	1.93 ± 0.15

[a]Effective concentrations (EC_{50}) needed to reach Y_{max}/2, [b]Maximum fraction of carboxyfluorescein released compared to total dye released upon addition of Triton-X 100. [c]n is the Hill coefficient. Standard deviation from three independent experiments is reported.

Within each series, it was determined that the nature of the π-rich or π-poor aromatic rings incorporated did not have a significant impact on CPPM activity. By comparing CPPMs from both series, it was determined that the nature of the CPPM backbone also had a negligible effect on CPPM activity. Although many of our previous SAR studies were based on the imide system, in this paper all further testing was conducted with the diester system since backbone architecture had little impact on results and this system offers more options for structural tuning.
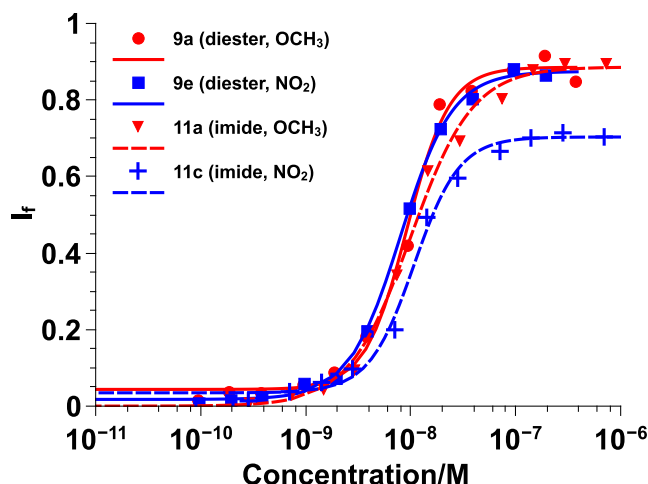
Figure 2.14. Diester vs. imide Hill plots for π-rich CPPMs **9a** and **12a** (red) and π-poor CPPMs **9e** and **12c** (blue) using 100 nm PC large unilamellar vesicles swelled with carboxyfluorescein. Data was fit to the Hill Equation and I_f represents the fraction of dye released. Solid lines represent diester-based CPPMs and dashed lines represent imide random copolymer-based CPPMs.

To further probe the effect of π-electronics on CPPM activity, dye-swelled vesicles were prepared by adding negatively charged PS lipids (20 mol%) to PC lipids. This lipid composition was selected in order to exploit potentially favorable π-anion interactions that can occur between anionic lipids and electron deficient aromatic systems while also capitalizing on electron repulsions between anionic lipids and electron-rich aromatic systems.[58] Based on the nature of π-interactions, it was anticipated that CPPM activity would trend based on π-electron density, with π-poor CPPMs exhibiting better activity due to favorable π-anion interactions. In contrast, π-rich polymers were expected to have weaker activity due to electron repulsion between the anionic lipids and the electron-rich aromatic rings. For these studies, polymers **9a**, **c**, and **e** were tested and the results were compared to those obtained for PC vesicles. A summary of the EC_{50}, $I_{f,max}$, and n values can be found in **Table 2.4.**

Table 2.4 EC_{50}, $I_{f,max}$, and Hill coefficient n values for diester homopolymer-based CPPM activity using 100 nm EYPC/Brain PS (80/20) large unilamellar vesicles swelled with carboxyfluorescein.

CPPM	$EC_{50}{}^{a}$ (nM)	$I_{f,max}{}^{b}$	n^{c}
9a	9.10	0.89	1.34
9c	11.69	0.90	1.14
9e	11.90	0.89	1.47

[a] Effective concentrations (EC_{50}) needed to reach $I_{f,max}/2$, [b] Maximum fraction of carboxyfluorescein released compared to total dye released upon addition of Triton-X 100. [c] n is the Hill coefficient Standard deviation from three independent experiments is reported.

In addition, representative overlays of π-rich and π-poor polymers tested with PC and PC/PS vesicles can be found in Figure 2.15. EC_{50} values for polymers **9a, c,** and **e** tested with PC/PS vesicles were similar to those obtained from studies with PC vesicles. There was also little difference in the Hill Plots for these polymers, regardless of the nature of the π-rich or π-poor aromatic ring incorporated or type of vesicles used for the study.
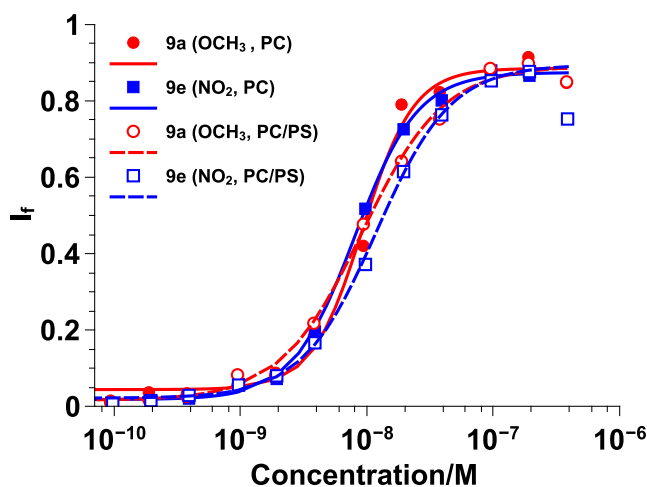
Figure 2.15. Anionic vs. zwitterionic vesicle Hill plots for π-rich polymer **9a** (red) and π-poor polymer **9e** (blue) using two types of 100 nm large unilamellar vesicles swelled with carboxyfluorescein: PC (solid lines) and PC/PS (80/20, dashed lines). Data was fit to the Hill Equation. I_{f} represents the fraction of dye released.

Based on these results, a set of diester random copolymers was designed that had a more dilute hydrophobic content to be sure that the results observed were not due to the CPPM hydrophobic content being too high. The CPPMs designed are shown in Figure 2.7. A summary of the EC_{50}, $I_{f,max}$, and n values can be found in Table 2.5 for PC and Table 2.6 for PC/PS vesicles. In addition, representative overlays for the diester random copolymers as they compare to their corresponding diester homopolymers for PC and PC/PS vesicles can be observed in Figure 2.16 and Figure 2.17, respectively.

Table 2.5. EC_{50}, Y_{max}, and Hill coefficient n values for diester random copolymer-based CPPM activity using 100 nm EYPC large unilamellar vesicles swelled with carboxyfluorescein.

CPPM	EC_{50}^{a} (nM)	$I_{f,max}^{b}$	n^{c}
15a	6.50	0.80	1.76
15c	5.60	0.79	1.99
15e	6.74	0.72	1.87

[a] Effective concentrations (EC_{50}) needed to reach $I_{f,max}/2$, [b] Maximum fraction of carboxyfluorescein released compared to total dye released upon addition of Triton-X 100. [c] n is the Hill coefficient Standard deviation from three independent experiments is reported.

Table 2.6. EC_{50}, Y_{max}, and Hill coefficient n values for diester random copolymer-based CPPM activity using 100 nm EYPC/Brain PS (80/20) large unilamellar vesicles swelled with carboxyfluorescein.

CPPM	EC_{50}^{a} (nM)	$I_{f,max}^{b}$	n^{c}
15a	27.94	0.87	1.91
15c	28.96	0.87	1.91
15e	44.59	0.88	1.46

[a] Effective concentrations (EC_{50}) needed to reach $I_{f,max}/2$, [b] Maximum fraction of carboxyfluorescein released compared to total dye released upon addition of Triton-X 100. [c] n is the Hill coefficient Standard deviation from three independent experiments is reported.
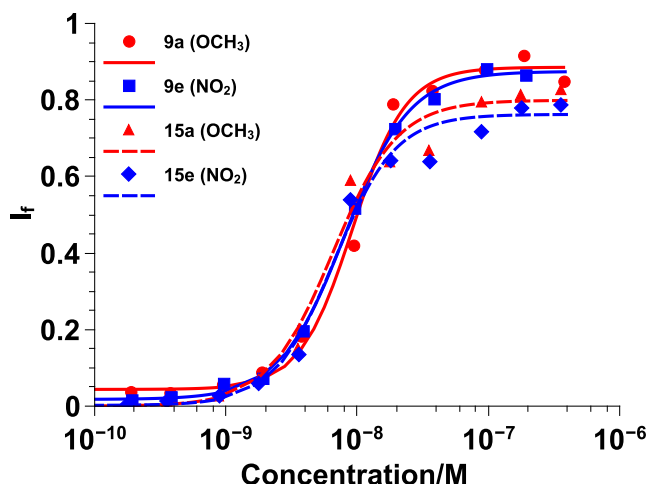
Figure 2.16. Homopolymer vs. random copolymer Hill plots for π-rich polymers **9a** and **15a** (red) and π-poor polymers **9e** and **15e** (blue) using 100 nm PC large unilamellar vesicles swelled with carboxyfluorescein. Data was fit to the Hill Equation and I_f represents the fraction of dye released. Solid lines represent diester homopolymers and dashed lines represent diester random copolymers.

EC$_{50}$ values for **14a, c,** and **e** were similar to those obtained for **9a, c,** and **e** when tested with PC vesicles and the overlays of the Hill plots in Figure 2.16 further suggest that there was little difference between the activity of the diester homopolymers and the less hydrophobic random copolymers. When tested with PC/PS vesicles, there was a slight increase in EC$_{50}$ values for the random copolymers as compared to the homopolymers and there was a noticeable shift in the Hill plots in Figure 2.17. However, the shift was about the same for all diester random copolymers and thus attributed to the lower hydrophobic content and not due to the π-electronics of the system. Since no trend was observed, it was concluded that π-electronics do not play a major role in CPPM activity. Alternatively, it is possible that the assay used here does not have the fidelity to distinguish the subtleties of π –interactions despite the fact that these same assays previously illustrated that adding hydrophobicity improves activity, with aromatic groups outperforming aliphatic groups. [32,33] Even though we were able to synthesize a series of polymers that contained aromatic groups with an electrostatic

potential range of -29.69 to 15.57 kcal/mol, it is also possible that the structural modifications made to the polymers may not have been significant enough to impact CPPM activity. While it is likely that overall CPPM hydrophobicity and cationic charge are more influential design parameters than π-electronics, these results indicate that a wide range of aromatic groups can be incorporated into the polymer structures with limited impact on CPPM activity. From a design standpoint, this opens up additional ways in which CPPMs can be modified without inhibiting their performance.
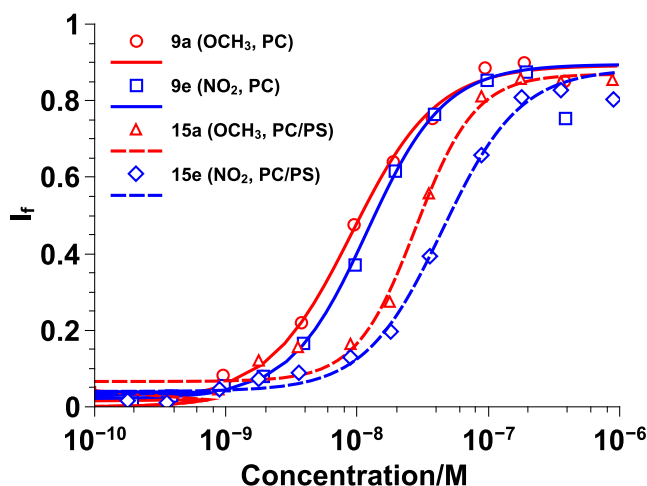
Figure 2.17. Homopolymer vs. random copolymer Hill plots for π-rich polymers **9a** and **15a** (red) and π-poor polymers **9e** and **15e** (blue) using 100 nm PC/PS (80/20) large unilamellar vesicles swelled with carboxyfluorescein. Data was fit to the Hill Equation and I_f represents the fraction of dye released. Solid lines represent diester homopolymers and dashed lines represent random copolymers.

2.5   Conclusion

For this study, aromatic groups containing electron donating and electron withdrawing groups were chemically incorporated into CPPM structures as a way to tune π-interactions. It was hypothesized that tuning the quadrupole moments of the aromatic rings would provide additional control over CPPM activity. When synthesizing the monomers for these studies, it was established through small molecule synthesis that

highly electron-withdrawing groups could not be chemically incorporated into the diester versions of our oxanorbornene monomers because it spontaneously induced a retro-Diels-Alder reaction.

Within the synthetically accessible series, vesicle dye release experiments were performed as a way to determine the CPPMs' EC_{50} values and assess their relative activities. It was shown using PC vesicles that polymer backbone did not impact activity for the π-rich/ π-poor CPPMs and that the electron donating or electron withdrawing groups as well as the relative hydrophobic content did not impact activity either. Diester CPPMs were also tested with PC vesicles containing 20% PS anionic lipids in efforts to more thoroughly understand π-membrane interactions.

However, it would seem that only overall hydrophobicity dictated polymer activity and not the incorporated electron donating or electron withdrawing groups. Although it is possible that the assay used could not distinguish the subtleties of π-interactions, it is also likely that the structural modifications made to the polymers were not significant enough to impact CPPM activity, despite the fact that molecules containing aromatic rings with an electrostatic potential range of -29.69 kcal/mol to 15.57 +kcal/mol were explored. This suggests that other design parameters, such as overall hydrophobicity and cationic charge, have a greater impact on CPPM activity. The results also indicate that a wide range of aromatic groups can be incorporated into the polymer structures with limited impact on CPPM activity. This is encouraging from a design standpoint as it expands potential functionality without impacting activity. Understanding these design principles will help guide the development of future CPPMs.

2.6   References

(1)   Cooley, C. B.; Trantow, B. M.; Nederberg, F.; Kiesewetter, M. K.; Hedrick, J. L.; Waymouth, R. M.; Wender, P. A. J. Am. Chem. Soc. 2009, 131, 16401-16403.

(2)   Futaki, S.; Suzuki, T.; Ohashi, W.; Yagami, T.; Tanaka, S.; Ueda, K.; Sugiura, Y. The Journal of biological chemistry 2001, 276, 5836-5840.

(3)   Geihe, E. I.; Cooley, C. B.; Simon, J. R.; Kiesewetter, M. K.; Edward, J. A.; Hickerson, R. P.; Kaspar, R. L.; Hedrick, J. L.; Waymouth, R. M.; Wender, P. A. Proc. Natl. Acad. Sci. U. S. A. 2012, 109, 13171-13176.

(4)   Lindgren, M.; Langel, U. Methods Mol Biol 2011, 683, 3-19.

(5)   Morris, M. C.; Depollier, J.; Mery, J.; Heitz, F.; Divita, G. Nat. Biotechnol. 2001, 19, 1173-1176.

(6)   Opalinska, J. B.; Gewirtz, A. M. Nat. Rev. Drug Discovery 2002, 1, 503-514.

(7)   Patel, L. N.; Zaro, J. L.; Shen, W. C. Pharm. Res. 2007, 24, 1977-1992.

(8)   Sgolastra, F.; deRonde, B. M.; Sarapas, J. M.; Som, A.; Tew, G. N. Accounts Chem Res 2013, 46, 2977-2987.

(9)   Wender, P. A.; Mitchell, D. J.; Pattabiraman, K.; Pelkey, E. T.; Steinman, L.; Rothbard, J. B. Proceedings of the National Academy of Sciences of the United States of America 2000, 97, 13003-13008.

(10)   Bechara, C.; Sagan, S. FEBS Lett. 2013, 587, 1693-1702.

(11)   Joliot, A.; Pernelle, C.; Deagostinibazin, H.; Prochiantz, A. Proc. Natl. Acad. Sci. U. S. A. 1991, 88, 1864-1868.

(12)   Green, M.; Loewenstein, P. M. Cell 1988, 55, 1179-1188.

(13)   Frankel, A. D.; Pabo, C. O. Cell 1988, 55, 1189-1193.

(14)   Derossi, D.; Joliot, A. H.; Chassaing, G.; Prochiantz, A. J. Biol. Chem. 1994, 269, 10444-10450.

(15)   Fawell, S.; Seery, J.; Daikh, Y.; Moore, C.; Chen, L. L.; Pepinsky, B.; Barsoum, J. Proc. Natl. Acad. Sci. U. S. A. 1994, 91, 664-668.

(16)   Vives, E.; Brodin, P.; Lebleu, B. J. Biol. Chem. 1997, 272, 16010-16017.

(17)   Tezgel, A. O.; Telfer, J. C.; Tew, G. N. Biomacromolecules 2011, 12, 3078-3083.

(18)   Yin, L. C.; Tang, H. Y.; Kim, K. H.; Zheng, N.; Song, Z. Y.; Gabrielson, N. P.; Lu, H.; Cheng, J. J. Angew. Chem., Int. Ed. Engl. 2013, 52, 9182-9186.

(19)   Gabrielson, N. P.; Lu, H.; Yin, L. C.; Kim, K. H.; Cheng, J. J. Mol. Ther. 2012, 20, 1599-1609.

(20)   Tang, H. Y.; Yin, L. C.; Kim, K. H.; Cheng, J. J. Chem. Sci. 2013, 4, 3839-3844.

(21)   Stanzl, E. G.; Trantow, B. M.; Vargas, J. R.; Wender, P. A. Accounts Chem Res 2013, 46, 2944-2954.

(22)   Tezgel, A. O.; Gonzalez-Perez, G.; Telfer, J. C.; Osborne, B. A.; Minter, L. M.; Tew, G. N. Mol. Ther. 2013, 21, 201-209.

(23)   Futaki, S. Adv. Drug Deliv. Rev. 2005, 57, 547-558.

(24)   Mishra, A.; Lai, G. H.; Schmidt, N. W.; Sun, V. Z.; Rodriguez, A. R.; Tong, R.; Tang, L.; Cheng, J.; Deming, T. J.; Kamei, D. T.; Wong, G. C. Proc. Natl. Acad. Sci. U. S. A. 2011, 108, 16883-16888.

(25)   Zaro, J. L.; Shen, W. C. Exp. Cell. Res. 2005, 307, 164-173.

(26)   Thoren, P. E.; Persson, D.; Isakson, P.; Goksor, M.; Onfelt, A.; Norden, B. Biochem. Biophys. Res. Commun. 2003, 307, 100-107.

(27)   Suzuki, T.; Futaki, S.; Niwa, M.; Tanaka, S.; Ueda, K.; Sugiura, Y. The Journal of biological chemistry 2002, 277, 2437-2443.

(28)   Takeuchi, T.; Kosuge, M.; Tadokoro, A.; Sugiura, Y.; Nishi, M.; Kawata, M.; Sakai, N.; Matile, S.; Futaki, S. ACS Chem. Biol. 2006, 1, 299-303.

(29)   Hennig, A.; Gabriel, G. J.; Tew, G. N.; Matile, S. J. Am. Chem. Soc. 2008, 130, 10338-10344.

(30)   Sakai, N.; Matile, S. J. Am. Chem. Soc. 2003, 125, 14348-14356.

(31)   Schmidt, N. W.; Lis, M.; Zhao, K.; Lai, G. H.; Alexandrova, A. N.; Tew, G. N.; Wong, G. C. J. Am. Chem. Soc. 2012, 134, 19207-19216.

(32)   Som, A.; Reuter, A.; Tew, G. N. Angew. Chem., Int. Ed. Engl. 2012, 51, 980-983.

(33)   Som, A.; Tezgel, A. O.; Gabriel, G. J.; Tew, G. N. Angew. Chem., Int. Ed. Engl. 2011, 50, 6147-6150.

(34)   Perret, F.; Nishihara, M.; Takeuchi, T.; Futaki, S.; Lazar, A. N.; Coleman, A. W.; Sakai, N.; Matile, S. J. Am. Chem. Soc. 2005, 127, 1114-1115.

(35)   Nishihara, M.; Perret, F.; Takeuchi, T.; Futaki, S.; Lazar, A. N.; Coleman, A. W.; Sakai, N.; Matile, S. Org. Biomol. Chem. 2005, 3, 1659-1669.

(36)   Sakai, N.; Futaki, S.; Matile, S. Soft Matter 2006, 2, 636-641.

(37)   Sakai, N.; Takeuchi, T.; Futaki, S.; Matile, S. Chembiochem : a European journal of chemical biology 2005, 6, 114-122.

(38)   Almeida, P. F.; Pokorny, A. Biochemistry 2009, 48, 8083-8093.

(39)   Almeida, P. F.; Pokorny, A. Methods in molecular biology 2010, 618, 155-169.

(40)   Yau, W. M.; Wimley, W. C.; Gawrisch, K.; White, S. H. Biochemistry 1998, 37, 14713-14718.

(41)   Killian, J. A.; von Heijne, G. Trends Biochem. Sci. 2000, 25, 429-434.

(42)   White, S. H.; Wimley, W. C. Annual review of biophysics and biomolecular structure 1999, 28, 319-365.

(43)   Wimley, W. C.; White, S. H. Nature structural biology 1996, 3, 842-848.

(44)   Morris, M. C.; Vidal, P.; Chaloin, L.; Heitz, F.; Divita, G. Nucleic Acids Res. 1997, 25, 2730-2736.

(45)   Morris, M. C.; Deshayes, S.; Heitz, F.; Divita, G. Biol. Cell 2008, 100, 201-217.

(46)   Caesar, C. E.; Esbjorner, E. K.; Lincoln, P.; Norden, B. Biochemistry 2006, 45, 7682-7692.

(47)   Yezid, H.; Konate, K.; Debaisieux, S.; Bonhoure, A.; Beaumelle, B. The Journal of biological chemistry 2009, 284, 22736-22746.

(48)   Gabriel, G. J.; Pool, J. G.; Som, A.; Dabkowski, J. M.; Coughlin, E. B.; Muthukumar, M.; Tew, G. N. Langmuir : the ACS journal of surfaces and colloids 2008, 24, 12489-12495.

(49)   Thaker, H. D.; Sgolastra, F.; Clements, D.; Scott, R. W.; Tew, G. N. J. Med. Chem. 2011, 54, 2241-2254.

(50)   Braun, P.; von Heijne, G. Biochemistry 1999, 38, 9778-9782.

(51)   Strandberg, E.; Morein, S.; Rijkers, D. T.; Liskamp, R. M.; van der Wel, P. C.; Killian, J. A. Biochemistry 2002, 41, 7190-7198.

(52)   John Haynes, W.; Zhou, X. L.; Su, Z. W.; Loukin, S. H.; Saimi, Y.; Kung, C. FEBS Lett. 2008, 582, 1514-1518.

(53)   Gromiha, M. M.; Suwa, M. Int. J. Biol. Macromol. 2005, 35, 55-62.

(54)   Gromiha, M. M. Biophys. Chem. 2003, 103, 251-258.

(55)   Arbuzova, A.; Wang, L.; Wang, J.; Hangyas-Mihalyne, G.; Murray, D.; Honig, B.; McLaughlin, S. Biochemistry 2000, 39, 10330-10339.

(56)   Lienkamp, K.; Madkour, A. E.; Musante, A.; Nelson, C. F.; Nusslein, K.; Tew, G. N. Journal of the American Chemical Society 2008, 130, 9836-9843.

(57)   Nanjappan, P.; Czarnik, A. W. J. Org. Chem. 1986, 51, 2851-2853.

(58)   Schottel, B. L.; Chifotides, H. T.; Dunbar, K. R. Chem. Soc. Rev. 2008, 37, 68-83.

CHAPTER 3

DEVELOPMENT OF ROMP-BASED PROTEIN MIMICS FOR EFFICIENT SIRNA

DELIVERY INTO HUMAN T CELLS

3.1   Introduction:

RNA interference (RNAi), discovered almost two decades ago, continues to be an important tool to probe molecular pathways and to potentially treat diseases.[1-5] Small interfering RNA (siRNA), which represents one RNAi approach, must be present in the cytosol so that the siRNA guide strand can be incorporated into the RISC complex and degrade its complementary mRNA. This leads to transient, sequence-specific, post-transcriptional gene knockdown,[6-8] which is advantageous for discrete biological and clinical applications,[1-5] a strategy of critical importance in the context of the immune system and T cells.[9-12]

T cells are key components of the immune system. They orchestrate essential functions during the immune response to pathogens, chronic inflammation, and autoimmune disorders.[10] Harnessing the capabilities of RNAi would allow immunologists to explore molecular pathways leading to a better understanding of T cell activation, signaling, and other biological processes, eventually providing new treatment options for autoimmune diseases.[9-12] Unfortunately, progress in this area has been severely limited due to the lack of robust delivery technologies for T cell lines and primary cells.[10,12-17] Three major strategies are routinely used for siRNA delivery into T cells and primary cells: electroporation, viral vectors, and transfection.[12-17] The use of electroporation and viral vectors both have severe drawbacks, which include high cell death and potential mutagenic/immunogenic effects, respectively.[14,16] Transfection is generally a safer

alternative, with higher cell survival rates; however, many current delivery vehicles exhibit low efficiencies in T cell lines and primary cells.[13,15,17] Although designing successful carriers for T cells has been a challenge, highly modular protein transduction domain mimics (PTDMs), sometimes referred to as cell-penetrating peptide mimics (CPPMs), have been used successfully in other more easily transfected cell types and can provide insight for the design of more efficient delivery vehicles.[18-20]

Inspiration for PTDMs is derived from proteins with translocation abilities, such as the HIV-1 TAT and *Antennapedia* homeodomain proteins, as well as other protein transduction domains (PTDs) and cell-penetrating peptides (CPPs) that exhibit delivery capabilities.[21-23] PTDMs incorporate important features of PTDs and CPPs critical for intracellular delivery[24-29], including cationic charge content provided by guanidinium groups, and partial hydrophobicity contributed by the backbone architecture and/or the incorporation of hydrophobic monomers.[18,19] Although some PTDs and CPPs, such as CADY and MPG, possess these key features and have already been designed and commercialized for siRNA delivery, PTDMs offer many distinct advantages over their peptide counterparts.[30,31] Moving away from a peptide-based architecture provides protection from proteolysis and avoids solid phase peptide synthesis. Additionally, a non-peptidic system offers many more structural options, since it is not restricted to the incorporation of known amino acids.[18,19,32] Consequently, different chemistries can be used to design molecules, and chemical compositions can be tuned more widely to improve delivery of specific cargo.[18,19,32] This design rationale has proven successful in creating more potent antimicrobial peptide mimics, where the key features, including their facially amphiphilic architecture,[33-35] were incorporated into synthetic scaffolds to yield new antimicrobial agents.[19,35-37]

In the realm of delivery reagents, several groups have demonstrated the utility of synthetic, guanidinium-rich, polymeric scaffolds to deliver siRNA.[18,19,38-44] Ring-opening metathesis polymerization (ROMP)[20,45-47], polymethacrylamide[42,48], arginine-grafted bioreducible polydisulfide[40,41], and oligocarbonate[38,39,44] scaffolds have all been developed and screened for siRNA delivery. The successful design of PTDMs will further the understanding of the key features necessary for efficient delivery, as well as enable the development of more effective delivery reagents.[18,19,32]

Related to this long term goal, in 2008, the Tew research group first reported the development of polymeric guanidinium-rich PTDMs based on a ROMP scaffold that mimics PTDs/CPPs, such as TAT_{49-57} and oligoarginine (R9).[19,49,50] Initial studies aimed to understand the effects of PTDM length[51], hydrophobicity[52], aromaticity[53], aromatic π-electronics[54], and sequence segregation of cationic/hydrophobic components[55] on membrane interactions and cellular uptake.[43] In early 2013, we extended this platform to include siRNA delivery. It was demonstrated that our PTDMs delivered FITC-siRNA into Jurkat T cells with efficiencies greater than 90% and achieved 50% knockdown of NOTCH1 protein in human T cells from human peripheral blood mononuclear cells (hPBMCs).[20] Due to the initial success of siRNA delivery using these PTDMs, further understanding of the relationship between PTDM structure and siRNA delivery efficiency in T cells was desired.

Herein we document our efforts to tune ROMP-based PTDM structures for improved siRNA delivery. Structure activity relationships using Jurkat T cells and hPBMCs were used to probe how polymer charge content and the addition of a segregated, hydrophobic block impacted siRNA internalization and delivery efficiencies. Specifically, two polymer series were developed, homopolymers and block copolymers, with matching cationic charge contents (Figure 3.1). All block copolymers contained a

constant hydrophobic block of approximately five repeat units. It should be noted that guanidinium moieties were incorporated to mimic arginine residues and phenyl moieties were incorporated in the block copolymer PTDMs to mimic phenylalanine residues, both of which have been shown to play critical roles in membrane interactions.[27,29,43,51-54,57,58] In this study, we elucidate the essential design parameters for siRNA delivery using our PTDMs, which can be used to develop the next generation of highly efficient transfection reagents.

3.2 PTDM Design and Characterization

Proteins and peptides have been utilized extensively for intracellular delivery applications.[18,32,60-62] These materials, however, have presented many limitations, including long and costly synthetic procedures, as well as poor stability, all of which can be avoided by leveraging more versatile synthetic platforms. In this report, ROMP with Grubbs' third generation catalyst was used to synthesize all PTDMs since it is a fast, efficient, and functional group tolerant method that also allows for good control over molecular weights and dispersities. The living nature of many ROMP polymerizations also enables the synthesis both of homopolymers and block copolymers, and allows the influence of an added hydrophobic block on internalization and delivery efficiencies to be evaluated within the same monomer chemistry.[63-71] Additionally, the oxanorbornene-based dual-functional monomer platform is quite versatile, allowing for the incorporation of the same or different functionalities to tune the polymer structures at the monomer level.[18] For this particular endeavor, a monomer containing two Boc-protected guanidinium groups (**dG**; Figure 3.1**)** and a second monomer containing a methyl group and a phenyl group (**MePh**; Figure 3.1) were synthesized.

71
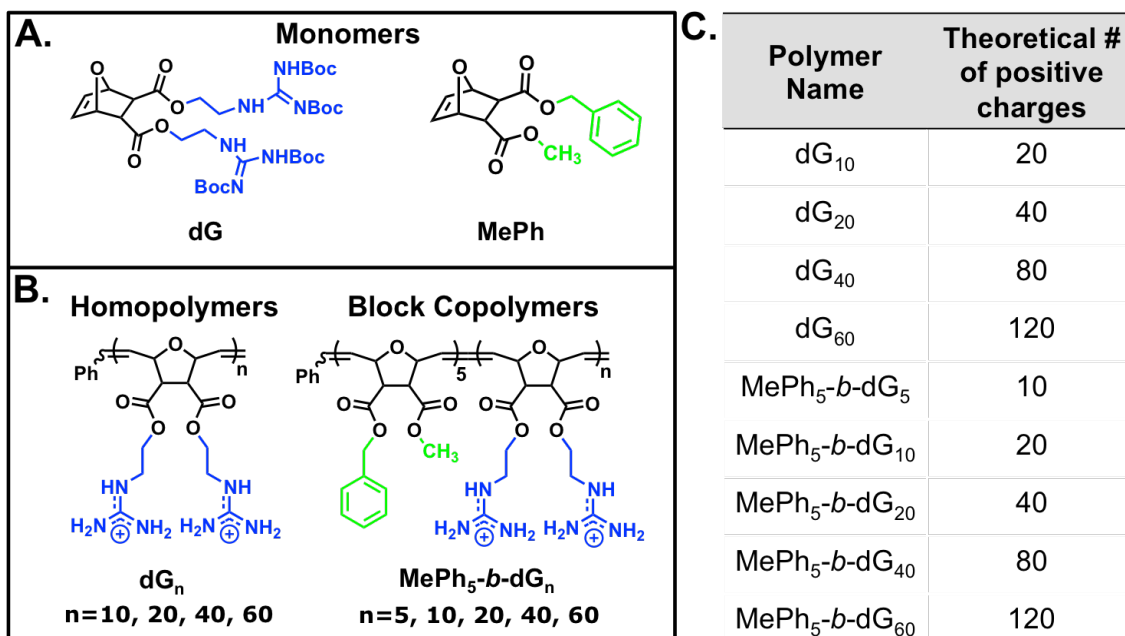
Figure 3.1. Monomer and polymer structures used for this study. A) Monomer structures. B) Polymer structures. C) Table summarizing the polymer nomenclature and the corresponding number of positive charges each polymer contains. Blue represents cationic moieties and green represents hydrophobic moieties.

All molecular weight characterization for these libraries of polymers are summarized in Table 3.1, Table 3.2, Figure 3.2, Figure 3.3, Figure 3.4, and Figure 3.5. Guanidinium moieties were selected as the cations because they have been previously shown to yield superior uptake and delivery efficiencies as compared to their ammonium counterparts found in lysine and ornithine.[27]

Table 3.1. Molecular weight characterization of boc-protected homopolymers **5a-f** and block copolymers **6a-f**.

Polymer	M_n^a (Da)	M_w^a (Da)	M_p^a (Da)	$Đ^a$ (M_w/M_n)
5a	4,300	4,600	4,500	1.06
5b	6,400	6,800	6,700	1.07
5c	12,700	13,400	13,500	1.06
5d	23,600	27,200	30,500	1.15
5e	40,500	45,400	48,700	1.12
5f	50,200	59,200	71,000	1.18
6a	5,400	5,900	5,900	1.08
6b	8,300	9,000	9,300	1.08
6c	16,000	17,100	17,500	1.07
6d	27,600	31,500	36,800	1.14
6e	36,800	41,300	46,700	1.12
6f	45,000	57,100	71,100	1.27

[a]Number average molecular weight (M_n), weight average molecular weight (M_w), molecular weight at the peak maximum (M_p), and dispersity indices ($Đ=M_w/M_n$) determined by GPC using poly(methyl methacrylate) (PMMA) standards, tetrahydrofuran (THF) as the eluent, and toluene as the flow marker.
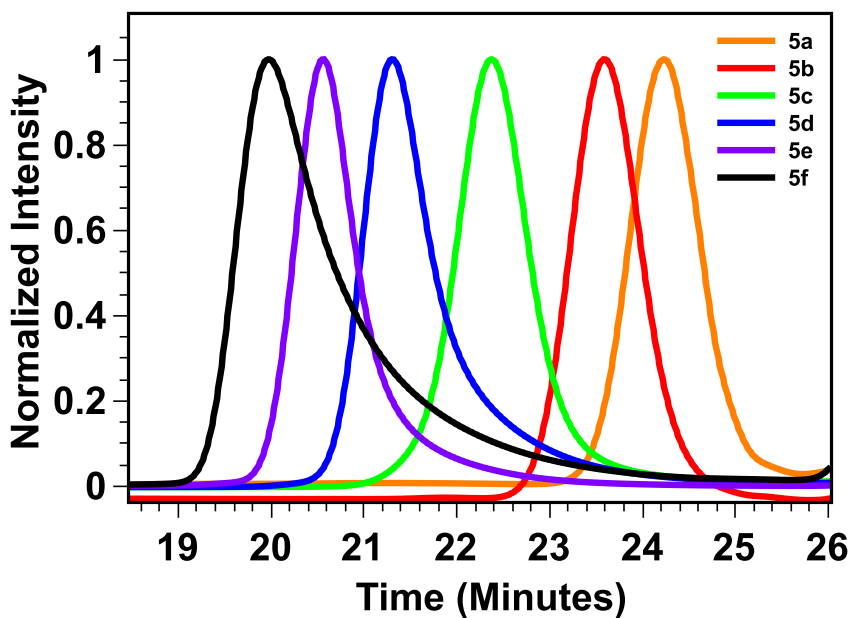
Figure 3.2. THF GPC chromatograms for boc-protected homopolymers PTDMs **5a-f**. A summary of molecular weight data can be found in **Table 3.1**.
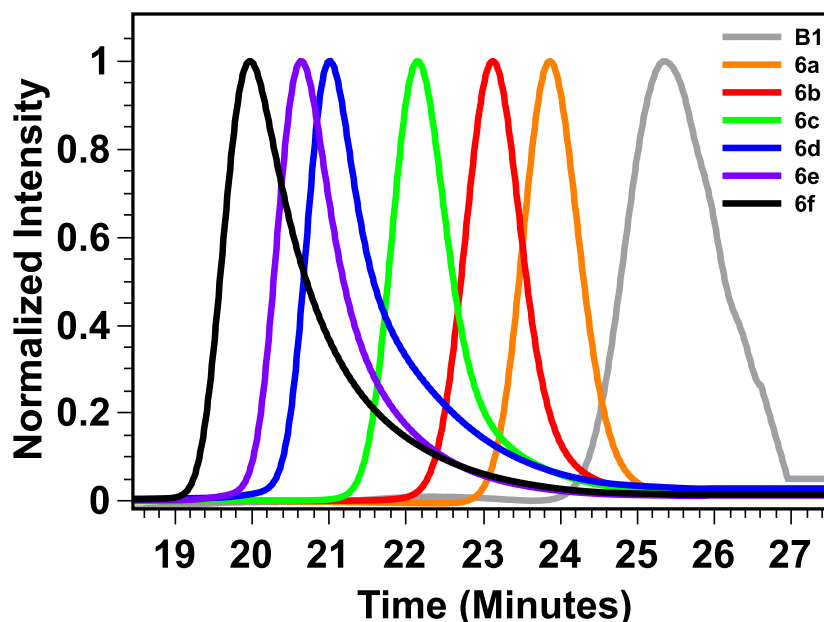
Figure 3.3. THF GPC chromatograms for boc-protected block copolymer PTDMs **6a-f**. **B1** (grey) is a representative chromatogram for the first block of the BCP PTDMs. A summary of molecular weight data can be found in **Table 3.1**.

Table 3.2. Molecular weight characterization of deprotected homopolymers dG_n and block copolymers **MePh$_5$-*b*-dG$_n$**.

Polymer	M_n^a (Da)	M_w^a (Da)	M_p^a (Da)	$Đ^a$ (M_w/M_n)
dG_5	8,800	9,300	9,000	1.05
dG_{10}	11,400	12,000	11,700	1.05
dG_{20}	18,300	19,400	19,400	1.06
dG_{40}	31,500	33,900	36,000	1.08
dG_{60}	45,600	49,100	50,800	1.08
dG_{80}	57,100	80,400	67,500	1.41
MePh$_5$-*b*-dG$_5$	10,200	10,900	10,100	1.07
MePh$_5$-*b*-dG$_{10}$	14,900	15,800	15,200	1.06
MePh$_5$-*b*-dG$_{20}$	21,800	23,500	23,500	1.08
MePh$_5$-*b*-dG$_{40}$	33,300	36,600	39,500	1.10
MePh$_5$-*b*-dG$_{60}$	39,700	43,700	45,600	1.10
MePh$_5$-*b*-dG$_{80}$	n.d.[b]	n.d.[b]	n.d.[b]	n.d.[b]

[aNumber average molecular weight (M_n), weight average molecular weight (M_w), molecular weight at the peak maximum (M_p), and dispersity indices ($Đ=M_w/M_n$) determined by GPC using poly(methyl methacrylate) (PMMA) standards, 2,2,2-trifluoroethanol (TFE) with 20 mM NaTFA salt as the eluent, and methanol as the flow marker. [b]not determined (n.d.) due to insolubility in TFE eluent.
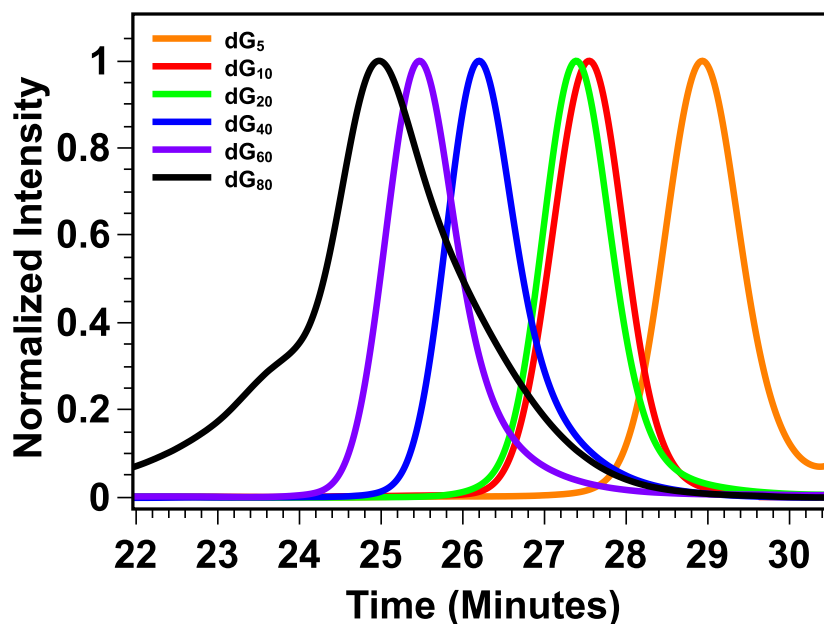
Figure 3.4. TFE GPC chromatograms for deprotected homopolymer PTDMs. A summary of molecular weight data can be found in **Table 3.2**.
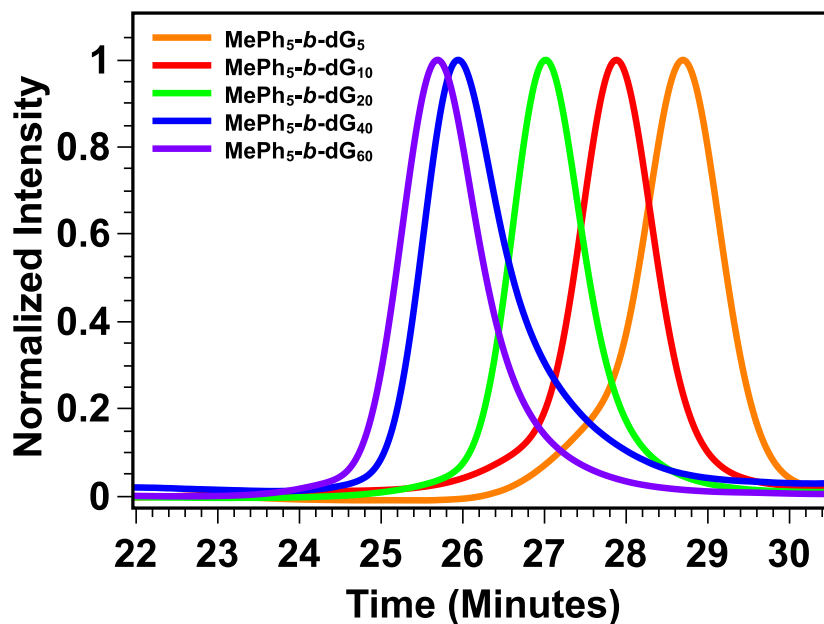
Figure 3.5. TFE GPC chromatograms for deprotected block copolymer PTDMs. A summary of molecular weight data can be found in **Table 3.2**.

The number average molecular weight (M_n) for the homopolymerization of the **dG**

monomer increased linearly with monomer to initiator ratio ([M]/[I]), while maintaining low

dispersities. This indicated that it polymerized in a controlled fashion and can be used to synthesize both homopolymers and block copolymers (Figure 3.6).
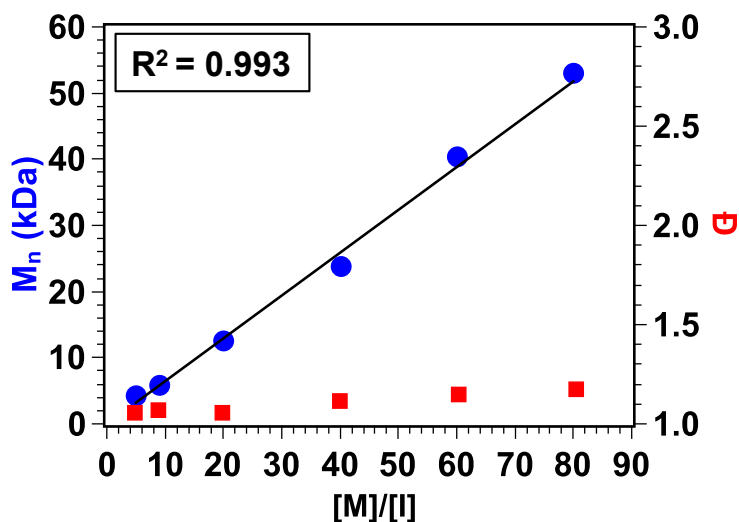
Figure 3.6. Plot of number average molecular weight (M_n) and dispersity index (Đ) with respect to monomer / initiator [M]/[I] ratio for the dG_m series. The linear relationship (R^2 = 0.993) reflects the controlled nature of the polymerization.

Homopolymer and block copolymer PTDMs were synthesized to determine how the cationic charge content, as well as the incorporation of a segregated hydrophobic region, impacted siRNA delivery. To that end, PTDMs with increasing amounts of cationic charge were synthesized, as documented in Figure 3.1. Since the cationic monomer contains two guanidinium groups, the number of charges is reported as twice the degree of polymerization (Figure 3.1C). In addition, block copolymer PTDMs were designed with segregated hydrophobic and cationic domains, as shown in Figure 3.1 These were specifically designed because the incorporation of a hydrophobic domain has been shown to improve internalization and delivery efficiencies through interactions with hydrophobic lipids.[31] The performance of the block copolymers was compared to their corresponding homopolymer derivatives, which contained the same charge content, in order to assess the effect of incorporating a hydrophobic block. In both cases, the

charge content was varied up to 160 charges (80 repeat units); however, PTDMs with 160 charges had limited solubility and were therefore not used for any biological studies. Overall, this series of PTDMs provided insight into key design parameters for efficient siRNA internalization and delivery.

3.3 FITC-siRNA Delivery

Preliminary studies were conducted using fluorescein isothiocyanate (FITC) labeled siRNA (FITC-siRNA), to assess trends in internalization efficiencies in Jurkat T cells resulting from differences in PTDM charge content and the presence or absence of a hydrophobic block. The fluorescent label on the siRNA allowed cell populations to be analyzed using flow cytometry. Jurkat T cells were selected because they are typically difficult to transfect and manipulate.[10,12-17] The N:P ratio, which is the ratio of the number of positively charged nitrogen atoms in the PTDMs to the number of negatively charged phosphate atoms in siRNA, used for complex formation between PTDMs and siRNA was 8:1 and was established by screening FITC-siRNA internalization efficiencies (Figure 3.7 and Figure 3.8) as a function of N:P ratio in addition to using gel retardation assays to assess siRNA complexation. This N:P ratio used was consistent with our previous publication.[20] Gel retardation assays for PTDM/siRNA complexes at N:P ratios of 0.5:1, 1:1, 2:1, 4:1, 8:1, and 12:1 are shown below (Figure 3.9-Figure 3.17).
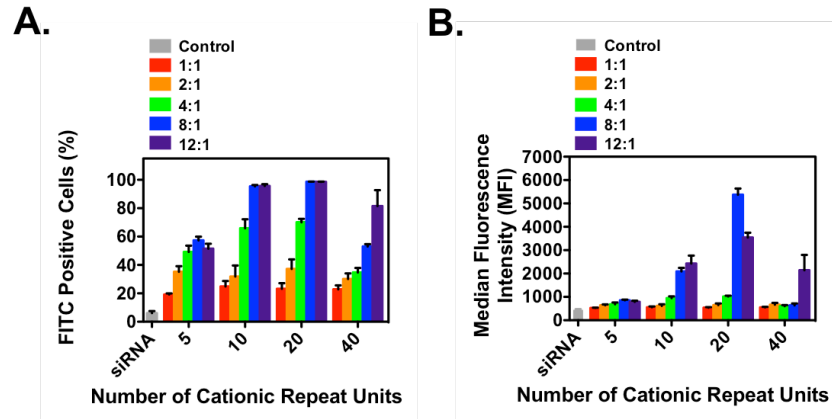
Figure 3.7. N/P ratio screening for FITC-siRNA delivery into Jurkat T cells using ROMP-based PTDMs. Jurkat T cells (cell density = 4×10^5 cells/mL) were treated with polymer/FITC-siRNA complexes with an N:P ratio = 8:1 in complete media for four hours at 37°C and compared with untreated cells and cells only receiving FITC-siRNA. A) Percent positive cells. B) MFI of the cell population. Each data point represents the mean ± SEM of three independent experiments.
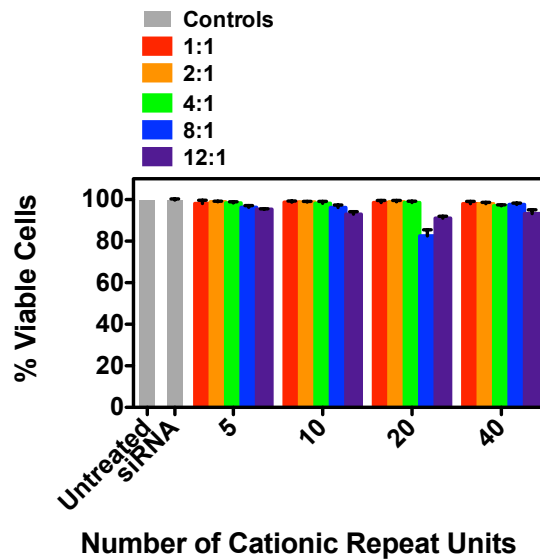
Figure 3.8. Percent viable cells using a 7-Amino-actinomycin (7-AAD) Jurkat T Cell viability assay. Jurkat T cells (cell density = 4×10^5 cells/mL) were treated with PTDM/FITC-siRNA complexes with an N:P ratio = 8:1 in complete media for four hours at 37°C and compared with untreated cells and cells only receiving FITC-siRNA. Cells were stained at four hours. Each data point represents the mean ± SEM of three independent experiments.
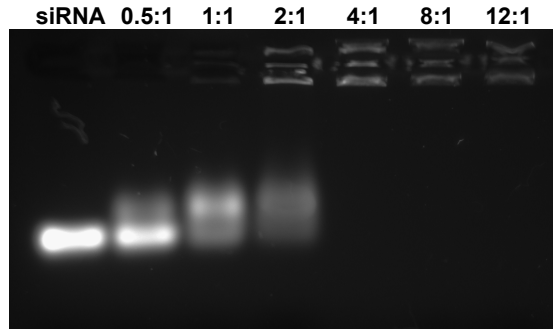
Figure 3.9. Gel retardation assay to assess PTDM / siRNA complex formation using dG_{10}. All samples were run on a 0.8% agarose gel and the N:P ratios tested ranged from 0.5:1 to 12:1, with 1 µg of siRNA per well.
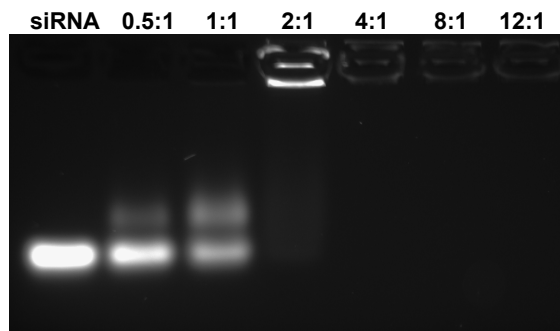
Figure 3.10. Gel retardation assay to assess PTDM / siRNA complex formation using dG_{20}. All samples were run on a 0.8% agarose gel and the N:P ratios tested ranged from 0.5:1 to 12:1, with 1 µg of siRNA per well.
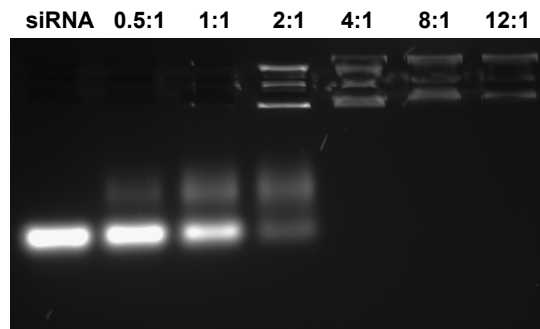
Figure 3.11. Gel retardation assay to assess PTDM / siRNA complex formation using dG_{40}. All samples were run on a 0.8% agarose gel and the N:P ratios tested ranged from 0.5:1 to 12:1, with 1 µg of siRNA per well.
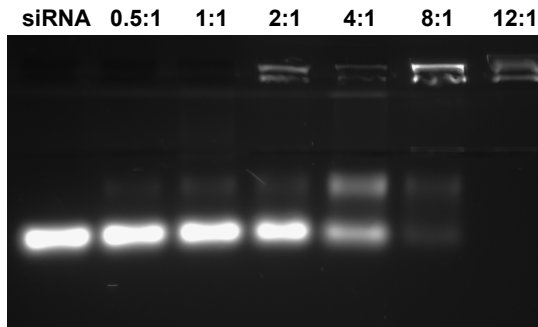
Figure 3.12. Gel retardation assay to assess PTDM / siRNA complex formation using dG$_{60}$. All samples were run on a 0.8% agarose gel and the N:P ratios tested ranged from 0.5:1 to 12:1, with 1 µg of siRNA per well.
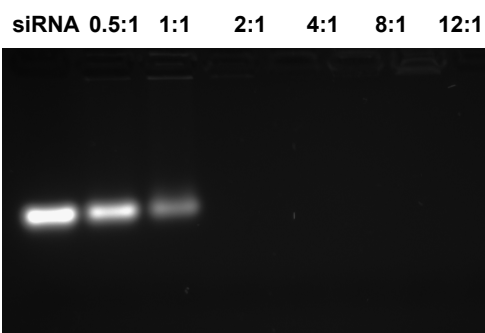
Figure 3.13. Gel retardation assay to assess PTDM / siRNA complex formation using MePh$_5$-*b*-dG$_5$. All samples were run on a 0.8% agarose gel and the N:P ratios tested ranged from 0.5:1 to 12:1, with 1 µg of siRNA per well.
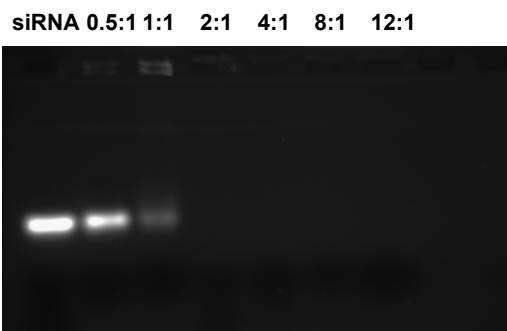
Figure 3.14. Gel retardation assay to assess PTDM / siRNA complex formation using MePh$_5$-*b*-dG$_{10}$. All samples were run on a 0.8% agarose gel and the N:P ratios tested ranged from 0.5:1 to 12:1, with 1 µg of siRNA per well.
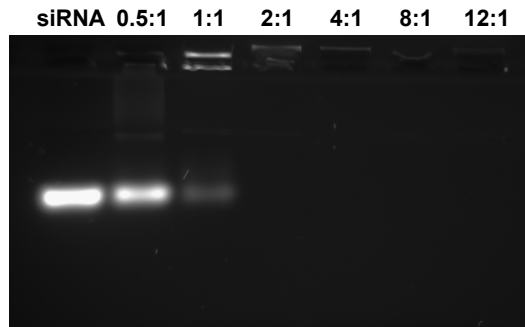
Figure 3.15. Gel retardation assay to assess PTDM / siRNA complex formation using MePh$_5$-*b*-dG$_{20}$. All samples were run on a 0.8% agarose gel and the N:P ratios tested ranged from 0.5:1 to 12:1, with 1 µg of siRNA per well.
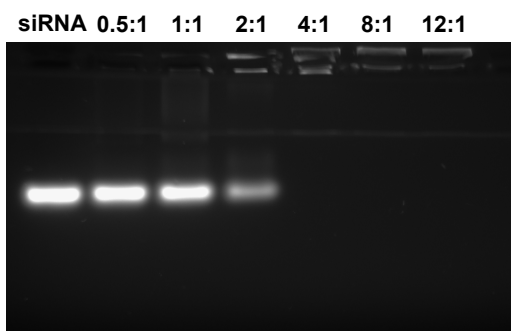
Figure 3.16. Gel retardation assay to assess PTDM / siRNA complex formation using MePh$_5$-*b*-dG$_{40}$. All samples were run on a 0.8% agarose gel and the N:P ratios tested ranged from 0.5:1 to 12:1, with 1 µg of siRNA per well.
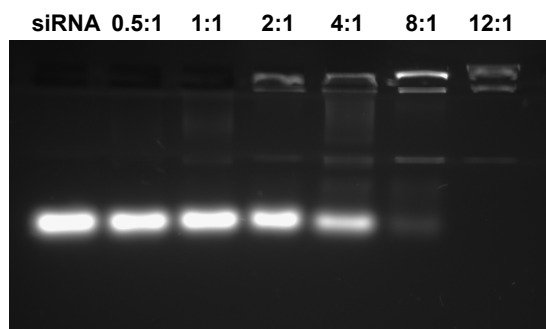
Figure 3.17. Gel retardation assay to assess PTDM / siRNA complex formation using MePh$_5$-*b*-dG$_{60}$. All samples were run on a 0.8% agarose gel and the N:P ratios tested ranged from 0.5:1 to 12:1, with 1 µg of siRNA per well.

In brief, it was demonstrated that shorter polymers (40 charges or less) completely complexed siRNA at lower N:P ratios than longer polymers (80 charges or more). In terms of media composition, it was previously reported that our ROMP-based PTDMs do not experience significant reduction in performance when tested in the presence of serum.[20] Therefore, all cell data was collected in the presence of serum.[20]

A summary of FITC-siRNA internalization efficiencies for homopolymer and block copolymer PTDMs is shown in Figure 3.18, where Figure 3.18A presents the percentage of the cell population that received FITC-siRNA and Figure 3.18B presents the median fluorescence intensity (MFI) of the cell populations. In both data sets, PTDM internalization efficiencies increased in a charge-dependent manner up to approximately 40 charges (**dG$_{20}$** and **MePh$_5$-*b*-dG$_{20}$**) and then diminish at higher charge contents. **MePh$_5$-*b*-dG$_{20}$**, with an MFI of 2,300, delivered the most siRNA, three times more than the next best PTDM, **MePh$_5$-*b*-dG$_{10}$**, with an MFI of 800. This demonstrates that there is an optimal guanidinium content necessary for efficient internalization and above that charge content, the carriers are no longer as effective and show reduced performance.
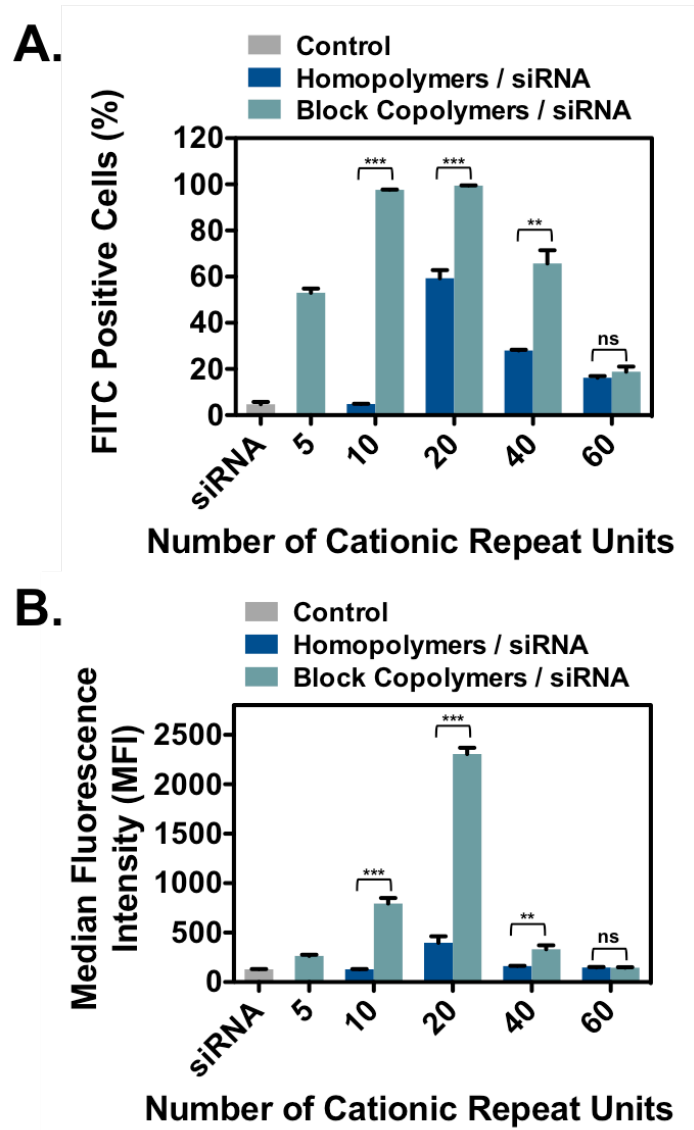
Figure 3.18. FITC-siRNA internalization in Jurkat T cells using homopolymer and block copolymer PTDMs. Jurkat T cells (cell density = 4×10^5 cells/mL) were treated with PTDM/FITC-siRNA complexes with an N:P ratio = 8:1 in complete medium for four hours at 37°C and compared to cells only receiving FITC-siRNA. All data was normalized to an untreated control. A) Percent FITC positive cells. B) Median fluorescence intensity (MFI) of the cell population. Data represents the mean ± SEM of three independent experiments. * = $p < 0.05$, ** = $p < 0.01$, *** = $p < 0.001$, ns = not significant, as calculated by the unpaired two-tailed student t-test. * represents significance between homopolymer and block copolymer PTDMs with the same charge content.
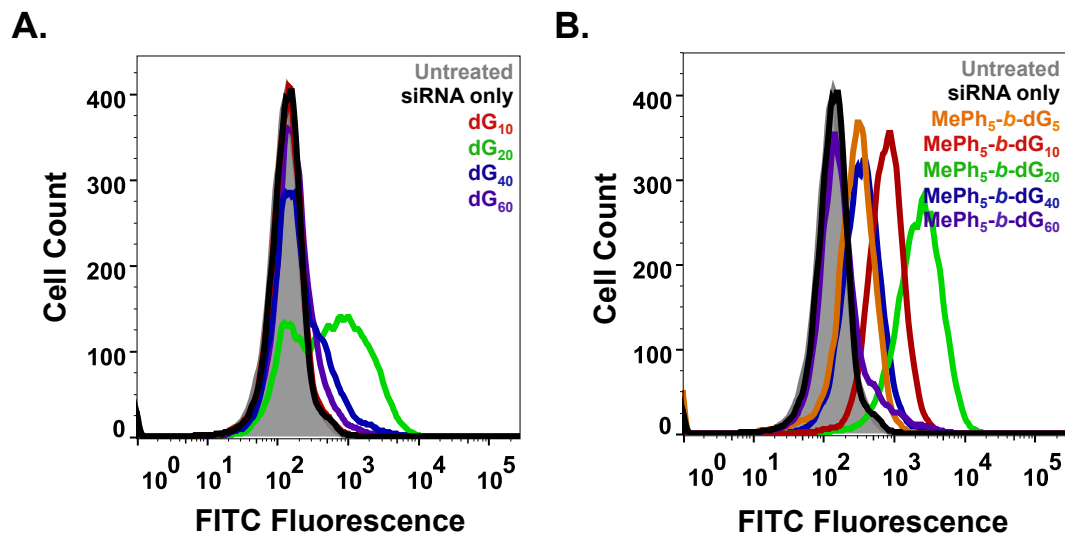
Figure 3.19. Representative histograms for FITC-siRNA delivery into Jurkat T cells using ROMP-based protein mimics. Jurkat T cells (cell density = 4×10^5 cells/mL) were treated with polymer/FITC-siRNA complexes with an N/P ratio = 8/1 in complete media for four hours at 37°C and compared with untreated cells and cells only receiving FITC-siRNA. A) Overlay of representative histograms for cells treated with homopolymer/siRNA complexes. B) Overlay of representative histograms for cells treated with block copolymer/siRNA complexes.

From this data set, it can also be seen that the block copolymer PTDMs significantly outperformed their homopolymer counterparts, particularly at charge contents of 40 or less. Both **MePh$_5$-*b*-dG$_{20}$** and **MePh$_5$-*b*-dG$_{10}$** had MFI values that were six times higher than their corresponding homopolymers (**dG$_{20}$** and **dG$_{10}$**, respectively). At larger charge contents, MFI values were similarly diminished for both homopolymer and block copolymer PTDMs. The block copolymer PTDM with 80 charges (**MePh$_5$-*b*-dG$_{40}$**) delivered FITC-siRNA to 66% of the cell population, which is approximately double the cell population that its homopolymer PTDM counterpart, **dG$_{40}$,** could reach. The observation that block copolymers outperformed their homopolymer counterparts is consistent with other reported guanidinium-rich siRNA transport molecules.[39,48] In addition to Figure 3.18, flow cytometry histograms can be found in Figure 3.19. PTDMs were also tested for their ability to deliver FITC-siRNA into HeLa cells to demonstrate

that they enabled internalization in adherent cells and to establish trends in a second cell type. Block copolymer PTDMs containing 20 and 40 charges (**MePh$_5$-*b*-dG$_{10}$** and **MePh$_5$-*b*-dG$_{20}$**) were shown to deliver double the amount of siRNA than their homopolymer counterparts. PTDMs with 80 charges (**dG$_{40}$** and **MePh$_5$-*b*-dG$_{40}$**) were able to deliver the most siRNA, with similar MFIs of 4,100 and 4,500, respectively. A significant drop-off in internalization efficiency for the largest charged segment was still observed (Figure 3.26 -Figure 3.29). All polymer-treated cells showed greater than 90% viability using 7-AAD/Annexin V staining (Figure 3.21-Figure 3.24, Figure 3.30-Figure 3.31).
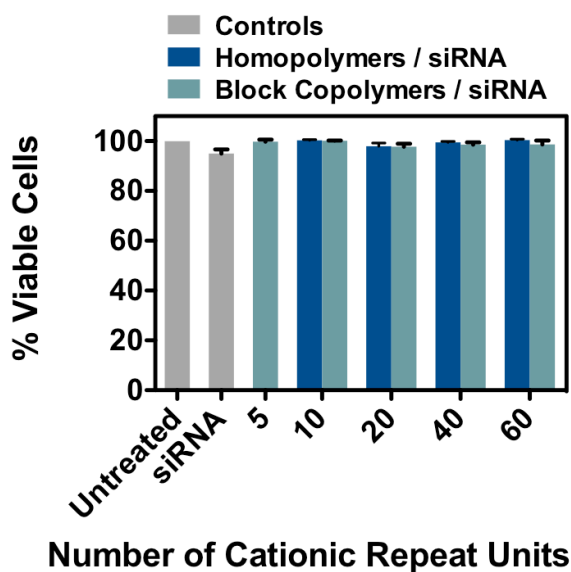
Figure 3.20. Percent viable cells using a 7-Amino-actinomycin (7-AAD) Jurkat T Cell viability assay. Jurkat T cells (cell density = 4x10^5 cells/mL) were treated with PTDM/FITC-siRNA complexes with an N:P ratio = 8:1 in complete media for four hours at 37°C and compared with untreated cells and cells only receiving FITC-siRNA. Cells were stained at four hours. Each data point represents the mean ± SEM of three independent experiments.
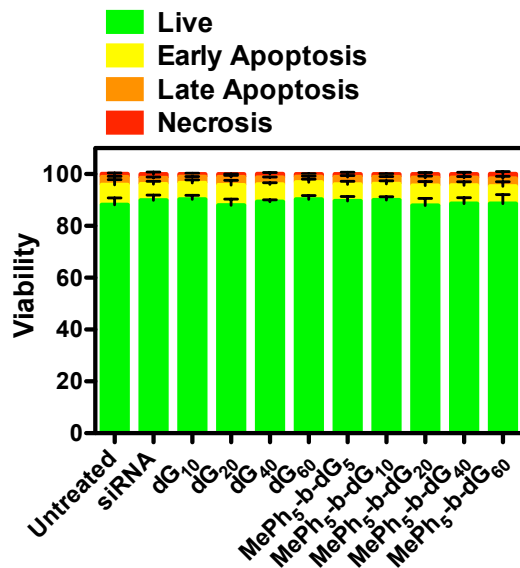
Figure 3.21. Percent viable cells using a 7-Amino-actinomycin (7-AAD) and Annexin-V Jurkat T cell viability assay. Jurkat T cells (cell density = 4×10^5 cells/mL) were treated with polymer/FITC-siRNA complexes with an N:P ratio = 8:1 in complete media for four hours at 37°C and compared with untreated cells and cells only receiving FITC-siRNA. Cells were stained at four hours. Each data point represents the mean ± SEM of three independent experiments.

In a separate viability study, promising PTDM/siRNA complexes were compared to samples that were treated with PTDMs alone in the same working concentrations used for complex formation. Cells were harvested four hours after treatment and washed. Samples were split and viability was determined on one half of the cells. The other half were re-plated in fresh serum-containing medium and viability was assessed after an additional 24 hours of incubation. This procedure not only assessed PTDM toxicity at the maximum free concentrations, but it also probed longer-term toxicity effects of the treatment. All cells exhibited greater than 90% viability as assessed by 7-AAD/Annexin V staining both at the four-hour and 24-hour time points (Figure 3.22-Figure 3.24). In addition, cells were also counted at the 24-hour time point to measure cell proliferation. All cell populations were found to approximately double over the 24-

hour period, suggesting that PTDM/siRNA treatment did not impair cell growth (Figure 3.25).
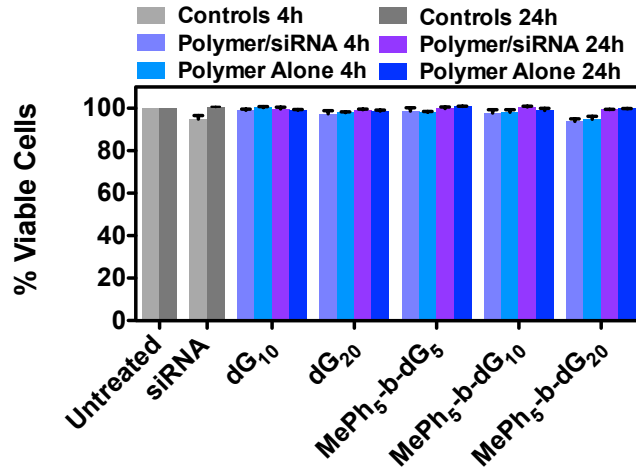
Figure 3.22. Percent viable cells using a 7-Amino-actinomycin (7-AAD) Jurkat T Cell viability assay. Jurkat T cells (cell density = $4x10^5$ cells/mL) were treated with PTDM/FITC-siRNA complexes with an N:P ratio = 8:1 or the same concentration of polymer with no siRNA in complete media for four hours at 37°C and compared with untreated cells and cells only receiving FITC-siRNA. Half of the cell populations ($2x10^5$ cells) were stained at four hours. The other half ($2x10^5$ cell) were re-plated in complete media and stained at 24 hours. Each data point represents the mean ± SEM of three independent experiments.
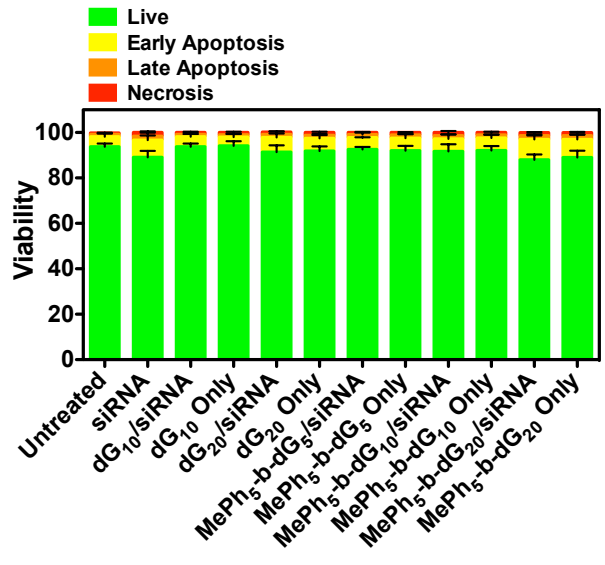
Figure 3.23. Percent viable cells using a 7-Amino-actinomycin (7-AAD) and Annexin-V Jurkat T cell viability assay at the four hour time point. Jurkat T cells (cell density = 4×10^5 cells/mL) were treated with PTDM/FITC-siRNA complexes with an N:P ratio = 8:1 or the same concentration of PTDM with no siRNA in complete media for four hours at 37°C and compared with untreated cells and cells only receiving FITC-siRNA. Half the cell populations (2×10^5 cells) were stained at four hours and the other half (2×10^5 cells) were re-plated for a 24 hour time point. Each data point represents the mean ± SEM of three independent experiments.
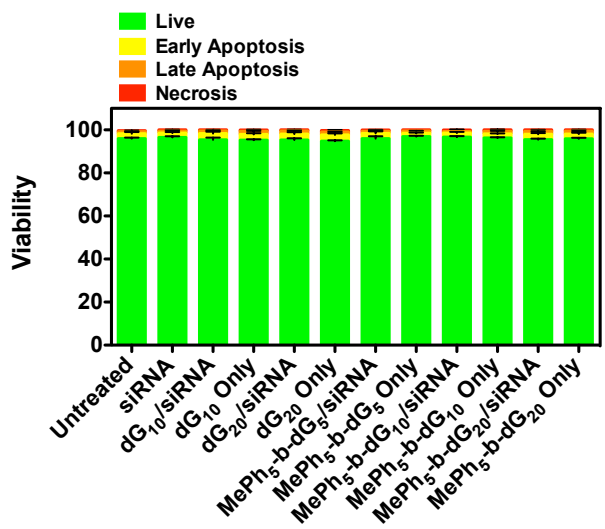
Figure 3.24. Percent viable cells using a 7-Amino-actinomycin (7-AAD) and Annexin-V Jurkat T cell viability assay at the 24 hour time point. Jurkat T cells (cell density = 4×10^5 cells/mL) were treated with PTDM/FITC-siRNA complexes with an N:P ratio = 8:1 or the same concentration of PTDM with no siRNA in complete media for four hours at 37°C and compared with untreated cells and cells only receiving FITC-siRNA. Half the cell populations (2×10^5 cells) were stained at four hours and the other half (2×10^5 cells) were re-plated and stained at the 24 hour time point. Each data point represents the mean ± SEM of three independent experiments.

Cell Counts

In addition to viability staining at 4 and 24 hr, cells were counted at 24 hr to assess proliferation. 1/20 dilution of each experimental well in trypan blue was used for cell counts. Since Jurkat T cells have a doubling time of 24 hr, it was anticipated that healthy cell populations would double by the 24 hr time point. Cells were not counted at the 4 hr time point since they were initially counted at the start of the experiment.
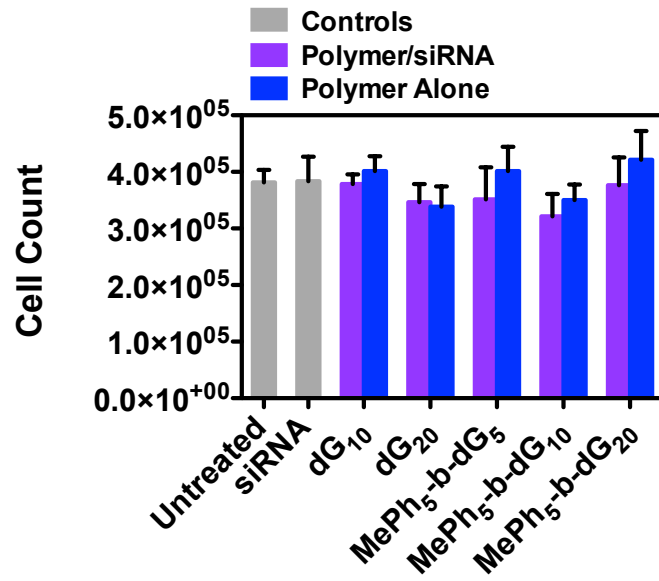
Figure 3.25. Cell counts 24 hours following PTDM/FITC-siRNA or polymer alone treatments. Jurkat T cells (cell density = 4×10^5 cells/mL) were treated with PTDM/FITC-siRNA complexes with an N:P ratio = 8:1 in complete or the same concentration of PTDM with no siRNA media for four hours at 37°C and compared with untreated cells and cells only receiving FITC-siRNA. The entire cell population was counted 24 hours. Comparison wells receiving polymer and no siRNA were also used as controls. Each data point represents the mean ± SEM of three independent experiments.
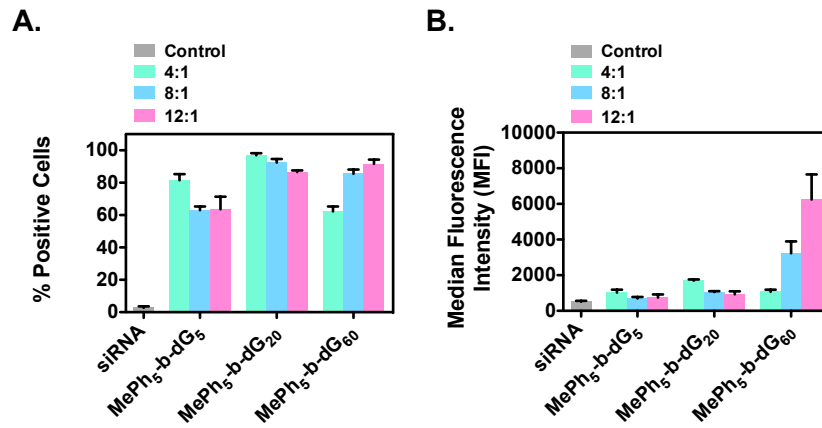
Figure 3.26. N:P ratio screening for FITC-siRNA delivery into HeLa cells using ROMP-based PTDMs. HeLa cells (cell density = 5×10^4 cells/mL 48 hours prior to experiment; 70-90% confluent on the day of the experiment) treated with polymer/FITC-siRNA complexes with an N:P ratio of either 4:1, 8:1, or 12:1 in complete media for four hours at 37°C and compared cells only receiving FITC-siRNA. All data was compared to an untreated control. A) Percent positive cells. B) MFI of the cell population. Each data point represents the mean ± SEM of three independent experiments.
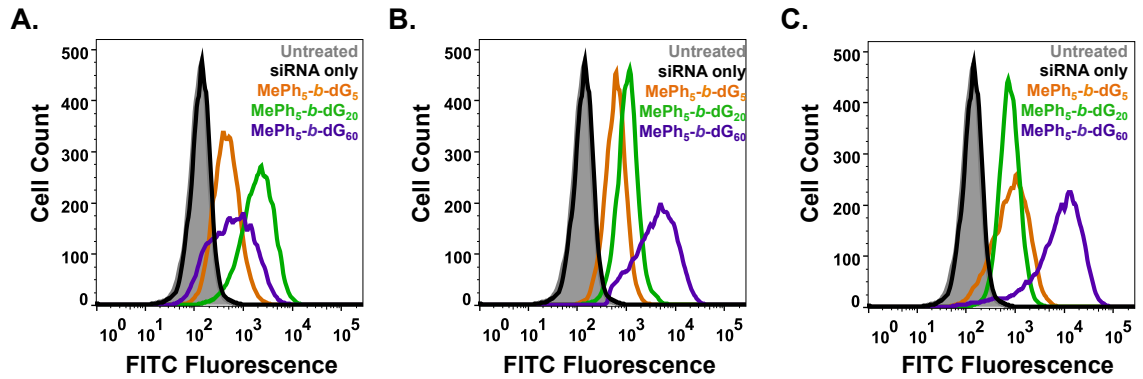
Figure 3.27. Representative histograms for FITC-siRNA delivery into HeLa cells using ROMP-based PTDMs. HeLa cells (cell density = 5×10^4 cells/mL 48 hours prior to experiment; 70-90% confluent on the day of the experiment) treated with polymer/FITC-siRNA complexes with an N:P ratio = 8:1 in complete media for four hours at 37°C and compared cells only receiving FITC-siRNA and to an untreated control. A) Overlay of representative histograms for cells treated with PTDM/siRNA complexes with an N:P = 4:1. B) Overlay of representative histograms for cells treated with PTDM/siRNA complexes with an N:P = 8:1. C) Overlay of representative histograms for cells treated with PTDM/siRNA complexes with an N:P = 12:1.
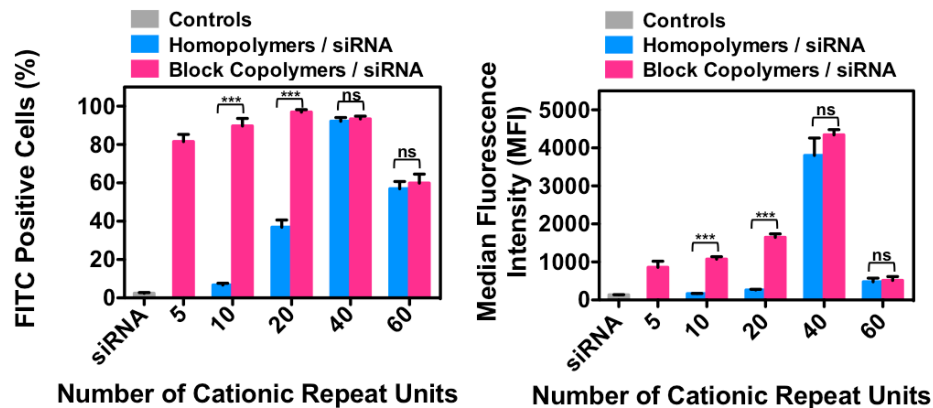
Figure 3.28. FITC-siRNA delivery into HeLa cells using ROMP-based protein mimics. HeLa cells (cell density = 5×10^4 cells/mL 48 hours prior to experiment; 70-90% confluent on the day of the experiment) treated with polymer/FITC-siRNA complexes with an N:P ratio = 8:1 in complete media for four hours at 37°C and compared cells only receiving FITC-siRNA. All data was normalized to an untreated control. A) Percent positive cells. B) MFI) of the cell population. Each data point represents the mean ± SEM of three independent experiments.
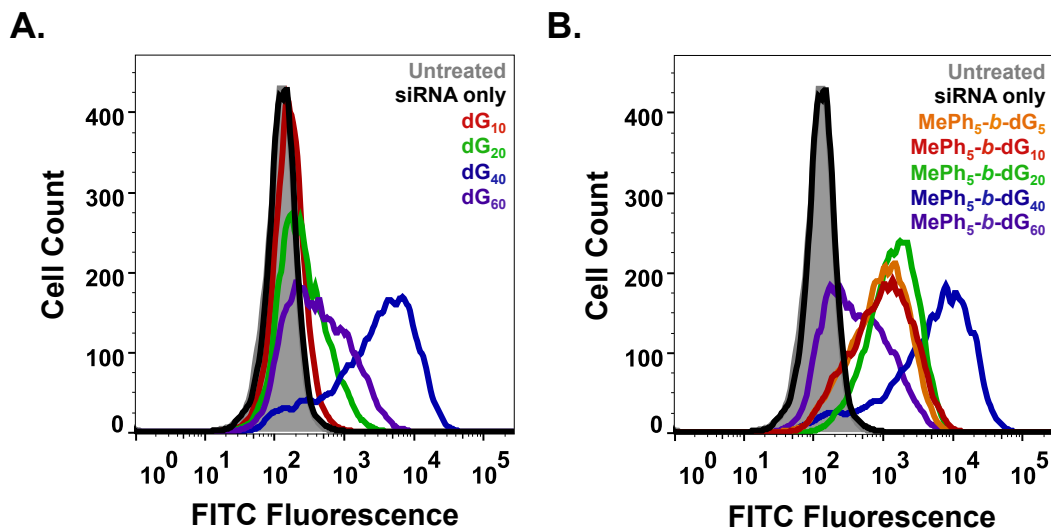
Figure 3.29. Representative histograms for FITC-siRNA delivery into HeLa cells using ROMP-based protein mimics. HeLa cells (cell density = 5x10^4 cells/mL 48 hours prior to experiment; 70-90% confluent on the day of the experiment) treated with polymer/FITC-siRNA complexes with an N:P ratio = 8:1 in complete media for four hours at 37°C and compared cells only receiving FITC-siRNA and to an untreated control. A) Overlay of representative histograms for cells treated with homopolymer/siRNA complexes. B) Overlay of representative histograms for cells treated with block copolymer/siRNA complexes.
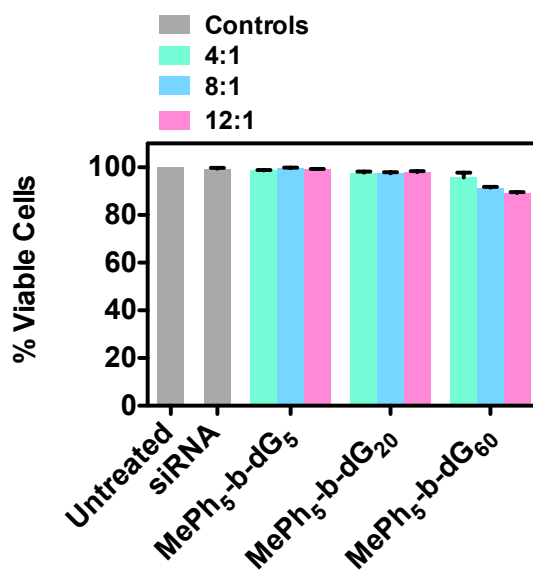
Figure 3.30. Percent viable cells using a 7-Amino-actinomycin (7-AAD) HeLa cell viability assay. HeLa cells (cell density = 5x10^4 cells/mL 48 hours prior to experiment; 70-90% confluent on the day of the experiment) were treated with polymer/FITC-siRNA complexes with an N:P ratio of either 4:1, 8:1, or 12:1 in complete media for four hours at 37°C and compared with untreated cells and cells only receiving FITC-siRNA. Cells were stained at four hours. Each data point represents the mean ± SEM of three independent experiments.
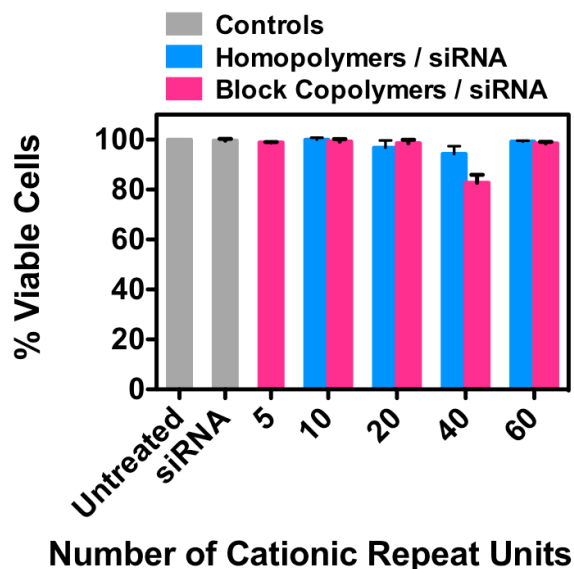
Figure 3.31. Percent viable cells using a 7-Amino-actinomycin (7-AAD) HeLa cell viability assay. HeLa cells (cell density = 5×10^4 cells/mL 48 hours prior to experiment; 70-90% confluent on the day of the experiment) were treated with polymer/FITC-siRNA complexes with an N:P ratio = 8:1 in complete media for four hours at 37°C and compared with untreated cells and cells only receiving FITC-siRNA. Cells were stained at four hours. Each data point represents the mean ± SEM of three independent experiments.

Based on these results, two block copolymer PTDMs, **MePh$_5$-*b*-dG$_5$** and **MePh$_5$-*b*-dG$_{20}$,** were compared to a range of commercial reagents commonly used for siRNA internalization and delivery, including R9 (peptide, Peptide2.0), DeliverX (peptide, Affymetrix), Xfect (polymer, ClonTech), N-Ter (peptide, Sigma Aldrich), and RNAiMAX (lipid, Life Technologies). In addition, JetPEI, a common polyethyleneimine-based pDNA delivery reagent, was included. All commercial reagents were used as directed by the vendor. A summary of FITC-siRNA internalization efficiencies for block copolymer PTDMs and commercial reagents is shown in Figure 3.32, where Figure 3.32A presents the percentage of the cell population that received FITC-siRNA and Figure 3.32B presents the MFI of the cell populations. **MePh$_5$-*b*-dG$_5$** and **MePh$_5$-*b*-dG$_{20}$** were both shown to enable internalization in a greater percentage of cells than the

93

commercial reagents (Figure 3.32A). In addition, **MePh$_5$-*b*-dG$_{20}$** resulted in a nearly 10-fold greater MFI than the commercial reagents, indicating it was able to deliver quantitatively more cargo inside the cells (Figure 3.32B-Figure 3.33**).** Viability was assessed using 7-AAD / Annexin V staining (Figure 3.33). All samples had greater than 90% viability, with the exception of samples treated with RNAiMAX, which had viabilities closer to 80% (Figure 3.34). This data demonstrates the superiority of our PTDMs for siRNA delivery compared to common commercial reagents and establishes these materials as viable delivery vehicles for hard-to-transfect T cell lines, for which options for efficient delivery are limited.
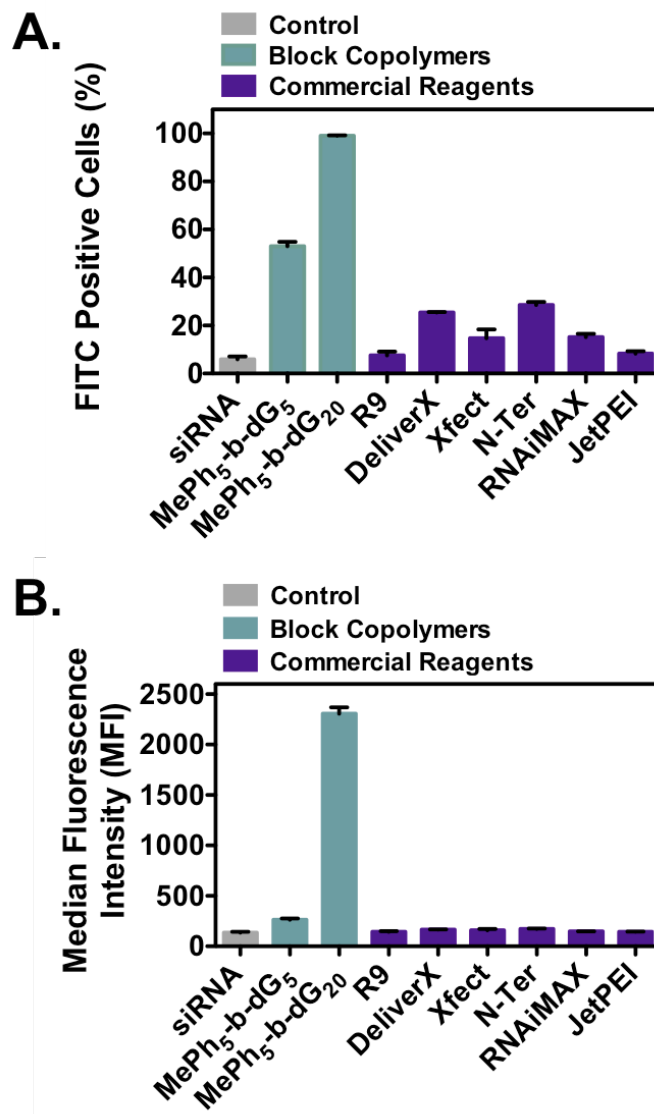
Figure 3.32. Comparison of PTDM and commercial reagent FITC-siRNA internalization efficiencies in Jurkat T cells (cell density = 4×10^5 cells/mL). Cells treated with PTDM/FITC-siRNA complexes with an N:P ratio = 8:1 or with commercial reagent/FITC-siRNA complexes (used as directed) in complete medium for four hours at 37°C and compared to cells only receiving FITC-siRNA. All data was normalized to untreated controls. A) Percent FITC positive cells. B) Median fluorescence intensity (MFI) of the cell population. Data represents the mean ± SEM of three independent experiments. All PTDM data is statistically different from the commercial reagents (p <0.001) as calculated by the unpaired two-tailed student t-test.
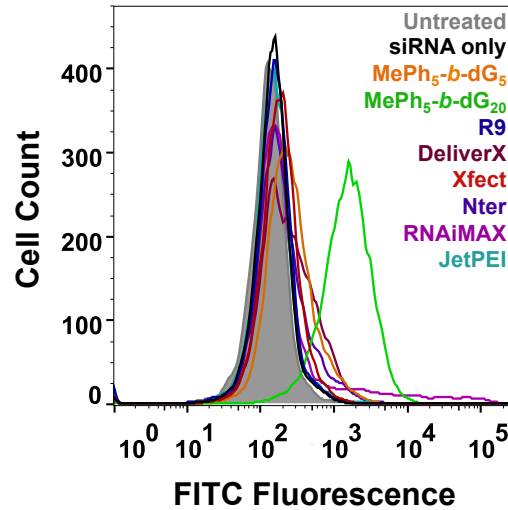
Figure 3.33. Representative histograms for FITC-siRNA delivery into Jurkat T cells using ROMP-based protein mimics and commercially available reagents. Jurkat T cells (cell density = 4×10^5 cells/mL) were treated with polymer/FITC-siRNA complexes with an N:P ratio = 8:1 in complete media for four hours at 37°C and compared with untreated cells and cells only receiving FITC-siRNA.
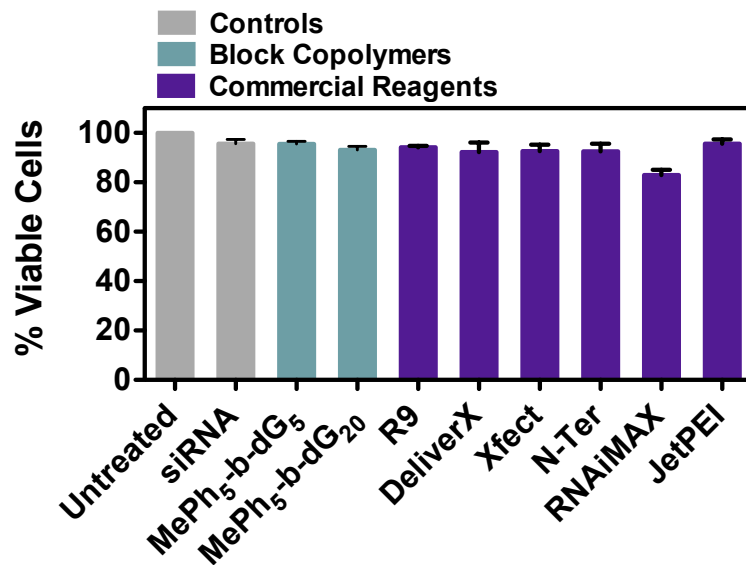
Figure 3.34. Percent viable cells using a 7-Amino-actinomycin (7-AAD) Jurkat T Cell viability assay. Jurkat T cells (cell density = 4×10^5 cells/mL) were treated with PTDM/FITC-siRNA complexes with an N:P ratio = 8:1 or commercial reagents/FITC-siRNA complexes used as directed in complete media for four hours at 37°C and compared with untreated cells and cells only receiving FITC-siRNA. Cells were stained at four hours. Each data point represents the mean ± SEM of three independent experiments.

3.4 Delivery of Biologically Active siRNA to *NOTCH1*

Based on the FITC-siRNA internalization results from Jurkat T cells, four promising PTDMs (**MePh$_5$-*b*-dG$_5$, MePh$_5$-*b*-dG$_{10}$, MePh$_5$-*b*-dG$_{20}$**, and **dG$_{20}$**) were screened for delivery of a biologically active siRNA to *NOTCH1*. NOTCH1 was selected as the primary target for siRNA knockdown studies because it represents an active gene in T cells. Unlike looking at a reporter gene, which is not required for normal cellular activities, the gene of interest is required for cellular function and represents a more sophisticated and realistic system for knockdown assessment. Although NOTCH1 protein is constitutively expressed in Jurkat T cells, it is a mutation in the *NOTCH1* gene together with increased NOTCH1 protein stability that gives the T cell line its immortality, thus making down regulation of NOTCH1 expression difficult to monitor. To overcome this limitation, hPBMCs were used in *NOTCH1* down regulation experiments. At the same time, demonstrating robust delivery into primary T cells is of critical practical importance. hPBMCs, which are a mixed population of primary lymphocytes and monocytes obtained from human donors, were cultured overnight to enrich for the viable cell population, most of which were CD4+ and CD8+ T cells. Surface staining cells at the 48 hour time point to check for CD4 and CD8 expression revealed that approximately 30% of the population was CD8+ and approximately 50% of the population was CD4+. The gating strategy for this determination is shown in Figure 3.35.
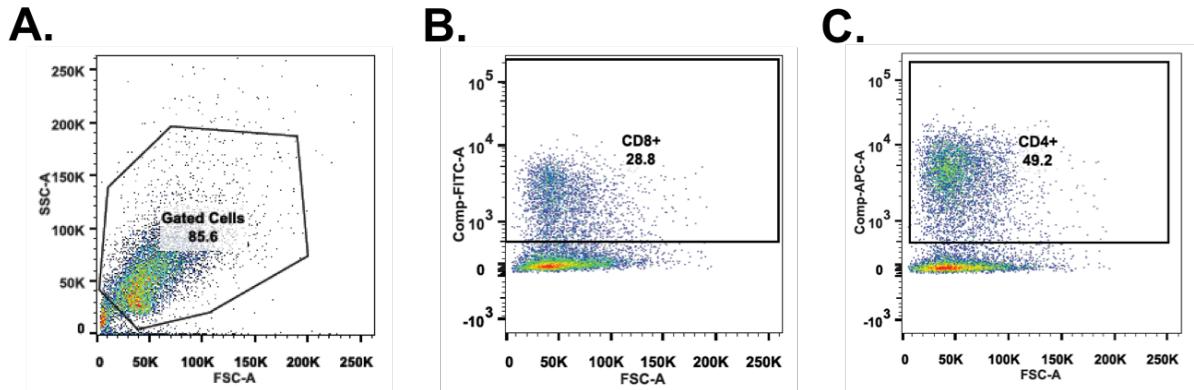
Figure 3.35. Representative flow cytometry cell gating to determine the fraction of the population that represent CD8+T cells and CD4+ T cells. A) Plot of forward vs. side scatter showing the gate on the cell population used for analysis. B) Plot of FITC fluorescence vs. forward scatter showing the gate on the FITC-positive cells (CD8+ T cells). C) Plot of APC fluorescence vs. forward scatter showing the gate on the APC-positive cells (CD4+ T cells).

In these experiments, hPBMCs were treated with PTDM/siRNA complexes for four hours in serum-containing medium. A fixed amount of siRNA (100nM) was used for each experiment to assess the effect PTDM structure has on knockdown efficiencies. Specifically, within the block copolymer architecture, the length of the cationic sequence was examined. After four hours, the cells were transferred to anti-CD3 and anti-CD28-coated well plates for stimulation and allowed to incubate for 48 hours. T cell stimulation will result in an induction in NOTCH1 expression and allow us to assess the effect treatment had on NOTCH1 protein levels in comparison to untreated samples. This time point was selected because it is the point of maximum protein expression, and we expect the cells that successfully received siRNA to *NOTCH1* would have decreased protein expression compared to the untreated controls. Flow cytometry was used as the primary method to analyze protein expression, enabling us to stain for protein content and quantify the extent to which protein levels were reduced on a per cell basis.

The percent relative protein expression data for these experiments is shown in Figure 3.36, all gated histograms are shown in Figure 3.37, and a summary of the MFI data can be found in Figure 3.38. In this case, percent relative protein expression is the MFI of the total population multiplied by the percent NOTCH1 positive population all normalized to an untreated blank.
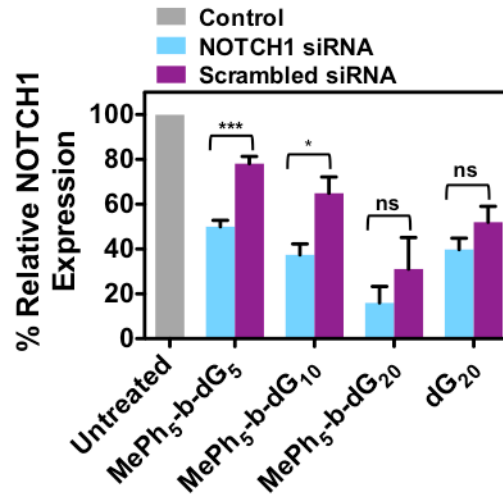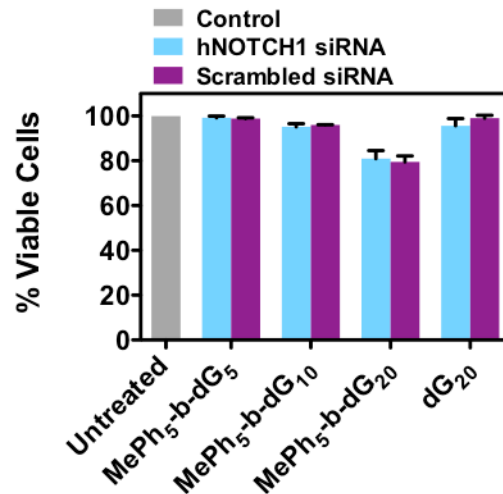
Figure 3.36. Relative NOTCH1 expression levels in PBMCs and their corresponding viabilities (cell density = 1×10^6 cells/mL). Cells were treated with PTDM/NOTCH1 siRNA complexes or PTDM/scrambled siRNA with an N:P ratio = 8:1 in complete media for four hours at 37°C. After treatment, cells were washed and then stimulated with plate-bound anti-CD3 and anti-CD28 for 48 hours. All data was normalized to an untreated control (grey bar). A) Relative NOTCH1 levels in PBMCs after 48-hour treatment with PTDM/NOTCH1 siRNA (light blue bars) or PTDM/scrambled siRNA complexes (purple bars). B) Percent viable cells following staining with 7-AAD. Data represents the mean ± SEM of four independent experiments using cells isolated from different donors. * = $p <$ 0.05, ** = $p < 0.01$, *** = $p < 0.001$, ns = not significant, as calculated by the unpaired two-tailed student *t*-test.
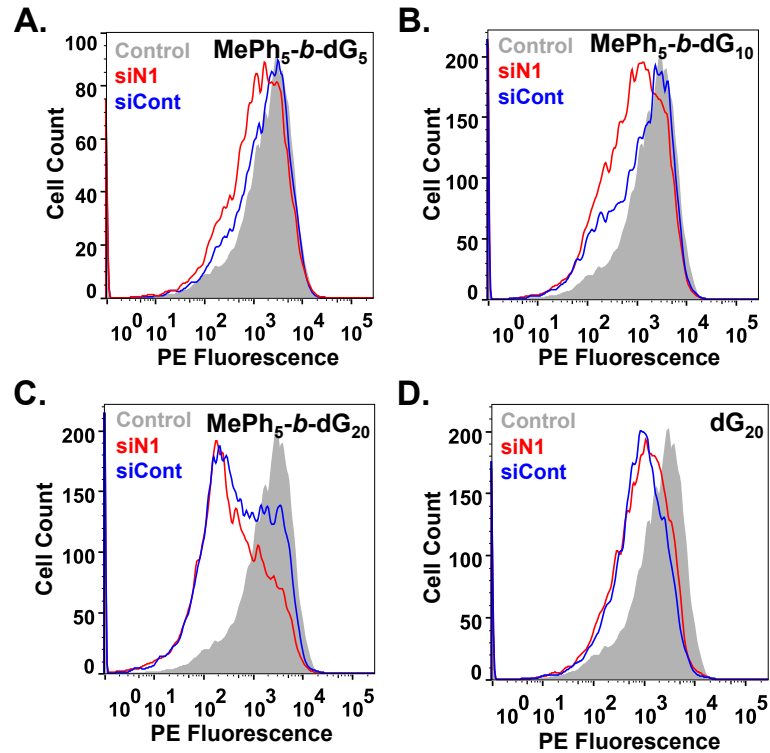
Figure 3.37. Representative histograms for *hNOTCH1* knockdown in PBMCs using ROMP-based PTDMs. PBMCs (cell density = 1×10^6 cells/mL). Cells treated with PTDM/siN1 complexes or PTDM/siCont with an N:P ratio = 8:1 in complete media for four hours at 37°C. After treatment, cells were washed and then stimulated with plate-bound anti-CD3 and anti-CD28 for 48 hours. Untreated samples, samples receiving *hNOTCH1* siRNA (siN1), and samples receiving scrambled control siRNA (siCont) are represented in grey, red, and blue, respectively.

For the PTDM with the shortest cationic sequence, **MePh$_5$-*b*-dG$_5$**, NOTCH1 expression was reduced to ~50%, which is significant given that *NOTCH1* is not a reporter gene. Doubling the cationic length with **MePh$_5$-*b*-dG$_{10}$** resulted in a lower NOTCH1 expression of ~37%. The lowest NOTCH1 expression obtained, ~16%, was observed for **MePh$_5$-b-dG$_{20}$**. This data was consistent with the previous data shown in Figure 3.18 and Figure 3.32, which support the suggestion that this PTDM is able to deliver the most siRNA into PBMCs. In fact, it appears that for these experiments with 100 nM siRNA that **MePh$_5$-*b*-dG$_{20}$** delivers too much siRNA since resolution was lost between the target (light blue bars) and scrambled siRNA (purple bars), a common observation when excess siRNA is

present intracellularly.[72-75] Although reducing the siRNA concentration may help limit these effects[73-75], sequence overlaps with target and off-target mRNAs are also a contributing factor and may be present, even at reduced concentrations.[72,76] Better screening for scrambled controls that avoid the target mRNA sequence would be expected to improve the specificity of NOTCH1 knockdown experiments.[76] While the primary goal of this study was to explore how the polymer structures impact siRNA delivery efficiencies, future studies will be geared towards optimizing these materials for improved specificity.

When evaluating protein expression, it was critical to assess cell viability to ensure that diminished protein expression was not due to cell death. Since monitoring protein content by flow cytometry requires cells to be fixed, cell samples were split after harvest to determine cell viability on the unfixed population. hPBMC viability was assessed by staining with 7-AAD, a DNA-intercalating dye that is excluded from live cells but taken up by dead and dying cells that have compromised membrane integrity. As shown in Figure 3.36B, all samples were greater than 80% viable, which suggests that reduced protein expression in the cells is a consequence of PTDM/siRNA treatment and not due to cell death.
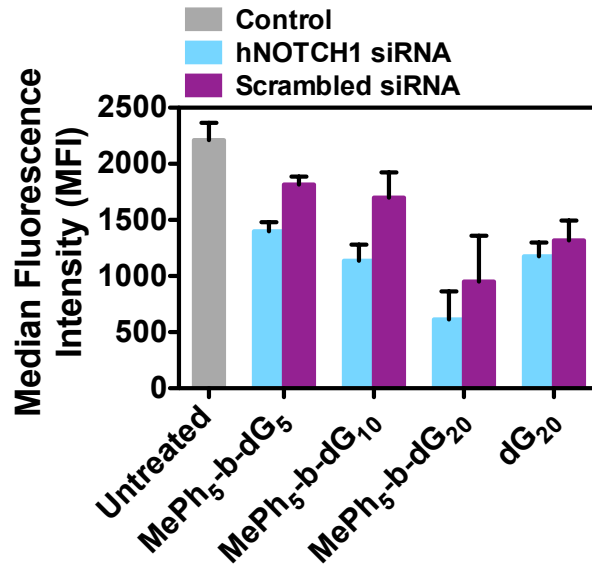
Figure 3.38. MFI for hNOTCH1 protein in hPBMCs (cell density = 1×10^6 cells/mL). Cells treated with PTDM/hNOTCH1 siRNA complexes or PTDM/scrambled siRNA with an N/P ratio = 8/1 in complete media for four hours at 37°C. After treatment, cells were washed and then stimulated with plate-bound anti-CD3 and anti-CD28 for 48 hours. All data was normalized to an untreated control. Each data point represents the mean ± SEM of four independent experiments.

In addition to using flow cytometry, a western blot was used to monitor protein reduction in cells treated with siRNA to *NOTCH1* or treated with scrambled siRNA as they compared to untreated cells for **MePh$_5$-*b*-dG$_{20}$** (Figure 3.39). This data was consistent with the flow cytometry data.
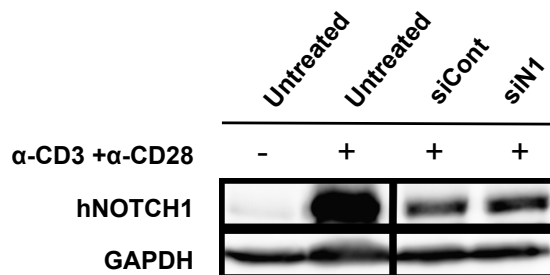
Figure 3.39. Western blot analysis showing knockdown of NOTCH1 by **MePh$_5$-*b*-dG$_{20}$**. Unstimulated, untreated cells (lane 1), untreated, stimulated cells (lane 2), treated with **MePh$_5$-*b*-dG$_{20}$**/scrambled siRNA complexes (siCont, lane 3) or **MePh$_5$-*b*-dG$_{20}$**/NOTCH1 siRNA complexes (siN1, lane 4). Total protein lysates were immunoblotted with antibodies that detect the active NOTCH1 intracellular domain and GAPDH. Untreated, unstimulated PBMCs (lane 1) were included as a negative control of the active NOTCH1 intracellular domain. siCont stands for scrambled siRNA and siN1 stands for siRNA to *NOTCH1*.

3.5 Conclusions

RNAi is an attractive approach to study gene function and has potential for therapeutic applications involving T cells due to its transient knockdown of target proteins; however, difficulties in delivery to these cell types limit its use. In efforts to address an unmet need in the area of T cell delivery and to better understand how polymer composition impacts delivery and knockdown efficiencies, we report the development of two guanidinium-rich PTDM series for siRNA delivery. Homopolymer and block copolymer PTDMs with varying cationic charge contents were tested to assess the role of cationic charge content and the addition of a segregated, hydrophobic block in the internalization of FITC-siRNA in Jurkat T cells and knockdown of *hNOTCH1* in hPBMCs. FITC-siRNA internalization in Jurkat T cells demonstrated that there was an optimal cationic charge content necessary for efficient delivery (40 charges), which, once surpassed, resulted in diminished delivery capabilities. Cells incubated with PTDMs and their corresponding siRNA complexes exhibited greater than 90% viability using 7-AAD/Annexin-V staining. Block copolymers also significantly outperformed commercial reagents designed for siRNA delivery, making these PTDMs potential alternatives for T cell siRNA transfections. Based on the FITC-siRNA internalization results, select PTDM candidates were screened for knockdown of *NOTCH1* in hPBMCs. For this set of PTDMs, protein expression was reduced as the cationic charge content increased, with the block copolymer PTDM **MePh$_5$-*b*-dG$_{20}$** providing the most reduction in protein expression. Viability data indicated that knockdown was due to PTDM/siRNA treatment and not cell death. Overall, optimization of the cationic charge content led to improved delivery efficiencies, as well as improved knockdown efficiencies. This demonstrates the importance of understanding the essential PTDM design parameters for delivery of siRNA and will help guide the design of the next generation of efficient PTDMs.

3.6 Acknowledgement

3.7 References

(1)   de Planque, M. R.; Bonev, B. B.; Demmers, J. A.; Greathouse, D. V.; Koeppe, R. E., 2nd; Separovic, F.; Watts, A.; Killian, J. A. *Biochemistry* **2003**, *42*, 5341-5348.

(2)   Kim, J.; Lee, S. H.; Choe, J.; Park, T. G. *J Gene Med* **2009**, *11*, 804-812.

(3)   Mello, C. C.; Conte, D. *Nature* **2004**, *431*, 338-342.

(4)   Vicentini, F. T. M. D.; Borgheti-Cardoso, L. N.; Depieri, L. V.; Mano, D. D.; Abelha, T. F.; Petrilli, R.; Bentley, M. V. L. B. *Pharm. Res.* **2013**, *30*, 915-931.

(5)   Whitehead, K. A.; Langer, R.; Anderson, D. G. *Nat. Rev. Drug Discov.* **2009**, *8*, 129-138.

(6)   Carthew, R. W. *Curr. Opin. Cell Biol.* **2001**, *13*, 244-248.

(7)   Elbashir, S. M.; Harborth, J.; Lendeckel, W.; Yalcin, A.; Weber, K.; Tuschl, T. *Nature* **2001**, *411*, 494-498.

(8)   Meister, G.; Tuschl, T. *Nature* **2004**, *431*, 343-349.

(9)   Behlke, M. A. *Mol. Ther.* **2006**, *13*, 644-670.

(10)   Mantei, A.; Rutz, S.; Janke, M.; Kirchhoff, D.; Jung, U.; Patzel, V.; Vogel, U.; Rudel, T.; Andreou, I.; Weber, M.; Scheffold, A. *European Journal of Immunology* **2008**, *38*, 2616-2625.

(11)   Rutz, S.; Scheffold, A. *Arthritis Res. Ther.* **2004**, *6*, 78-85.

(12)   Freeley, M.; Long, A. *Biochem. J.* **2013**, *455*, 133-147.

(13)   Goffinet, C.; Keppler, O. T. *Faseb Journal* **2006**, *20*, 500-+.

(14)   Lai, W.; Chang, C. H.; Farber, D. L. *J. Immunol. Methods* **2003**, *282*, 93-102.

(15)   Marodon, G.; Mouly, E.; Blair, E. J.; Frisen, C.; Lemoine, F. M.; Klatzmann, D. *Blood* **2003**, *101*, 3416-3423.

(16)   McManus, M. T.; Haines, B. B.; Dillon, C. P.; Whitehurst, C. E.; van Parijs, L.; Chen, J. Z.; Sharp, P. A. *J. Immunol.* **2002**, *169*, 5754-5760.

(17)   Zhang, Y. F.; Lu, H. Z.; LiWang, P.; Sili, U.; Templeton, N. S. *Mol. Ther.* **2003**, *8*, 629-636.

(18)   deRonde, B. M.; Tew, G. N. *Biopolymers* **2015**.

(19)   Sgolastra, F.; deRonde, B. M.; Sarapas, J. M.; Som, A.; Tew, G. N. *Acc. Chem. Res.* **2013**.

(20)   Tezgel, A. O.; Gonzalez-Perez, G.; Telfer, J. C.; Osborne, B. A.; Minter, L. M.; Tew, G. N. *Mol Ther* **2013**, *21*, 201-209.

(21)   Frankel, A. D.; Pabo, C. O. *Cell* **1988**, *55*, 1189-1193.

(22)   Green, M.; Loewenstein, P. M. *Cell* **1988**, *55*, 1179-1188.

(23)   Joliot, A.; Pernelle, C.; Deagostinibazin, H.; Prochiantz, A. *Proc Natl Acad Sci U S A* **1991**, *88*, 1864-1868.

(24)   Derossi, D.; Chassaing, G.; Prochiantz, A. *Trends Cell Biol* **1998**, *8*, 84-87.

(25)   Derossi, D.; Joliot, A. H.; Chassaing, G.; Prochiantz, A. *J Biol Chem* **1994**, *269*, 10444-10450.

(26)   Fawell, S.; Seery, J.; Daikh, Y.; Moore, C.; Chen, L. L.; Pepinsky, B.; Barsoum, J. *Proc Natl Acad Sci U S A* **1994**, *91*, 664-668.

(27)   Mitchell, D. J.; Kim, D. T.; Steinman, L.; Fathman, C. G.; Rothbard, J. B. *J. Pept. Res.* **2000**, *56*, 318-325.

(28)   Vives, E.; Brodin, P.; Lebleu, B. *J Biol Chem* **1997**, *272*, 16010-16017.

(29)   Wender, P. A.; Mitchell, D. J.; Pattabiraman, K.; Pelkey, E. T.; Steinman, L.; Rothbard, J. B. *Proc. Natl. Acad. Sci. U. S. A.* **2000**, *97*, 13003-13008.

(30)   Crombez, L.; Morris, M. C.; Deshayes, S.; Heitz, F.; Divita, G. *Curr. Pharm. Design* **2008**, *14*, 3656-3665.

(31)   Simeoni, F.; Morris, M. C.; Heitz, F.; Divita, G. *Nucleic Acids Res.* **2003**, *31*, 2717-2724.

(32)   Stanzl, E. G.; Trantow, B. M.; Vargas, J. R.; Wender, P. A. *Acc Chem Res* **2013**, *46*, 2944-2954.

(33)   Brogden, K. A. *Nat Rev Microbiol* **2005**, *3*, 238-250.

(34)   Som, A.; Vemparala, S.; Ivanov, I.; Tew, G. N. *Biopolymers* **2008**, *90*, 83-93.

(35)   Gabriel, G. J.; Som, A.; Madkour, A. E.; Eren, T.; Tew, G. N. *Mater Sci Eng R Rep* **2007**, *57*, 28-64.

(36)   Kuroda, K.; Caputo, G. A. *Wiley Interdiscip Rev Nanomed Nanobiotechnol* **2013**, *5*, 49-66.

(37)   Tew, G. N.; Scott, R. W.; Klein, M. L.; Degrado, W. F. *Acc Chem Res* **2010**, *43*, 30-39.

(38)   Cooley, C. B.; Trantow, B. M.; Nederberg, F.; Kiesewetter, M. K.; Hedrick, J. L.; Waymouth, R. M.; Wender, P. A. *J Am Chem Soc* **2009**, *131*, 16401-16403.

(39)   Geihe, E. I.; Cooley, C. B.; Simon, J. R.; Kiesewetter, M. K.; Edward, J. A.; Hickerson, R. P.; Kaspar, R. L.; Hedrick, J. L.; Waymouth, R. M.; Wender, P. A. *Proc Natl Acad Sci U S A* **2012**, *109*, 13171-13176.

(40)   Kim, S. H.; Jeong, J. H.; Kim, T. I.; Kim, S. W.; Bull, D. A. *Mol Pharm* **2009**, *6*, 718-726.

(41)   Kim, S. H.; Jeong, J. H.; Ou, M.; Yockman, J. W.; Kim, S. W.; Bull, D. A. *Biomaterials* **2008**, *29*, 4439-4446.

(42)   Tabujew, I.; Freidel, C.; Krieg, B.; Helm, M.; Koynov, K.; Mullen, K.; Peneva, K. *Macromol Rapid Commun* **2014**, *35*, 1191-1197.

(43)   Tezgel, A. O.; Telfer, J. C.; Tew, G. N. *Biomacromolecules* **2011**, *12*, 3078-3083.

(44)   Wender, P. A.; Huttner, M. A.; Staveness, D.; Vargas, J. R.; Xu, A. F. *Mol Pharm* **2015**, *12*, 742-750.

(45)   Kolonko, E. M.; Kiessling, L. L. *J Am Chem Soc* **2008**, *130*, 5626-+.

(46)   Kolonko, E. M.; Pontrello, J. K.; Mangold, S. L.; Kiessling, L. L. *J Am Chem Soc* **2009**, *131*, 7327-7333.

(47)   Strong, L. E.; Kiessling, L. L. *J Am Chem Soc* **1999**, *121*, 6193-6196.

(48)   Treat, N. J.; Smith, D.; Teng, C.; Flores, J. D.; Abel, B. A.; York, A. W.; Huang, F.; McCormick, C. L. *ACS Macro Lett* **2012**, *1*, 100-104.

(49)   Gabriel, G. J.; Madkour, A. E.; Dabkowski, J. M.; Nelson, C. F.; Nusslein, K.; Tew, G. N. *Biomacromolecules* **2008**, *9*, 2980-2983.

(50)   Hennig, A.; Gabriel, G. J.; Tew, G. N.; Matile, S. *J. Am. Chem. Soc.* **2008**, *130*, 10338-10344.

(51)   Hennig, A.; Gabriel, G. J.; Tew, G. N.; Matile, S. *J Am Chem Soc* **2008**, *130*, 10338-10344.

(52)   Som, A.; Tezgel, A. O.; Gabriel, G. J.; Tew, G. N. *Angew Chem Int Ed Engl* **2011**, *50*, 6147-6150.

(53)   Som, A.; Reuter, A.; Tew, G. N. *Angew Chem Int Ed Engl* **2012**, *51*, 980-983.

(54)   deRonde, B. M.; Birke, A.; Tew, G. N. *Chem Eur J* **2015**, *21*, 3013-3019.

(55)   Sgolastra, F.; Minter, L. M.; Osborne, B. A.; Tew, G. N. *Biomacromolecules* **2014**, *15*, 812-820.

(56)   Osborne, B. A.; Minter, L. M. *Nature Reviews Immunology* **2007**, *7*, 64-75.

(57)   White, S. H.; Wimley, W. C. *Annu. Rev. Biophys. Biomol. Struct.* **1999**, *28*, 319-365.

(58)   Wimley, W. C.; White, S. H. *Nat. Struct. Biol.* **1996**, *3*, 842-848.

(59)   Lienkamp, K.; Madkour, A. E.; Musante, A.; Nelson, C. F.; Nusslein, K.; Tew, G. N. *J Am Chem Soc* **2008**, *130*, 9836-9843.

(60)   Deshayes, S.; Morris, M.; Heitz, F.; Divita, G. *Adv Drug Deliv Rev* **2008**, *60*, 537-547.

(61)   Elliott, G.; O'Hare, P. *Cell* **1997**, *88*, 223-233.

(62)   Lindgren, M.; Langel, U. *Cell-Penetrating Peptides: Methods and Protocols* **2011**, *683*, 3-19.

(63)   Love, J. A.; Morgan, J. P.; Trnka, T. M.; Grubbs, R. H. *Angew Chem Int Ed Engl* **2002**, *41*, 4035-4037.

(64)   Cannizzo, L. F.; Grubbs, R. H. *Macromolecules*, *21*, 1961-1967.

(65)   Schwab, P.; France, M. B.; Ziller, J. W.; Grubbs, R. H. *Angew Chem Int Ed Engl* **1995**, *34*, 2039-2041.

(66)   Singh, R.; Czekelius, C.; Schrock, R. R. *Macromolecules* **2006**, *39*, 1316-1317.

(67)   Bielawski, C. W.; Grubbs, R. H. *Prog. Polym. Sci.* **2007**, *32*, 1-29.

(68)   Schrock, R. R.; Hoveyda, A. H. *Angew Chem Int Ed Engl* **2003**, *42*, 4592-4633.

(69)   Trnka, T. M.; Grubbs, R. H. *Acc Chem Res* **2001**, *34*, 18-29.

(70)   Bielawski, C. W.; Grubbs, R. H. *Angew Chem Int Ed Engl* **2000**, *39*, 2903-2906.

(71)   Bielawski, C. W.; Benitez, D.; Grubbs, R. H. *J Am Chem Soc* **2003**, *125*, 8424-8425.

(72)   Fedorov, Y.; Anderson, E. M.; Birmingham, A.; Reynolds, A.; Karpilow, J.; Robinson, K.; Leake, D.; Marshall, W. S.; Khvorova, A. *RNA* **2006**, *12*, 1188-1196.

(73)   Jackson, A. L.; Linsley, P. S. *Nat. Rev. Drug Discov.* **2010**, *9*, 57-67.

(74)   Persengiev, S. P.; Zhu, X.; Green, M. R. *RNA* **2004**, *10*, 12-18.

(75)   Semizarov, D.; Frost, L.; Sarthy, A.; Kroeger, P.; Halbert, D. N.; Fesik, S. W. *Proc. Natl. Acad. Sci. U. S. A.* **2003**, *100*, 6347-6352.

(76)   Jackson, A. L.; Burchard, J.; Schelter, J.; Chau, B. N.; Cleary, M.; Lim, L.; Linsley, P. S. *RNA* **2006**, *12*, 1179-1187.

CHAPTER 4

CRITICAL HYDROPHOBIC CONTENT IN ROMP-BASED PROTEIN MIMICS

REQUIRED FOR EFFICENT SIRNA INTERNALIZATION

4.1   Introduction

Intracellular delivery of therapeutics, particularly siRNA, continues to be a challenge for the biomedical community.[1,2]   Transient gene knockdown plays an important role in the exploration of molecular pathways and in the development of more advanced treatment options; the field, however, needs a clearer understanding of how to efficiently and reliably deliver bioactive molecules across cellular membranes, particularly in primary human cells.[2-8]   Nature, however, is already capable of designing proteins that can perform these functions.[9-11]   One example is HIV-1 TAT, which is responsible for the spread of the viral genome of HIV.[9,10]   This protein contains a region referred to as a protein transduction domain (PTD), which is primarily responsible for its ability to enter cells.[12-14]   These regions in proteins are generally cation-rich, containing lysine and arginine residues which aid in cellular uptake. Structure-activity relationships (SARs) related to this protein, as well as others such the *Antennapedia* homeodomain protein, led to the development of cell-penetrating peptides (CPPs). These peptides are capable of delivering cargo such as small molecules, siRNA, pDNA, and proteins into cells using covalent or non-covalent interactions.[15-20] Three examples of CPPs include TAT$_{49-57}$, which is an arginine-rich peptide based on the PTD of the HIV-1 TAT protein, and Pep-1 and MPG, which are lysine-rich primary, amphipathic peptides.[13,14,20-24]

Although extensive work has been devoted to exploring CPPs for siRNA delivery applications[24-27], the extension of design principles learned from these systems to the development of synthetic mimics, referred to as cell-penetrating peptide mimics

(CPPMs) or protein transduction domain mimics (PTDMs), offers many distinct advantages.[28,29] Breaking out of the synthetic confinement of amino acids, a wider range of chemistries can be used to manipulate key features of CPPs, including a segregated hydrophobic component and cationic charge content, primarily in the form of guanidinium moieties.[28] The field of mimetic polymer chemistry has demonstrated the utility of a range of polymer scaffolds for the development of siRNA delivery reagents[28,30,31], including an oxanorbornene-based scaffold[28,30,32], a polymethacrylamide-based scaffold[33], an arginine-grafted bioreducible polydisulfide-based scaffold[34,35], and an oligocarbonate-based scaffold.[36-38] A similar design rationale was successfully used for the design of antimicrobial peptides, where the facially amphiphilic structures of antimicrobial peptides were successfully mimicked using highly modular synthetic scaffolds.[39-43] In order to realize the full potential of these PTDM materials and continue to improve internalization and delivery efficiencies, extensive SARs studies are necessary to elucidate key design parameters.

To this end, our research group has devoted an extensive amount of research into understanding how the structures of our ring-opening metathesis (ROMP) based protein mimics influence their membrane interactions[29,40,44-48], cellular uptake efficiencies[29,49], and siRNA delivery efficiencies.[30,32] With respect to siRNA delivery, our group has demonstrated the utility of our platform for the successful internalization of siRNA and for the knockdown of active biological genes in T cells.[30,32] Previous SARs established that there was a critical cationic block length required for efficient siRNA delivery, which, not surprisingly, showed some cell-type dependencies.[32] Additionally, the incorporation of a fixed-length, segregated, hydrophobic segment into our block copolymer PTDM structures improved siRNA internalization efficiencies by six fold compared to their homopolymer counterparts with the same relative cationic block

lengths.[32] From our preliminary studies, a great deal was learned about the cationic block length of our PTDMs;[32] however, further studies were needed to understand how the amount and type of hydrophobic content influenced siRNA internalization efficiencies.

Many literature reports demonstrate that adding hydrophobicity, either through direct incorporation or through the use of bulky counter ions, generally improves membrane interactions, cellular uptake, and delivery efficiencies of CPPs and their synthetic mimics.[30,32,37,47,48,50-55] Pep-1 and MPG, two common CPPs used for protein and siRNA delivery, respectively, have primary amphipathic structures and their hydrophobic components improve membrane interactions and internalization efficiencies.[23,24] In light of these trends and the wide variety of hydrophobic groups available, it is important to understand how the lengths within our PTDMs and the nature of the hydrophobic moiety impacts siRNA internalization efficiencies. At the same time, the need to optimize the cationic block length should not be overlooked either as it also influences the PTDM design landscape.

Structure activity relationships using Jurkat T cells and HeLa cells were used to probe how the length and the nature of the hydrophobic block impacted siRNA internalization efficiencies. To explore the length of the hydrophobic block, two series of diblock copolymers (n + m) with symmetric (n = m) or asymmetric (n ≠ m) block lengths were synthesized (Figure 4.2.1). In a separate series of PTDMs, the hydrophobic side chain composition was varied to probe how the relative hydrophobicity impacted siRNA internalization. After initial testing, this set of PTDMs was further expanded to incorporate additional hydrophobic side chains to elucidate the hydrophobic window for which our PTDMs had optimal activity. Relative hydrophobicities of the hydrophobic building blocks were estimated using HPLC retention times to guide the selection of

structures used for analysis.   Probing the effects of hydrophobicity on siRNA internalization efficiencies enabled us to better elucidate the essential design principles for our PTDMs.

4.2   Initial PTDM Design and Characterization

In this report, we document the use of ring-opening metathesis polymerization (ROMP) for the synthesis of block copolymer (BCP) PTDMs with varying hydrophobic block lengths. ROMP is a facile polymerization method that is functional group tolerant and allows for good control over molecular weights and dispersities.[59-66] In addition, we continue to exploit the versatile, dual-functional oxanorbornene-based monomer platform as a means to tailor the overall polymer properties; in this case with a focus on the hydrophobic block length and moieties incorporated as side chains. The monomers and polymers designed and synthesized for this study are summarized in Figure 4.2.1. The guanidinium-rich monomer (**dG**), shown in its boc-protected form and meant to mimic arginine residues, was used as the cationic component of the BCP PTDMs.   This selection was made based on previous literature that demonstrates the superior performance of guanidinium moieties over their ammonium counterparts, which are reminiscent of lysine and ornithine residues.[67]
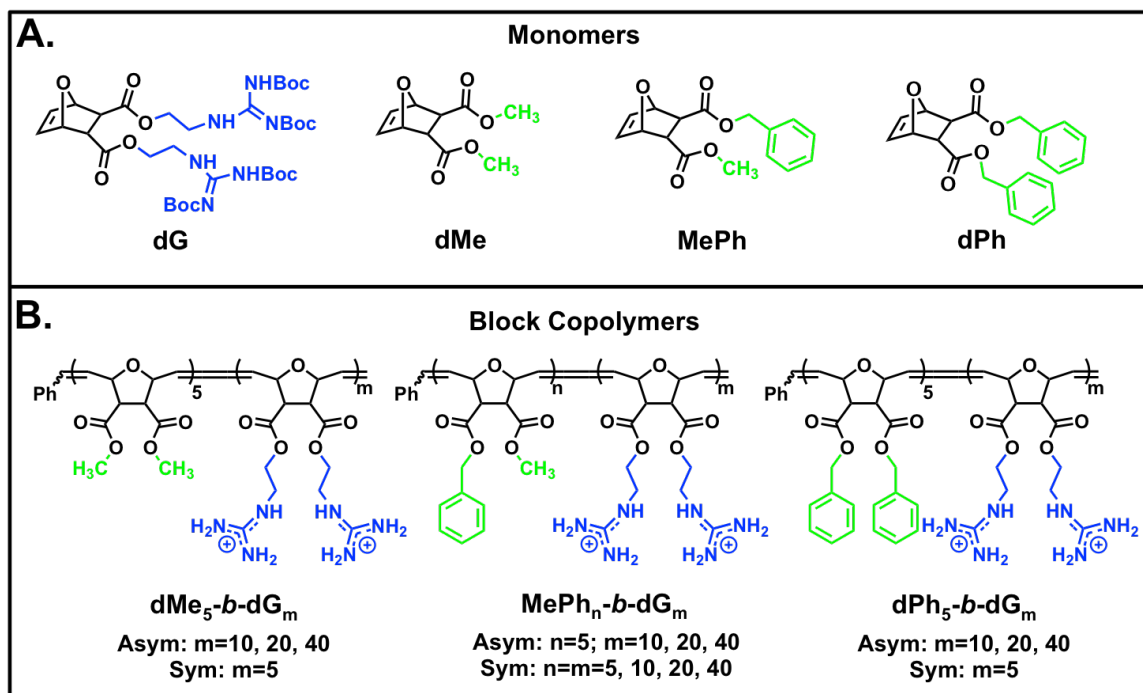
Figure 4.1. Monomer and polymer structures used for this study. A) Monomer structures B) Polymer Structures. Blue represents cationic moieties and green represents hydrophobic moieties.

The three initial hydrophobic monomers were designed to contain either two methyl substituents (dimethyl, **dMe**), one methyl and one phenyl substituent (methyl phenyl, **MePh**), or two phenyl substituents (diphenyl, **dPh**) (Figure 4.2.1A) and were selected because HPLC retention times indicated that they spanned a range of hydrophobicities. These retention times were 14.2 min (**dMe**), 27.8 min (**MePh**), and 36.1 min (**dPh**). The phenyl-based hydrophobic groups have also demonstrated useful activities in prior studies[30,32,44,47] **MePh**, which has traditionally been selected by our group as the hydrophobic component of PTDMs for siRNA delivery, was used to synthesize BCPs with symmetric ($n = m$) or asymmetric ($n \neq m$, with n being fixed at five for all polymers in the series) block sizes. This allowed us to explore how the length of the hydrophobic block impacts internalization efficiencies at a fixed cationic charge length. A summary

113

of molecular weight data for the block polymer PTDMs is shown in Figure 3.3, Figure 3.5, Table 4.1, and Table 4.2, Figure 4.2, and Figure 4.3.

Table 4.1. Molecular weight characterization of Boc-protected block copolymer PTDMs from the MePh$_n$-b-dG$_m$, dMe$_5$-b-dG$_m$, and dPh$_5$-b-dG$_m$ series.

Polymer	M$_n$[a] (Da)	M$_w$[a] (Da)	M$_p$[a] (Da)	Đ[a] (M$_w$/M$_n$)
25a	5,400	5,900	5,900	1.08
25b	8,300	9,000	9,300	1.08
25c	16,000	17,100	17,500	1.07
25d	27,600	31,500	36,800	1.14
25e	9,900	10,800	11,100	1.09
25f	19,800	21,400	22,800	1.08
25g	31,600	38,400	44,700	1.22
26a	5,500	5,800	5,900	1.06
26b	9,500	10,300	10,600	1.08
26c	14,600	15,900	16,600	1.09
27a	5,200	5,600	5,700	1.08
27b	8,500	9,300	9,500	1.09
27c	14,400	16,100	17,100	1.11

[a]Number average molecular weight (M$_n$), weight average molecular weight (M$_w$), molecular weight at the peak maximum (M$_p$), and dispersity indices (Đ=M$_w$/M$_n$) determined by GPC using poly(methyl methacrylate) (PMMA) standards, tetrahydrofuran (THF) as the eluent, and toluene as the flow marker.
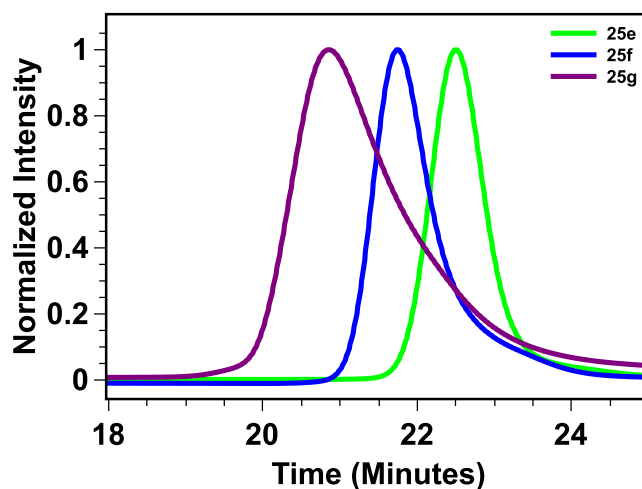
Figure 4.2. THF GPC chromatograms for boc-protected block copolymer PTDMs **25e-g**. A summary of molecular weight data can be found in **Table 4.1**.

Table 4.2. Molecular weight characterization of deprotected block copolymer PTDMs.

Polymer	M_n^a (Da)	M_w^a (Da)	M_p^a (Da)	$Đ^a$ (M_w/M_n)
MePh$_5$-*b*-dG$_5$	10,200	10,900	10,100	1.07
MePh$_5$-*b*-dG$_{10}$	14,900	15,800	15,200	1.06
MePh$_5$-*b*-dG$_{20}$	21,800	23,500	23,500	1.08
MePh$_5$-*b*-dG$_{40}$	33,300	36,600	39,500	1.10
MePh$_{10}$-*b*-dG$_{10}$	19,500	21,000	19,300	1.08
MePh$_{20}$-*b*-dG$_{20}$	29,600	33,200	30,700	1.12
MePh$_{40}$-*b*-dG$_{40}$	45,000	49,500	51,900	1.10
dMe$_5$-*b*-dG$_5$	12,300	12,900	12,500	1.05
dMe$_5$-*b*-dG$_{10}$	18,100	18,900	18,800	1.05
dMe$_5$-*b*-dG$_{20}$	24,000	25,300	25,500	1.05
dPh$_5$-*b*-dG$_5$	13,000	14,400	12,200	1.11
dPh$_5$-*b*-dG$_{10}$	17,600	19,200	17,200	1.09
dPh$_5$-*b*-dG$_{20}$	25,000	26,800	25,900	1.07

[a]Number average molecular weight (M_n), weight average molecular weight (M_w), molecular weight at the peak maximum (M_p), and dispersity indices ($Đ=M_w/M_n$) determined by GPC using poly(methyl methacrylate) (PMMA) standards, 2,2,2-trifluoroethanol (TFE) with 20 mM NaTFA salt as the eluent, and methanol as the flow marker.
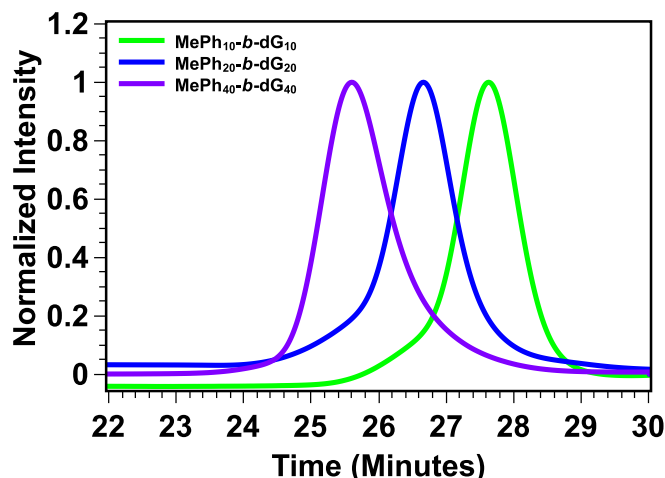
Figure 4.3. TFE GPC chromatograms for deprotected block copolymer PTDMs MePh$_{10}$-*b*-dG$_{10}$, MePh$_5$-*b*-dG$_{10}$, MePh$_5$-*b*-dG$_{20}$, and MePh$_5$-*b*-dG$_{40}$. A summary of molecular weight data can be found in **Table 4.2**.

In addition, BCPs containing a fixed hydrophobic block length of five consisting of **dMe**, **MePh**, or **dPh** hydrophobic blocks and a cationic charge block of five, ten, or twenty **dG** units were synthesized as a way to further probe the relationship between the

hydrophobic component and the length of the charged block for siRNA internalization efficiencies. A summary of molecular weight data for is shown in Figure 4.4, Figure 4.5, Figure 4.6, Figure 4.7, Table 4.1, and Table 4.2.
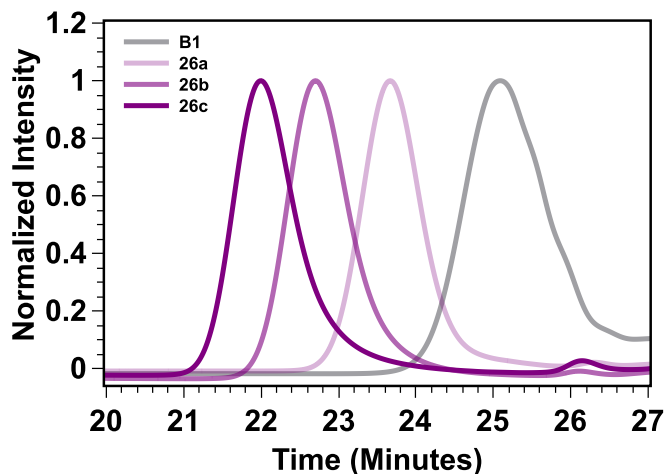
Figure 4.4. THF GPC chromatograms for boc-protected block copolymer PTDMs **26a-c**. A summary of molecular weight data can be found in **Table 4.1**.
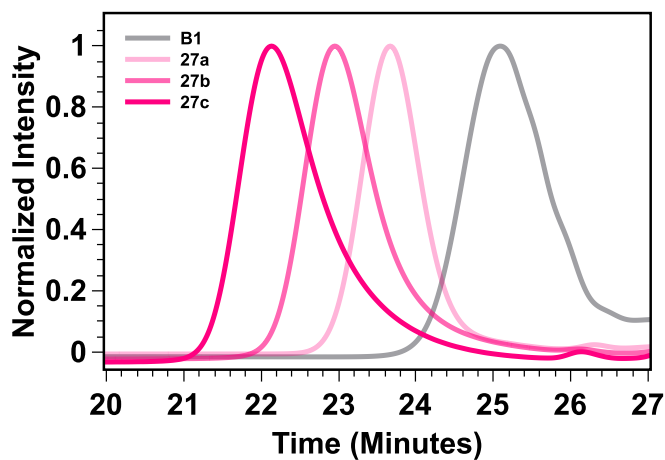
Figure 4.5. THF GPC chromatograms for boc-protected block copolymer PTDMs **8a-c**. A summary of molecular weight data can be found in **Table 4.1**.

117
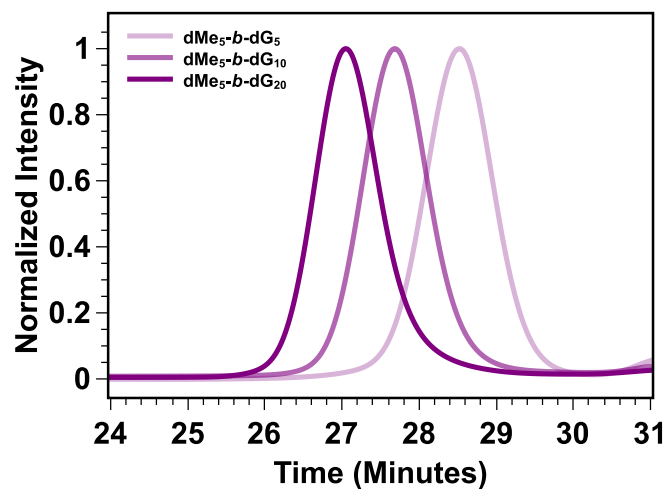
Figure 4.6. TFE GPC chromatograms for deprotected block copolymer PTDMs dMe$_5$-*b*-dG$_5$, dMe$_5$-*b*-dG$_{10}$, and dMe$_5$-*b*-dG$_{20}$. A summary of molecular weight data can be found in **Table 4.2**.
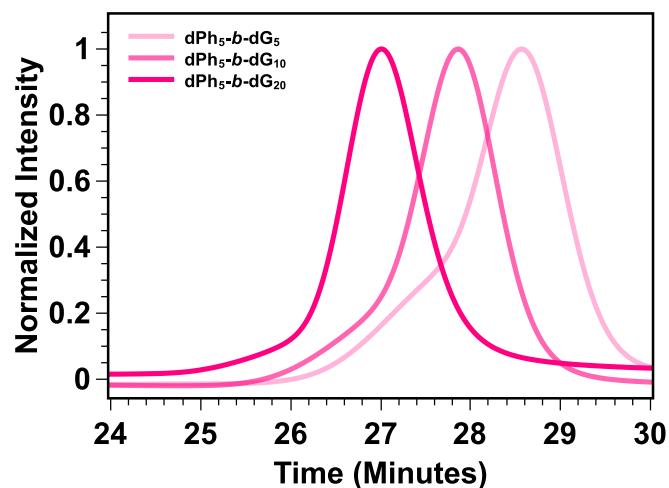
Figure 4.7. TFE GPC chromatograms for deprotected block copolymer PTDMs **dPh$_5$-*b*-dG$_5$**, **dPh$_5$-*b*-dG$_{10}$**, and **dPh$_5$-*b*-dG$_{20}$**. A summary of molecular weight data can be found in **Table 4.2**.

Previous work in this area documented the effect of cationic charge block length and the addition of a hydrophobic block had on siRNA internalization and delivery.[32] In that study, BCP PTDMs significantly outperformed their homopolymer counterparts, recapitulating the importance of an added hydrophobic component.[32] This study further

builds from this initial finding to explore how the quantity of hydrophobic repeat units and the type of hydrophobic moiety used impacts siRNA internalization efficiencies.

4.3 FITC-siRNA Delivery: Symmetric vs. Asymmetric

The first studies explored the MePh$_n$-b-dG$_m$ PTDM series. A total of seven PTDMs were designed to contain equal hydrophobic and cationic block lengths (symmetric, n = m = 5, 10, 20, and 40) and three contained a fixed hydrophobic block of five repeat units (asymmetric, n ≠ m) with cationic charge blocks of approximately 10, 20, and 40 repeat units. The cationic block length was varied from 5 to 40 based on our previous findings.[32] Fluorescein isothiocyanate (FITC) labeled siRNA (FITC-siRNA) was used to establish trends in siRNA internalization efficiency for both series in Jurkat T cells, a representative suspension cell type, and HeLa cells, a representative adherent cell type, using complete media. In this report, only FITC-labeled siRNA was used since we recently demonstrated the internalization relationship for our PTDMS between FITC-siRNA in Jurkats and siRNA for *NOTCH1* in human peripheral blood mononuclear cells (PBMCs)*. The N:P ratios for these experiments, which are the ratios of the number of positively charged nitrogen atoms in the PTDMs to the number of negatively charged phosphate atoms in the FITC-siRNA, were set at 8:1 and 4:1, respectively, and were previously optimized by our group.[32] The selection of these N:P ratios were further supported by gel retardation assays, which demonstrated that all PTDMs fully bound siRNA at N:P ratios of 4:1 or less (Figure 4.8-Figure 4.20).
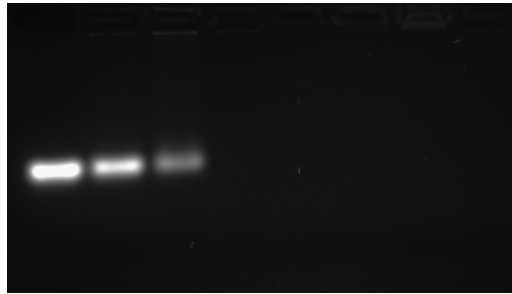
Figure 4.8. Gel retardation assay to assess PTDM / siRNA complex formation using MePh$_5$-*b*-dG$_5$. All samples were run on a 0.8% agarose gel and the N:P ratios tested ranged from 0.5:1 to 12:1, with 1 µg of siRNA per well.
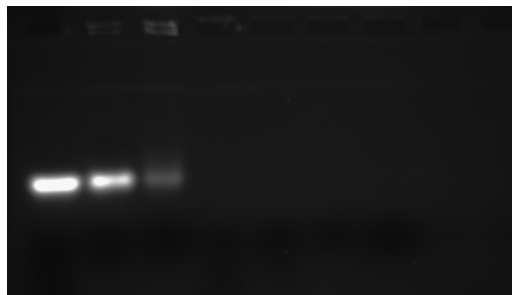
Figure 4.9. Gel retardation assay to assess PTDM / siRNA complex formation using MePh$_5$-*b*-dG$_{10}$. All samples were run on a 0.8% agarose gel and the N:P ratios tested ranged from 0.5:1 to 12:1, with 1 µg of siRNA per well.
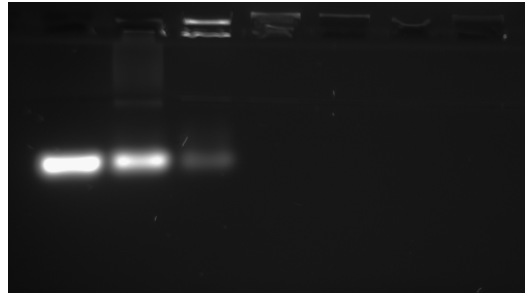
Figure 4.10. Gel retardation assay to assess PTDM / siRNA complex formation using MePh$_5$-*b*-dG$_{20}$. All samples were run on a 0.8% agarose gel and the N:P ratios tested ranged from 0.5:1 to 12:1, with 1 µg of siRNA per well.
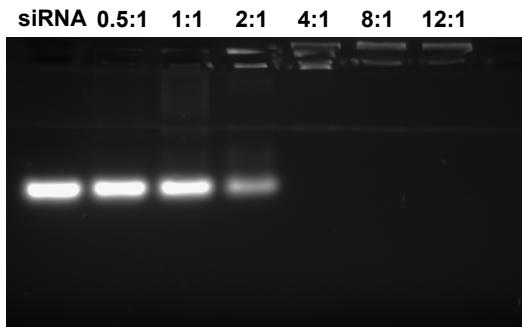
Figure 4.11. Gel retardation assay to assess PTDM / siRNA complex formation using MePh$_5$-*b*-dG$_{40}$. All samples were run on a 0.8% agarose gel and the N:P ratios tested ranged from 0.5:1 to 12:1, with 1 μg of siRNA per well.
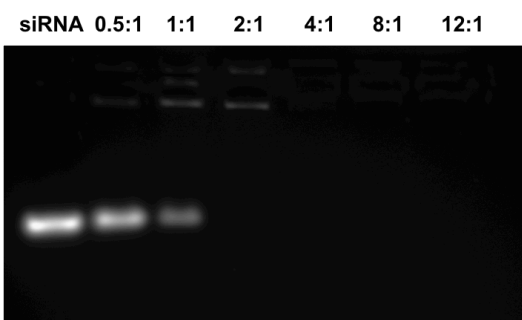
Figure 4.12. Gel retardation assay to assess PTDM / siRNA complex formation using MePh$_{10}$-*b*-dG$_{10}$. All samples were run on a 0.8% agarose gel and the N:P ratios tested ranged from 0.5:1 to 12:1, with 1 μg of siRNA per well.

Figure 4.13. Gel retardation assay to assess PTDM / siRNA complex formation using MePh$_{20}$-*b*-dG$_{20}$. All samples were run on a 0.8% agarose gel and the N:P ratios tested ranged from 0.5:1 to 12:1, with 1 μg of siRNA per well.

Figure 4.14. Gel retardation assay to assess PTDM / siRNA complex formation using MePh$_{40}$-*b*-dG$_{40}$. All samples were run on a 0.8% agarose gel and the N:P ratios tested ranged from 0.5:1 to 12:1, with 1 µg of siRNA per well.

Figure 4.15. Gel retardation assay to assess PTDM / siRNA complex formation using dMe$_5$-*b*-dG$_5$. All samples were run on a 0.8% agarose gel and the N:P ratios tested ranged from 0.5:1 to 12:1, with 1 µg of siRNA per well.

Figure 4.16. Gel retardation assay to assess PTDM / siRNA complex formation using dMe$_5$-*b*-dG$_{10}$. All samples were run on a 0.8% agarose gel and the N:P ratios tested ranged from 0.5:1 to 12:1, with 1 µg of siRNA per well.

siRNA 0.5:1 1:1 2:1 4:1 8:1 12:1

Figure 4.17. Gel retardation assay to assess PTDM / siRNA complex formation using dMe$_5$-*b*-dG$_{20}$. All samples were run on a 0.8% agarose gel and the N:P ratios tested ranged from 0.5:1 to 12:1, with 1 µg of siRNA per well.

siRNA 0.5:1 1:1 2:1 4:1 8:1 12:1
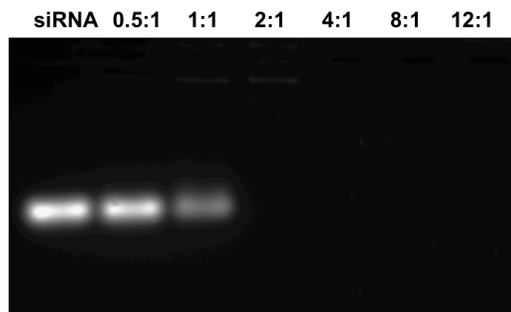
Figure 4.18. Gel retardation assay to assess PTDM / siRNA complex formation using dPh$_5$-*b*-dG$_5$. All samples were run on a 0.8% agarose gel and the N:P ratios tested ranged from 0.5:1 to 12:1, with 1 µg of siRNA per well.

siRNA 0.5:1 1:1 2:1 4:1 8:1 12:1
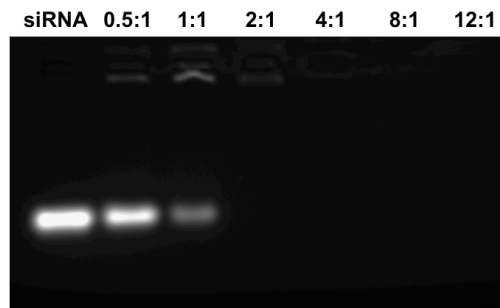
Figure 4.19. Gel retardation assay to assess PTDM / siRNA complex formation using dPh$_5$-*b*-dG$_{10}$. All samples were run on a 0.8% agarose gel and the N:P ratios tested ranged from 0.5:1 to 12:1, with 1 µg of siRNA per well.

siRNA 0.5:1 1:1 2:1 4:1 8:1 12:1
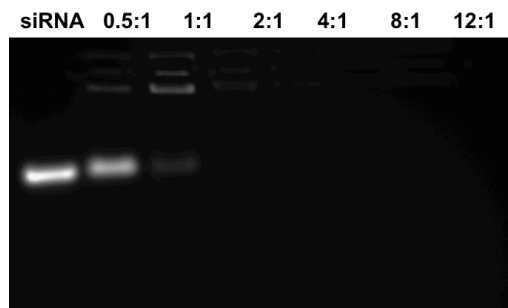
Figure 4.20. Gel retardation assay to assess PTDM / siRNA complex formation using dPh$_5$-*b*-dG$_{20}$. All samples were run on a 0.8% agarose gel and the N:P ratios tested ranged from 0.5:1 to 12:1, with 1 μg of siRNA per well.

A summary of FITC-siRNA internalization efficiencies for these symmetric and asymmetric PTDMs is shown in Figure 4.3.14, where Figure 4.3.14A and Figure 4.3.14B present the percentage of the cell population that received FITC-siRNA and Figure 4.3.14C and Figure 4.3.14D present the median fluorescence intensity (MFI) of the cell populations. The corresponding flow cytometry histograms are shown in Figure 4.22 and Figure 4.23 for Jurkat T cells and HeLa cells, respectively.

MePh$_n$-b-dG$_m$ PTDM Series with Symmetric (n=m) or Asymmetric (n≠m) Block Lengths
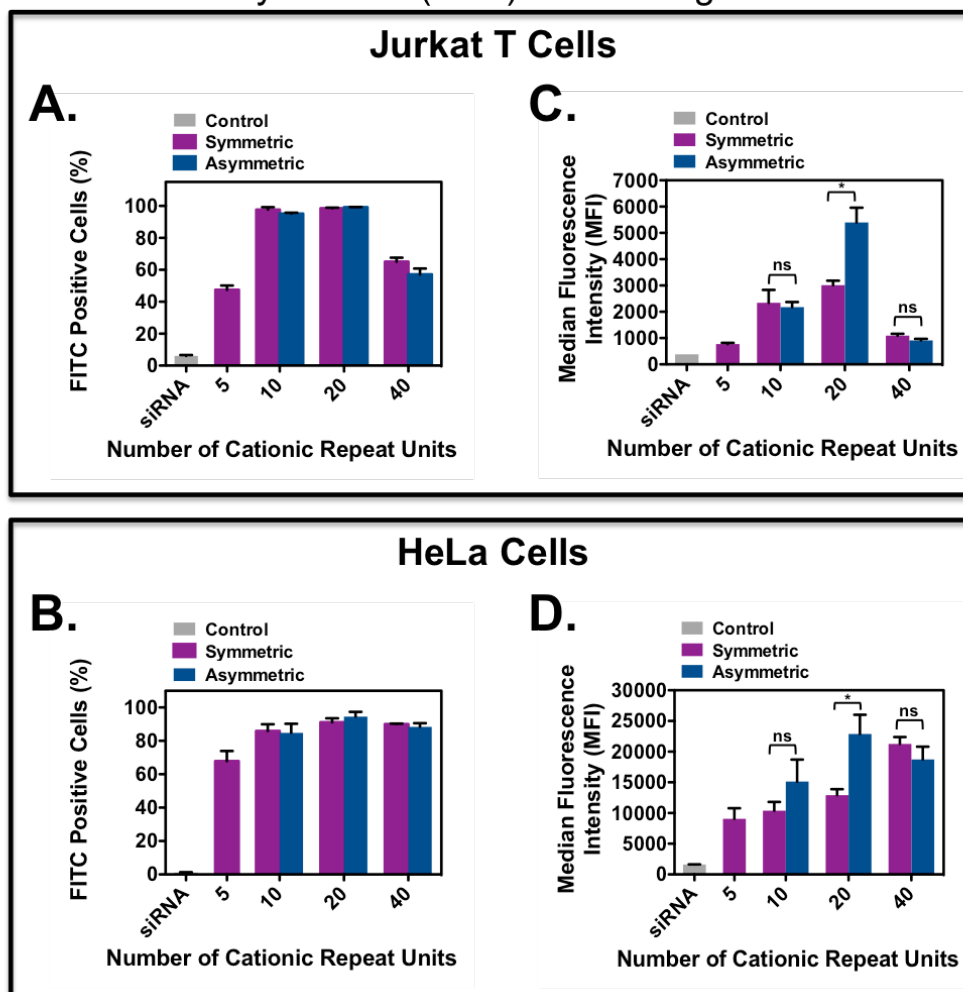
Figure 4.21. FITC-siRNA delivery into Jurkat T cells and HeLa cells using symmetric and asymmetric ROMP-based protein mimics. Jurkat T cells (cell density = 4x10^5 cells/mL) treated with polymer/FITC-siRNA complexes with an N:P ratio = 8:1 in complete media for four hours at 37°C and compared cells only receiving FITC-siRNA. HeLa cells (cell density = 5x10^4 cells/mL 48 hours prior to experiment; 70-90% confluent on the day of the experiment) treated with polymer/FITC-siRNA complexes with an N/P ratio = 4/1 in complete media for four hours at 37°C and compared cells only receiving FITC-siRNA. All data was compared to an untreated control. A) Percent positive Jurkat T cells. B) Percent positive HeLa cells. C) Median fluorescence intensity (MFI) of the Jurkat T cell population. D) Median fluorescence intensity (MFI) of the HeLa cell population. Each data point represents the mean ± SEM of three independent experiments. * = $p < 0.05$ and ns = not significant, as calculated by the unpaired two-tailed student t-test. Statistics represents significance between symmetric and asymmetric block copolymer PTDMs with the same cationic charge content.
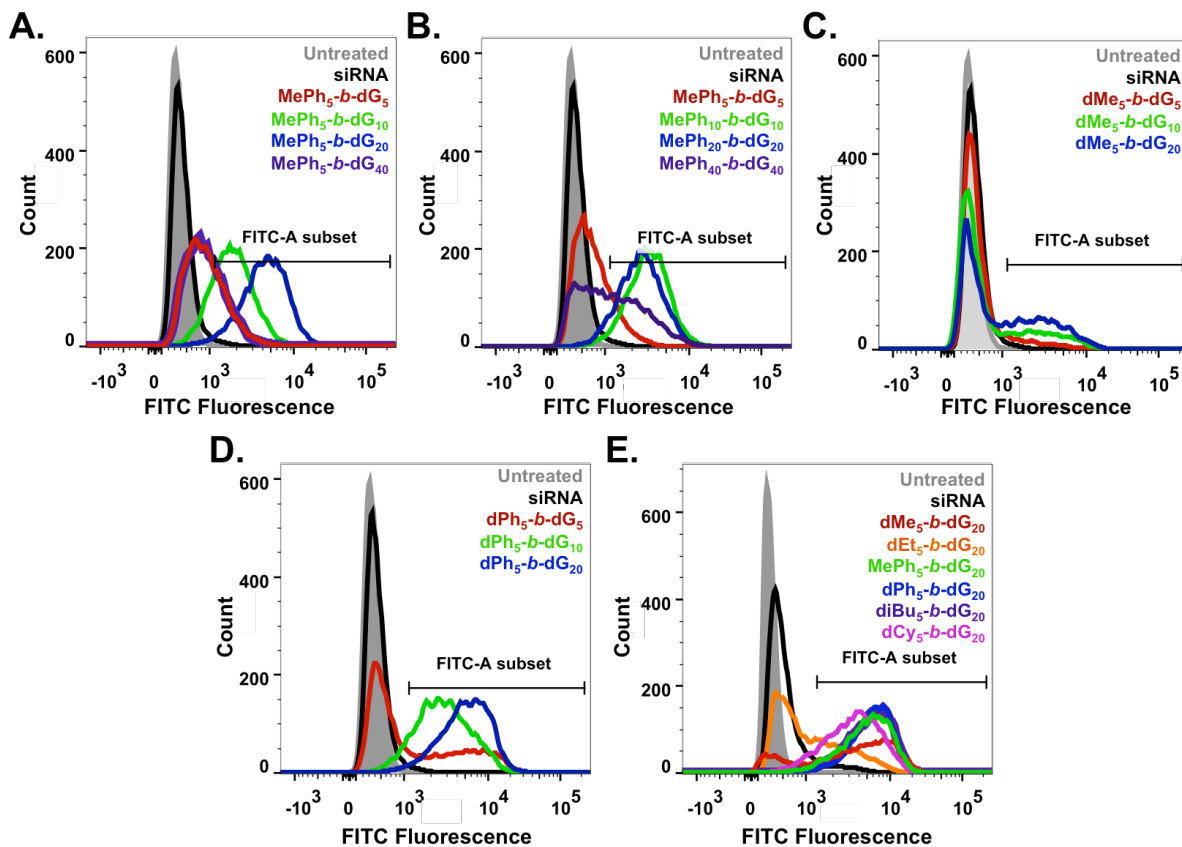
Figure 4.22. Representative histograms for FITC-siRNA delivery into Jurkat T cells using ROMP-based protein mimics. Jurkat T cells (cell density = 4×10^5 cells/mL) were treated with polymer/FITC-siRNA complexes with an N/P ratio = 8/1 in complete media for four hours at 37°C and compared with untreated cells and cells only receiving FITC-siRNA. A) Overlay of representative histograms for cells treated with asymmetric block copolymer/siRNA complexes. B) Overlay of representative histograms for cells treated with symmetric block copolymer/siRNA complexes. C) Overlay of representative histograms for cells treated with the dimethyl block copolymer/siRNA complexes. D) Overlay of representative histograms for cells treated with the diphenyl block copolymer/siRNA complexes. E) Overlay of representative histograms for cells treated with block copolymer/siRNA complexes, where the block copolymers have a constant cationic charge content of 20.
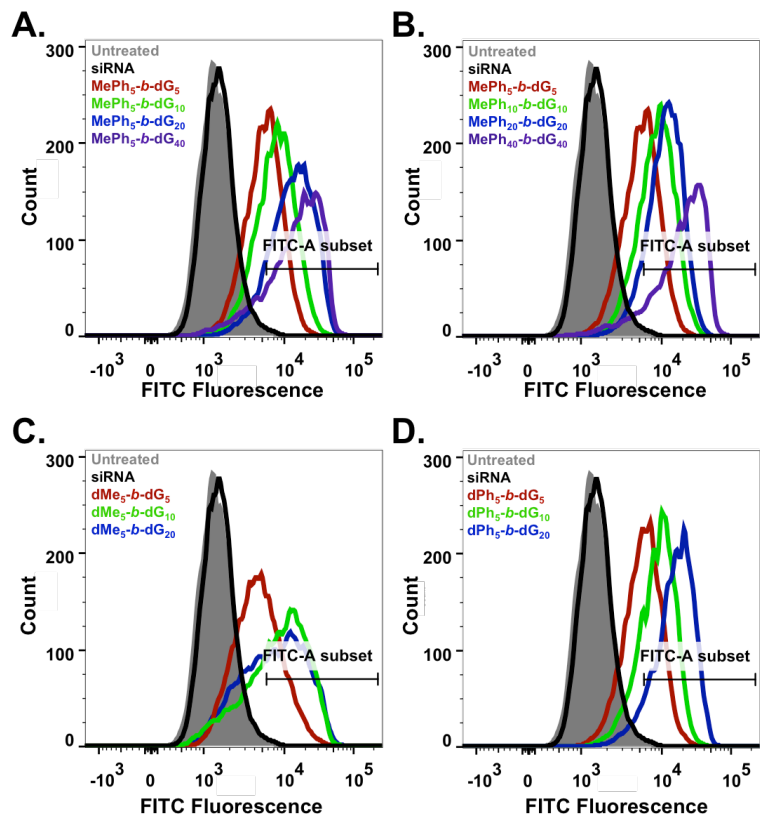
Figure 4.23. Representative histograms for FITC-siRNA delivery into HeLa cells using ROMP-based protein mimics. HeLa cells (cell density = 5×10^4 cells/mL 48 hours prior to experiment; 70-90% confluent on the day of the experiment) treated with polymer/FITC-siRNA complexes with an N/P ratio = 8/1 in complete media for four hours at 37°C and compared cells only receiving FITC-siRNA and to an untreated control. A) Overlay of representative histograms for cells treated with asymmetric block copolymer/siRNA complexes. B) Overlay of representative histograms for cells treated with symmetric block copolymer/siRNA complexes. C) Overlay of representative histograms for cells treated with the dimethyl block copolymer/siRNA complexes. D) Overlay of representative histograms for cells treated with the diphenyl block copolymer/siRNA complexes.

All PTDM-treated cells showed greater than 85% viability using 7-AAD staining (Figure 4.24 and Figure 4.25).
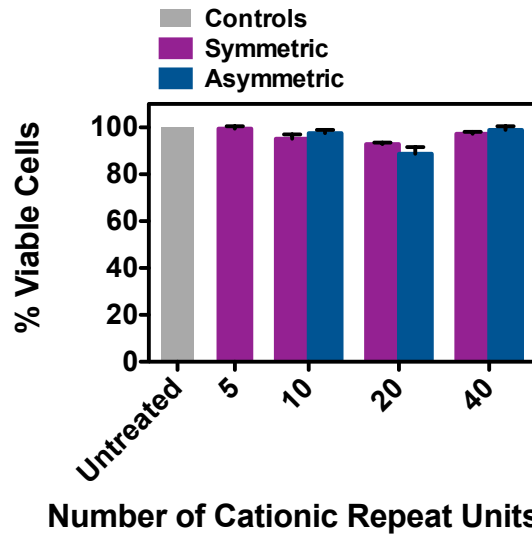
Figure 4.24. Percent viable Jurkat T cells using a 7-Amino-actinomycin (7-AAD) viability assay. Jurkat T cells (cell density = 4×10^5 cells/mL) were treated with polymer/FITC-siRNA complexes with an N/P ratio = 8/1 in complete media for four hours at 37°C and compared with untreated cells and cells only receiving FITC-siRNA. Cells were stained at four hours. Each data point represents the mean ± SEM of three independent experiments.
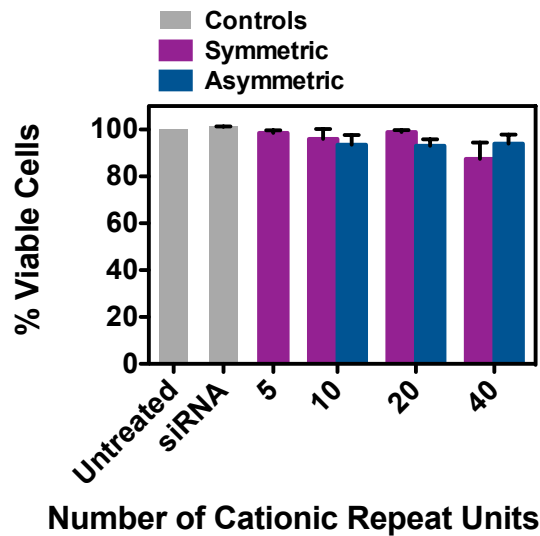
Figure 4.25. Percent viable cells using a 7-Amino-actinomycin (7-AAD) HeLa cell viability assay. HeLa cells (cell density = 5×10^4 cells/mL 48 hours prior to experiment; 70-90% confluent on the day of the experiment) were treated with polymer/FITC-siRNA complexes with an N/P ratio = 8/1 in complete media for four hours at 37°C and compared with untreated cells and cells only receiving FITC-siRNA. Cells were stained at four hours. Each data point represents the mean ± SEM of three independent experiments.

For both cell types, symmetric and asymmetric PTDMs containing the same cationic charge contents were able to deliver to the same percentages of the cell populations (Figure 4.3.14A and Figure 4.3.14B) regardless of the different hydrophobic block lengths. When looking at the MFI data, PTDMs with five, ten, and forty cationic repeat units lead to similar internalization amounts regardless of the hydrophobic block length; however, for PTDMs with 20 cationic repeat units, the asymmetric PTDM **MePh$_5$-*b*-dG$_{20}$**, significantly outperformed its symmetric counterpart (Figure 4.3.14C and Figure 4.3.14D). For both cell types, **MePh$_5$-*b*-dG$_{20}$** had double the fluorescence intensity of **MePh$_{20}$-*b*-dG$_{20}$**. This result demonstrates that the relationship between hydrophobicity and cationic block length is not always trivial and that increasing the hydrophobic block length further does not guarantee superior performance.[37] In addition, this result suggests that a certain ratio between hydrophobic and cationic block lengths is necessary for efficient internalization.

4.4 FITC-siRNA Delivery: Varying the hydrophobic block

To further probe the relationship between hydrophobic and cationic block lengths, PTDMs with a fixed hydrophobic block length of five repeat units of either low (**dMe**), moderate (**MePh**), or high hydrophobicity (**dPh**) were prepared and studied. The relative hydrophobicities of these monomers was determined using HPLC and can be found in Table 4.3. The given retention times were 14.2 min, 27.8 min, and 36.1 min, respectively, where larger HPLC retention times reflect increased hydrophobicity. Based on previous results and those shown in Figure 2, the hydrophobic block length was held constant at five repeat units while the cationic block length was varied from five to twenty. This generated a total of nine PTDMs. FITC-siRNA was again used to establish trends in siRNA internalization efficiency in Jurkat T cells and HeLa cells using complete media. The N:P ratios were set at 8:1 and 4:1, respectively, and were supported by gel

retardation assays, which demonstrated that all PTDMs bound siRNA at N:P ratios of 4:1 or less (Figure 4.8-Figure 4.20). A summary of FITC-siRNA internalization efficiencies for the PTDMs with variable hydrophobic block compositions is shown in Figure 4.4.1, where Figure 4.4.1A and Figure 4.4.1B present the percentage of the cell populations that received FITC-siRNA and Figure 4.4.1C and Figure 4.4.1D present the MFIs of the cell populations. All PTDM-treated cells showed greater than 85% viability using 7-AAD staining (Figure 4.27 and Figure 4.28**)**.

MePh$_n$-*b*-dG$_m$ PTDM Series with Symmetric (n=m) or Asymmetric (n≠m) Block Lengths
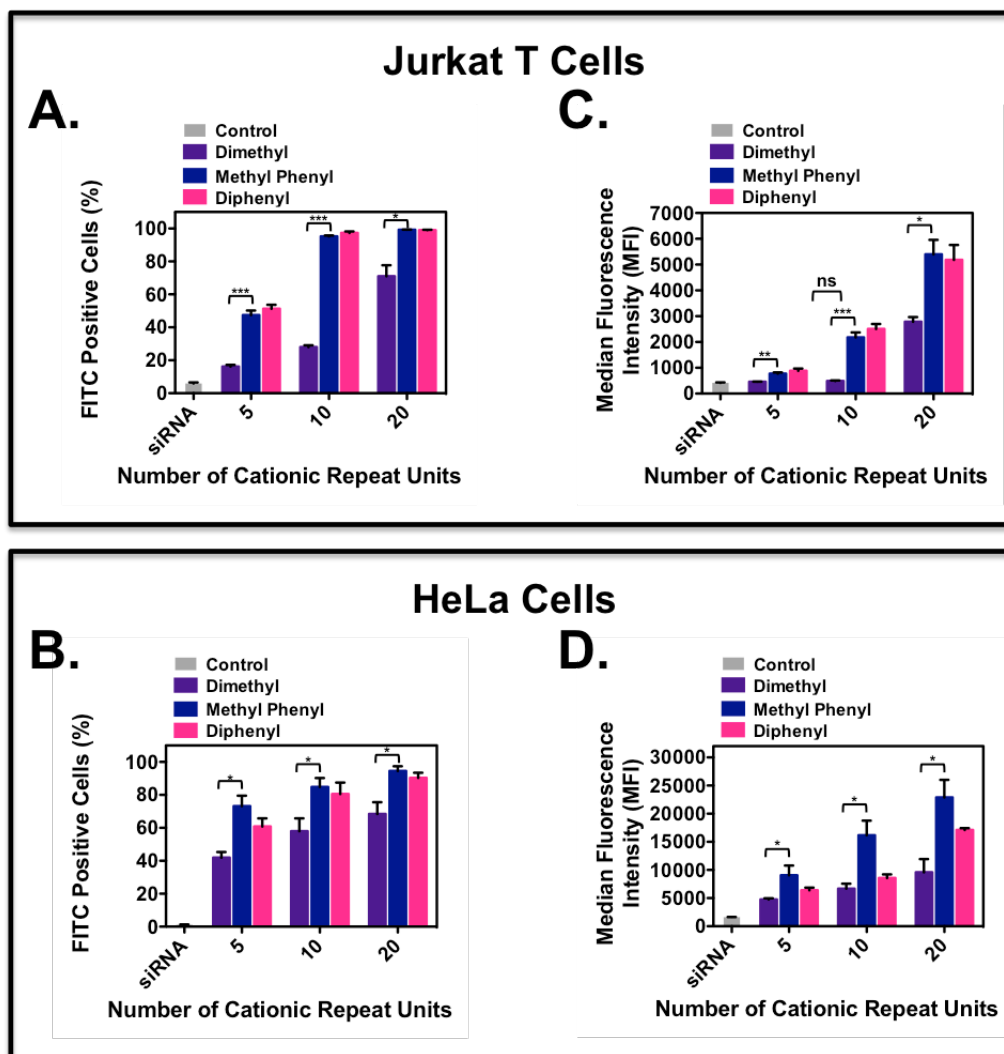
Figure 4.26. FITC-siRNA delivery into Jurkat T cells and HeLa cells using ROMP-based protein mimics with different hydrophobic blocks. Jurkat T cells (cell density = 4x10^5 cells/mL) treated with polymer/FITC-siRNA complexes with an N:P ratio = 8:1 in complete media for four hours at 37°C and compared cells only receiving FITC-siRNA. HeLa cells (cell density = 5x10^4 cells/mL 48 hours prior to experiment; 70-90% confluent on the day of the experiment) treated with polymer/FITC-siRNA complexes with an N/P ratio = 4/1 in complete media for four hours at 37°C and compared cells only receiving FITC-siRNA. All data was compared to an untreated control. A) Percent positive Jurkat T cells. B) Median fluorescence intensity (MFI) of the Jurkat T cell population. C) Percent positive HeLa cells. D) Median fluorescence intensity (MFI) of the HeLa cell population. Each data point represents the mean ± SEM of three independent experiments. * = *p* < 0.05, ** = *p* < 0.01, *** = *p* < 0.001 as calculated by the unpaired two-tailed student *t*-test. Statistics represents significance between **dMe**-containing and **MePh**-containing PTDMs.
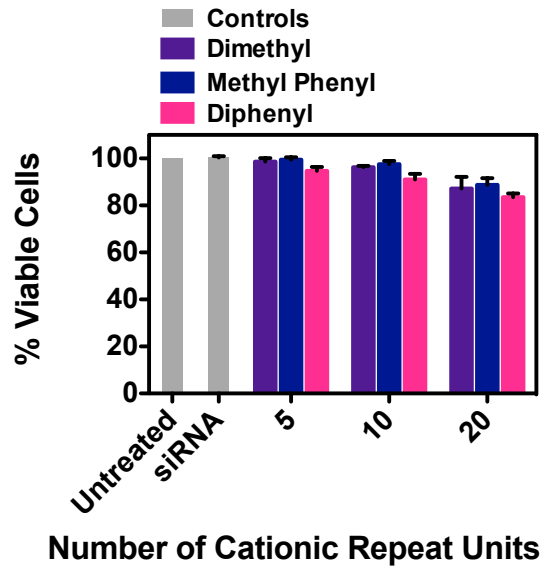
Figure 4.27. Percent viable Jurkat T cells using a 7-Amino-actinomycin (7-AAD) viability assay. Jurkat T cells (cell density = 4×10^5 cells/mL) were treated with polymer/FITC-siRNA complexes with an N/P ratio = 8/1 in complete media for four hours at 37°C and compared with untreated cells and cells only receiving FITC-siRNA. Cells were stained at four hours. Each data point represents the mean ± SEM of three independent experiments.
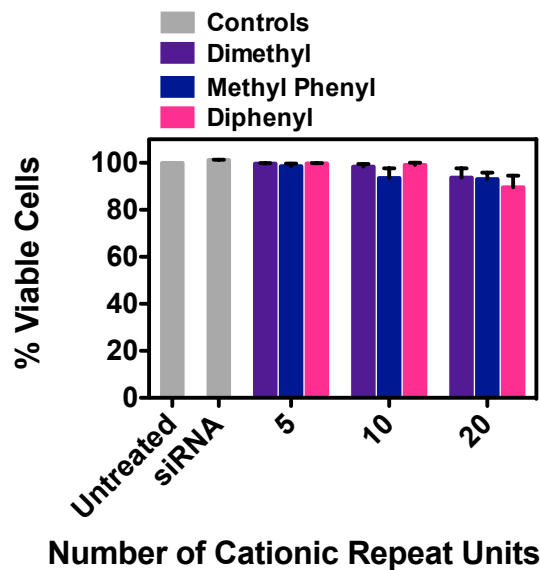
Figure 4.28. Percent viable cells using a 7-Amino-actinomycin (7-AAD) HeLa cell viability assay. HeLa cells (cell density = 5×10^4 cells/mL 48 hours prior to experiment; 70-90% confluent on the day of the experiment) were treated with polymer/FITC-siRNA complexes with an N/P ratio = 8/1 in complete media for four hours at 37°C and compared with untreated cells and cells only receiving FITC-siRNA. Cells were stained at four hours. Each data point represents the mean ± SEM of three independent experiments.

132

For both cell types, **MePh-** and **dPh**-containing PTDMs with the same cationic block length were able to deliver to the same percentages of the cell populations; however, in all cases, the **dMe**-containing PTDMs delivered to a significantly smaller percentage of the population, particularly at the lower cationic block lengths. This percentage increased from 20% (**dMe$_5$-b-dG$_5$**) to 80% (**dMe$_5$-b-dG$_{20}$**), supporting the idea that cationic charge blocks larger than five (up to 20) improve FITC-siRNA internalization efficiencies. In addition, for Jurkat T cells, the MFIs for the **MePh-** and **dPh**-containing PTDMs were not statistically different but were significantly higher when compared to the **dMe**-containing PTDMs. Specifically, **MePh$_5$-b-dG$_{10}$** and **dPh$_5$-b-dG$_{10}$** had four times the fluorescence intensity of **dMe$_5$-b-dG$_{10}$,** and at higher cationic block lengths, **MePh$_5$-b-dG$_{20}$** and **dPh$_5$-b-dG$_{20}$** had double the fluorescence intensity of **dMe$_5$-b-dG$_{20}$**. This observed trend was similar for HeLa cells when comparing the **MePh$_5$-b-dG$_m$** series to the **dMe$_5$-b-dG$_m$** series, with the **MePh**-containing PTDMs having roughly double the fluorescence intensity regardless of the cationic block length. Taken together, this data suggests that there may be a minimum hydrophobic block length necessary for efficient siRNA internalization, but there also seems to be a limit to which increasing the hydrophobicity improves siRNA internalization.

4.5   Expanding the Hydrophobic Monomer Set

To further understand the hydrophobic window necessary for optimal internalization and gain more insight regarding the tunability of the hydrophobic domain, several additional monomers were designed. In order to select the appropriate PTDMs, a series of hydrophobic monomers were synthesized and analyzed using HPLC to assess their relative hydrophobicities in addition to calculating logP values using MarvinSketch (ChemAxon Ltd).[68] Monomers with longer retention times required more organic component in the mobile phase in order to be eluted and are considered to be

more hydrophobic. The corresponding HPLC chromatograms can also be found in

Figure 4.29.

Table 4.3. Summary of Monomers and Their Corresponding HPLC Retention Times and LogP Values.

Monomer Name	Monomer Abbreviation	HPLC Rt[a] (min)	LogP[b]
Dimethyl	dMe	14.2	0.05
Methyl ethyl	MeEt	17.3	0.41
Diethyl	dEt	21.1	0.77
Methyl Propyl	MePr	21.8	0.93
Methyl Butyl	MeBu	25.8	1.38
Methyl Phenyl	MePh	27.8	1.78
Dipropyl	dPr	28.6	1.81
Diisobutyl	diBu	34.8	2.54
Dibutyl	dBu	34.9	2.70
Diphenyl	dPh	36.1	3.50
Dicyclohexyl	dCy	44.2	4.28
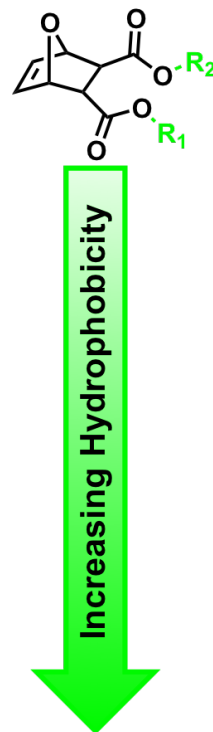
[a]HPLC data collected using a linear gradient from 100% water to 100% CH_3CN at a flow rate of 1 mL/min. HPLC Detection Wavelength = 215 nm. [b]LogP is the octanol/water partition coefficient. All values were calculated using MarvinSketch (ChemAxon Ltd.)

The values were obtained by eluting the monomers on a C_8 column using a linear

gradient from 100% water with 0.1% TFA to 100% acetonitrile with 0.1% TFA at a flow

rate of 1 mL/minute.   Monomers with longer retention times required more organic

component in the mobile phase in order to be eluted and are considered to be more
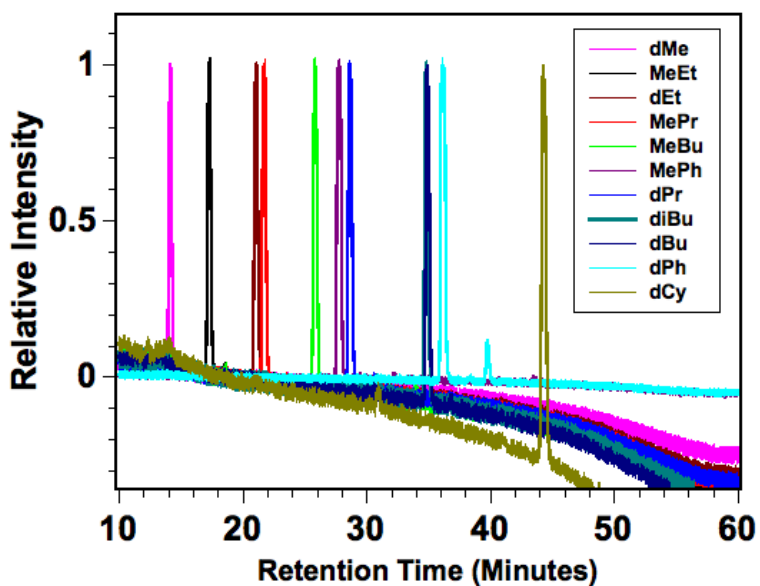
hydrophobic.

Figure 4.29. Overlay of HPLC chromatograms for hydrophobic monomers.

A plot of HPLC retention time (RT) as it relates to logP value can be found in Figure 4.30. The linear relationship between HPLC retention and logP value supports the use of HPLC RTs as a viable, experimental method for assessing relative monomer hydrophobicity.[56-58] Alternatively, it also allows more confidence with calculated logP values for this monomer class going forward. A summary of the monomers synthesized, along with their corresponding HPLC RTs and logP values are reported in Table 4.5.1. The monomer names reflect the substituents used for the monomer R groups, R_1 and R_2, which can either be the same or different. The wide variety of hydrophobic monomers synthesized in Table 4.5.11 also highlights the versatility of the diester monomer platform. [69]

135
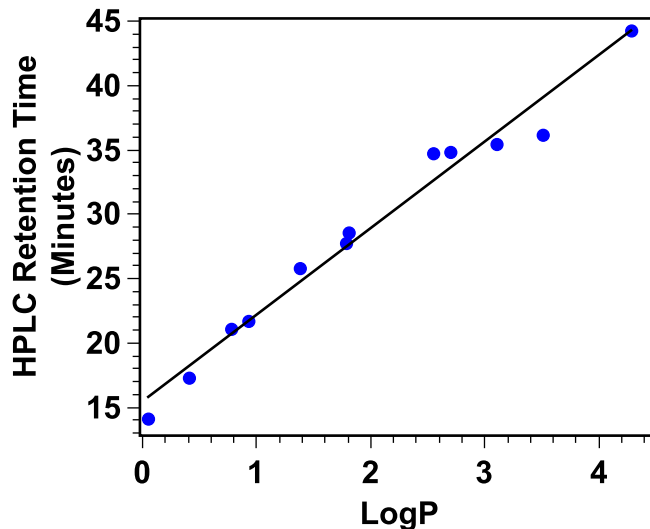
Figure 4.30. Plot of HPLC RT as it relates to LogP value. R^2=0.975. All value correspond to HPLC retention times found in **Table 4.3** of the main text.

The original hydrophobic monomers used for this study were **dMe**, **MePh**, and **dPh**, which had HPLC RTs of 14.2 min, 27.8 min, and 36.1 minutes, respectively. From the eleven monomers in Table 4.3, three new candidates were selected based on their overall hydrophobiciies; **diEt** falls in the hydrophobic window between **dMe** and **MePh**, **diBu** has similar hydrophobicity to **MePh** and **dPh**, and **dCy** is the most hydrophobic of the eleven monomers. These new monomers and their corresponding polymers are summarized in Figure 4.31.
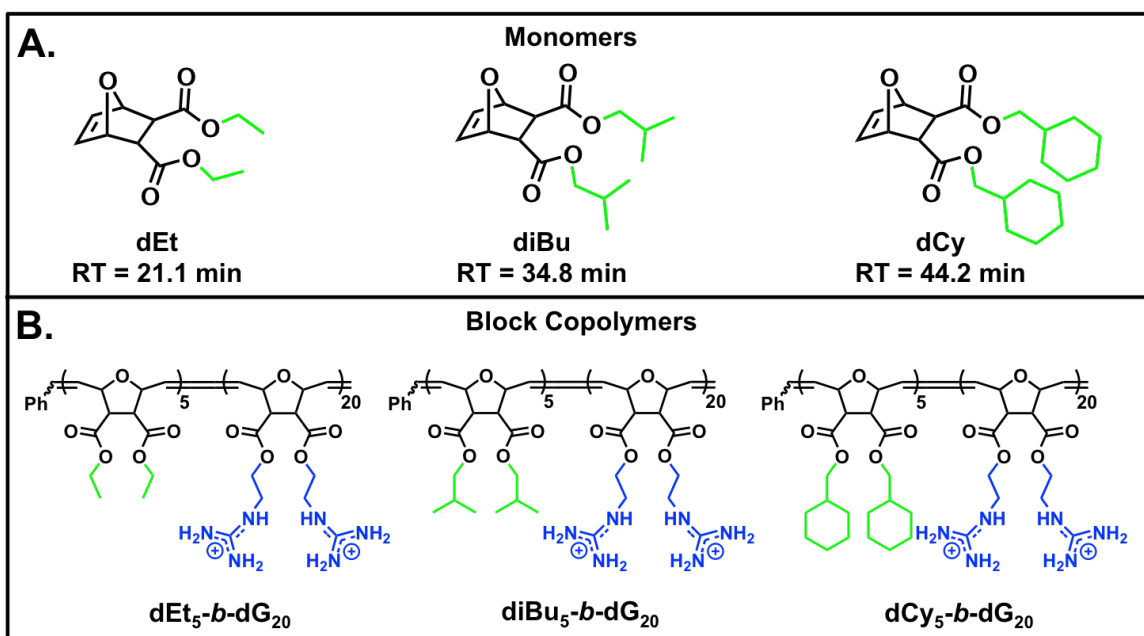
Figure 4.31. Additional monomer and polymer structures used for this study based on monomer hydrophobicity estimates. A) Monomer structures B) Polymer Structures. Blue represents cationic moieties and green represents hydrophobic moieties.

Given the similar trends observed with cationic block length compared to our previous study,[32] only one cationic block length, 20 repeat units, was selected for study. The molecular weight data for this series is summarized in Figure 4.32, Figure 4.33, Table 4.4, and Table 4.5. For all FITC-siRNA experiments performed with these polymers the N:P ratios used were 8:1 and 4:1 for Jurkat T cells and HeLa cells, respectively. Gel retardation assays supported these selections (Figure 4.34-Figure 4.36). A summary of the FITC-siRNA internalization data can be found in Figure 4.37 while the median fluorescence intensity values for these PTDMs, plotted as a function of the monomers' HPLC RTs, is shown in Figure 4.38. All PTDM-treated cells showed greater than 85% viability using 7-AAD staining (Figure 4.39). This plot shows the initial three PTDMs (**dMe₅-*b*-dG₂₀**, **MePh₅-*b*-dG₂₀**, and **dPh₅-*b*-dG₂₀**, red circles) with the three new PTDMs (**dEt₅-*b*-dG₂₀**, **diBu₅-*b*-dG₂₀**, and **dCy₅-*b*-dG₂₀**, blue circles).

Table 4.4. Molecular Weight Characterization of deprotected block copolymer PTDMs.

Polymer	M_n^a (Da)	M_w^a (Da)	M_p^a (Da)	$Đ^a$ (M_w/M_n)
28	15,100	16,100	16,600	1.06
29	16,000	17,100	17,500	1.07
30	16,200	17,200	17,400	1.06

[a]Number average molecular weight (M_n), weight average molecular weight (M_w), molecular weight at the peak maximum (M_p), and dispersity indices ($Đ=M_w/M_n$) determined by GPC using poly(methyl methacrylate) (PMMA) standards, tetrahydrofuran (THF) as the eluent, and toluene as the flow marker.
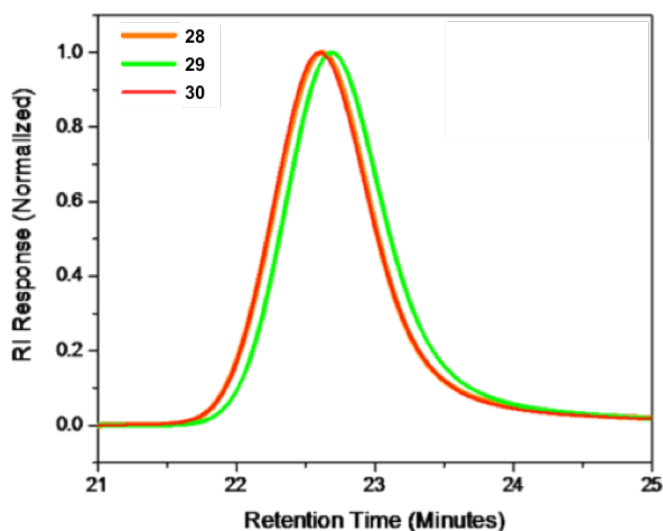
Figure 4.32. THF GPC chromatograms for boc-protected block copolymer PTDMs **28-30**. A summary of molecular weight data can be found in Table 4.5.2.

Table 4.5. Molecular Weight Characterization of deprotected block copolymer PTDMs.

Polymer	$M_n{}^a$ (Da)	$M_w{}^a$ (Da)	$M_p{}^a$ (Da)	$Đ^a$ (M_w/M_n)
dEt$_5$-*b*-dG$_{20}$	24,800	26,300	25,900	1.06
diBu$_5$-*b*-dG$_{20}$	25,700	27,600	26,100	1.06
dCy$_5$-*b*-dG$_{20}$	27,200	29,500	27,500	1.06

[a]Number average molecular weight (M_n), weight average molecular weight (M_w), molecular weight at the peak maximum (M_p), and dispersity indices ($Đ=M_w/M_n$) determined by GPC using poly(methyl methacrylate) (PMMA) standards, 2,2,2-trifluoroethanol (TFE) with 20 mM NaTFA salt as the eluent, and methanol as the flow marker.
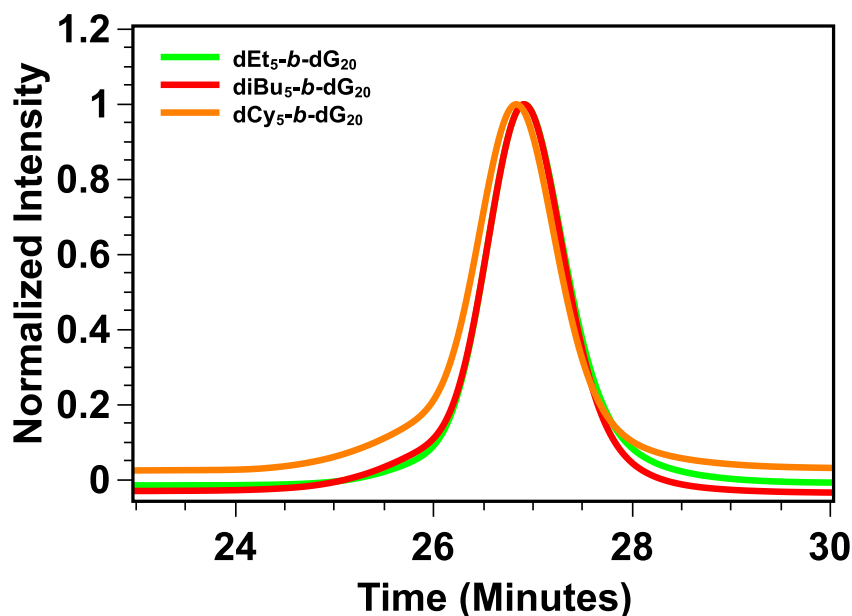
Figure 4.33. TFE GPC chromatograms for deprotected block copolymer PTDMs dEt$_5$-*b*-dG$_{20}$, diBu$_5$-*b*-dG$_{20}$, and dCy$_5$-*b*-dG$_{20}$. A summary of molecular weight data can be found in **Table 4.5**.
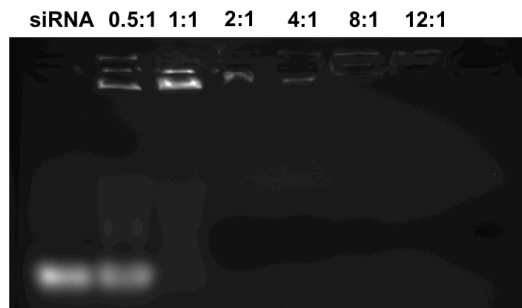
Figure 4.34. Gel retardation assay to assess PTDM / siRNA complex formation using dEt$_5$-*b*-dG$_{20}$. All samples were run on a 0.8% agarose gel and the N:P ratios tested ranged from 0.5:1 to 12:1, with 1 µg of siRNA per well.
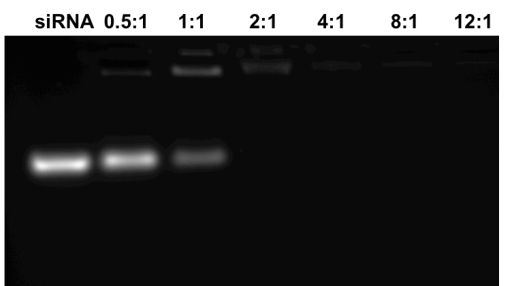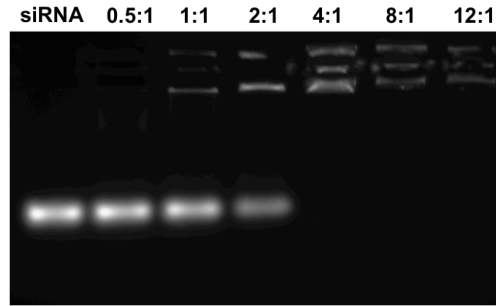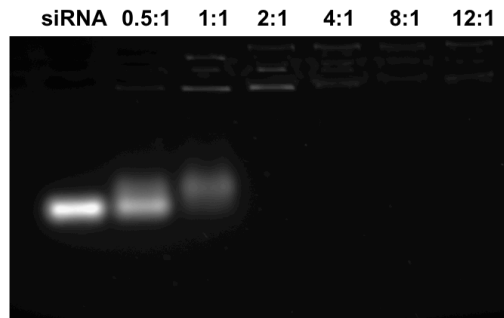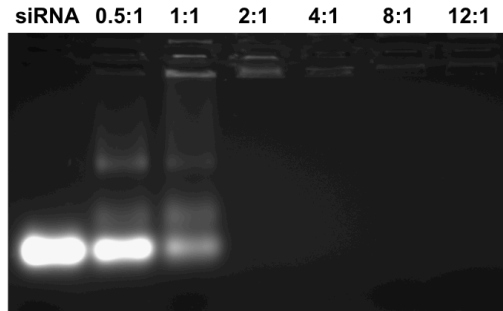
Figure 4.35. Gel retardation assay to assess PTDM / siRNA complex formation using diBu$_5$-*b*-dG$_{20}$. All samples were run on a 0.8% agarose gel and the N:P ratios tested ranged from 0.5:1 to 12:1, with 1 µg of siRNA per well.
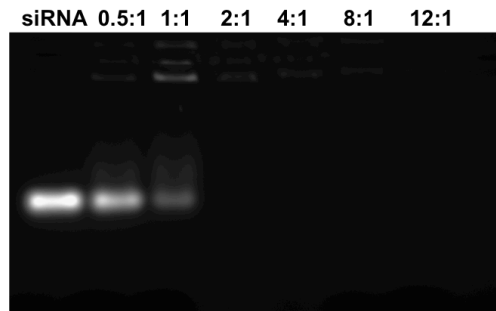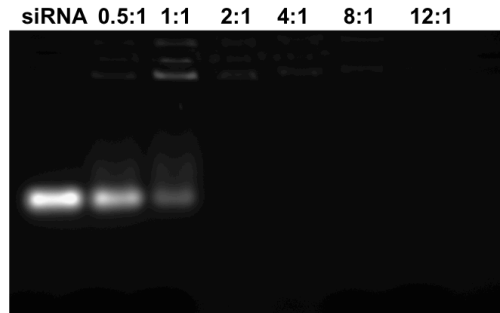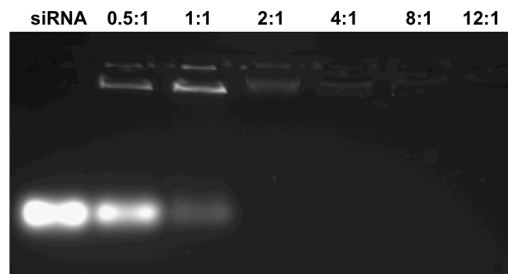

Figure 4.36. Gel retardation assay to assess PTDM / siRNA complex formation using dCy$_5$-*b*-dG$_{20}$. All samples were run on a 0.8% agarose gel and the N:P ratios tested ranged from 0.5:1 to 12:1, with 1 µg of siRNA per well.
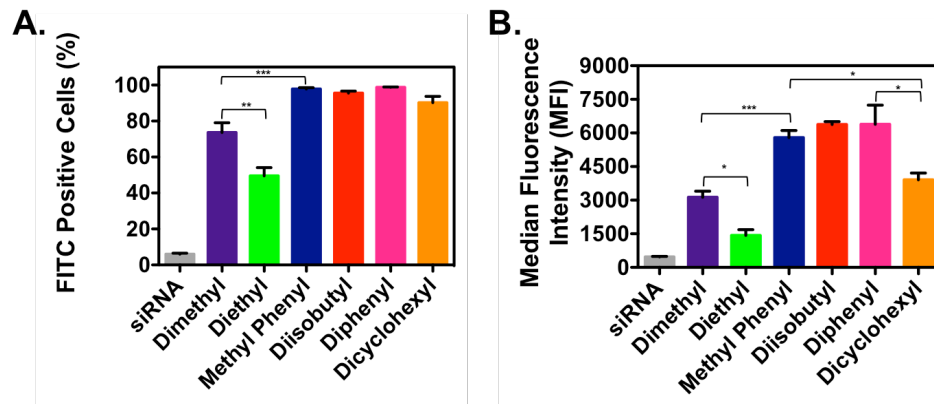

Figure 4.37. FITC-siRNA delivery into Jurkat T cells using ROMP-based protein mimics containing the same cationic charge content but different hydrophobic blocks. Jurkat T cells (cell density = 4x10^5 cells/mL) treated with polymer/FITC-siRNA complexes with an N/P ratio = 8/1 in complete media for four hours at 37°C and compared cells only receiving FITC-siRNA. All data was compared to an untreated control. A) Percent positive Jurkat T cells. B) Median fluorescence intensity (MFI) of the Jurkat T cell population. * p = < 0.05, ** = $p < 0.01$, *** = $p < 0.001$, ns = not significant, as calculated by the unpaired two-tailed student *t*-test. * represents significance between block copolymer PTDMs with the same charge content.
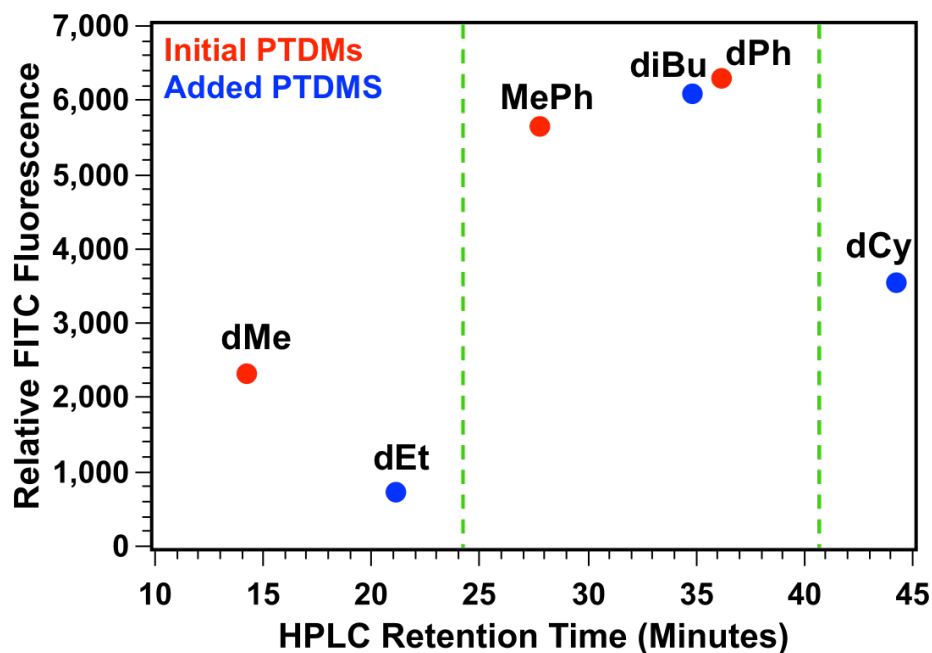
Figure 4.38. Plot of relative FITC fluorescence as it relates to monomer HPLC retention times. Green dashed lines indicate the hydrophobic window for optimal PTDM performance. Red data points represent hydrophobic monomers initially used. Blue data points represent hydrophobic monomers added after monomer hydrophobicity assessment by HPLC.
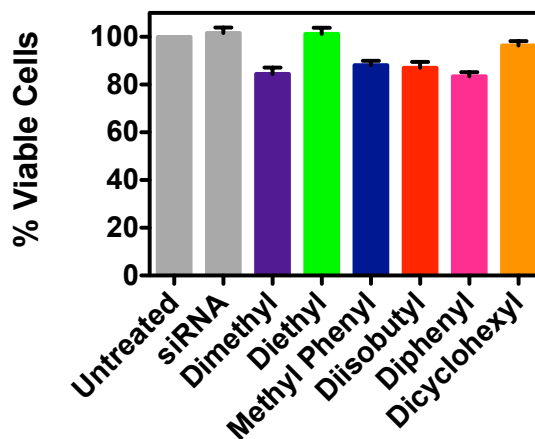
Figure 4.39. Percent viable Jurkat T cells using a 7-Amino-actinomycin (7-AAD) viability assay. Jurkat T cells (cell density = 4×10^5 cells/mL) were treated with polymer/FITC-siRNA complexes with an N/P ratio = 8/1 in complete media for four hours at 37°C and compared with untreated cells and cells only receiving FITC-siRNA. Cells were stained at four hours. Each data point represents the mean ± SEM of three independent experiments.

141

From the initial studies, there appeared to be a hydrophobic threshold (**dMe** < **MePh** ~ **dPh**) for efficient internalization shown by the green dashed line near 24 minutes. The new **dEt**-containing PTDM appears to support this hypothesis given that it delivers similar amounts of FITC-siRNA compared to the **dMe**-containing PTDM despite being more hydrophobic. Increasing the monomer hydrophobicity with **diBu**-containing PTDMs beyond the "threshold value" yields internalization values similar to **MePh**- and **dPh**-containing PTDMs; however, a further increase in the monomer hydrophobicity to **dCy** yields a PTDM that generates lower FITC-siRNA internalization than the three PTDMs composed of monomer HPLC RTs of 27.8 minutes to 36.1 minutes. This would suggest a window of optimal hydrophobicity when using these PTDMs for siRNA internalization. Furthermore, polymers that fall within this critical hydrophobic window are comprised of both aromatic and non-aromatic-containing PTDMs, suggesting that overall hydrophobicity may be more important than monomer composition.

4.6 Conclusions

Understanding the structural components of carrier molecules necessary for efficient siRNA internalization is critical for the development of more efficient delivery reagents. In efforts to better determine appropriate design principles for our ROMP-based PTDMs, several new PTDMs were designed to understand how the length and relative hydrophobicity of the non-charged block had on FITC-siRNA internalization efficiencies in Jurkat T cells, a suspension cell type, and HeLa cells, an adherent cell type. Initially a set of symmetric (n = m) and asymmetric (n ≠ m, with n being fixed at five for all polymers in the series) BCP PTDMs were tested with m = 5, 10, 20, or 40. At fixed cationic block lengths, the percentage of the cell population receiving FITC-siRNA remained the same regardless of the hydrophobic block length; however, the asymmetric **MePh$_5$-*b*-dG$_{20}$** had twice the fluorescence intensity of **MePh$_{20}$-*b*-dG$_{20}$**,

demonstrating the complex relationship between hydrophobic and cationic block lengths. In a separate series of polymers, the hydrophobic block length was held constant at five repeat units, but the hydrophobic component was varied from **dMe-**, to **MePh-**, to **dPh**-based repeat units, which represent a range of hydrophobicities. In this series, the **dMe**-based PTDMs exhibited diminished internalization efficiencies in comparison to their more hydrophobic counterparts (**MePh**- and **dPh**-based PTDMs). This suggested there was a minimum hydrophobicy required for efficient internalization. HPLC retention times were used to assess the relative hydrophobicity of monomers and to select a few for the design of additional PTDMs prepared, (**dEt-*b*-dG$_{20}$**, **diBu-*b*-dG$_{20}$**, and **dCy-*b*-dG$_{20}$**) to more fully explore this optimal hydrophobic window. An approximately 10 minute retention time window between 27 and 37 (or logP values of 1.78 and 3.50) was shown to yield optimal PTDM siRNA internalization efficiencies. Below this threshold, PTDMs lack sufficient hydrophobicity to promote efficient internalization and the PTDM above this hydrophobicity also showed diminished internalization capabilities. The polymers that fall within the critical hydrophobic window are comprised of both aromatic and non-aromatic-containing PTDMs, suggesting that overall hydrophobicity may be more important than monomer composition. Overall, optimization of PTDM hydrophobicity led to a better understanding of the structural components necessary for efficient siRNA internalization, which will be used in the future to guide the development of superior delivery reagents.

4.7   Acknowledgement

this chapter. Mass spectral data were obtained at the University of Massachusetts Mass Spectrometry Facility, which is supported in part by NSF. Flow cytometry data were obtained using the Flow Cytometry Core Facility at the University of Massachusetts Amherst, which is supported in part by NSF.

4.8   References

(1)   Lorenzer, C.; Dirin, M.; Winkler, A. M.; Baumann, V.; Winkler, J. J Control Release 2015, 203, 1-15.
(2)   Whitehead, K. A.; Langer, R.; Anderson, D. G. Nat Rev Drug Discov 2009, 8, 129-138.
(3)   Deshayes, S.; Morris, M. C.; Divita, G.; Heitz, F. Cell Mol Life Sci 2005, 62, 1839-1849.
(4)   Fonseca, S. B.; Pereira, M. P.; Kelley, S. O. Adv Drug Deliv Rev 2009, 61, 953-964.
(5)   Heitz, F.; Morris, M. C.; Divita, G. Brit J Pharmacol 2009, 157, 195-206.
(6)   Park, T. G.; Jeong, J. H.; Kim, S. W. Adv Drug Deliv Rev 2006, 58, 467-486.
(7)   Snyder, E. L.; Dowdy, S. F. Pharm Res 2004, 21, 389-393.
(8)   Thomas, M.; Klibanov, A. M. Appl Microbiol Biotechnol 2003, 62, 27-34.
(9)   Frankel, A. D.; Pabo, C. O. Cell 1988, 55, 1189-1193.
(10)   Green, M.; Loewenstein, P. M. Cell 1988, 55, 1179-1188.
(11)   Joliot, A.; Pernelle, C.; Deagostinibazin, H.; Prochiantz, A. Proc. Natl. Acad. Sci. U. S. A. 1991, 88, 1864-1868.
(12)   Vives, E.; Brodin, P.; Lebleu, B. Journal of Biological Chemistry 1997, 272, 16010-16017.
(13)   Mitchell, D. J.; Kim, D. T.; Steinman, L.; Fathman, C. G.; Rothbard, J. B. Journal of Peptide Research 2000, 56, 318-325.
(14)   Wender, P. A.; Mitchell, D. J.; Pattabiraman, K.; Pelkey, E. T.; Steinman, L.; Rothbard, J. B. Proceedings of the National Academy of Sciences of the United States of America 2000, 97, 13003-13008.
(15)   Lindgren, M.; Langel, U. Cell-Penetrating Peptides: Methods and Protocols 2011, 683, 3-19.
(16)   Siprashvili, Z.; Reuter, J. A.; Khavari, P. A. Molecular Therapy 2004, 9, 721-728.
(17)   Opalinska, J. B.; Gewirtz, A. M. Nature Reviews Drug Discovery 2002, 1, 503-514.
(18)   Patel, L. N.; Zaro, J. L.; Shen, W. C. Pharmaceutical Research 2007, 24, 1977-1992.
(19)   Futaki, S.; Suzuki, T.; Ohashi, W.; Yagami, T.; Tanaka, S.; Ueda, K.; Sugiura, Y. Journal of Biological Chemistry 2001, 276, 5836-5840.
(20)   Morris, M. C.; Depollier, J.; Mery, J.; Heitz, F.; Divita, G. Nature Biotechnology 2001, 19, 1173-1176.
(21)   Morris, M. C.; Deshayes, S.; Heitz, F.; Divita, G. Biology of the Cell 2008, 100, 201-217.

(22)   Morris, M. C.; Vidal, P.; Chaloin, L.; Heitz, F.; Divita, G. Nucleic Acids Research 1997, 25, 2730-2736.

(23)   Boisguerin, P.; Deshayes, S.; Gait, M. J.; O'Donovan, L.; Godfrey, C.; Betts, C. A.; Wood, M. J.; Lebleu, B. Adv Drug Deliv Rev 2015, 87, 52-67.

(24)   Crombez, L.; Morris, M. C.; Deshayes, S.; Heitz, F.; Divita, G. Curr. Pharm. Design 2008, 14, 3656-3665.

(25)   Huang, Y. W.; Lee, H. J.; Tolliver, L. M.; Aronstam, R. S. Biomed Res Int 2015, 2015, 834079.

(26)   Simeoni, F.; Morris, M. C.; Heitz, F.; Divita, G. Nucleic Acids Res. 2003, 31, 2717-2724.

(27)   deRonde, B. M.; Tew, G. N. Biopolymers 2015, 104, 265-280.

(28)   Sgolastra, F.; Minter, L. M.; Osborne, B. A.; Tew, G. N. Biomacromolecules 2014, 15, 812-820.

(29)   Tezgel, A. O.; Gonzalez-Perez, G.; Telfer, J. C.; Osborne, B. A.; Minter, L. M.; Tew, G. N. Mol Ther 2013, 21, 201-209.

(30)   Vader, P.; van der Aa, L. J.; Storm, G.; Schiffelers, R. M.; Engbersen, J. F. Curr Top Med Chem 2012, 12, 108-119.

(31)   deRonde, B. M.; Torres, J. A.; Minter, L. M.; Tew, G. N. Biomacromolecules 2015, 16, 3172–3179.

(32)   Tabujew, I.; Freidel, C.; Krieg, B.; Helm, M.; Koynov, K.; Mullen, K.; Peneva, K. Macromol. Rapid Commun. 2014, 35, 1191-1197.

(33)   Kim, S. H.; Jeong, J. H.; Kim, T. I.; Kim, S. W.; Bull, D. A. Mol. Pharm. 2009, 6, 718-726.

(34)   Kim, S. H.; Jeong, J. H.; Ou, M.; Yockman, J. W.; Kim, S. W.; Bull, D. A. Biomaterials 2008, 29, 4439-4446.

(35)   Cooley, C. B.; Trantow, B. M.; Nederberg, F.; Kiesewetter, M. K.; Hedrick, J. L.; Waymouth, R. M.; Wender, P. A. J. Am. Chem. Soc. 2009, 131, 16401-16403.

(36)   Geihe, E. I.; Cooley, C. B.; Simon, J. R.; Kiesewetter, M. K.; Edward, J. A.; Hickerson, R. P.; Kaspar, R. L.; Hedrick, J. L.; Waymouth, R. M.; Wender, P. A. Proc. Natl. Acad. Sci. U. S. A. 2012, 109, 13171-13176.

(37)   Wender, P. A.; Huttner, M. A.; Staveness, D.; Vargas, J. R.; Xu, A. F. Mol. Pharm. 2015, 12, 742-750.

(38)   Brogden, K. A. Nat. Rev. Microbiol. 2005, 3, 238-250.

(39)   Gabriel, G. J.; Som, A.; Madkour, A. E.; Eren, T.; Tew, G. N. Mater Sci Eng R Rep 2007, 57, 28-64.

(40)   Kuroda, K.; Caputo, G. A. WIREs Nanomed. Nanobiotechnol. 2013, 5, 49-66.

(41)   Som, A.; Vemparala, S.; Ivanov, I.; Tew, G. N. Biopolymers 2008, 90, 83-93.

(42)   Tew, G. N.; Scott, R. W.; Klein, M. L.; Degrado, W. F. Acc. Chem. Res. 2010, 43, 30-39.

(43)   deRonde, B. M.; Birke, A.; Tew, G. N. Chemistry 2015, 21, 3013-3019.

(44)   Gabriel, G. J.; Madkour, A. E.; Dabkowski, J. M.; Nelson, C. F.; Nusslein, K.; Tew, G. N. Biomacromolecules 2008, 9, 2980-2983.

(45)   Hennig, A.; Gabriel, G. J.; Tew, G. N.; Matile, S. J Am Chem Soc 2008, 130, 10338-10344.

(46)   Som, A.; Reuter, A.; Tew, G. N. Angew Chem Int Ed Engl 2012, 51, 980-983.

(47)   Som, A.; Tezgel, A. O.; Gabriel, G. J.; Tew, G. N. Angew Chem Int Ed Engl 2011, 50, 6147-6150.

(48) Tezgel, A. O.; Telfer, J. C.; Tew, G. N. Biomacromolecules 2011, 12, 3078-3083.

(49) Futaki, S.; Ohashi, W.; Suzuki, T.; Niwa, M.; Tanaka, S.; Ueda, K.; Harashima, H.; Sugiura, Y. Bioconjug Chem 2001, 12, 1005-1011.

(50) Katayama, S.; Hirose, H.; Takayama, K.; Nakase, I.; Futaki, S. J Control Release 2011, 149, 29-35.

(51) Rothbard, J. B.; Jessop, T. C.; Lewis, R. S.; Murray, B. A.; Wender, P. A. J Am Chem Soc 2004, 126, 9506-9507.

(52) Takeuchi, T.; Kosuge, M.; Tadokoro, A.; Sugiura, Y.; Nishi, M.; Kawata, M.; Sakai, N.; Matile, S.; Futaki, S. ACS Chem Biol 2006, 1, 299-303.

(53) Nishihara, M.; Perret, F.; Takeuchi, T.; Futaki, S.; Lazar, A. N.; Coleman, A. W.; Sakai, N.; Matile, S. Org Biomol Chem 2005, 3, 1659-1669.

(54) Sakai, N.; Futaki, S.; Matile, S. Soft Matter 2006, 2, 636-641.

(55) Morris, M. C.; Depollier, J.; Mery, J.; Heitz, F.; Divita, G. Nat Biotechnol 2001, 19, 1173-1176.

(56) Thaker, H. D.; Cankaya, A.; Scott, R. W.; Tew, G. N. ACS Med Chem Lett 2013, 4, 481-485.

(57) Thaker, H. D.; Som, A.; Ayaz, F.; Lui, D.; Pan, W.; Scott, R. W.; Anguita, J.; Tew, G. N. J Am Chem Soc 2012, 134, 11088-11091.

(58) Thaker, H. D.; Sgolastra, F.; Clements, D.; Scott, R. W.; Tew, G. N. J Med Chem 2011, 54, 2241-2254.

(59) Bielawski, C. W.; Benitez, D.; Grubbs, R. H. J Am Chem Soc 2003, 125, 8424-8425.

(60) Bielawski, C. W.; Grubbs, R. H. Angew Chem Int Ed Engl 2000, 39, 2903-2906.

(61) Bielawski, C. W.; Grubbs, R. H. Prog. Polym. Sci. 2007, 32, 1-29.

(62) Cannizzo, L. F.; Grubbs, R. H. Macromolecules, 21, 1961-1967.

(63) Love, J. A.; Morgan, J. P.; Trnka, T. M.; Grubbs, R. H. Angew Chem Int Ed Engl 2002, 41, 4035-4037.

(64) Schwab, P.; France, M. B.; Ziller, J. W.; Grubbs, R. H. Angew Chem Int Ed Engl 1995, 34, 2039-2041.

(65) Singh, R.; Czekelius, C.; Schrock, R. R. Macromolecules 2006, 39, 1316-1317.

(66) Trnka, T. M.; Grubbs, R. H. Acc Chem Res 2001, 34, 18-29.

(67) Mitchell, D. J.; Kim, D. T.; Steinman, L.; Fathman, C. G.; Rothbard, J. B. J Pept Res 2000, 56, 318-325.

(68) Lienkamp, K.; Madkour, A. E.; Musante, A.; Nelson, C. F.; Nusslein, K.; Tew, G. N. J Am Chem Soc 2008, 130, 9836-9843.

CHAPTER 5

PERSPECTIVE AND FUTURE DIRECTIONS

5.1   Perspective

Looking forward, intracellular delivery of siRNA, pDNA, proteins, and other biologics will be at the forefront of the development of more sophisticated therapeutic treatment options. In turn, this will require equally sophisticated and well understand delivery systems to be designed to meet the challenges associated with the cellular internalization of these complex molecules.[1] It is further anticipated that CPPMs and PTDMs will play critical roles in this area. Early structure-activity relationship studies on proteins led to the elucidation of essential design features for CPPs and enabled protein mimics to be developed. These essential features include cationic charge content, often in the form of guanidinium moieties, and hydrophobic content, often completely segregated from the cationic component.[1-3] The extension of these design principles to polymers represents another critical step in our fundamental understanding and is expected to produce some of the most useful CPPMs and PTDMs.

One of the major strengths of polymeric CPPMs and PTDMs is the tunability of their scaffolds.[1] Researchers over the last decade have demonstrated that a wide range of polymer backbones such as poly(oxa)norbornene[,3-14], polymethacrylamide[15], poly(disulfide-amine)[16-21], oligocarbonate[22,23], and polydisulfide[24,25]can be used to display key features of CPPs while the development of new backbone chemistries is ongoing. Additionally, polymeric mimics offer the ability to tune molecular compositions and molecular weights more easily and with more structural options than offered by peptide-base scaffolds.[1] This allows elegant, well-controlled structure-property relationship studies to be performed in order to understand the influence polymer structures and compositions have on bioactive cargo internalization and delivery. Unfortunately, the

role structure plays in efficient bioactive cargo internalization and delivery is often underappreciated. Many researchers put their primary focus on establishing the therapeutic potential of a material as opposed to understanding how or why a material works and if a better design exists. Moving forward, however, a more complete understanding of the structural components necessary for efficient internalization and delivery is critical for the development of the next generation of delivery reagents.

5.2   Future Directions

This thesis primarily documented structure-activity relationships with ROMP-based protein mimics to elucidate the essential design principles that govern efficient membrane interactions as well as siRNA internalization and delivery.[14,26] The findings presented here defined the critical cationic charge content and the ideal hydrophobic window for efficient siRNA delivery.[14] These parameters are expected to serve as guidelines for the future development of PTDMs for siRNA delivery applications. It is also anticipated that future structure-activity relationship studies will be extended to include the imide-based ROMP scaffold, which our group has extensively explored using biophysical assays as well as to use both ROMP scaffolds to explore how complex size trends with PTDM structures using dynamic light scattering (DLS) and cryogenic transmission electron microscopy (cryo-TEM). Further structure-activity relationship studies can be performed to understand how the nature of the cation impacts delivery efficiency by varying it from guanidinium moieties to ammonium or phosphonium moieties.

More broadly, given the highly cationic nature of the PTDMs developed for this thesis work, the siRNA PTDM library can be adapted for the delivery of plasmid DNA (pDNA). Plasmid DNA delivery is advantageous because it is self-sustaining and allows for the prolonged expression of proteins within cells. In addition, there is an extensive

library of commercially available plasmids, allowing for a range of potential therapeutic applications.   Given that siRNA and pDNA both consist of negatively charged nucleobases, they both would interact with cationic PTDMs through electrostatic interactions, allowing the siRNA PTDMs to be used as a starting point for pDNA delivery.[27] Further optimization would likely be necessary to account for the much larger size of pDNA compared to siRNA, which would require more charges to be screened and for the cargo to be condensed considerably prior to delivery.[28-32] Being able to deliver pDNA would not only show the versatility of our molecules but would also open up new areas of biology to explore.[33-35]

Looking forward, as delivery capabilities continue to improve, the possibilities open up for more sophisticated treatment options. One such option is the co-delivery of multiple cargoes. Currently, many researchers have started exploring the co-delivery of siRNAs and chemotherapeutics, such as Paclitaxel or Doxorubicin.[36-39] The siRNA in these treatments is used to knockdown genes that are providing cells with chemotherapeutic resistance.[36-39] Transient knockdown of these pathways restores the chemotherapeutic agent's potency and reduces the need for the development of new cancer drugs.[36-39]   Given that our ROMP-based protein mimics have demonstrated successful siRNA delivery, adaptation of this platform to the co-delivery of siRNA and small molecules is likely feasible.

Another area where co-delivery could be advantageous is in relation to the CRISPR (clustered regularly interspaced short palindromic repeats)/Cas-9 system, which is an RNA-guided endonuclease technology currently being used for genome editing and repair. CRISPRs are sequences of prokaryotic DNA that consist of short base-pair sequences that are regularly repeated. Cas9, in particular, is a CRISPR associated (Cas) endonuclease.[40-42] For this system to function, a guide RNA (gRNA) needs to be co-expressed since it is this component that enables targeting of the specific

DNA sequenced to be modified.[40-42] Previous literature has demonstrated the co-delivery of the gRNA and Cas9 proteins by lipid-mediated delivery and through covalent attachment of the components to CPPs.[43,44] In both cases, they found it advantageous to deliver both the protein and guide RNA (gRNA) at the same time.[43,44] They mention that using pDNA for this application has severe drawbacks, including that they may insert themselves into the genome permanently and disrupt endogenous genes or may leave the cell susceptible to long term exposure of the CRISPR/Cas9 components and potentially leading to unwanted side effects.[43,44] They also note that using mRNA presents the problems of stability of the mRNA during delivery and potential immunogenicity effects from inserted foreign nucleic acids into the cell.[43,44]

Given our groups history of designing PTDMs for siRNA and protein delivery, our platforms can likely be extended to the delivery of the components for the CRISPR/Cas-9 system. Proof-of-concept experiments charting the co-delivery of model RNAs and proteins, such as AlexaFluor-labeled siRNA and enhanced green fluorescent protein (EGFP) can be used to screen potential PTDMs for these applications. This platform can then be evaluated using bioactive siRNA and proteins to demonstrate that the co-delivery process did not alter molecular function. Following this pre-screening, the platform can easily be extended to the CRISPR/Cas-9 system. Given the versatility of the PTDM platform, it can be envisaged that either one PTDM or a mixture of PTDMs could be used for the delivery of both components. In addition, the proven success of this system in hard-to-transfect cell types opens the possibilities of extending this platform to stem cells. Since stem cells can be differentiated into many cell types, correcting the genome at this stage would permanently correct the mutation and produce a wide range of cells expressing the correct sequences.

Overall, CPPMs and PTDMs appear to have an important role to play in the area of bioactive cargo delivery, having already demonstrated their ability to perform in the

arena of new immunological research and fundamental cell biology. Therapeutic delivery for the treatment of human disease, though a more difficult and complex issue, remains the ultimate goal. While the challenge is daunting, CPPMs and PTDMs are a promising technology undergoing continual refinement and offering many potential advantages. This thesis work provides considerably more insight into how PTDM structure and composition impact their overall delivery capabilities and will no doubt help guide the future development of efficient PTDM for intracellular delivery.

5.3   References

(1)   deRonde, B. M.; Tew, G. N. *Biopolymers* 2015, 104, 265-280.
(2)   Stanzl, E. G.; Trantow, B. M.; Vargas, J. R.; Wender, P. A. *Acc. Chem. Res.* 2013, **46**, 2944-2954.
(3)   Sgolastra, F.; deRonde, B. M.; Sarapas, J. M.; Som, A.; Tew, G. N. *Acc. Chem. Res.* 2013.
(4)   Gabriel, G. J.; Madkour, A. E.; Dabkowski, J. M.; Nelson, C. F.; Nusslein, K.; Tew, G. N. *Biomacromolecules* 2008, **9**, 2980-2983.
(5)   Hennig, A.; Gabriel, G. J.; Tew, G. N.; Matile, S. *J Am Chem Soc* 2008, **130**, 10338-10344.
(6)   Kolonko, E. M.; Kiessling, L. L. *J Am Chem Soc* 2008, **130**, 5626-5627.
(7)   Kolonko, E. M.; Pontrello, J. K.; Mangold, S. L.; Kiessling, L. L. *J Am Chem Soc* 2009, **131**, 7327-7333.
(8)   Sgolastra, F.; Minter, L. M.; Osborne, B. A.; Tew, G. N. *Biomacromolecules* 2014, **15**, 812-820.
(9)   Som, A.; Reuter, A.; Tew, G. N. *Angewandte Chemie* 2012, **51**, 980-983.
(10)   Som, A.; Tezgel, A. O.; Gabriel, G. J.; Tew, G. N. *Angewandte Chemie* 2011, **50**, 6147-6150.
(11)   Strong, L. E.; Kiessling, L. L. *J Am Chem Soc* 1999, **121**, 6193-6196.
(12)   Tezgel, A. O.; Gonzalez-Perez, G.; Telfer, J. C.; Osborne, B. A.; Minter, L. M.; Tew, G. N. *Molecular therapy : the journal of the American Society of Gene Therapy* 2013, **21**, 201-209.
(13)   Tezgel, A. O.; Telfer, J. C.; Tew, G. N. *Biomacromolecules* 2011, **12**, 3078-3083.
(14)   deRonde, B. M.; Torres, J. A.; Minter, L. M.; Tew, G. N. *Biomacromolecules* 2015, 16, 3172–3179.
(15)   Treat, N. J.; Smith, D.; Teng, C.; Flores, J. D.; Abel, B. A.; York, A. W.; Huang, F.; McCormick, C. L. *ACS macro letters* 2012, **1**, 100-104.
(16)   Kim, S. H.; Jeong, J. H.; Kim, T. I.; Kim, S. W.; Bull, D. A. *Mol. Pharm.* 2009, **6**, 718-726.
(17)   Kim, S. H.; Jeong, J. H.; Ou, M.; Yockman, J. W.; Kim, S. W.; Bull, D. A. *Biomaterials* 2008, **29**, 4439-4446.
(18)   Kim, T. I.; Kim, S. W. *Reactive & functional polymers* 2011, **71**, 344-349.
(19)   Kim, T. I.; Lee, M.; Kim, S. W. *Biomaterials* 2010, **31**, 1798-1804.

(20)   Kim, T. I.; Ou, M.; Lee, M.; Kim, S. W. *Biomaterials* 2009, **30**, 658-664.

(21)   Ou, M.; Wang, X. L.; Xu, R.; Chang, C. W.; Bull, D. A.; Kim, S. W. *Bioconjugate chemistry* 2008, **19**, 626-633.

(22)   Cooley, C. B.; Trantow, B. M.; Nederberg, F.; Kiesewetter, M. K.; Hedrick, J. L.; Waymouth, R. M.; Wender, P. A. *J Am Chem Soc* 2009, **131**, 16401-16403.

(23)   Geihe, E. I.; Cooley, C. B.; Simon, J. R.; Kiesewetter, M. K.; Edward, J. A.; Hickerson, R. P.; Kaspar, R. L.; Hedrick, J. L.; Waymouth, R. M.; Wender, P. A. *P Natl Acad Sci USA* 2012, **109**, 13171-13176.

(24)   Bang, E. K.; Gasparini, G.; Molinard, G.; Roux, A.; Sakai, N.; Matile, S. *J Am Chem Soc* 2013, **135**, 2088-2091.

(25)   Gasparini, G.; Bang, E. K.; Molinard, G.; Tulumello, D. V.; Ward, S.; Kelley, S. O.; Roux, A.; Sakai, N.; Matile, S. *J Am Chem Soc* 2014, **136**, 6069-6074.

(26)   deRonde, B. M.; Birke, A.; Tew, G. N. *Chem. Eur. J.* 2015, **21**, 3013-3019.

(27)   Scholz, C.; Wagner, E. *J. Control Rel.* 2012, **161**, 554-565.

(28)   Luo, D.; Saltzman, W. M. *Nat. Biotechnol.* 2000, **18**, 33-37.

(29)   Heitz, F.; Morris, M. C.; Divita, G. *Brit J Pharmacol* 2009, **157**, 195-206.

(30)   Park, T. G.; Jeong, J. H.; Kim, S. W. *Adv Drug Deliver Rev* 2006, **58**, 467-486.

(31)   Thomas, M.; Klibanov, A. M. *Appl Microbiol Biot* 2003, **62**, 27-34.

(32)   Wolff, J. A.; Malone, R. W.; Williams, P.; Chong, W.; Acsadi, G.; Jani, A.; Felgner, P. L. *Science* 1990, **247**, 1465-1468.

(33)   Johnston, S. A.; Qu, B. X.; McGuire, M.; Stemke-Hale, K.; Sykes, K. *Developments in biologicals* 2000, **104**, 3-8.

(34)   Meerak, J.; Wanichwecharungruang, S. P.; Palaga, T. *Vaccine* 2013, **31**, 784-790.

(35)   Laddy, D. J.; Weiner, D. B. *International reviews of immunology* 2006, **25**, 99-123.

(36)   Li, J. M.; Zhang, W.; Su, H.; Wang, Y. Y.; Tan, C. P.; Ji, L. N.; Mao, Z. W. *International journal of nanomedicine* 2015, **10**, 3147-3162.

(37)   Sun, T. M.; Du, J. Z.; Yao, Y. D.; Mao, C. Q.; Dou, S.; Huang, S. Y.; Zhang, P. Z.; Leong, K. W.; Song, E. W.; Wang, J. *ACS nano* 2011, **5**, 1483-1494.

(38)   Wei, W.; Lv, P. P.; Chen, X. M.; Yue, Z. G.; Fu, Q.; Liu, S. Y.; Yue, H.; Ma, G. H. *Biomaterials* 2013, **34**, 3912-3923.

(39)   Chen, W.; Yuan, Y.; Cheng, D.; Chen, J.; Wang, L.; Shuai, X. *Small* 2014, **10**, 2678-2687.

(40)   Pellagatti, A.; Dolatshad, H.; Valletta, S.; Boultwood, J. *Archives of toxicology* 2015, **89**, 1023-1034.

(41)   Pu, J.; Frescas, D.; Zhang, B.; Feng, J. *Experimental biology and medicine* 2015, **240**, 1065-1070.

(42)   Riordan, S. M.; Heruth, D. P.; Zhang, L. Q.; Ye, S. Q. *Cell & bioscience* 2015, **5**, 33.

(43)   Zuris, J. A.; Thompson, D. B.; Shu, Y.; Guilinger, J. P.; Bessen, J. L.; Hu, J. H.; Maeder, M. L.; Joung, J. K.; Chen, Z. Y.; Liu, D. R. *Nat Biotechnol* 2015, **33**, 73-80.

(44)   Ramakrishna, S.; Kwaku Dad, A. B.; Beloor, J.; Gopalappa, R.; Lee, S. K.; Kim, H. *Genome research* 2014, **24**, 1020-1027.

CHAPTER 6

EXPERIMENTAL

6.1 Materials and Instrumentation

Materials

Maleic anhydride, maleimide, furan, 4-dimethylaminopyridine (DMAP), 1-(3-Dimethylaminopropyl)-3-ethylcarbodiimide hydrochloride (EDC), 1,3-di-boc-2-(2-hydroxyethyl)guanidine, benzyl alcohol, 3,5-dinitrobenzyl alcohol, 3-nitrobenzyl alcohol, 3,5-bis(trifluoromethyl)benzyl alcohol, 3-trifluoromethylbenzyl alcohol, 3,5-difluorobenzyl alcohol, 3,5-dimethylbenzyl alcohol, 3,5-dimethoxybenzyl alcohol, N-boc-ethanolamine, diisopropyl azodicarboxylate (DIAD), triphenylphosphine, ethyl vinyl ether, trifluoroacetic acid (TFA), methanol (MeOH), 1-propanol, 1-butanol, isobutanol, cyclohexylmethanol, ethyl acetate (EtOAc) dimethyl sulfoxide (DMSO), pentane, 2,2,2-trifluoroethanol (TFE), water, and tetrahydrofuran (THF) were obtained as reagent grade from Aldrich, Fisher Scientific, Fluka or Acros and used as received. 3rd generation Grubbs catalyst (Dichloro-di(3-bromopyridino)-N,N'- Dimesitylenoimidazolino-Ru=CHPh; G3) was synthesized as described previously by Grubbs and coworkers.[1] Dichloromethane (CH_2Cl_2) (HPLC grade, Fisher Scientific) was distilled from CaH2 under nitrogen. Spectra/Por® 6 dialysis membranes with a MWCO of 2,000 g/mol and Biotech CD dialysis tubing with a MWCO of 100-500 g/mol were purchased from Spectrum Medical Industries. Egg yolk phosphatidylcholine (EYPC) brain phosphatidylserine (brain PS) lipids were purchased from Avanti Polar Lipids Inc. and 5(6)-carboxyfluorescein (CF) was purchased from Fluka. Sterile, RNase-free phosphate buffered saline (Amresco) and heparin, from porcine intestinal mucosa, were purchased from VWR and bovine serum albumin (BSA) and DMEM/high with L-glutamine and sodium pyruvate were

purchased from Sigma Aldrich and used as received. FITC-siRNA (sc-36869), siRNA to *hNOTCH1* (sc-36095), and RNase-free water were purchased from Santa Cruz Biotechnologies and R9, DeliverX Plus siRNA, Xfect, N-ter, RNAiMAX, and JetPEI were purchased from Peptide 2.0, Inc., Affymetrix, Clontech, Sigma Aldrich, Life Technologies, and Polyplus Transfection, respectively. Gibco RPMI 1640 glutaMAX and fetal bovine serum were purchased from Life Technologies and Penicillin/Streptomycin (10K/10K), MEM non-essential amino acids solution (10 mM, 100X), and sodium pyruvate solution (100 mM) were purchased from Lonza. Anti-human CD3 epsilon MAb (Clone UCHT1) and human CD28 MAb (Clone 37407) were purchased from R&D Systems, anti-human NOTCH1 PE, Annexin V PE apoptosis detection kit, 7-AAD viability stain, and Foxp3/transcription faction staining buffer set were purchased from eBiosciences. hPBMCs were purchased from from Stemcell Technologies, Inc. in 2.5×10^6 cells/aliquot (Product # 70047.2). For experiments, cells from different donors were used. The company obtained these cells using institutional review board approved consent forms and protocols.

Instrumentation

^{1}H and ^{13}C NMR spectra were recorded at 300 MHz and 75 MHz, respectively, using a Bruker DPX-300 NMR spectrometer. Chemical shifts (δ) are reported in ppm and coupling constants (J) in Hz. The abbreviations used for splitting patterns are: s, singlet; d, doublet; dd, doublet of doublets; t, triplet; tt, triplet of triplets; q, quartet; m, multiplet; comp, overlapping multiplets of magnetically non-equivalent protons; br, broad. Mass spectral data were obtained at the University of Massachusetts, Mass Spectrometry Facility from a JEOL JMS 700 instrument (JEOL, Peabody, MA). A CombiFlash® RF 200 automated chromatography system with a variable UV-Vis detector (λ= 200-780 nm, Teledyne ISCO, Lincoln, NE) was used for purification of monomer 13. 120 g RediSep

Rf Flash Columns were used for the separations. All other compounds were purified using standard silica gel chromatography methods.

A CombiFlash® RF 200 automated chromatography system with a variable UV-Vis detector (λ= 200-780 nm, Teledyne ISCO, Lincoln, NE) was used for purification of monomer **13**. 120 g Redi*Sep* Rf Flash Columns were used for the separations. All other compounds were purified using standard silica gel chromatography methods.

Gel permeation chromatography (GPC) chromatograms for boc-protected polymers were obtained using an Agilent 1260 series system equipped with a refractive index (RI) and ultraviolet (UV) detectors, a PL Gel 5 µm guard column con two 5 µm analytical Mixed-C columns and a 5 µm analytical Mixed-D column (Agilent). All columns were connected in series and incubated at 40 °C. THF was used as the eluent with a flow rate of 1.0 mL/min. ~ 3 mg/mL samples were prepared using THF as the diluent and toluene as the flow marker. All samples were filtered through 0.45 µm PTFE syringe filters (Restek, Bellefonte, PA) Polymethyl methacrylate and polystyrene standards were used for the calibration. Dye release assays were performed using a Biotek SynergyMx fluorescence plate reader that was incubated to 25 °C.

GPC chromatograms for deprotected polymers were obtained using an Agilent 1260 series system equipped with a refractive index (RI) and ultraviolet (UV) detectors, an HFIPgel guard column (7 mm x 50 mm; Agilent) and three HFIPgel columns (7 mm x 300 mm; Agilent). All columns were connected in series and incubated at 40 °C. TFE with 20 mM NaTFA salt was used as the eluent with a flow rate of 1.0 mL/min. ~ 3 mg/mL samples were prepared using TFE with 20 mM NaTFA salt as the diluent and methanol as the flow marker. All samples were filtered through a 0.45 µm PTFE syringe

filters (Restek, Bellefonte, PA). Poly(methyl methacrylate) standards were used for the calibration.

Flow cytometry (FCM) experiments were performed using a Becton Dickinson LSRII (BD Biosciences) with eight color analysis capabilities and two excitation lasers: 488 nm and 633 nm or a BD Dual LSRFortessa with eighteen color analysis capabilities and five excitation lasers: 355nm (UV), 405 nm, 488 nm 561 nm, and 640 nm. Fluorescence signals were collected for 10,000 cells.

HPLC was carried out a HP 5890 HPLC system equipped with a photodiode array detector using an Agilent Zorbax SB-C$_8$, 80 Å, 4.6 x 150 mm ID (5 µm) column. Samples were eluted using a linear gradient of 100% water with 0.1% TFA to 100% acetonitrile with 0.1% TFA over 60 minutes at a flow rate of 1 mL/min, and were detected using a wavelength of 215 nm.

6.2 Synthesis of π-rich and π-poor Half-esters
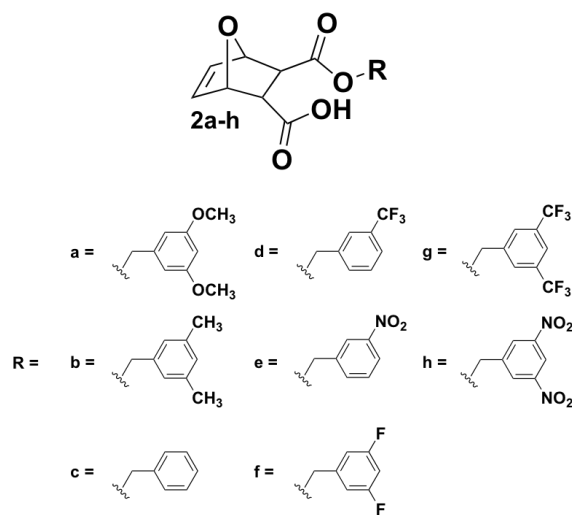
Figure 6.1 Half-ester final products 2a-h.

Synthesis of 2a: The procedure reported by Lienkamp *et al*. was followed with minor modifications.[2] One equivalent of **1**, 1.25 equivalents of the corresponding substituted benzyl alcohol, and 10 mol% DMAP were dissolved in a minimal amount of freshly distilled CH_2Cl_2 and the reaction mixture was stirred under nitrogen at RT overnight. The reaction mixture for **2a** was concentrated *via* rotary evaporation and the half ester was recrystallized from a mixture of chloroform/hexanes (3:1, v/v) and isolated *via* vacuum filtration. **2a** was then dried under vacuum at RT overnight.

Yield: 52 %, white crystals

^{1}H NMR (300 MHz, DMSO-d_6): δ 12.44 (br, 1H), 6.54 (s, 2H), 6.45 (comp, 3H), 5.12 (s, 2H), 4.94 (q, 2H), 3.73 (s, 6H), 2.79 (m, 2H);

^{13}C NMR (75 MHz, DMSO-d_6): δ 172.82, 171.60, 160.60, 138.42, 136.85, 136.67, 105.69, 99.76, 80.27, 79.93, 65.90, 55.29, 46.92, 46.21;

HR-MS (FAB) *m/z* [M+H]$^+$: 334.1053 (calc.), 334.1047 (found)

Synthesis of 2b-f: The procedure reported by Lienkamp *et al*. was followed with minor modifications.[2] One equivalent of **1**, 1.25 equivalents of the corresponding substituted benzyl alcohols, and 10 mol% DMAP were dissolved in a minimal amount of freshly distilled CH_2Cl_2 and the reaction mixture was stirred under nitrogen at RT overnight. **2b-f** precipitated from solution and were isolated *via* vacuum filtration and washed with cold CH_2Cl_2. **2b-f** were then dried under vacuum at RT overnight.

2b. 43 %, white powder

^{1}H NMR (300 MHz, DMSO-d_6): δ 12.41 (br, 1H), 6.95 (s, 3H), 6.45 (m, 2H), 5.10 (s, 2H), 4.92 (q, 2H), 2.76 (s, 2H), 2.26, (s, 6H)

^{13}C NMR (75 MHz, DMSO-d_6): δ 172.72, 171.56, 137.48, 136.76, 136.60, 135.83, 129.39, 125.85, 80.17, 79.83, 66.03, 46.78, 46.03, 20.92;

HR-MS (FAB) *m/z* [M+H]$^+$: 303.1262 (calc.), 303.1253 (found)

2c. Yield: 60 %, white powder

^{1}H NMR (300 MHz, DMSO-*d$_6$*): δ 12.46 (br, 1H), 7.36 (comp, 5H), 6.45 (m, 2H), 5.12 (m, 2H), 5.01 (q, 2H), 2.77 (d, 2H);

^{13}C NMR (75 MHz, DMSO-*d$_6$*): δ 172.74, 171.59, 136.79, 136.61, 136.07, 128.45, 128.05, 128.02, 80.18, 79.84, 65.99, 46.82, 46.10;

HR-MS (FAB) *m/z* [M+H]$^+$: 275.0914 (calc.), 275.0903 (found)

2d. Yield: 58 %, white powder

^{1}H NMR (300 MHz, DMSO-*d$_6$*): δ 12.46 (br, 1H), 7.76 (br, 1H), 7.70 (comp, 2H), 7.62 (m, 1H), 6.47 (m, 2H), 5.13 (comp, 4H), 2.82 (q, 2H);

^{13}C NMR (75 MHz, DMSO-*d$_6$*): δ 172.87, 171.68, 137.66, 136.67, 136.63, 131.98, 129.58, 129.18, 126.10, 124.71, 124.48, 122.49, 80.29, 79.94, 65.22, 47.01, 46.15;

HR-MS (FAB) *m/z* [M+H]$^+$: 343.0793 (calc.), 343.0804 (found)

2e. Yield: 47 %, white powder

^{1}H NMR (300 MHz, DMSO-*d$_6$*): δ 12.44 (br, 1H), 8.25 (m, 1H), 8.19 (m, 1H), 7.84 (m, 1H), 7.68 (m, 1H), 6.47 (m, 2H), 5.17 (comp, 4H), 2.82 (q, 2H);

^{13}C NMR (75 MHz, DMSO-*d$_6$*): δ 172.75, 171.60, 147.83, 138.41, 136.66, 136.58, 134.43, 130.01, 122.86, 122.48, 80.22, 79.91, 64.75, 46.97, 46.07;

HR-MS (FAB) *m/z* [M+H]$^+$: 320.0770 (calc.), 320.1766 (found)

2f. Yield: 41 %, white powder

^{1}H NMR (300 MHz, DMSO-*d$_6$*): δ 12.47 (br, 1H), 7.15 (comp, 3H), 6.47 (m, 2H), 5.14, (d, 2H), q (5.04, 2H), 2.82 (d, 2H);

^{13}C NMR (75 MHz, DMSO-d_6): δ 172.88, 171.57, 164.20, 164.03, 160.94, 160.77, 140.75 (t, 9.6 Hz), 136.88, 136.66, 110.63 (m), 103.24 (t, 25.7 Hz), 80.30, 79.93, 64.59, 47.03, 46.17;

HR-MS (FAB) *m/z* [M+H]$^+$: 320.0770 (calc.), 320.1766 (found)

Synthesis of 2g-h: The procedure reported by Lienkamp *et.al*. was followed with minor modifications.[2] One equivalent of **1**, 1.25 equivalents of the corresponding substituted benzyl alcohols, and 10 mol% DMAP were dissolved in a minimal amount of freshly distilled CH_2Cl_2 and the reaction mixture was stirred under nitrogen at RT overnight. Product purification was attempted using column chromatography with EtOAc / CH_2Cl_2 (1:4, v/v). Although all starting material was removed, **2g-h** were unstable in solution and byproducts from the retro Diels-Alder reaction were observed in the corresponding ^{1}H NMR spectra. The ^{1}H NMR peaks for the corresponding unstable product are listed below and impurities are omitted. The impurity was isolated for **2h** by column chromatography using CH_2Cl_2 / MeOH (9:1, v/v) and identified by ^{1}H NMR, ^{13}C NMR, and HR-MS (FAB).

2g. ^{1}H NMR (300 MHz, DMSO-d_6): δ 12.55 (br, 1H), 8.08 (comp, 3H), 6.47 (m, 2H), 5.18 (comp, 4H), 2.84 (q, 2H);

2h. ^{1}H NMR (300 MHz, DMSO-d_6): δ 12.39 (br, 1H), 8.79 (m, 1H), 8.67 (m, 2H), 6.48 (m, 2H), 5.31 (br, 2H), (d, 2H), 2.85 (q, 2H);

Impurity peaks: δ 8.70, 8.58, 6.58, 5.45, 5.36, 5.34, 5.26, 4.75, 3.30;
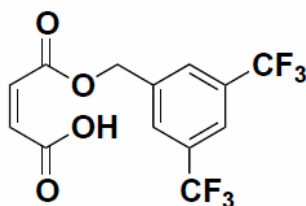
Figure 6.2. Structure of the Retro-Diels-Alder impurity **4g**.

Half-ester Impurity 4g:

^{1}H NMR (300 MHz, DMSO-d_6): δ 13.06 (br, 1H), 8.11 (comp, 3H), 6.47 (d, 2H), 5.37, (s, 2H);

^{13}C NMR (75 MHz, DMSO-d_6): δ 166.52, 165.16, 139.35, 132.04, 130.43 (q, 33.23 Hz), 128.74, 128.47, 125.13, 121.79, 121.52, 64.56;

HR-MS (FAB) *m/z* [M+H]$^+$: 343.0237 (calc.), 343.0417 (found).

6.3   Synthesis of π-rich and π-poor Diester Monomers:
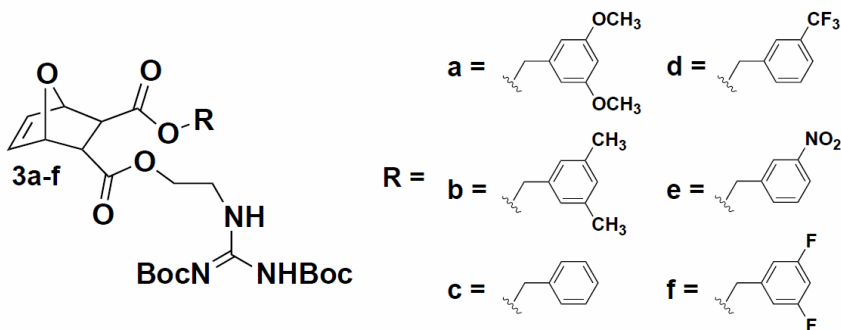
Figure 6.3. Diester monomer final products **3a-f**.

6.3.1   Synthesis of 3a-f:

The procedure reported by Lienkamp *et.al.* was followed with minor modifications.[2]   One equivalent of **2a-f**, one equivalent of 1,3-Di-Boc-2-(2-hydroxyethyl)guanidine, and 10 mol% DMAP were dissolved in CH$_2$Cl$_2$ and stirred at RT under nitrogen.   The solution

was then cooled down to 0°C in an ice bath and one equivalent of EDC was added. The solution was allowed to stir overnight under nitrogen and gradually return to RT. The reaction mixture was then concentrated *via* rotary evaporation and purified by either column chromatography with EtOAc/CH$_2$Cl$_2$ (1/4, v/v) as the eluent or by using a CombiFlash purification system, with a 120 g silica cartridge and EtOAc/CH$_2$Cl$_2$ (1/4, v/v) as the eluent. Pure fractions were combined and then concentrated *via* rotary evaporation. The sample was dried under vacuum overnight at RT to obtain a white solid.

3a: Yield 77 %, white powder

^{1}H NMR (300 MHz, DMSO-d_6): δ 11.48 (s, 1H), 8.41 (t, 1H), 6.50 (m, 2H), 6.45 (comp, 3H), 5.16 (d, 2H), 4.97 (q, 2H), 4.10 (m, 1H), 3.95 (m, 1H), 3.73 (s, 6H), 2.87 (q, 2H), 1.46 (s, 9H), 1.37 (s, 9H);

^{13}C NMR (75 MHz, CD$_3$CN): δ 172.92, 172.67, 164.93, 162.32, 157.75, 154.12, 139.81, 138.01, 137.96, 107.15, 100.85, 84.47, 81.81, 81.75, 79.94, 67.54, 64.03, 56.40, 48.18, 47.91, 40.62, 28.81, 28.52;

HR-MS (FAB) *m/z* [M+H]$^+$: 620.2819 (calc.), 620.2819 (found)

3b: Yield 74 %, white powder

^{1}H NMR (300 MHz, DMSO-d_6): δ 11.49 (br, 1H), 8.41 (t, 1H), 6.94 (br, 3H), 6.46 (m, 2H), 5.14 (d, 2H), 4.95 (q, 2H), 4.11 (m, 1H), 3.92 (m, 1H), 3.50 (m, 2H), 2.84 (q, 2H), 2.25 (s, 6H), 1.46 (s, 9H), 1.37 (s, 9H);

^{13}C NMR (75 MHz, CD$_3$CN): 172.90, 172.71, 164.95, 157.75 154.14, 139.47, 138.02, 137.97, 137.33, 130.98, 127.54, 84.50, 81.81, 81.78, 79.95, 67.92, 63.99, 48.16, 47.84, 40.67, 28.85, 28.55, 21.72;

HR-MS (FAB) *m/z* [M+H]$^+$: 588.2921 (calc.), 588.2908 (found)

3c: Yield 80 %, white powder

^{1}H NMR (300 MHz, DMSO-d_6): δ 12.46 (br, 1H), 7.34 (m, 5H), 6.46 (m, 2H), 5.11 (d, 2H), 5.01 (q, 2H), 2.77 (d, 2H);

^{13}C NMR (75 MHz, CD$_3$CN): δ 172.48, 172.29, 164.51, 157.33, 153.70, 137.57, 137.50, 137.06, 129.41, 129.21, 129.09, 84.04, 81.34, 81.32, 79.51, 67.37, 63.56, 47.68, 47.40, 40.20, 28.35, 28.06;

HR-MS (FAB) *m/z* [M+H]$^+$: 560.2608 (calc.), 560.2616 (found)

3d: Yield: 58 %, white powder

^{1}H NMR (300 MHz, DMSO-d_6): δ 11.49 (s, 1H), 8.42, (t, 1H), 7.67 (comp, 4H), 6.47 (t, 2H), 5.16 (comp, 4H), 4.10 (m, 1H), 3.94 (m, 1H), 3.49 (m, 2H), 2.88 (q, 2H), 1.45 (s, 9H), 1.35 (s, 9H)

^{13}C NMR (75 MHz, CD$_3$CN): δ 172.87, 172.73, 164.95, 163.70, 157.78, 154.16, 138.88, 138.02, 133.27, 130.78, 126.14 (m), 84.50, 81.84, 79.97, 66.91, 64.05, 48.09, 47.98, 40.65, 28.86, 28.56,

HR-MS (FAB) *m/z* [M+H]$^+$: 628.2482 (calc.), 628.2459 (found)

3e: Yield: 60 %, white powder

^{1}H NMR (300 MHz, DMSO-d_6): δ 11.47 (s, 1H), 8.41 (t, 1H), 8.21 (m, 1H), 7.83 (m, 1H), 7.69 (t, 1H), 6.47 (m, 2H), 5.18 (m, 4H), 4.11 (m, 1H), 3.96 (m, 1H), 3.49 (comp, 2H), 2.90 (q, 2H), 1.45 (s, 9H), 1.36 (s, 9H);

^{13}C NMR (75 MHz, CD$_3$CN): δ 172.87, 172.71, 164.91, 157.74, 154.12, 139.66, 137.99, 135.62, 131.16, 124.24, 124.02, 84.49, 81.84, 81.79, 79.96, 66.45, 64.07, 48.01, 47.97, 40.64, 28.78, 28.49

HR-MS (FAB) *m/z* [M+H]$^+$: 605.2441 (calc.), 605.2423 (found)

3f: Yield: 70 %, white powder

^{1}H NMR (300 MHz, DMSO-d_6): δ 11.47 (s, 1H), 8.41 (t, 1H), 7.18 (m, 1H), 7.09 (comp, 2H), 6.48 (m, 2H), 5.18 (s, 2H), 5.07 (q, 2H), 4.11 (m, 1H), 3.98 (m, 1H), 3.49 (m, 2H), 2.90 (q, 2H), 1.45 (s, 9H), 1.37 (s, 9H);

^{13}C NMR (75 MHz, CD$_3$CN): δ 171.54, 171.26, 164.61, 164.44, 163.57, 161.34, 161.17, 156.41, 152.79, 140.63 (t, J = 9.55 Hz), 136.66, 110.49 (m), 103.10 (t, J = 25.5 Hz), 83.14, 80.47, 78.61, 64.83, 62.75, 46.73, 46.68, 39.33, 27.49, 27.19;

HR-MS (FAB) *m/z* [M+H]$^+$: 596.2420 (calc.), 596.2409 (found)
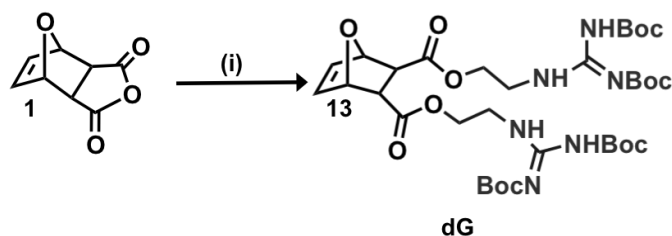
Figure 6.4. Synthesis of diguanidine monomer. i)1,3-di-boc-2-(2-hydroxyethyl)guanidine, DMAP, EDC, CH$_2$Cl$_2$, 0°C to RT, overnight;

The procedure reported by Lienkamp *et.al.* was followed with minor modifications.[2] One equivalent of **1**, two equivalents of 1,3-Di-Boc-2-(2-hydroxyethyl)guanidine, and 10 mol% DMAP were dissolved in CH$_2$Cl$_2$ and the reaction mixture was stirred overnight at RT under nitrogen. After one day, the solution was cooled down to 0°C in ice bath and one equivalent of EDC was added. The solution was allowed to stir overnight under nitrogen and gradually return to RT. The reaction mixture was then concentrated *via* rotary evaporation and purified using a CombiFlash purification system, with a 120 g silica cartridge and EtOAc/CH$_2$Cl$_2$ (1/4, v/v) as the eluent. Pure fractions were combined and then concentrated *via* rotary evaporation. The sample was dried under vacuum overnight at RT to obtain a white solid.

Yield = 60 %, white solid

^{1}H NMR (300 MHz, DMSO-d_6): δ 11.49 (s, 2H), 8.24 (s, 2H), 6.47 (s, 2H), 5.16 (s, 2H), 4.14 (comp, 2H), 4.04 (comp, 2H), 3.53 (m, 4H), 2.82 (s, 2H), 1.47 (s, 18H), 1.39 (s, 18H);

^{13}C NMR (75 MHz, CD$_3$CN): δ 172.43, 164.51, 157.35, 153.72, 137.56, 84.05, 81.41, 79.50, 63.72, 47.49, 40.21, 28.38, 28.09;

HR-MS (FAB) m/z [M+H]$^{+}$: 755.3827 (calc.), 755.3814 (found).

6.4 Synthesis of π-rich and π-poor Imide Monomers
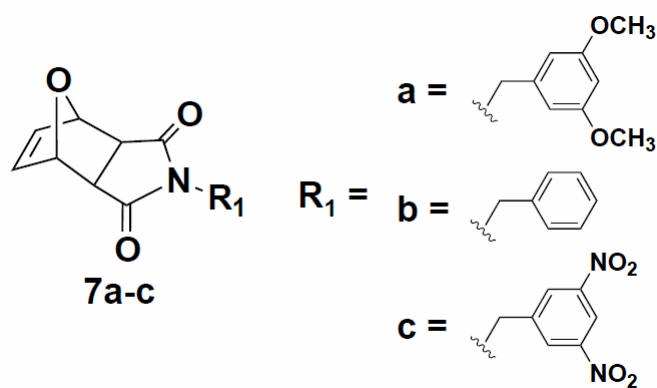
Figure 6.5. Imide monomer final products **7a-c**.

Synthesis of 7a-c: The procedure reported by Som *et.al.* was followed with minor modifications.[5] 1 equivalent of oxanorbornene imide (**6**), 1.25 equivalents of the corresponding alcohol, and one equivalent of triphenyl phosphine were dissolved in 40 mL of freshly distilled THF under nitrogen and subsequently cooled to 0C using an ice bath. Upon cooling, 1 equivalent of DIAD was added drop-wise to the solution. The reaction was allowed to stir overnight and gradually return to RT. The reaction was then concentrated using rotary evaporation and the product was recrystallized using diethyl ether and further purified by column chromatography using gradient elution with EtOAc and CH$_2$Cl$_2$ to yield pure **7a-c**.

7a: Yield: 92 %, white powder

^{1}H NMR (300 MHz, CDCl$_3$): δ 6.52 (t, 2H), 6.44 (d, 2H), 6.34 (t, 1H), 5.31 (s, 2H), 4.60 (s, 2H), 3.75 (s, 6H) 2.88 (s, 2H);

^{13}C NMR (75 MHz, CDCl$_3$): δ 175.99, 161.02, 137.60, 136.42, 105.33, 100.02, 55.04, 47.67, 81.23, 42.46;

HR-MS (FAB) *m/z* [M+H]$^+$: 315.1107 (calc.), 315.1139 (found).

7b: Yield: 90 %, white powder

^{1}H NMR (300 MHz, CDCl$_3$): δ 7.30 (comp, 5H), 6.52 (s, 2H), 5.35 (s, 2H), 4.73 (s, 2H), 2.91 (s, 2H);

^{13}C NMR (75 MHz, CDCl$_3$): δ 176.03, 136.65, 135.54, 128.85, 127.90, 127.09, 80.83, 42.57, 42.36;

HR-MS (FAB) *m/z* [M+H]$^+$: 451.2193 (calc.), 451.2183 (found).

7c: Yield: 95 %, white powder (protect from light)

^{1}H NMR (300 MHz, CDCl$_3$): δ 8.97 (br, 1H), 8.49 (br, 2H), 6.56 (s, 2H), 5.33 (s, 2H), 4.84 (s, 2H), 2.97 (s, 2H);

^{13}C NMR (75 MHz, CDCl$_3$): δ 175.69, 148.79, 139.64, 136.68, 128.31, 118.50, 81.27 47.74, 41.22;

HR-MS (FAB) *m/z* [M+H]$^+$: 256.0974 (calc.), 256.0961 (found).
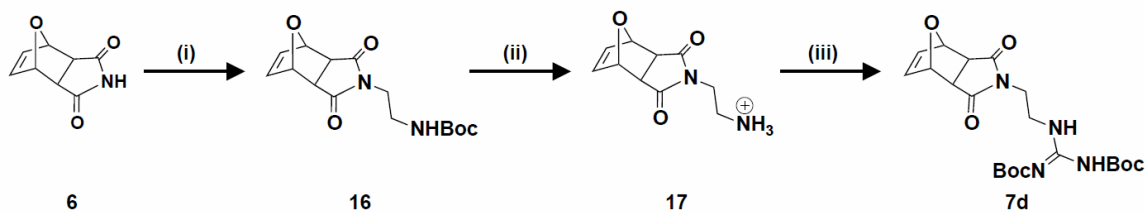
Figure 6.6. Synthesis of guanidine-containing monomer. i) N-Boc-ethanolamine, PPh$_3$, DIAD, THF, RT, 18 hr; ii) TFA/CH$_2$Cl$_2$ (1:1), RT, 3 hr; iii) Guanidinium triflate, NEt$_3$, CH$_2$Cl$_2$, RT, 18 hr;

Synthesis of 6: 1 equivalent of maleimide and 1.4 equivalents of furan were dissolved in 100 mL of EtOAc. The reaction was stirred for 3 h at 90 °C. After 3 h, the reaction was cooled to RT to allow the product to precipitate. The exo Diels-Alder product, **6**, was isolated by vacuum filration and was allowed to dry under vacuum at RT overnight. The spectroscopic data matched previous reports.[6]

6: Yield = 55 %, white powder
^{1}H NMR (300 MHz, DMSO-d_6): δ 11.17 (br, 1H), 6.53 (s, 2H), 5.11 (s, 2H), 2.85 (s, 2H);

Synthesis of 18: The procedure reported by Schmidt *et.al.* was followed with minor modifications.[7] 1 equivalent of oxanorbornene imide, 1.15 equivalent of N-boc-ethanolamine, and 1 equivalent of triphenylphosphine were added to 100 mL of freshly distilled THF under nitrogen and cooled to 0 °C using an ice bath. 1 equivalent of DIAD was then added drop-wise to solution and the reaction was subsequently allowed to warm to room temperature and stir overnight. After overnight stirring, the reaction was concentrated using rotary evaporation and precipitated twice into diethyl ether to yield **16**. The product was isolated by vacuum filtration and allowed to dry. The intermediate yield was 56 %. **16** was deprotected in 2 mL of trifluoroacetic acid (TFA) and precipitated into diethyl ether to yield **17**. **17** was then directly dissolved in 100 mL of CH$_2$Cl$_2$ along with triethylamine and 1 equivalent of 1,3-di-boc-2-(trifluoromethylsulfonyl)guanidine and allowed to stir at RT for 12 hr. After 12 hr, the

solution was concentrated using rotary evaporation and washed with 10% potassium hydrogen sulfate (3x25mL), saturated sodium bicarbonate (3x25mL), and subsequently precipitated into diethyl ether to yield **18**.

18: Yield: 85 %, white powder

^{1}H NMR (300 MHz, CDCl$_3$): δ 11.43 (br, 1H), 8.46 (s, 1H), 6.51 (s, 2H), 5.26 (s, 2H), 3.69 (comp, 4H), 2.87 (s, 2H), 1.53 (s, 9H) 1.47 (s, 9H);

^{13}C NMR (75 MHz, DMSO-d_6): δ 176.30, 156.65, 153.02, 136.54, 83.33, 80.97, 47.65, 39.02,

HR-MS (FAB) *m/z* [M+H]$^+$: 451.2193 (calc.), 451.2183 (found).

6.5   Synthesis of π-rich and π-poor Polymers:
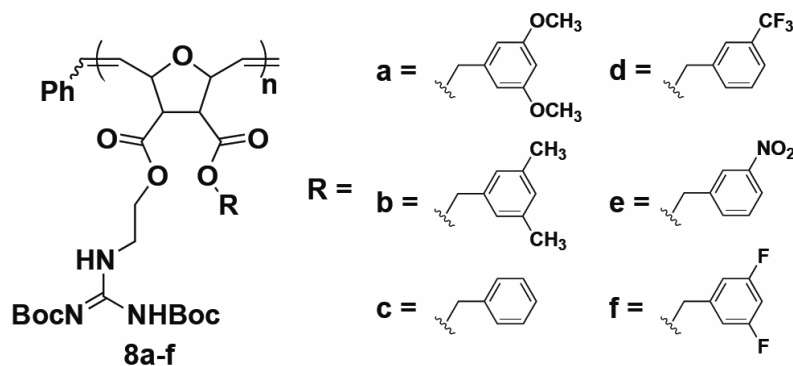
Figure 6.7. Protected diester homopolymer CPPMs final products **8a-f**.

Synthesis of 8a-f: 20 equivalents of **3a-f** and one equivalent of G3 catalyst were each dissolved in 1.5 mL of dry CH$_2$Cl$_2$ in separate Schlenk flasks. The catalyst flask also contained a small stir bar. Three freeze-pump-thaw cycles were used to remove air. Following the third thaw step, the monomer flask was kept under nitrogen while the catalyst flask remained under vacuum. The corresponding monomer **3a-f** was then cannulated into the vigorously stirring catalyst solution at RT. After 1hr, the reaction was quenched with 3 mL of ethyl vinyl ether. The quenched polymer solutions were allowed

to stir overnight at RT. The solutions were then transferred to 20 mL scintillation vials and concentrated *via* rotary evaporation. The crude polymers (**8a-f**) were then dissolved in a minimal amount of THF and added drop-wise to 100 mL of stirring pentanes to precipitate the polymer. After 5-10 minutes of stirring, **8a-f** were isolated *via* vacuum filtration using fine sinter funnels. Polymers were dried under vacuum at RT overnight.

8a: ^{1}H NMR (300 MHz, Acetone-d_6): δ 11.63 (br, 1H), 8.44 (br, 1H), 6.55 (comp, 2H), 6.43 (br, 1H), 5.98 (br, 1H), 5.68 (br, 1H), 5.14 (comp, 3H), 4.74 (br, 1H), 4.16 (br, 2H), 3.79 (br, 6H), 3.60 (br, 2H), 3.28 (br, 2H), 1.51 (s, 9H), 1.43 (s, 9H);

8b: ^{1}H NMR (300 MHz, Acetone-d_6): δ 11.62 (br, 1H), 8.40 (br, 1H), 6.95 (comp, 3H), 5.94 (br, 1H), 5.65 (br, 1H), 5.10 (comp, 3H), 4.70 (br, 1H), 4.10 (br, 2H), 3.57 (br, 2H), 3.22 (br, 2H), 1.49 (s, 9H), 1.42 (s, 9H);

8c: ^{1}H NMR (300 MHz, DMSO-d_6): δ 11.46 (br, 1H), 8.36 (br, 1H), 7.28 (br, 5H), 5.68 (br, 1H), 5.78 (br, 1H), 5.56 (br, 1H), 5.01 (comp, 3H), 4.54 (br, 1H), 3.98 (br, 2H), 3.43 (br, 2H), 3.20 (br, 2H), 1.39 (s, 9H), 1.33 (s, 9H);

8d: ^{1}H NMR (300 MHz, Acetone-d_6): δ 11.63 (br, 1H), 8.44 (br, 1H), 7.69 (comp, 4H), 5.98 (br, 1H), 5.70 (br, 1H), 5.25 (comp, 3H), 4.74 (br, 1H), 4.15 (br, 2H), 3.60 (br, 2H), 3.31 (br, 2H), 1.49 (s, 9H), 1.41 (s, 9H);

8e: ^{1}H NMR (300 MHz, Acetone-d_6): δ 11.60 (br, 1H), 8.42 (br, 1H), 8.23 (comp, 2H), 7.86 (br, 1H), 7.70 (br, 1H), 5.98 (br, 1H), 5.70 (br, 1H), 5.23 (comp, 3H), 4.73 (br, 1H), 4.17 (br, 2H), 3.60 (br, 2H), 3.33 (br, 2H), 1.49 (s, 9H), 1.42 (s, 9H);

8f: ^{1}H NMR (300 MHz, Acetone-d_6): δ 11.62 (br, 1H), 8.45 (br, 1H), 7.01 (comp, 3H), 5.98 (br, 1H), 5.70 (br, 1H), 5.17 (comp, 3H), 4.74 (br, 1H), 4.18 (br, 2H), 3.62 (br, 2H), 3.33 (br, 2H), 1.50 (s, 9H), 1.43 (s, 9H);
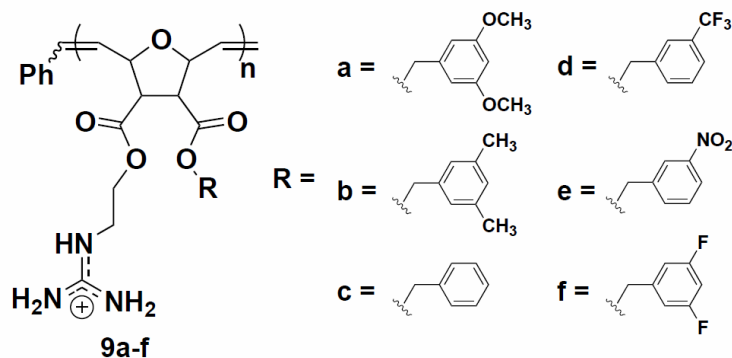
Figure 6.8. Deprotected diester homopolymer CPPM final products **9a-f**

Deprotection Procedure to Yield Polymers 9a-f: 8a-f were dissolved in 2 mL of CH$_2$Cl$_2$ and allowed to stir. 2 mL of TFA was then added drop-wise to the solution and allowed to stir overnight at RT. Excess TFA was removed by azeotropic distillation with MeOH. During this process, 5-7 mL of MeOH was added and then the sample was concentrated *via* rotary evaporation. This process was repeated 7-9 times to ensure complete TFA removal. Following this, samples were dissolved in a water/MeOH mixture, transferred to Spectra/Por® 6 dialysis membranes (MWCO=2,000 g/mol), and dialyzed against RO water until the conductivity of the water remained < 0.2 µS (2-3 days). **9a-f** were then isolated from water by lyophilization.

9a: ^{1}H NMR (300 MHz, CD$_3$CN): δ 7.79 (br, 1H), 7.08 (comp, 4H), 6.46 (comp, 3H), 5.86 (br, 1H), 5.63 (br, 1H), 5.03 (comp, 3H), 4.66 (br, 1H), 4.10 (br, 1H), 3.99 (br, 1H), 3.75 (br, 6H), 3.31 (comp, 4H);

9b: ^{1}H NMR (300 MHz, CD$_3$CN): δ 7.71 (comp, 2H), 7.33 (br, 1H), 6.95 (comp, 5 H), 5.85 (br, 1H), 5.63 (br, 1H), 5.01 (comp, 3H), 4.65 (br, 1H), 4.08 (br, 1H), 3.94 (br, 1H), 3.27 (comp, 4H), 2.27 (br, 6H);

9c: ^{1}H NMR (300 MHz, CD$_3$CN): δ 7.36 (comp, 6H), 7.05 (comp, 3H), 5.85 (br, 1H), 5.64 (br, 1H), 5.09 (comp, 3H), 4.66 (br, 1H), 4.08 (br, 2H), 3.92 (br, 1H), 3.28 (comp, 4H);

9d: ^{1}H NMR (300 MHz, CD$_3$CN): δ 7.64 (comp, 5H), 7.09 (comp, 4H), 5.86 (br, 1H), 5.64 (br, 1H), 5.12 (comp, 3H), 4.66 (br, 1H), 4.09 (br, 1H), 3.95 (br, 1H), 3.30 (comp, 4H);

9e: ^{1}H NMR (300 MHz, DMSO-d_6): δ 8.18 (comp, 2H), 7.70 (comp, 3H), 7.30 (comp, 4H), 5.82 (br, 1H), 5.61 (br, 1H), 5.37 (comp, 3H), 4.56 (br, 1H), 3.98 (comp, 2H), 3.28 (comp, 4H);

9f: ^{1}H NMR (300 MHz, DMSO-d_6): δ 7.81 (comp, 2H), 7.19 (comp, 6H), 5.84 (br, 1H), 5.61 (br, 1H), 5.08 (br, 3H), 4.57 (br, 1H), 4.01 (br, 2H), 3.26 (comp, 4H);
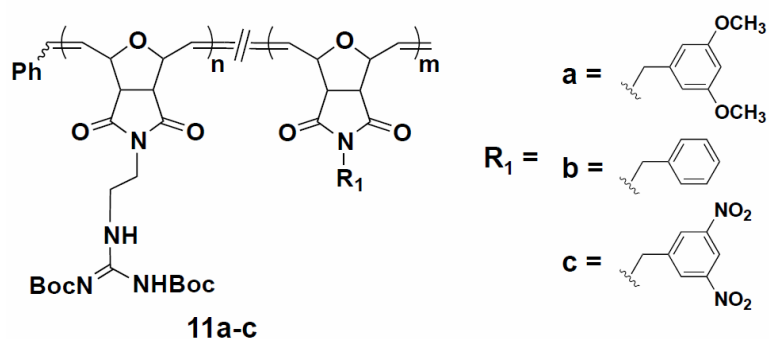
Figure 6.9. Protected imide random copolymer CPPM final products **11a-c**.

Synthesis of 11a-c: 20 equivalents of **7a-c** and 20 equivalents of **19** were each dissolved in 1.5 mL of dry CH$_2$Cl$_2$ in the same Schlenk flasks. 1 equivalent of G3 catalyst

was dissolved in 1.5 mL of dry CH_2Cl_2 in a separate Schlenk flask with a stir bar. Three freeze-pump-thaw cycles were used to remove air. Following the third thaw step, the monomer flask was kept under nitrogen while the catalyst flask remained under vacuum. The corresponding monomers **7a-c** and **18** were then cannulated into a vigorously stirring catalyst solution at RT. After 1hr, the reaction was quenched with 3 mL of ethyl vinyl ether. The quenched polymer solutions were allowed to stir overnight at RT. The solutions were then concentrated via rotary evaporation and redissolved in a minimal amount of CH_2Cl_2 added drop-wise to 100 mL of stirring diethyl ether to precipitate the polymer. After 5-10 minutes of stirring, **11a-c** were isolated *via* vacuum filtration using fine sinter funnels. Polymers were dried under vacuum at RT overnight.

11a: ^{1}H NMR (300 MHz, DMSO-d_6): δ 11.46 (m, 1H), 8.45 (br, 1H), 6.36 (br, 3H), 5.92 (br, 2H), 5.72 (br, 2H), 4.89 (br, 2H), 4.40 (br, 4H), 3.67 (br, 6H), 3.43 (br, 8H), 1.42 (s, 9H), 1.36 (s, 9H);

11b: ^{1}H NMR (300 MHz, DMSO-d_6): δ 11.47 (m, 1H), 8.46 (br, 1H), 7.25 (br, 5H), 5.92 (br, 2H), 5.72, (br, 2H), 4.89 (br, 2H), 4.46 (m, 4H), 3.40 (m, 8H), 1.42 (s, 9H), 1.36 (s, 9H)

11c: ^{1}H NMR (300 MHz, DMSO-d_6): δ 11.44 (m, 1H), 8.72 (br, 1H) 8.51 (br, 3H), 5.92 (br, 2H), 5.71 (br, 2H), 4.81 (br, 4H), 4.43 (br, 2H), 3.43 (comp, 8H), 1.46 (s, 9H), 1.40 (s, 9H);
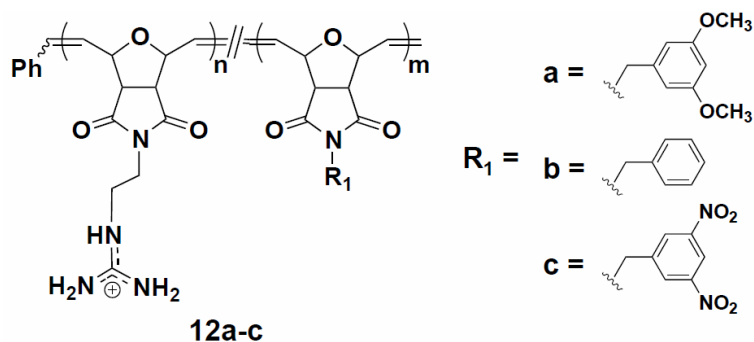
Figure 6.10. Deprotected imide random copolymer CPPM final products **12a-c**.

Deprotection Procedure to Yield Polymers 12a-c: 11a-c were dissolved in 2 mL of H_2Cl_2 and allowed to stir. 2 mL of TFA was then added drop-wise to the solution and allowed to stir overnight at RT. Excess TFA was removed by azeotropic distillation with MeOH. During this process, 5-7 mL of MeOH was added and then the sample was concentrated *via* rotary evaporation. This process was repeated 7-9 times to ensure complete TFA removal. Following this, samples were dissolved in 5-10 mL of water and lyophilized to isolate **12a-c**.

12a: ^{1}H NMR (300 MHz, DMSO-d_6): δ 7.28 (comp, 5H), 6.37 (br, 3H), 5.96 (br, 2H), 5.74 (br, 2H), 4.85 (br, 2H), 4.43 (br, 4H), 3.68 (br, 6H), 3.43 (comp, 8H);

12b: ^{1}H NMR (300 MHz, DMSO-d_6): δ 7.52 (comp, 10H), 5.96 (br, 2H), 5.74 (br, 2H), 4.87 (br, 2H), 4.49 (comp, 4H), 3.47 (comp, 8H);

12c: ^{1}H NMR (300 MHz, DMSO-d_6): δ 8.82 (br, 1H), 8.59 (br, 2H), 7.34 (br, 5H), 6.04 (br, 2H), 5.83 (br, 2H), 4.93 (br, 4H), 4.53 (br, 2H), 3.47 (comp, 8H);
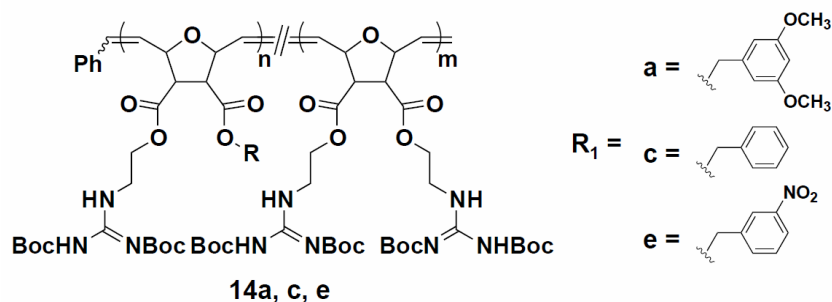
Figure 6.11. Protected diester random copolymer CPPM final products **14a, c, e**.

Synthesis of 14a, c, e: 12 equivalents of **13** and 8 equivalents of either **3a, 3c, or 3e** were dissolved in 1.5 mL of dry CH_2Cl_2 in one Schlenk flask and 1 equivalent of G3 catalyst was dissolved in 1.5 mL of dry CH_2Cl_2 in separate Schlenk flask containing a stir bar. Three freeze-pump-thaw cycles were used to remove air. Following the third thaw step, the monomer flask was kept under nitrogen while the catalyst flask remained under vacuum. The corresponding monomer solution mixture of **13** and either **14a, c, e** was then cannulated into the vigorously stirring catalyst solution at RT. After 1hr, the reaction was quenched with 3 mL of ethyl vinyl ether. The quenched polymer solutions were allowed to stir overnight at RT. The solutions were then transferred to 20 mL scintillation vials and concentrated *via* rotary evaporation. The crude polymers (**14a, c, e**) were then dissolved in a minimal amount of THF and added drop-wise to 100 mL of stirring pentanes to precipitate the polymer. After 5-10 minutes of stirring, **14a, c, e** were isolated *via* vacuum filtration using fine sinter funnels. Polymers were dried under vacuum at RT overnight.

14a: ^{1}H NMR (300 MHz, CD_3CN): δ 11.56 (br, 3H), 8.36 (br, 3H), 8.45 (comp, 3H), 5.88 (br, 2H), 5.61 (br, 2H), 5.02 (comp, 4H), 4.67 (br, 2H), 4.12 (comp, 6H), 3.75 (s, 6H), 3.52 (comp, 6H), 3.17 (br, 4H), 1.48 (s, 27H), 1.43 (s, 27H); n:m = 38:62

14c: ^{1}H NMR (300 MHz, CD$_3$CN): δ 11.56 (br, 3H), 8.36 (br, 3H), 7.34 (br, 5H), 5.88 (br, 2H), 5.61 (br, 2H), 5.08 (comp, 4H), 4.66 (br, 2H), 4.12 (comp, 6H), 3.52 (comp, 6H), 3.16 (br, 4H), 1.48 (s, 27H), 1.43 (s, 27H); n:m = 40:60

14e: ^{1}H NMR (300 MHz, CD$_3$CN): δ 11.55 (br, 3H), 8.36 (br, 3H), 8.17 (br, 2H), 7.74 (br, 1H), 7.60 (br, 1H), 5.88 (br, 2H), 5.63 (br, 2H), 5.11 (comp, 4H), 4.67 (br, 2H), 4.13 (comp, 6H), 3.56 (comp, 6H), 3.17 (br, 4H), 1.48 (s, 27H), 1.43 (s, 27H); n:m = 39:61
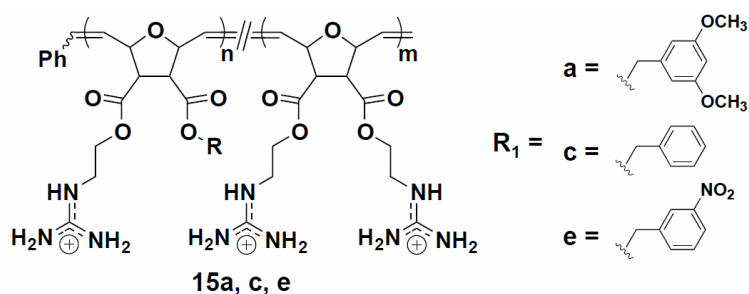
Figure 6.12. Deprotected diester random copolymer CPPM final products **15a, c, e**.

Deprotection Procedure to Yield Polymers 15a, c, e: 14a, c, e were dissolved in 2 mL of CH$_2$Cl$_2$ and allowed to stir. 2 mL of TFA was then added drop-wise to the solution and allowed to stir overnight at RT. Excess TFA was removed by azeotropic distillation with MeOH. During this process, 5-7 mL of MeOH was added and then the sample was concentrated *via* rotary evaporation. This process was repeated 7-9 times to ensure complete TFA removal. Following this, samples were dissolved in a water/MeOH mixture, transferred to Spectra/Por® 6 dialysis membranes (MWCO=2,000 g/mol), and dialyzed against RO water until the conductivity of the water remained < 0.2 µS. **15a, c, e** were then isolated from water by lyophilization.

15a: ¹H NMR (300 MHz, DMSO-d_6): δ 7.86 (br, 3H), 7.41 (comp, 12H), 6.47 (br, 3H), 5.83 (br, 2H), 5.60 (br, 2H), 4.99 (br, 4H), 4.58 (br, 2H), 4.04 (comp, 6H), 3.72 (br, 6H), 3.27 (comp, 10H).

15c: ¹H NMR (300 MHz, DMSO-d_6): δ 7.89 (comp, 5H), 7.33 (comp, 15H), 5.83 (br, 2H), 5.60 (br, 2H), 5.06 (br, 4H), 4.58 (br, 2H), 4.05 (comp, 6H), 3.27 (comp, 10H)

15e: ¹H NMR (300 MHz, DMSO-d_6): δ 8.19 (br, 3H), 7.56 (comp, 16H), 5.83 (br, 2H), 5.60 (br, 2H), 5.20 (br, 2H), 4.98 (br, 2H), 4.58 (br, 2H), 4.04 (comp, 6H), 3.29 (comp, 10H).

6.6 Synthesis of Monomers for the Exploration of Cationic Charge Content and Polymer Architecture on siRNA Internalization and Delivery
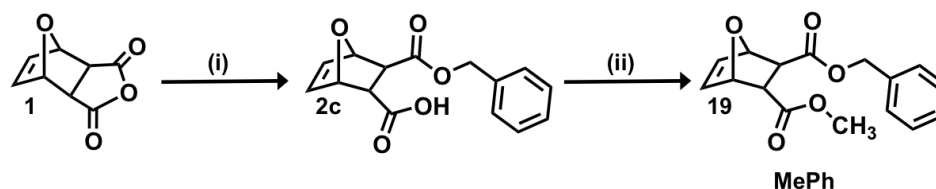
Figure 6.13. Synthesis of hydrophobic monomer **MePh**. i) Benzyl alcohol, DMAP, CH₂Cl₂, RT, overnight; ii) MeOH, DMAP, EDC, CH₂Cl₂, 0°C to RT, overnight;

Synthesis of 1: Maleic anhydride (100.0 g, 1.02 mol) was dissolved in 1 L toluene and 150 mL of furan (140.7 g, 2.05 mol) was added. The solution was stirred for 3 days at room temperature (RT) according to the literature. The product (**1**) was then filtered, washed with hexanes, and dried under vacuum overnight at RT to obtain a colorless powder. Spectroscopic data and yield were consistent with the literature.[2]

¹H NMR (300 MHz, DMSO-d_6): δ = 6.57 (s, 2H), 5.35 (s, 2H), 3.31 (s, 2H);

Synthesis of 2c: The procedure reported by Lienkamp *et al*. was followed with minor modifications.[2] One equivalent of **1**, 1.25 equivalents of the corresponding substituted benzyl alcohols, and 10 mol% DMAP were dissolved in a minimal amount of freshly distilled CH_2Cl_2 and the reaction mixture was stirred under nitrogen at RT overnight. **2** precipitated from solution and was isolated using vacuum filtration and washed with cold CH_2Cl_2. **2** was then dried under vacuum at RT overnight.

2. Yield: 60 %, white powder

^{1}H NMR (300 MHz, DMSO-d_6): δ = 12.46 (br, 1H), 7.36 (comp, 5H), 6.45 (m, 2H), 5.12 (m, 2H), 5.01 (q, 2H), 2.77 (d, 2H);

^{13}C NMR (75 MHz, DMSO-d_6): δ = 172.74, 171.59, 136.79, 136.61, 136.07, 128.45, 128.05, 128.02, 80.18, 79.84, 65.99, 46.82, 46.10;

HR-MS (FAB) *m/z* $[M+H]^+$: 275.0914 (calc.), 275.0903 (found).

Synthesis of 19 (MePh): The procedure reported by Lienkamp *et al*. was followed with minor modifications.[2] One equivalent of **2**, one equivalent of MeOH, and 10 mol% DMAP were dissolved in CH_2Cl_2 and stirred at RT under nitrogen. The solution was then cooled down to 0°C in an ice bath and one equivalent of EDC was added. The solution was allowed to stir overnight under nitrogen and gradually return to RT. The reaction mixture was then concentrated *via* rotary evaporation and purified by either column chromatography with EtOAc/CH_2Cl_2 (1/4, v/v) as the eluent or by using a CombiFlash purification system, with a 120 g silica cartridge and EtOAc/CH_2Cl_2 (1/4, v/v) as the eluent. Pure fractions were combined and then concentrated using rotary evaporation. The sample was dried under vacuum overnight at RT to obtain a white solid.

3: Yield 82 %, white powder.

^{1}H NMR (300 MHz, CD$_3$CN): δ = 7.38 (comp, 5H), 6.44 (comp, 2H), 5.14 (d, 2H), 5.06 (comp, 2H), 3.50 (s, 3H), 2.84 (q, 2H).

^{13}C NMR (75 MHz, CD$_3$CN): δ = 173.35, 172.84, 137.95, 137.91, 137.51, 129.84, 129.60, 129.50, 81.64, 81.63, 67.72, 52.75, 47.96, 47.89.

HR-MS (FAB) *m/z* [M+H]$^+$: 289.1076 (calc.), 289.1078 (found).

6.7 Synthesis of Polymers for the Exploration of Cationic Charge Content and Polymer Architecture on siRNA Internalization and Delivery
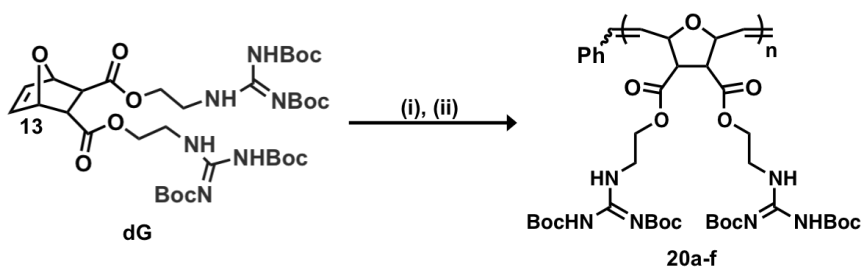
Figure 6.14. Synthesis of Boc-protected homopolymer PTDMs (20a-f). i) Dichloro-di(3-bromopyridino)-*N,N'*-Dimesitylenoimidazolino-Ru=CHPh (G3) catalyst, CH$_2$Cl$_2$, RT, 90 min; ii) Ethyl vinyl ether, RT, overnight; Polymers were synthesized with m = 5, 10, 20, 40, 60 and 80.

Homopolymer Synthesis of 20a-f: 5, 10, 20, 40, 60, or 80 equivalents of **13** and one equivalent of G3 catalyst were each dissolved in 1.5 mL of dry CH$_2$Cl$_2$ in separate schlenk flasks. The catalyst flask also contained a small stir bar. Three freeze-pump-thaw cycles were used to remove air. Following the third thaw step, the monomer flask was kept under nitrogen while the catalyst flask remained under vacuum. Monomer **13** was then cannulated into the vigorously stirring catalyst solution at RT. After 1.5 hr, the reaction was quenched with 3 mL of ethyl vinyl ether. The quenched polymer solutions were allowed to stir overnight at RT. The solutions were then transferred to 20 mL scintillation vials and concentrated using rotary evaporation. **20a-e** were then dissolved in a minimal amount of THF and added drop-wise to 100 mL of cold, stirring pentanes to precipitate the polymers. After 5-10 minutes of stirring, **20a-e** were isolated using

vacuum filtration with fine sinter funnels. Polymers were dried under vacuum at RT overnight.

20a (m=5): ^{1}H NMR (500 MHz, CD$_3$CN): δ = 11.53 (br, 2H), 8.35 (br, 2H), 5.88 (trans) and 5.62 (cis) (br, 2H total), 5.04 (cis) and 4.66 (trans) (br, 2H total), 4.17 (br, 4H), 3.56 (br, 4H), 3.17 (br, 2H), 1.47 (s, 18H), 1.42 (s, 18H).

20b (m=10): ^{1}H NMR (300 MHz, CD$_3$CN): δ = 11.52 (br, 2H), 8.35 (br, 2H), 5.86 (trans) and 5.59 (cis) (br, 2H total), 5.05 (cis) and 4.65 (trans) (br, 2H total), 4.17 (br, 4H), 3.55 (br, 4H), 3.15 (br, 2H), 1.46 (s, 18H), 1.41 (s, 18H).

20c (m=20): ^{1}H NMR (300 MHz, CD$_3$CN): δ = 11.54 (br, 2H), 8.35 (br, 2H), 5.86 (trans) and 5.59 (cis) (br, 2H total), 5.05 (cis) and 4.66 (trans) (br, 2H total), 4.17 (br, 4H), 3.55 (br, 4H), 3.14 (br, 2H), 1.46 (s, 18H), 1.41 (s, 18H).

20d (m=40): ^{1}H NMR (500 MHz, CD$_3$CN): δ = 11.54 (br, 2H), 8.35 (br, 2H), 5.86 (trans) and 5.61 (cis) (br, 2H total), 5.05 (cis) and 4.66 (trans) (br, 2H total), 4.16 (br, 4H), 3.55 (br, 4H), 3.14 (br, 2H), 1.46 (s, 18H), 1.41 (s, 18H).

20e (m=60): ^{1}H NMR (500 MHz, CD$_3$CN): δ = 11.54 (br, 2H), 8.35 (br, 2H), 5.86 (trans) and 5.61 (cis) (br, 2H total), 5.05 (cis) and 4.66 (trans) (br, 2H total), 4.17 (br, 4H), 3.56 (br, 4H), 3.17 (br, 2H), 1.46 (s, 18H), 1.41 (s, 18H).

20f (m=80): ^{1}H NMR (500 MHz, CD$_3$CN): δ = 11.54 (br, 2H), 8.35 (br, 2H), 5.86 (trans) and 5.61 (cis) (br, 2H total), 5.05 (cis) and 4.66 (trans) (br, 2H total), 4.16 (br, 4H), 3.55 (br, 4H), 3.15 (br, 2H), 1.46 (s, 18H), 1.41 (s, 18H).
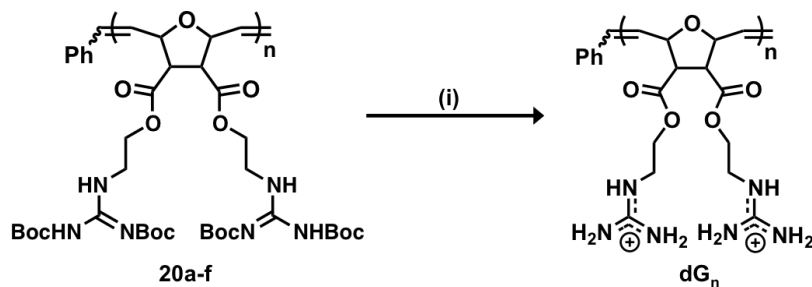
Figure 6.15. Deprotection of boc-protected homopolymers (**20a-f**) to yield the dG$_n$ series of PTDMs. i) TFA/CH$_2$Cl$_2$ (1:1), RT, overnight. dG$_n$ series further purified by dialysis with molecular weight cut-off : 100-500 g/mol.

Deprotection Procedure to Yield dG Polymer Series: 20a-e were dissolved in 2 mL of CH$_2$Cl$_2$ and allowed to stir. 2 mL of TFA was then added drop-wise to the solution and allowed to stir overnight at RT. Excess TFA was removed by azeotropic distillation with MeOH. During this process, 5-7 mL of MeOH was added and then the sample was concentrated using rotary evaporation. This process was repeated 7-9 times to ensure complete TFA removal. Following this, samples were dissolved in a water/MeOH mixture, transferred to Biotech CE dialysis tubing membranes with a MWCO 100-500 g/mol and dialyzed against RO water until the conductivity of the water remained < 0.2 μS (2-3 days on dialysis). The dG series was then aqueous filtered and isolated from water by lyophilization.

dG$_5$: ^{1}H NMR (500 MHz, DMSO-d_6): δ = 7.93 (br, 2H), 7.42 (br, 8H), 5.84 (trans) and 5.60 (cis) (br, 2H total), 4.96 (cis) and 4.63 (trans) (br, 2H total), 4.10 (br, 4H), 3.38 (br, 4H), 3.33 (br, 2H).

dG$_{10}$: ^{1}H NMR (300 MHz, DMSO-d_6): δ = 7.99 (br, 2H), 7.43 (br, 8H), 5.83 (trans) and 5.60 (cis) (br, 2H total), 4.96 (cis) and 4.62 (trans) (br, 2H total), 4.05 (br, 4H), 3.40 (br, 4H), 3.27 (br, 2H).

dG$_{20}$: ^{1}H NMR (300 MHz, DMSO-d_6): δ = 7.98 (br, 2H), 7.43 (br, 8H), 5.82 (trans) and 5.57 (cis) (br, 2H total), 4.96 (cis) and 4.57 (trans) (br, 2H total), 4.05 (br, 4H), 3.37 (br, 4H), 3.28 (br, 2H).

dG$_{40}$: ^{1}H NMR (500 MHz, DMSO-d_6): δ = 7.98 (br, 2H), 7.44 (br, 8H), 5.82 (trans) and 5.58 (cis) (br, 2H total), 4.97 (cis) and 4.61 (trans) (br, 2H total), 4.03 (br, 4H), 3.40 (br, 4H), 3.27 (br, 2H).

dG$_{60}$: ^{1}H NMR (500 MHz, DMSO-d_6): δ = 7.98 (br, 2H), 7.44 (br, 8H), 5.82 (trans) and 5.58 (cis) (br, 2H total), 4.97 (cis) and 4.57 (trans) (br, 2H total), 4.03 (br, 4H), 3.38 (br, 4H), 3.28 (br, 2H).

dG$_{80}$: ^{1}H NMR (500 MHz, DMSO-d_6): δ = 7.98 (br, 2H), 7.43 (br, 8H), 5.82 (trans) and 5.58 (cis) (br, 2H total), 4.96 (cis) and 4.57 (trans) (br, 2H total), 4.03 (br, 4H), 3.37 (br, 4H), 3.32 (br, 2H).
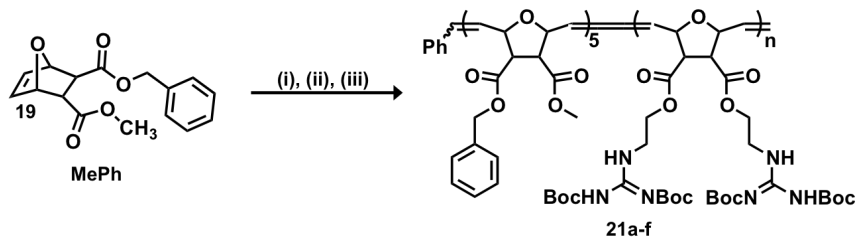
Figure 6.16. Synthesis of Boc-protected block copolymer PTDMs (21a-f). i) Dichloro-di(3-bromopyridino)-*N,N'*-Dimesitylenoimidazolino-Ru=CHPh (G3) catalyst, CH_2Cl_2, RT, 10 min; ii) dG, CH_2Cl_2, RT, 90 min; iii) Ethyl vinyl ether, RT, overnight; Polymers were synthesized with n = 5, 10, 20, 40, 60 and 80.

Block Copolymer Synthesis of 21a-f: 5 equivalents of **19**, 5, 10, 20, 40, 60, or 80 equivalents of **13,** and one equivalent of G3 catalyst were each dissolved in 1.5 mL of dry CH_2Cl_2 in separate schlenk flasks. The catalyst flask also contained a small stir bar. Three freeze-pump-thaw cycles were used to remove air. Following the third thaw step, the flasks containing **13** and **19** were kept under nitrogen while the catalyst flask remained under vacuum. Monomer **19** was then cannulated into the vigorously stirring catalyst solution at RT. After 10 min, a small aliquot (0.05 mL) was removed from the solution for analysis and then monomer **13** was cannulated into the vigorously stirring polymerization solution at RT reaction. After 1.5 hr, the polymerizations were quenched with 3 mL of ethyl vinyl ether and allowed to stir overnight at RT. The solutions were then transferred to 20 mL scintillation vials and concentrated using rotary evaporation. **21a-f** were then dissolved in a minimal amount of THF and added drop-wise to 100 mL of cold, stirring pentanes to precipitate the polymers. After 5-10 minutes of stirring, **21a-f** were isolated using vacuum filtration with fine sinter funnels. Polymers were dried under vacuum at RT overnight.
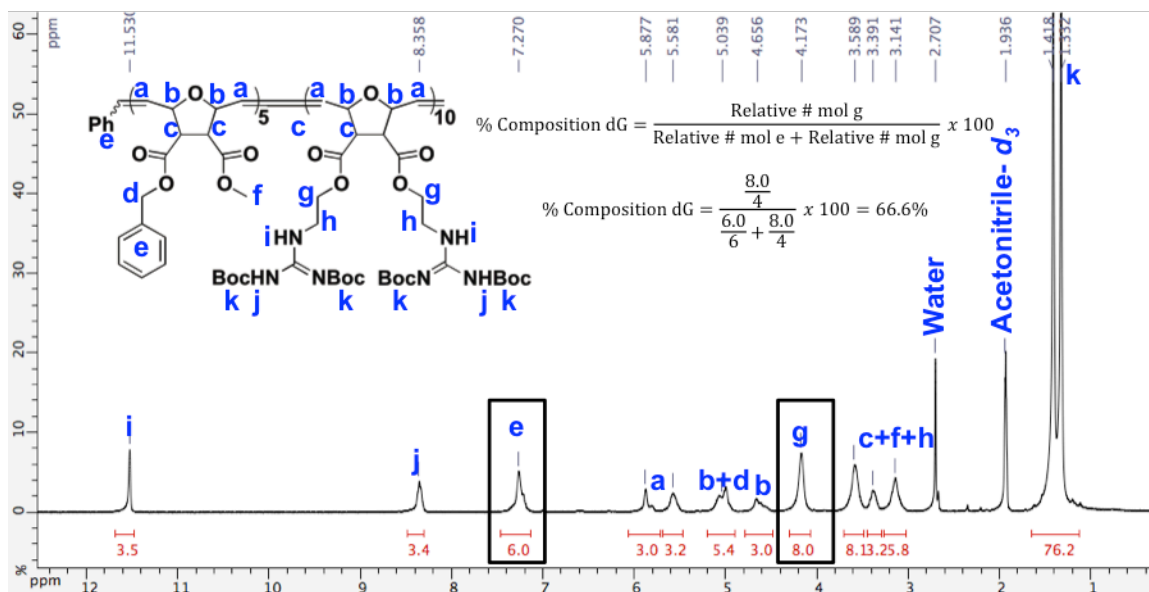
Figure 6.17. Representative ^{1}H NMR spectrum of **21b** to demonstrate the determination of block copolymer composition from unique peaks from each distinct repeat unit (dG and MePh). Data reflects true integrations for the polymer peaks and are not modified to display the number of hydrogen atoms expected to be found for each monomer, when analyzed independently.

Note: All ^{1}H NMR data reported below for **21a-f** reflects the numbers of hydrogen atoms expected to be found for each type of monomer repeat unit and do not necessarily reflect their relative abundance in the polymer samples.

21a (n=5; m=5): ^{1}H NMR (300 MHz, CD$_3$CN): δ = 11.53 (br, 2H), 8.35 (br, 2H), 7.34 (br, 6H), 5.86 (trans) and 5.60 (cis) (comp, 4H total), 5.07 (comp, 2H), 5.07 (cis) and 4.65 (trans) (comp, 4H), 4.17 (br, 4H), 3.51 (comp, 7H), 3.15 (br, 4H), 1.47 (s, 18H), 1.42 (s, 18H).

n:m = 5 : 5

21b (n=5; m=10): ^{1}H NMR (500 MHz, CD$_3$CN): δ = 11.54 (br, 2H), 8.36 (br, 2H), 7.33 (br, 6H), 5.86 (trans) and 5.59 (cis) (comp, 4H total), 5.05 (comp, 2H), 5.05 (cis) and

4.64 (trans) (comp, 4H total), 4.17 (br, 4H), 3.55 (comp, 7H), 3.14 (br, 4H), 1.46 (s, 18H), 1.41 (s, 18H).

n:m = 5 : 10

21c (n=5; m=20): ^{1}H NMR (500 MHz, CD$_3$CN): δ = 11.54 (br, 2H), 8.35 (br, 2H), 7.34 (br, 6H), 5.86 (trans) and 5.60 (cis) (comp, 4H) total, 5.05 (comp, 2H) 5.05 (cis) and 4.65 (trans) (comp, 4H total), 4.16 (br, 4H), 3.55 (comp, 7H), 3.15 (br, 4H), 1.46 (s, 18H), 1.41 (s, 18H).

n:m = 5 : 20

21d (n=5; m=40): ^{1}H NMR (500 MHz, CD$_3$CN): δ = 11.54 (br, 2H), 8.35 (br, 2H), 7.34 (br, 6H), 5.86 (trans) and 5.61 (cis) (comp, 4H) total, 5.05 (comp, 2H) 5.05 (cis) and 4.66 (trans) (comp, 4H total), 4.17 (br, 4H), 3.55 (comp, 7H), 3.14 (br, 4H), 1.46 (s, 18H), 1.41 (s, 18H).

n:m = 5 : 40

21e (n=5; m=60): ^{1}H NMR (500 MHz, CD$_3$CN): δ = 11.54 (br, 2H), 8.35 (br, 2H), 7.34 (br, 6H), 5.86 (trans) and 5.60 (cis) (comp, 4H) total, 5.05 (comp, 2H) 5.05 (cis) and 4.66 (trans) (comp, 4H total), 4.16 (br, 4H), 3.55 (comp, 7H), 3.14 (br, 4H), 1.46 (s, 18H), 1.41 (s, 18H).

n:m = 5 : 60

21f (n=5; m=80): ^{1}H NMR (500 MHz, CD$_3$CN): δ = 11.54 (br, 2H), 8.35 (br, 2H), 7.34 (br, 6H), 5.86 (trans) and 5.61 (cis) (comp, 4H) total, 5.05 (comp, 2H) 5.05 (cis) and 4.66 (trans) (comp, 4H total), 4.17 (br, 4H), 3.55 (comp, 7H), 3.14 (br, 4H), 1.46 (s, 18H), 1.41 (s, 18H).

n:m = 5 : 80
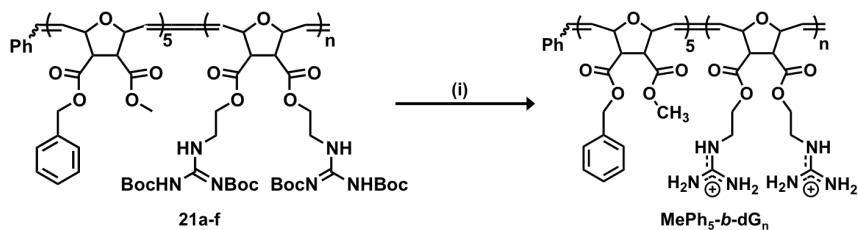
Figure S6.18. Deprotection of boc-protected block copolymers (**21a-f**) to yield the MePh$_5$-*b*-dG$_n$ series of PTDMs. i) TFA/CH$_2$Cl$_2$ (1:1), RT, overnight. MePh$_5$-*b*-dG$_n$ series further purified by dialysis with molecular weight cut-off : 100-500 g/mol.

Deprotection Procedure to Yield MePh$_5$-*b*-dG$_n$ Polymer Series: 21a-f were dissolved in 2 mL of CH$_2$Cl$_2$ and allowed to stir. 2 mL of TFA was then added drop-wise to the solution and allowed to stir overnight at RT. Excess TFA was removed by azeotropic distillation with MeOH. During this process, 5-7 mL of MeOH was added and then the sample was concentrated using rotary evaporation. This process was repeated 7-9 times to ensure complete TFA removal. Following this, samples were dissolved in a water/MeOH mixture, transferred to Biotech CE dialysis tubing membranes with a MWCO 100-500 g/mol and dialyzed against RO water until the conductivity of the water remained < 0.2 µS (2-3 days on dialysis). The MePh$_5$-*b*-dG$_n$ series was then aqueous filtered and isolated from water by lyophilization.

MePh$_5$-*b*-dG$_5$: ^{1}H NMR (300 MHz, CD$_3$CN-d_6): δ = 7.88 (br, 2H), 7.35 (comp, 6H), 7.07 (comp, 8H), 5.87 (trans) and 5.62 (cis) (br, 4H total), 5.07 (comp, 2H), 5.07 (cis) and 4.68 (trans) (comp, 4H total), 4.15 (br, 4H), 3.42 (comp, 7H), 3.20 (br, 4H).

MePh$_5$-*b*-dG$_{10}$: ^{1}H NMR (500 MHz, DMSO-d_6): δ 7.96 (br, 2H), 7.39 (comp, 14H), 5.83 (trans) and 5.59 (cis) (comp, 4H total), 5.01 (comp, 2H), 5.01 (cis) and 4.58 (trans) (comp, 4H total), 4.07 (4H, br), 3.38 (7H, br), 3.27 (4H, br);

MePh$_5$-*b*-dG$_{20}$: ^{1}H NMR (500 MHz, DMSO-d_6): δ 7.98 (br, 2H), 7.40 (comp, 14H), 5.83 (trans) and 5.59 (cis) (comp, 4H total), 5.03 (comp, 2H), 5.03 (cis) and 4.61 (trans) (comp, 4H total), 4.04 (4H, br), 3.40 (7H, br), 3.28 (4H, br);

MePh$_5$-*b*-dG$_{40}$: ^{1}H NMR (500 MHz, DMSO-d_6): δ 7.98 (br, 2H), 7.44 (comp, 14H), 5.82 (trans) and 5.59 (cis) (comp, 4H total), 4.97 (comp, 2H), 4.97 (cis) and 4.58 (trans) (comp, 4H total), 4.10 (4H, br), 3.40 (7H, br), 3.28 (4H, br);

MePh$_5$-*b*-dG$_{60}$: ^{1}H NMR (500 MHz, DMSO-d_6): δ 7.99 (br, 2H), 7.44 (comp, 14H), 5.82 (trans) and 5.58 (cis) (comp, 4H total), 4.97 (comp, 2H), 4.97 (cis) and 4.61 (trans) (comp, 4H total), 4.04 (4H, br), 3.40 (7H, br), 3.28 (4H, br);

MePh$_5$-*b*-dG$_{80}$: ^{1}H NMR (500 MHz, DMSO-d_6): δ = 7.99 (br, 2H), 7.33 (comp, 14H), 5.84 (trans) and 5.57 (cis) (comp, 4H total), 4.97 (comp, 2H), 4.97 (cis) and 4.60 (trans) (comp, 4H total), 4.04 (4H, br), 3.40 (7H, br), 3.31 (4H, br);

6.8 Synthesis of Monomers for the Exploration of Hydrophobic Content Effects on siRNA Internalization
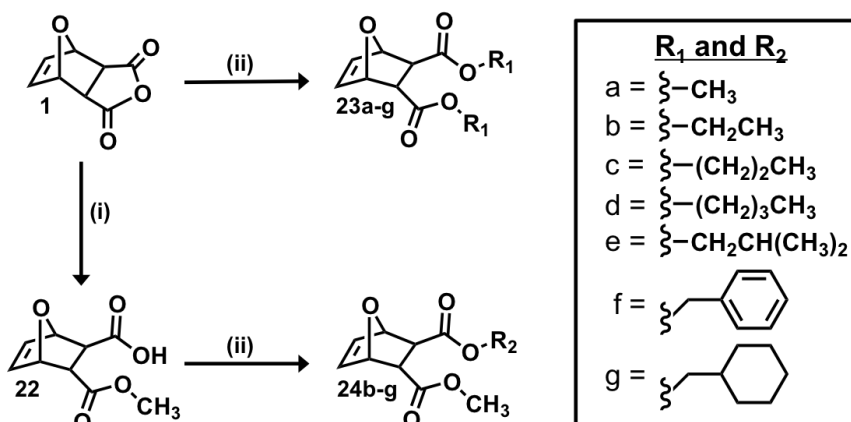
Figure 6.19. Synthesis of hydrophobic monomers. i) Methanol, DMAP, CH_2Cl_2, RT, overnight; ii) R_1OH or R_2OH, DMAP, EDC, CH_2Cl_2, 0°C to RT, overnight;

Synthesis of 1: Maleic anhydride (100.0 g, 1.02 mol) was dissolved in 1 L toluene and 150 mL of furan (140.7 g, 2.05 mol) was added. The solution was stirred for 3 days at room temperature (RT) according to the literature. The product (**1**) was then filtered, washed with hexanes, and dried under vacuum overnight at RT to obtain a colorless powder. Spectroscopic data and yield were consistent with the literature.[2]

^{1}H NMR (300 MHz, DMSO-d_6): δ = 6.57 (s, 2H), 5.35 (s, 2H), 3.31 (s, 2H);

Synthesis of 22: The procedure reported by Lienkamp *et al*. was followed with minor modifications.[2] One equivalent of **1**, 1.25 equivalents of methanol, and 10 mol% DMAP were dissolved in a minimal amount of freshly distilled CH_2Cl_2 and the reaction mixture was stirred under nitrogen at RT overnight. The reaction was rotary evaporated to remove CH2Cl2 and **2** was subsequently recrystallized from a mixture of chloroform/hexanes (3/1, v/v). **2** was later isolated by vacuum filtration and allowed to dry under vacuum at RT overnight.

2. Yield: 62 %, white powder

^{1}H NMR (500 MHz, DMSO-d_6): δ = 12.35 (br, 1H), 6.45 (q, 2H), 5.08 (s, 2H), 3.54 (s, 3H), 2.72 (s, 2H);

^{13}C NMR (125 MHz, DMSO-d_6): δ = 172.66, 172.11, 136.73, 136.61, 80.05, 79.72, 51.49, 46.69, 45.99;

HR-MS (FAB) *m/z* [M+H]$^+$: 199.0606 (calc.), 199.0611 (found).

Synthesis of 23a-g: The procedure reported by Lienkamp *et al*. was followed with minor modifications.[2] Since both substituents to be added to theses monomers was identical, there was no need to isolate the half-ester intermediate as in the case for monomers **24b-g**. For this reaction, one equivalent of **1**, two equivalents of R$_1$OH, and 10 mol% DMAP were dissolved in CH_2Cl_2 and stirred at RT under nitrogen. The solution was then cooled down to 0°C in an ice bath and one equivalent of EDC was added. The solution was allowed to stir overnight under nitrogen and gradually return to RT. The reaction mixture was then concentrated using rotary evaporation and purified using a CombiFlash purification system, with a 120 g silica cartridge and EtOAc/CH_2Cl_2 (1/4, v/v) as the eluent. Pure fractions were combined and then concentrated using rotary evaporation. The sample was dried under vacuum overnight at RT to obtain a white solid.

23a (dMe): Yield 76 %, white powder.

^{1}H NMR (500 MHz, DMSO-d_6): δ = 6.46 (s, 2H), 5.11 (s, 2H), 3.55 (s, 6H), 2.82 (s, 2H);

^{13}C NMR (125 MHz, DMSO-d_6): δ = 171.70, 136.61, 79.74, 51.63, 46.23;

HR-MS (FAB) *m/z* [M+H]$^+$: 213.0763 (calc.), 213.0749 (found).

23b (dEt): Yield 74 %, white powder.

^{1}H NMR (500 MHz, DMSO-d_6): δ = 6.46 (s, 2H), 5.10 (s, 2H), 4.01 (m, 4H), 2.78 (s, 2H), 1.16 (t, 6H);

^{13}C NMR (125 MHz, DMSO-d_6): δ = 171.13, 136.59, 79.76, 60.17, 46.18, 13.93;

HR-MS (FAB) *m/z* [M+H]$^+$: 241.1076 (calc.), 241.1097 (found).

23c (dPr): Yield 70 %, opaque oil.

^{1}H NMR (500 MHz, DMSO-d_6): δ = 6.46 (s, 2H), 5.10 (s, 2H), 3.92 (m, 4H), 2.80 (s, 2H), 1.55 (m, 4H), 0.87 (t, 6H);

^{13}C NMR (125 MHz, DMSO-d_6): δ = 171.20, 136.60, 79.86, 65.74, 46.22, 21.39, 10.25;

HR-MS (FAB) *m/z* [M+H]$^+$: 269.1389 (calc.), 269.1374 (found).

23d (dBu): Yield 82 %, white, waxy solid.

^{1}H NMR (500 MHz, DMSO-d_6): δ = 6.46 (s, 2H), 5.09 (s, 2H), 3.96 (m, 4H), 2.78 (s, 2H), 1.52 (m, 4H), 1.31 (m, 4H), 0.88 (t, 6H);

^{13}C NMR (125 MHz, DMSO-d_6): δ =171.18, 136.58, 79.85, 63.95, 46.19, 30.05, 19.59, 13.53;

HR-MS (FAB) *m/z* [M+H]$^+$: 297.1702 (calc.), 297.1711 (found).

23e (diBu): Yield 47 %, white powder.

^{1}H NMR (500 MHz, DMSO-d_6): δ = 6.47 (s, 2H), 5.09 (s, 2H), 3.74 (comp, 4H), 2.82 (s, 2H), 1.83 (m, 2H), 0.87 (d, 12H);

^{13}C NMR (125 MHz, DMSO-d_6): δ = 171.10, 136.58, 79.92, 70.18, 46.25, 27.11, 18.86;

HR-MS (FAB) *m/z* [M+H]$^+$: 297.1702 (calc.), 297.1643 (found).

23f (dPh): Yield 80 %, white powder.

^{1}H NMR (500 MHz, CD$_3$CN): δ = 7.34 (comp, 10H), 6.44 (s, 2H), 5.16 (s, 2H), 4.97 (comp, 4H), 2.87 (s, 2H);

^{13}C NMR (125 MHz, CD$_3$CN): δ = 172.37, 137.52, 137.03, 129.41, 129.14, 129.06, 81.30, 67.26, 47.58;

HR-MS (FAB) *m/z* [M+H]$^+$: 365.1389 (calc.), 365.1385 (found).

23g (dCy): Yield 67 %, white powder.

^{1}H NMR (500 MHz, DMSO-*d$_6$*): δ = 6.46 (s, 2H), 5.09 (s, 2H), 3.76 (comp, 4H), 2.79 (s, 2H), 1.65 (comp, 10H), 1.54 (s, 2H), 1.17 (comp, 6H), 0.92 (comp, 4H);

^{13}C NMR (125 MHz, DMSO-*d$_6$*): δ = 171.61, 137.07, 80.40, 69.69, 46.69, 36.93, 29.56, 26.35, 25.88.

HR-MS (FAB) *m/z* [M+H]$^+$: 377.2328 (calc.), 377.2299 (found).

Synthesis of 24b-g: The procedure reported by Lienkamp *et al*. was followed with minor modifications.[2] One equivalent of **22**, one equivalent of R$_2$OH, and 10 mol% DMAP were dissolved in CH$_2$Cl$_2$ and stirred at RT under nitrogen. The solution was then cooled down to 0°C in an ice bath and one equivalent of EDC was added. The solution was allowed to stir overnight under nitrogen and gradually return to RT. The reaction mixture was then concentrated *via* rotary evaporation and purified using a CombiFlash purification system, with a 120 g silica cartridge and EtOAc/CH$_2$Cl$_2$ (1/4, v/v) as the eluent. Pure fractions were combined and then concentrated using rotary evaporation. The sample was dried under vacuum overnight at RT to obtain a white solid.

24b (MeEt): Yield 75 %, opaque oil.

^{1}H NMR (500 MHz, DMSO-*d$_6$*): δ = 6.46 (s, 2H), 5.10 (s, 2H), 4.01 (m, 2H), 3.56 (s, 3H), 2.80 (s, 2H), 1.15 (m, 3H);

^{13}C NMR (125 MHz, DMSO-d_6): δ = 171.71, 171.17, 136.62, 79.76, 60.27, 51.52, 46.27, 46.16, 13.97;

HR-MS (FAB) *m/z* [M+H]$^+$: 227.0919 (calc.), 227.0911 (found).

24c (MePr): Yield 65 %, opaque oil.

^{1}H NMR (500 MHz, DMSO-d_6): δ = 6.46 (s, 2H), 5.11 (s, 2H), 3.92 (m, 2H), 3.56 (s, 3H), 2.81 (s, 2H), 1.55 (m, 2H), 0.87 (t, 3H);

^{13}C NMR (125 MHz, DMSO-d_6): δ = 171.69, 171.24, 136.63, 136.59, 79.81, 79.76, 65.01, 51.55, 46.29, 46.15, 21.40, 10.24;

HR-MS (FAB) *m/z* [M+H]$^+$:

24d (MeBu): Yield 69 %, opaque oil.

^{1}H NMR (500 MHz, CD$_3$CN): δ = 6.46 (s, 2H), 5.10 (s, 2H), 3.96 (m, 2H), 3.55 (s, 3H), 2.80 (s, 2H), 1.52 (m, 2H), 1.31 (m, 2H), 0.88 (t, 3H);

^{13}C NMR (125 MHz, DMSO-d_6): δ = 171.67, 171.23, 136.63, 136.59, 79.82, 79.77, 84.02, 51.54, 46.28, 46.15, 30.07, 18.56, 13.55;

HR-MS (FAB) *m/z* [M+H]$^+$: 255.1232 (calc.), 255.1229 (found).

24f (MePh): Yield 82 %, white powder.

^{1}H NMR (500 MHz, CD$_3$CN): δ = 7.38 (comp, 5H), 6.44 (comp, 2H), 5.14 (d, 2H), 5.06 (comp, 2H), 3.50 (s, 3H), 2.84 (q, 2H).

^{13}C NMR (125 MHz, CD$_3$CN): δ = 173.35, 172.84, 137.95, 137.91, 137.51, 129.84, 129.60, 129.50, 81.64, 81.63, 67.72, 52.75, 47.96, 47.89.

HR-MS (FAB) *m/z* [M+H]$^+$: 289.1076 (calc.), 289.1078 (found).

6.9 Synthesis of Polymers for the Exploration of Hydrophobic Content Effects on siRNA Internalization

Polymer	Monomer
25a-g	MePh (**24f**)
26a-c	dMe (**23a**)
27a-c	dPh (**23f**)
28	dEt (**23b**)
29	diBu (**23e**)
30	dCy (**23g**)
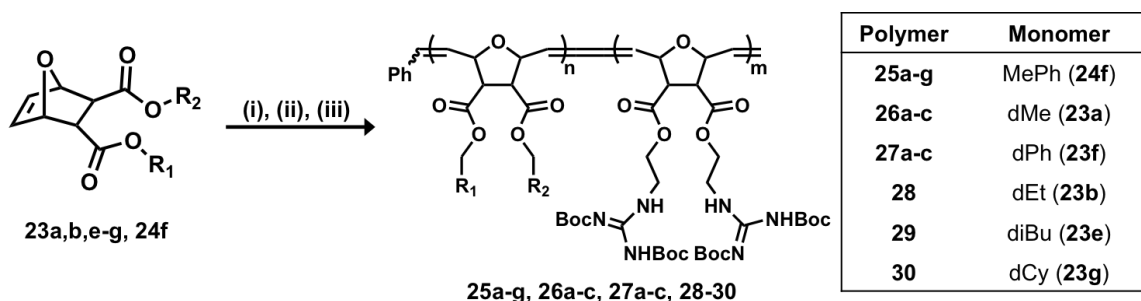
Figure 6.20. Synthesis of Boc-protected block copolymer PTDMs (**25a-f, 26a-c, 27a-c, 28-30**). i) Dichloro-di(3-bromopyridino)-*N,N'*-Dimesitylenoimidazolino-Ru=CHPh (G3) catalyst, CH$_2$Cl$_2$, RT, 10 min; ii) dG, CH$_2$Cl$_2$, RT, 90 min; iii) Ethyl vinyl ether, RT, overnight;

Block Copolymer Synthesis of 25a-g, 26a-c, 27a-c, 28-30: 5, 10, 20, or 40 equivalents of hydrophobic monomers (**23a,b,e-g** or **24f**), 5, 10, 20, or 40 equivalents of **18,** and one equivalent of G3 catalyst were each dissolved in 1.5 mL of dry CH$_2$Cl$_2$ in separate schlenk flasks. The catalyst flask also contained a small stir bar. Three freeze-pump-thaw cycles were used to remove air. Following the third thaw step, the flasks containing **23a,b,e-g** or **24f** and **13** were kept under nitrogen while the catalyst flask remained under vacuum. Monomer **23a,b,e-g** or **24f** was then cannulated into the vigorously stirring catalyst solution at RT. After 10 min, a small aliquot (0.05 mL) was removed from the solution for analysis and then monomer **13** was cannulated into the vigorously stirring polymerization solution at RT reaction. After 1.5 hr, the polymerizations were quenched with 3 mL of ethyl vinyl ether and allowed to stir overnight at RT. The solutions were then transferred to 20 mL scintillation vials and concentrated using rotary evaporation. **25a-g, 26a-c, 27a-c,** and **28-30** were then dissolved in a minimal amount of THF and added drop-wise to 100 mL of cold, stirring pentanes to precipitate the polymers. After 5-10 minutes of stirring, **25a-g, 26a-c, 27a-c,** and **28-30** were isolated using vacuum filtration with fine sinter funnels. Polymers were dried under vacuum at RT overnight.

Note: All ^{1}H NMR data reported below for **25a-g, 26a-c, 27a-c,** and **28-30** reflects the numbers of hydrogen atoms expected to be found for each type of monomer repeat unit and do not necessarily reflect their relative abundance in the polymer samples. An example of the NMR block copolymer composition calculation is shown in Figure 6.17.

25a (n=5; m=5): ^{1}H NMR (300 MHz, CD$_3$CN): δ = 11.53 (br, 2H), 8.35 (br, 2H), 7.34 (br, 6H), 5.86 (trans) and 5.60 (cis) (comp, 4H total), 5.07 (comp, 2H), 5.07 (cis) and 4.65 (trans) (comp, 4H), 4.17 (br, 4H), 3.51 (comp, 7H), 3.15 (br, 4H), 1.47 (s, 18H), 1.42 (s, 18H);

n:m = 5 : 5

25b (n=5; m=10): ^{1}H NMR (500 MHz, CD$_3$CN): δ = 11.54 (br, 2H), 8.36 (br, 2H), 7.33 (br, 6H), 5.86 (trans) and 5.59 (cis) (comp, 4H total), 5.05 (comp, 2H), 5.05 (cis) and 4.64 (trans) (comp, 4H total), 4.17 (br, 4H), 3.55 (comp, 7H), 3.14 (br, 4H), 1.46 (s, 18H), 1.41 (s, 18H);

n:m = 5 : 10

25c (n=5; m=20): ^{1}H NMR (500 MHz, CD$_3$CN): δ = 11.54 (br, 2H), 8.35 (br, 2H), 7.34 (br, 6H), 5.86 (trans) and 5.60 (cis) (comp, 4H) total, 5.05 (comp, 2H) 5.05 (cis) and 4.65 (trans) (comp, 4H total), 4.16 (br, 4H), 3.55 (comp, 7H), 3.15 (br, 4H), 1.46 (s, 18H), 1.41 (s, 18H);

n:m = 5 : 20

25d (n=5; m=40): ^{1}H NMR (500 MHz, CD$_3$CN): δ = 11.54 (br, 2H), 8.35 (br, 2H), 7.34 (br, 6H), 5.86 (trans) and 5.61 (cis) (comp, 4H) total, 5.05 (comp, 2H) 5.05 (cis) and 4.66

(trans) (comp, 4H total), 4.17 (br, 4H), 3.55 (comp, 7H), 3.14 (br, 4H), 1.46 (s, 18H), 1.41 (s, 18H).

n:m = 5 : 40

25e (n=10; m=10): ^{1}H NMR (500 MHz, CD$_3$CN): δ = δ =11.54 (br, 2H), 8.35 (br, 2H), 7.33 (br, 5H), 5.84 (trans) and 5.61 (cis) (comp, 4H) total, 5.07 (comp, 2H), 5.00 (cis) and 4.66 (trans) (comp, 4H total), 4.16 (br, 4H), 3.56 (comp, 7H), 3.14 (br, 4H), 1.46 (s, 18H), 1.41 (s, 18H);

n:m = 10 : 10

25f (n=20; m=20): ^{1}H NMR (500 MHz, CD$_3$CN): δ = δ =11.54 (br, 2H), 8.35 (br, 2H), 7.33 (br, 5H), 5.82 (trans) and 5.60 (cis) (comp, 4H) total, 5.07 (comp, 2H), 4.99 (cis) and 4.65 (trans) (comp, 4H total), 4.18 (br, 4H), 3.56 (comp, 7H), 3.14 (br, 4H), 1.47 (s, 18H), 1.41 (s, 18H);

n:m = 20 : 20

25g (n=40; m=40): ^{1}H NMR (500 MHz, CD$_3$CN): δ =11.53 (br, 2H), 8.35 (br, 2H), 7.33 (br, 5H), 5.83 (trans) and 5.59 (cis) (comp, 4H) total, 5.07 (comp, 2H), 5.00 (cis) and 4.66 (trans) (comp, 4H total), 4.17 (br, 4H), 3.56 (comp, 7H), 3.14 (br, 4H), 1.47 (s, 18H), 1.41 (s, 18H);

n:m = 40 : 40

26a (n=5; m=5): ^{1}H NMR (500 MHz, CD$_3$CN): δ =11.54 (br, 2H), 8.35 (br, 2H), 5.85 (trans) and 5.59 (cis) (comp, 4H) total, 5.00 (cis) and 4.65 (trans) (comp, 4H total), 4.16 (br, 4H), 3.63 (comp, 10H), 3.14 (br, 4H), 1.47 (s, 18H), 1.41 (s, 18H);

n:m = 5 : 5

26b (n=5; m=10): ^{1}H NMR (500 MHz, CD$_3$CN): δ = 11.54 (br, 2H), 8.35 (br, 2H), 5.86 (trans) and 5.60 (cis) (comp, 4H) total, 4.99 (cis) and 4.66 (trans) (comp, 4H total), 4.16 (br, 4H), 3.60 (comp, 10H), 3.13 (br, 4H), 1.47 (s, 18H), 1.41 (s, 18H);

n:m = 5 : 10

26c (n=5; m=20): ^{1}H NMR (500 MHz, CD$_3$CN): δ = 11.54 (br, 2H), 8.35 (br, 2H), 5.86 (trans) and 5.60 (cis) (comp, 4H) total, 4.99 (cis) and 4.66 (trans) (comp, 4H total), 4.16 (br, 4H), 3.60 (comp, 10H), 3.14 (br, 4H), 1.46 (s, 18H), 1.41 (s, 18H);

n:m = 5 : 20

27a (n=5; m=5): ^{1}H NMR (500 MHz, CD$_3$CN): δ = 11.54 (br, 2H), 8.35 (br, 2H), 7.28 (br, 6H), 5.86 (trans) and 5.60 (cis) (comp, 4H total), 4.97 (cis) and 4.66 (trans) (comp, 4H), 4.16 (br, 4H), 3.55 (comp, 7H), 3.15 (br, 4H), 1.46 (s, 18H), 1.41 (s, 18H);

n:m = 5 : 5

27b (n=5; m=10): ^{1}H NMR (500 MHz, CD$_3$CN): δ = 11.54 (br, 2H), 8.35 (br, 2H), 7.28 (br, 6H), 5.86 (trans) and 5.59 (cis) (comp, 4H total), 4.97 (cis) and 4.66 (trans) (comp, 4H), 4.16 (br, 4H), 3.55 (comp, 7H), 3.15 (br, 4H), 1.46 (s, 18H), 1.41 (s, 18H);

n:m = 5 : 10

27c (n=5; m=20): ^{1}H NMR (500 MHz, CD$_3$CN): δ = 11.54 (br, 2H), 8.35 (br, 2H), 7.28 (br, 6H), 5.86 (trans) and 5.61 (cis) (comp, 4H total), 4.97 (cis) and 4.65 (trans) (comp, 4H), 4.16 (br, 4H), 3.55 (comp, 7H), 3.15 (br, 4H), 1.46 (s, 18H), 1.41 (s, 18H);

n:m = 5 : 20

28 (n=5; m=20): ^{1}H NMR (500 MHz, CD_2Cl_2): δ = 11.54 (br, 2H), 8.47 (br, 2H); 5.92 (trans) and 5.64 (cis) (comp, 4H total), 5.13 (cis) and 4.73 (trans) (comp, 4H), 4.26 (comp, 4H), 4.15 (br, 4H), 3.65 (comp, 4H), 3.19 (br, 4H), 1.53 (s, 18H), 1.47 (s, 18H), 1.27 (br, 6H);

n:m = 4 : 21

29 (n=5; m=20): ^{1}H NMR (500 MHz, CD_2Cl_2): δ = 11.54 (br, 2H), 8.48 (br, 2H); 5.92 (trans) and 5.64 (cis) (comp, 4H total), 5.14 (cis) and 4.73 (trans) (comp, 4H), 4.26 (comp, 4H), 3.86 (br, 4H), 3.65 (comp, 4H), 3.18 (br, 4H) 1.93 (br, 2H), 0.94 (br, 12H);

n:m = 6 : 19

30 (n=5; m=20): ^{1}H NMR (500 MHz, CD_2Cl_2): δ = 11.54 (br, 2H), 8.48 (br, 2H); 5.92 (trans) and 5.64 (cis) (comp, 4H total), 5.13 (cis) and 4.73 (trans) (comp, 4H), 4.26 (comp, 7H), 4.15 (br, 2H), 3.64 (comp, 8H), 3.18 (br, 4H), 1.74 (br, 4H), 1.49 (comp, 46H), 1.27 (comp, 4H), 0.98 (br, 2H);

n:m = 6 : 19

Polymer	Monomer
MePh$_n$-*b*-dG$_m$	MePh (**24f**)
dMe$_n$-*b*-dG$_m$	dMe (**23a**)
dPh$_n$-*b*-dG$_m$	dPh (**23f**)
dEt$_n$-*b*-dG$_m$	dEt (**23b**)
diBu$_n$-*b*-dG$_m$	diBu (**23e**)
dCy$_n$-*b*-dG$_m$	dCy (**23g**)

25a-g, 26a-c, 27a-c, 28-30
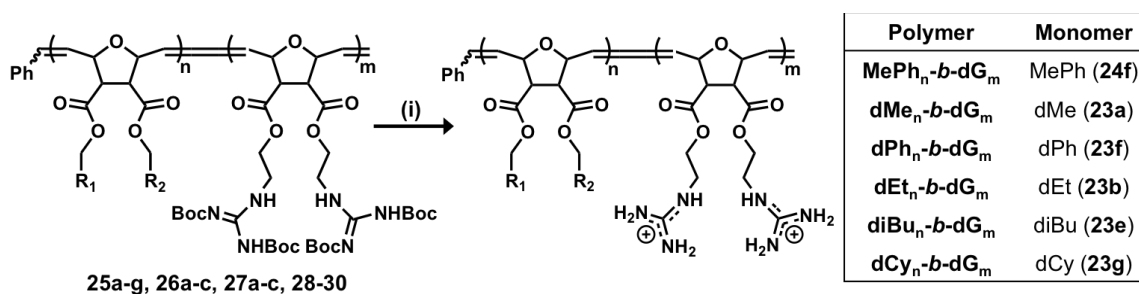
Figure 6.21. Deprotection of boc-protected block copolymers (6a-f) to yield the BCP of PTDMs. I) TFA/CH$_2$Cl$_2$ (1:1), RT, overnight. BCP PTDMs further purified by dialysis using membranes with molecular weight cut-off : 100-500 g/mol.

Deprotection Procedure to Yield MePh$_n$-*b*-dG$_m$, dMe$_n$-*b*-dG$_m$, dPh$_n$-*b*-dG$_m$, dEt$_n$-*b*-dG$_m$, diBu$_n$-*b*-dG$_m$, and dCy$_n$-*b*-dG$_m$ Polymers: 25a-g, 26a-c, 27a-c, and **28-30** were

dissolved in 2 mL of CH$_2$Cl$_2$ and allowed to stir. 2 mL of TFA was then added drop-wise to the solution and allowed to stir overnight at RT. Excess TFA was removed by azeotropic distillation with MeOH. During this process, 5-7 mL of MeOH was added and then the sample was concentrated using rotary evaporation. This process was repeated 7-9 times to ensure complete TFA removal. Following this, samples were dissolved in a water/MeOH mixture, transferred to Biotech CE dialysis tubing membranes with a MWCO 100-500 g/mol and dialyzed against RO water until the conductivity of the water remained < 0.2 µS (2-3 days on dialysis). The MePh$_5$-b-dG$_m$ series was then aqueous filtered and isolated from water by lyophilization.

MePh$_5$-b-dG$_5$: ^{1}H NMR (500 MHz, CD$_3$CN-d_6): δ = 7.88 (br, 2H), 7.35 (comp, 6H), 7.07 (comp, 8H), 5.87 (trans) and 5.62 (cis) (br, 4H total), 5.07 (comp, 2H), 4.92 (cis) and 4.68 (trans) (comp, 4H total), 4.15 (br, 4H), 3.42 (comp, 7H), 3.20 (br, 4H).

MePh$_5$-b-dG$_{10}$: ^{1}H NMR (500 MHz, DMSO-d_6): δ 7.96 (br, 2H), 7.39 (comp, 14H), 5.83 (trans) and 5.59 (cis) (comp, 4H total), 5.01 (comp, 2H), 4.93 (cis) and 4.58 (trans) (comp, 4H total), 4.07 (4H, br), 3.38 (7H, br), 3.27 (4H, br);

MePh$_5$-b-dG$_{20}$: ^{1}H NMR (500 MHz, DMSO-d_6): δ 7.98 (br, 2H), 7.40 (comp, 14H), 5.83 (trans) and 5.59 (cis) (comp, 4H total), 5.03 (comp, 2H), 4.92 (cis) and 4.61 (trans) (comp, 4H total), 4.04 (4H, br), 3.40 (7H, br), 3.28 (4H, br);

MePh$_5$-b-dG$_{40}$: ^{1}H NMR (500 MHz, DMSO-d_6): δ 7.98 (br, 2H), 7.44 (comp, 14H), 5.82 (trans) and 5.59 (cis) (comp, 4H total), 4.97 (comp, 2H), 4.97 (cis) and 4.58 (trans) (comp, 4H total), 4.10 (4H, br), 3.40 (7H, br), 3.28 (4H, br);

MePh$_{10}$-b-dG$_{10}$: ^{1}H NMR (500 MHz, DMSO-d_6): δ = 7.92 (br, 2H), 7.43 (comp, 6H), 7.32 (comp, 8H), 5.80 (trans) and 5.59 (cis) (br, 4H total), 5.04 (comp, 2H), 4.94 (cis) and 4.57 (trans) (comp, 4H total), 4.05 (br, 4H), 3.37 (comp, 7H), 3.21 (br, 4H);

MePh$_{20}$-b-dG$_{20}$: ^{1}H NMR (500 MHz, DMSO-d_6): δ = 7.96 (br, 2H), 7.43 (comp, 6H), 7.32 (comp, 8H), 5.80 (trans) and 5.59 (cis) (br, 4H total), 5.04 (comp, 2H), 4.94 (cis) and 4.57 (trans) (comp, 4H total), 4.04 (br, 4H), 3.36 (comp, 7H), 3.22 (br, 4H);

MePh$_{40}$-b-dG$_{40}$: ^{1}H NMR (500 MHz, DMSO-d_6): δ = 7.94 (br, 2H), 7.42 (comp, 6H), 7.32 (comp, 8H), 5.82 (trans) and 5.59 (cis) (br, 4H total), 5.06 (comp, 2H), 4.92 (cis) and 4.57 (trans) (comp, 4H total), 4.04 (br, 4H), 3.38 (comp, 7H), 3.24 (br, 4H);

dMe$_5$-*b*-dG$_5$: ^{1}H NMR (500 MHz, DMSO-d_6): δ = 7.88 (br, 2H), 7.35 (comp, 8H), 5.83 (trans) and 5.60 (cis) (br, 4H total), 4.90 (cis) and 4.59 (trans) (comp, 4H total), 4.04 (comp, 4H), 3.59 (br, 6H), 3.36 (br, 4H), 3.23 (br, 4H);

dMe$_5$-*b*-dG$_{10}$: ^{1}H NMR (500 MHz, DMSO-d_6): δ = 7.89 (br, 2H), 7.38 (comp, 8H), 5.86 (trans) and 5.60 (cis) (br, 4H total), 4.91 (cis) and 4.60 (trans) (comp, 4H total), 4.05 (comp, 4H), 3.60 (br, 6H), 3.38 (br, 4H), 3.24 (br, 4H);

dMe$_5$-*b*-dG$_{20}$: ^{1}H NMR (500 MHz, DMSO-d_6): δ = 7.89 (br, 2H), 7.39 (comp, 8H), 5.86 (trans) and 5.60 (cis) (br, 4H total), 4.92 (cis) and 4.59 (trans) (comp, 4H total), 4.05 (comp, 4H), 3.59 (br, 6H), 3.39 (br, 4H), 3.25 (br, 4H);

dPh$_5$-*b*-dG$_5$: ^{1}H NMR (500 MHz, DMSO-d_6): 7.89 (br, 2H), 7.26 (comp, 18H), 5.84 (trans) and 5.60 (cis) (br, 4H total), 4.97 (comp, 4H), 4.97 (cis) and 4.59 (trans) (comp, 4H total), 4.03 (br, 4H), 3.36 (comp, 4H), 3.23 (br, 4H);

dPh$_5$-*b*-dG$_{10}$: ^{1}H NMR (500 MHz, DMSO-d_6): δ = 7.91 (br, 2H), 7.36 (comp, 18H), 5.83 (trans) and 5.60 (cis) (br, 4H total), 4.97 (comp, 4H), 4.97 (cis) and 4.60 (trans) (comp, 4H total), 4.04 (br, 4H), 3.38 (comp, 4H), 3.23 (br, 4H);

dPh$_5$-*b*-dG$_{20}$: ^{1}H NMR (500 MHz, DMSO-d_6): δ = 7.96 (br, 2H), 7.35 (comp, 18H), 5.83 (trans) and 5.59 (cis) (br, 4H total), 4.97 (comp, 4H), 4.97 (cis) and 4.59 (trans) (comp, 4H total), 4.04 (br, 4H), 3.37 (comp, 4H), 3.24 (br, 4H);

dEt$_5$-*b*-dG$_{20}$: ^{1}H NMR (500 MHz, DMSO-d_6): δ = 7.97 (br, 2H), 7.43 (comp, 8H), 5.83 (trans) and 5.58 (cis) (br, 4H total), 4.96 (cis) and 4.57 (trans) (comp, 4H total), 4.05 (comp, 8H), 3.36 (comp, 4H), 3.24 (br, 4H), 1.15 (br, 6H);

diBu$_5$-*b*-dG$_{20}$: ^{1}H NMR (500 MHz, DMSO-d_6): δ = 7.97 (br, 2H), 7.43 (comp, 8H), 5.83 (trans) and 5.60 (cis) (br, 4H total), 4.96 (cis) and 4.57 (trans) (comp, 4H total), 4.04 (comp, 4H), 3.76 (br, 4H), 3.36 (comp, 4H), 3.24 (br, 4H), 1.83 (2H), 1.15 (br, 12H);

dCy$_5$-*b*-dG$_{20}$: ^{1}H NMR (500 MHz, DMSO-d_6): δ = 7.97 (br, 2H), 7.42 (comp, 8H), 5.82 (trans) and 5.59 (cis) (br, 4H total), 4.97 (cis) and 4.58 (trans) (comp, 4H total), 4.04 (comp, 6H), 3.77 (br, 2H), 3.36 (comp, 6H), 3.24 (br, 4H), 1.64 (comp, 10H), 1.17 (comp, 6H), 0.91 (comp, 4H);

6.10 Molecular Modeling

Aromatic groups studied were modeled using Spartan 2004 software (Wavefunction, Inc., Irvine, CA) to obtain electronic potential maps. These maps were then used to visualize difference in electron densities of various aromatic groups, including those incorporated into amino acids phenylalanine, tyrosine, and tryptophan as well as electron-rich and electron-poor systems incorporated into our CPPMs. Electrostatic potential values for the center of all aromatic rings modeled were also determined.

6.11 Vesicle Preparation and Dye Release Assays

Preparation of EYPC-LUVs⊃CF.[7,8] A thin lipid film was prepared by concentrating a solution of 25 mg EYPC in chloroform *via* rotary evaporation at RT. The sample was further dried under vacuum overnight at RT protected from light. Lipids were hydrated for 1 hr with 1.0 mL CF/Tris saline buffer (10 mM Tris, 10 mM NaCl, 50 mM CF, pH 7.5) and vortexed every 15 min for 1 hr. The resulting suspension was then subjected to six freeze-thaw cycles (liquid N_2 to freeze and 25 °C water bath to thaw), and then extruded nine times through a polycarbonate membrane (pore size = 100 nm). Extra-vesicular dye was removed by size exclusion chromatography (Sephadex G-50 superfine, Sigma-Aldrich) with Tris saline buffer (10 mM Tris, 107 mM NaCl, pH 7.5). The vesicle stock solution recovered from the column was collected in 2-3 fractions and stored at 4°C protected from light. These vesicles were used for the following dye-release assay.

Preparation of EYPC/Brain PS (80/20)-LUVs⊃CF.   The vesicle preparation was identical to that of the EYPC-LUVs⊃CF, with the exception that 20% Brain PS lipids, by weight, were used for the preparation.

Dye-release Assay.[59] All fluorescence measurements were taken at 25 °C with an excitation wavelength of 492 nm and an emission wavelength of 517 nm using a Biotek SynergyMx fluorescence plate reader. 1960 µL of Tris saline buffer was added to each well of a 12-well plate along with 20 µL of a working solution of EYPC-LUVs⊃CF (diluted to a post-triton fluorescence of 70,000 counts). After shaking in the plate reader for 3 minutes at 25 °C, the baseline fluorescence, F_0, was read. Then, 20 µL polymer solutions (in DMSO) of varying concentrations were added to the wells while stirring. After shaking in the plate reader for 10 minutes at 25 °C, the fluorescence intensity (F_{10}) was measured again. 20 µL of Triton X-100 (5% in DMSO) was then added to each of the wells to lyse the vesicles and release all of the dye. The final fluorescence measurement (F_t) was taken after 3 minutes of shaking in the plate reader at 25 °C. A cartoon depiction of this assay can be seen in Figure 2.4.1. The results were normalized according to the baseline and Triton controls to yield fractional dye release (*Y)* according the equation S1.

$$I_f = (F_{10} - F_0) / (F_t - F_0) \tag{S1}$$

For Hill analysis, *Y* was plotted against polymer concentration, *c,* and fit to the Hill equation, S2, to give the effective concentration (EC_{50}), which is the concentration of polymer that results in 50 % of the maximum fluorescence intensity.

$$I_f = I_{f,0} + (I_{f,max} - I_{f,0}) / [(1 + c / EC_{50})^n] \tag{S2}$$

Where, $I_{f,0}$ and I_f are the minimum and maximum value of I obtained, respectively.

6.12 Polymer/siRNA Complexation Using Gel Retardation Assays

PTDMs were complexed with siRNA at N:P ratios of 0.5:1, 1:1, 2:1, 4:1, 8:1, and 12:1 in microfuge tubes, with the siRNA amount held constant at 1 µg. Complexes were

allowed to incubate at RT for 30 minutes prior to agarose gel electrophoresis with sodium boric acid conductive medium.

6.13 FITC-siRNA Uptake in Jurkat T Cells

General Procedure

Polymers were dissolved in sterile DMSO to make 1 mM stock solutions. Polymers were stored at -20 °C in 50 µL aliquots. On the day of the experiment, Jurkat T cells were harvested, centrifuged, counted, and re-suspended in complete cell growth medium with 10% FBS to a density of $4x10^5$ cells/mL (1 mL final volume in a 12-well plate). Polymers with charge contents less than 40 were diluted to 0.1 mM with PBS and polymers with charge contents of 40 or larger were diluted to 0.005 mM with PBS (pH 7.4). Polymers were mixed with siRNA (10 µM stock solution, 50 nM in final well) at an N/P ratio, where N is the number of positively charged nitrogen groups in the polymer structures and P is the number of negatively charged phosphate groups in the FITC-siRNA duplexes, of 8/1 in PBS (100 µL total for each complex solution). This N/P ratio was previously optimized.[3] Complexes were incubated at RT for 30 minutes prior to adding them drop-wise to each well and gently pipetting the media in each well up and down to evenly mix in the complex solutions.. Cells were then incubated at 37 °C in a 5% CO_2 atmosphere for 4 hr. After 4 hr, cells were harvested and washed 3 times with 500 µL of a 20 U/mL heparin solution. Cells were either re-suspended in 200 µL of FACS wash buffer after the final wash for analysis or prepared for viability staining. See procedure below. For flow cytometry analysis, the fluorescence signal was collected for 10,000 cells. The cell populations were gated in order to assess the percent of positive cells, which reflected the percentage of the cell population that received FITC-siRNA. The calculated median

fluorescence intensity (MFI) represented the amount of cargo delivered to the cells. Results for percent positive cells and MFI can be found in the main text (**Figure 2**).

Comparison to Commercially Available Reagents

For experiments in which polymers were compared to commercially available reagents, the setup was identical to the general procedure with the exception that all commercially available reagents were handled in accordance with the recommended procedures. Summaries of these conditions are documented below. The concentration of siRNA in the final experiment wells remained at 50 nM for consistency. For flow cytometry analysis, the fluorescence signal was collected for 10,000 cells. The cell populations were gated in order to assess the percent of positive cells, which reflected the percentage of the cell population that received FITC-siRNA. The calculated MFI values reflected the amount of cargo delivered to the cells. Results for percent positive cells and MFI can be found in the main text (**Figure 3**).

R9. This reagent was purchased from Peptide 2.0 and dissolved in PBS to make a 1 mM stock solution. The N:P ratio used for this experiment was 8:1 to be consistent with the ratios used for the polymeric reagents.

DeliverX. This reagent was purchased from Affymetrix. The recommended reagent quantities were used as documented in the user manual. No further optimization was performed. For these experiments, DeliverX was first sonicated for five minutes to obtain a homogeneous solution. Following this, 5 µL of siRNA was dissolved in 45 µL of siRNA Buffer 1 and 7 µL of DeliverX was dissolved in 43 µL of siRNA Buffer 2. Both solutions were vortex mixed prior to mixing both solutions together. This solution was gently

vortex mixed and then allowed to incubate at RT for 20 minutes prior to adding it to the cell suspension.

Xfect. This reagent was purchased from CloneTech. Optimization was not required as per the directions on the company's website and in the user manual. The amounts of siRNA and polymer delivery reagent to be used for each transfection were pre-determined by the company based on the well size and volume of media to be used. For these experiments 5 µL of siRNA was added to in 45 µL of Xfect reaction buffer. In a separate tube, 8 uL of Xfect polymer solution was added to 42 µL of Xfect reaction buffer. Both samples were vortex mixed prior to adding the polymer solution to the siRNA solution and vortex mixing. The complex was allowed to incubate at RT for 20 minutes prior to adding it to the cell suspension.

N-ter. This reagent was purchased from Sigma Aldrich. The ratio of siRNA to transfection peptide to be used was documented in the user manual, where it was also noted that this ratio did not require further optimization. For these experiments, 5 µL of siRNA was added to 45 µL of PBS and 7 µL of N-ter was added to 43 µL of RNase-free water. The solutions were gently vortexed before combining them together. The combined solution was then vortexed and allowed to incubate at RT for 20 minutes prior to adding to the cell suspension.

RNAiMAX. This reagent was purchased from Life Technologies. The ratio of siRNA to transfection reagent used was documented in the user manual. For these experiments, 5 µL of siRNA was added to 45 µL of serum free media and 15 µL of RNAiMAX was added to 35 µL of serum free media. These solutions were gently vortexed before

combining the solutions and gently vortex mixing the combined solution. The complex was allowed to incubate at RT for 20 minutes prior to adding to the cell suspension.

JetPEI. This reagent was purchased from Polyplus Transfection. The ratio of siRNA to transfection reagent used was the same as documented for pDNA. For these experiments, 5 µL of siRNA was added to 45 µL of a 150 mM NaCl solution and 1.5 µL of JetPEI was added to 48.5 µL of a 150 mM NaCl solution. These solutions were gently vortexed before combining the solutions and gently vortex mixing the combined solution. The complex was allowed to incubate at RT for 30 minutes prior to adding to the cell suspension.

6.14 Viability in Jurkat T Cells

General Annexin V / 7-AAD Viability Assay Procedure

This assay was used to assess apoptosis (Annexin V staining) as well as overall viability (7-AAD staining), in order to have a more complete understanding of how polymer/siRNA treatment affected the cell populations. Following wash steps documented above, cells were washed with 200 µL of 1X Annexin V binding buffer and subsequently spun down. Cells were re-suspended in 100 µL of an PE-Annexin V / binding buffer stock solution (1.2 mL of binding buffer + 60 µL PE-Annexin; Solution was scaled up or down as needed.) Cells were then incubated at RT for 15 minutes protected from light. After the incubation, cells were brought up to 200 µL with Annexin V binding buffer and spun down. Cells were re-suspended in 200 µL of a 7-AAD stock solution (2.4 mL of binding buffer + 60 µL of 7-AAD stain; Solution was scaled up or down as needed) and transferred to FCM tubes for analysis. For flow cytometry analysis, the fluorescence signal was collected for 10,000 cells. The cell populations

were gated in order to assess the percent of positive cells, which reflected the percentage of dead cell in the population.

Viability at 4 and 24 hr

To assess cell viability at 4 and 24 hr, 4×10^5 cells/mL were treated as documented in the general FITC-siRNA uptake in Jurkat T cells procedure, with the exception that some cells were treated with just the polymer itself. After the 4 hr treatment, cells were split in half (2×10^5 cells/mL in each half) and washed three times with 500 µL of a 20 U/mL heparin solution. After the third wash, one half of the cells were viability stained as documented in the General Annexin V / 7-AAD viability assay procedure and analyzed by FCM and the other half were re-suspended in warm media and re-plated (2×10^5 cells/mL) for analysis at 24 hr. After 24 hr, the re-plated cells were harvested, washed three times with 500 µL of a 20 U/mL heparin solution, and prepared for viability staining and subsequent analysis. For flow cytometry analysis, the fluorescence signal was collected for 10,000 cells. The cell populations were gated in order to assess the percent of positive cells, which reflected the percentage of dead cell in the population. Note that the longer polymers with charge contents larger than 40 were not tested.

Cell Counts

In addition to viability staining at 4 and 24 hr, cells were counted at 24 hr to assess proliferation. 1/20 dilution of each experimental well in trypan blue was used for cell counts. Since Jurkat T cells have a doubling time of 24 hr, it was anticipated that healthy cell populations would double by the 24 hr time point. Cells were not counted at the 4 hr time point since they were initially counted at the start of the experiment.

6.15 FITC-siRNA Uptake in HeLa Cells

General Procedure

Polymers were dissolved in sterile DMSO to make 1 mM stock solutions. Polymers were stored at -20 °C in 50 µL aliquots. 48 hr prior to the experiment, HeLa T cells were trypsinized, harvested, centrifuged, counted, and re-suspended in complete cell growth medium with 10% FBS to a density of 5×10^4 cells/mL (1 mL final volume in a 12-well plate). Cells were then incubated for approximately 48 hr at 37 °C in a 5% CO_2 atmosphere to allow cells to become 70-90% confluent. On the day of the experiment, fresh media is added to the cells. Polymers with charge contents less than 40 were diluted to 0.1 mM with PBS and polymers with charge contents of 40 or larger were diluted to 0.005 mM with PBS (pH 7.4). Polymers were mixed with FITC-siRNA (10 µM stock solution, 50 nM in final well) at an N/P ratio of 4/1 in PBS (100 µL total for each complex solution). Complexes were incubated at RT for 30 minutes prior to adding them drop-wise to each well. The 12-well plate was gently rocked back and forth to help evenly distribute the complex solutions. Cells were then incubated at 37 °C in a 5% CO_2 atmosphere for 4 hr. After 4 hr, cells were trypsinized, harvested, and washed 3 times with 500 µL a 20 U/mL heparin solution. Cells were either re-suspended in 200 µL of FACS wash buffer after the final wash for analysis or prepared for viability staining. See procedure below. For flow cytometry analysis, the fluorescence signal was collected for 10,000 cells. The cell populations were gated in order to assess the percentage of positive cells, which reflected the percentage of the cell population that received FITC-siRNA. The calculated MFI represented the amount of cargo delivered to the cells.

6.16 Viability in HeLa Cells

General 7-AAD Viability Assay Procedure

Following the wash steps documented above, cells were re-suspended in 200 µL of a 7-AAD stock solution (2.4 mL of FACS wash buffer + 60 µL of 7-AAD stain; Solution was scaled up or down as needed) and transferred to FCM tubes for analysis. For flow cytometry analysis, the fluorescence signal was collected for 10,000 cells. The cell populations were gated in order to assess the percent of positive cells, which reflected the percentage of dead cell in the population.

6.17 hNOTCH1 Knockdown in Human Peripheral Blood Mononuclear Cells (hPBMCs)

Cell enrichment

The night before the experiment, human peripheral blood mononuclear cells (hPBMCs) were thawed and enriched for the viable cell population, a majority of which were T cells, overnight. In this process, hPBMCs were thawed, added to 9 mL of warmed media (RPMI 1640 with 10% FBS), centrifuged, re-suspended in 2 mL of warmed media, and added to two wells of a 6-well plate. Each well was brought up to 3 mL with warmed media and cells were incubated at 37 °C in a 5% CO_2 atmosphere overnight.

6.17.1 Well-plate coating

The night before the experiment, a 24-well plate was antibody-coated with a solution contain anti-CD3 and anti-CD28. For a stock solution that can coat 12 wells, 3.940 mL of PBS was added to a 15 mL centrifuge tube along with 40 µL of a 0.5 mg/mL solution of anti-CD3 in PBS and 20 µL of a 0.5 mg/mL solution of anti-CD28. The solution was

lightly vortexed and 300 µL of it was transferred to each of 12 wells. This stock solution preparation can be scaled up or down as needed.

hPBMC Treatment and Incubation

Polymers were dissolved in sterile DMSO to make 1 mM stock solutions. Polymers were stored at -20 °C in 50 µL aliquots. On the day of the experiment, hPBMCs were harvested, centrifuged, counted, and re-suspended in complete cell growth medium with 10% FBS to a density of 1×10^6 cells/mL (1 mL final volume in a 12-well plate). Polymers with charge contents less than 40 were diluted to 0.1 mM with PBS and polymers with charge contents of 40 or larger were diluted to 0.005 mM with PBS (pH 7.4). Polymers were mixed with siRNA (10 µM stock solution, 100 nM in final well) at an N/P ratio of 8/1 in PBS (100 µL total for each complex solution). This N/P ratio was previously optimized.[3] Complexes were incubated at RT for 30 minutes prior to adding them drop-wise to each well and gently pipetting the media in each well up and down to evenly mix in the complex solutions. Cells were then incubated at 37 °C in a 5% CO_2 atmosphere for 4 hr. After 4 hr, the cells were harvested, centrifuged, re-suspended in complete cell growth medium with 10% FBS and transferred to the coated well plate for stimulation. At least one untreated sample was transferred to an uncoated well to serve as a stimulation control. Cells were incubated at 37 °C in a 5% CO_2 atmosphere for 48 hr.

Flow Cytometry Analysis

Harvesting

After 48 hrs, cells were harvested, centrifuged, and washed with PBS. Cells were re-suspended in 200 µL of PBS and transferred to a 96-well plate. Cells were washed two additional times with FACS wash buffer. After the last wash, the cells were split in half, one part for intracellular staining for *hNOTCH1* protein and one part for viability staining.

Surface Staining

Following the wash steps documented above, cells were resuspended in 100 µL of FACS wash buffer and stained with 5 µL of FITC-labeled anti-CD8 and 5 µL of APC-labeled anti-CD4. Cells were incubated for 30 minutes on ice protected from light. After 30 minutes, the cells were brought up to 200 µL with FACS wash buffer and spun down. Cell were washed two additional times with 200 µL FACS wash buffer and then prepared for intracellular staining or viability staining. These stains were used to verify the CD4+ and CD8+ T cell populations present in the cell samples at 48 hours. The cell populations were roughly 30% CD8+ T cells and 50% CD4+ T cells.

Intracellular Staining

Following cell surface staining documented above, cells were re-suspended in 100 µL of the Foxp3 Fix/Perm Cocktail and incubated for 30 min on ice protected from light. After the 30 min incubation, the cells were brought up to 200 µL with the permeabilization wash buffer, which was prepared by diluting a 5 mL of a 10X stock solution in 45 mL of deionized water. Cells were washed three times with the permeablization wash buffer. After the third wash step, cells were re-suspended in 50 µL of the permeablization wash buffer, stained with 2 µL of anti-human NOTCH1 PE, and incubated for 30 min on ice protected light. After the 30 min incubation, cells were washed three times with the permeablization wash buffer and then re-suspended in 200 µL of FACS wash buffer and transferred to FCM tubes for analysis. For flow cytometry analysis, the fluorescence signal was collected for 10,000 cells. The cell populations were gated in order to assess the percent of positive cells, which reflected the percentage of the cell population expressing *hNOTCH1* protein. The calculated MFI represented the amount of *hNOTCH1* protein present in the cells. The percent relative protein expression represents the percent positive cells multiplied by the MFI, normalized to the blank, and

multiplied by 100%. Results for the percent relative protein expression can be found in the main text (**Figure 4**).

7-AAD Cell Viability Assay

Following the wash steps documented above, cells were re-suspended in 200 µL of a 7-AAD stock solution (2.4 mL of binding buffer + 60 µL of 7-AAD stain; Solution was scaled up or down as needed) and transferred to FCM tubes for analysis. For flow cytometry analysis, the fluorescence signal was collected for 10,000 cells. The cell populations were gated in order to assess the percent of positive cells, which reflected the percentage of dead cell in the population. Viability results can be found in the main text (**Figure 4**).

Western Blot

PBMCs, in the presence or absence of stimulation, were harvested at 48 hours post-treatment and whole cell lysates were prepared using RIPA buffer. Lysates were resolved on an 8% SDS-PAGE gel and transferred to nitrocellulose membranes. Membranes were blocked with 5% milk in PBST and probed with Anti-cleaved Notch1 Val1744 (D3B8, Cell Signaling Technology) or Anti-Glyceraldehyde-3-Phosphate Dehydrogenase Antibody (6C5, Merck Millipore). Membranes were then washed and incubated with their corresponding horseradish peroxidase-conjugated secondary antibodies (GE Healthcare). Oxidation of the chemiluminescent substrate (#34087, Thermo Fisher Scientific) was detected using a G:Box (Syngene).

6.18 Theoretical Calculations of LogP

The octanol/water partition coefficient (LogP) values for all hydrophobic monomers were calculated using MarvinSketch software (ChemAxon Ltd.). The weighted method was used, which provided a logP value that was the average of the Viswanadhan *et al.*, Klopman *et al.*, and PHYSPROP database methods.[4-6] Each method was given equal weight in the calculation to provide a more accurate estimate of the logP values.

6.19 HPLC

Relative hydrophobicities of monomers were also determined by HPLC using a method adapted from Thaker *et al.*[7] A linear gradient from 100% water with 0.1% TFA to 100% acetonitrile with 0.1% TFA over 60 minutes was used at a flow rate of 1 mL/minute. 5 mg/mL monomer solutions in DMSO were prepared for analysis. Samples that were more hydrophobic required higher percentages of acetonitrile to be present in the mobile phase to elute and, thus, correspond to higher retention times.

BIBLIOGRAPHY

Al-Badri, Z. M.; Som, A.; Lyon, S.; Nelson, C. F.; Nusslein, K.; Tew, G. N. Biomacromolecules 2008, 9, 2805-2810.

Almeida, P. F.; Pokorny, A. Biochemistry 2009, 48, 8083-8093.

Almeida, P. F.; Pokorny, A. Methods Mol Biol 2010, 618, 155-169.

Arbuzova, A.; Wang, L.; Wang, J.; Hangyas-Mihalyne, G.; Murray, D.; Honig, B.; McLaughlin, S. Biochemistry 2000, 39, 10330-10339.

Arnt, L.; Nusslein, K.; Tew, G. N. J Polym Sci A1 2004, 42, 3860-3864.

Arnt, L.; Tew, G. N. J Am Chem Soc 2002, 124, 7664-7665.

Arnt, L.; Tew, G. N. Macromolecules 2004, 37, 1283-1288.

Baker, T. J.; Luedtke, N. W.; Tor, Y.; Goodman, M. J Org Chem 2000, 65, 9054-9058.

Bang, E. K.; Gasparini, G.; Molinard, G.; Roux, A.; Sakai, N.; Matile, S. J Am Chem Soc 2013, 135, 2088-2091.

Bang, E. K.; Lista, M.; Sforazzini, G.; Sakai, N.; Matile, S. Chem Sci 2012, 3, 1752-1763.

Barnard, A.; Long, K.; Martin, H. L.; Miles, J. A.; Edwards, T. A.; Tomlinson, D. C.; Macdonald, A.; Wilson, A. J. Angew Chem Int Ed Engl 2015, 54, 2960-2965.

Barnard, A.; Long, K.; Yeo, D. J.; Miles, J. A.; Azzarito, V.; Burslem, G. M.; Prabhakaran, P.; T, A. E.; Wilson, A. J. Org Biomol Chem 2014, 12, 6794-6799.

Bechara, C.; Sagan, S. FEBS Lett. 2013, 587, 1693-1702.

Becker-Hapak, M.; McAllister, S. S.; Dowdy, S. F. Methods 2001, 24, 247-256.

Behlke, M. A. Mol. Ther. 2006, 13, 644-670.

Benko-Iseppon, A. M.; Galdino, S. L.; Calsa, T., Jr.; Kido, E. A.; Tossi, A.; Belarmino, L. C.; Crovella, S. Curr Protein Pept Sci 2010, 11, 181-188.

Bielawski, C. W.; Benitez, D.; Grubbs, R. H. J Am Chem Soc 2003, 125, 8424-8425.

Bielawski, C. W.; Grubbs, R. H. Angew Chem Int Ed Engl 2000, 39, 2903-2906.

Bielawski, C. W.; Grubbs, R. H. Prog. Polym. Sci. 2007, 32, 1-29.

Boisguerin, P.; Deshayes, S.; Gait, M. J.; O'Donovan, L.; Godfrey, C.; Betts, C. A.; Wood, M. J.; Lebleu, B. Adv Drug Deliv Rev 2015, 87, 52-67.

Bolintineanu, D. S.; Kaznessis, Y. N. Peptides 2011, 32, 188-201.

Braun, P.; von Heijne, G. Biochemistry 1999, 38, 9778-9782.

Brogden, K. A. Nat Rev Microbiol 2005, 3, 238-250.

Caesar, C. E.; Esbjorner, E. K.; Lincoln, P.; Norden, B. Biochemistry 2006, 45, 7682-7692.

Cannizzo, L. F.; Grubbs, R. H. Macromolecules, 21, 1961-1967.

Carthew, R. W. Curr Opin Cell Biol 2001, 13, 244-248.

Chen, W.; Yuan, Y.; Cheng, D.; Chen, J.; Wang, L.; Shuai, X. Small 2014, 10, 2678-2687.

Chung, H. H.; Harms, G.; Seong, C. M.; Choi, B. H.; Min, C.; Taulane, J. P.; Goodman, M. Biopolymers 2004, 76, 83-96.

Colak, S.; Nelson, C. F.; Nusslein, K.; Tew, G. N. Biomacromolecules 2009, 10, 353-359.

Cooley, C. B.; Trantow, B. M.; Nederberg, F.; Kiesewetter, M. K.; Hedrick, J. L.; Waymouth, R. M.; Wender, P. A. J Am Chem Soc 2009, 131, 16401-16403.

Copolovici, D. M.; Langel, K.; Eriste, E.; Langel, U. ACS Nano 2014, 8, 1972-1994.

Crombez, L.; Aldrian-Herrada, G.; Konate, K.; Nguyen, Q. N.; McMaster, G. K.; Brasseur, R.; Heitz, F.; Divita, G. Mol Ther 2009, 17, 95-103.

Crombez, L.; Morris, M. C.; Deshayes, S.; Heitz, F.; Divita, G. Curr. Pharm. Design 2008, 14, 3656-3665.

Dalby, B.; Cates, S.; Harris, A.; Ohki, E. C.; Tilkins, M. L.; Price, P. J.; Ciccarone, V. C. Methods 2004, 33, 95-103.

de Planque, M. R.; Bonev, B. B.; Demmers, J. A.; Greathouse, D. V.; Koeppe, R. E., 2nd; Separovic, F.; Watts, A.; Killian, J. A. Biochemistry 2003, 42, 5341-5348.

deRonde, B. M.; Birke, A.; Tew, G. N. Chem Eur J 2015, 21, 3013-3019.

deRonde, B. M.; Tew, G. N. Biopolymers 2015, 104, 265-280.

deRonde, B. M.; Torres, J. A.; Minter, L. M.; Tew, G. N. Biomacromolecules 2015, 16, 3172–3179.

Derossi, D.; Chassaing, G.; Prochiantz, A. Trends Cell Biol 1998, 8, 84-87.

Derossi, D.; Joliot, A. H.; Chassaing, G.; Prochiantz, A. J Biol Chem 1994, 269, 10444-10450.

Deshayes, S.; Morris, M. C.; Divita, G.; Heitz, F. Cell Mol Life Sci 2005, 62, 1839-1849.

Deshayes, S.; Morris, M.; Heitz, F.; Divita, G. Adv Drug Deliv Rev 2008, 60, 537-547.

Devine, D. A.; Hancock, R. E. Curr Pharm Des 2002, 8, 703-714.

El-Andaloussi, S.; Johansson, H. J.; Holm, T.; Langel, U. Mol Ther 2007, 15, 1820-1826.

Elbashir, S. M.; Harborth, J.; Lendeckel, W.; Yalcin, A.; Weber, K.; Tuschl, T. Nature 2001, 411, 494-498.

Elliott, G.; O'Hare, P. Cell 1997, 88, 223-233.

Elmquist, A.; Lindgren, M.; Bartfai, T.; Langel, U. Exp Cell Res 2001, 269, 237-244.

Ernst, J. T.; Bercerril, J.; Park, H. S.; Yin, H.; Hamilton, A. D. Angew Chem Int Ed Engl 2003, 42, 535-539.

Fairlie, D. P.; West, M. L.; Wong, A. K. Curr Med Chem 1998, 5, 29-62.

Fawell, S.; Seery, J.; Daikh, Y.; Moore, C.; Chen, L. L.; Pepinsky, B.; Barsoum, J. Proc Natl Acad Sci U S A 1994, 91, 664-668.

Fedorov, Y.; Anderson, E. M.; Birmingham, A.; Reynolds, A.; Karpilow, J.; Robinson, K.; Leake, D.; Marshall, W. S.; Khvorova, A. RNA 2006, 12, 1188-1196.

Felgner, P. L.; Gadek, T. R.; Holm, M.; Roman, R.; Chan, H. W.; Wenz, M.; Northrop, J. P.; Ringold, G. M.; Danielsen, M. Proc Natl Acad Sci U S A 1987, 84, 7413-7417.

Fillon, Y. A.; Anderson, J. P.; Chmielewski, J. J Am Chem Soc 2005, 127, 11798-11803.

Fire, A.; Xu, S.; Montgomery, M. K.; Kostas, S. A.; Driver, S. E.; Mello, C. C. Nature 1998, 391, 806-811.

Fishman, J. M.; Kiessling, L. L. Angew Chem Int Ed Engl 2013, 52, 5061-5064.

Fletcher, S.; Hamilton, A. D. Curr Opin Chem Biol 2005, 9, 632-638.

Fonseca, S. B.; Pereira, M. P.; Kelley, S. O. Adv Drug Deliv Rev 2009, 61, 953-964.

Frankel, A. D.; Pabo, C. O. Cell 1988, 55, 1189-1193.

Freeley, M.; Long, A. Biochem J 2013, 455, 133-147.

Freeley, M.; Long, A. J Immunol Methods 2013, 396, 116-127.

Futaki, S. Adv. Drug Deliv. Rev. 2005, 57, 547-558.

Futaki, S.; Nakase, I.; Suzuki, T.; Youjun, Z.; Sugiura, Y. Biochemistry 2002, 41, 7925-7930.

Futaki, S.; Suzuki, T.; Ohashi, W.; Yagami, T.; Tanaka, S.; Ueda, K.; Sugiura, Y. J Biol Chem 2001, 276, 5836-5840.

Gabriel, G. J.; Madkour, A. E.; Dabkowski, J. M.; Nelson, C. F.; Nusslein, K.; Tew, G. N. Biomacromolecules 2008, 9, 2980-2983.

Gabriel, G. J.; Pool, J. G.; Som, A.; Dabkowski, J. M.; Coughlin, E. B.; Muthukumar, M.; Tew, G. N. Langmuir : the ACS journal of surfaces and colloids 2008, 24, 12489-12495.

Gabriel, G. J.; Som, A.; Madkour, A. E.; Eren, T.; Tew, G. N. Mater Sci Eng R Rep 2007, 57, 28-64.

Gabriel, G. J.; Tew, G. N. Org Biomol Chem 2008, 6, 417-423.

Gabrielson, N. P.; Lu, H.; Yin, L. C.; Kim, K. H.; Cheng, J. J. Mol. Ther. 2012, 20, 1599-1609.

Gait, M. J. Cell Mol Life Sci 2003, 60, 844-853.

Gasparini, G.; Bang, E. K.; Molinard, G.; Tulumello, D. V.; Ward, S.; Kelley, S. O.; Roux, A.; Sakai, N.; Matile, S. J Am Chem Soc 2014, 136, 6069-6074.

Gehl, J. Acta Physiol Scand 2003, 177, 437-447.

Geihe, E. I.; Cooley, C. B.; Simon, J. R.; Kiesewetter, M. K.; Edward, J. A.;

Hickerson, R. P.; Kaspar, R. L.; Hedrick, J. L.; Waymouth, R. M.; Wender, P. A. P Natl Acad Sci USA 2012, 109, 13171-13176.

Gellman, S. H. Acc Chem Res 1998, 31, 173-180.

Goffinet, C.; Keppler, O. T. Faseb Journal 2006, 20, 500-+.

Goodman, C. M.; Choi, S.; Shandler, S.; DeGrado, W. F. Nat Chem Biol 2007, 3, 252-262.

Green, M.; Loewenstein, P. M. Cell 1988, 55, 1179-1188.

Gromiha, M. M. Biophys. Chem. 2003, 103, 251-258.

Gromiha, M. M.; Suwa, M. Int. J. Biol. Macromol. 2005, 35, 55-62.

Gros, E.; Deshayes, S.; Morris, M. C.; Aldrian-Herrada, G.; Depollier, J.; Heitz, F.; Divita, G. Biochim Biophys Acta 2006, 1758, 384-393.

Hammond, S. M.; Bernstein, E.; Beach, D.; Hannon, G. J. Nature 2000, 404, 293-296.

Hamuro, Y.; Schneider, J. P.; DeGrado, W. F. J Am Chem Soc 1999, 121, 12200-12201.

Hancock, R. E.; Diamond, G. Trends Microbiol 2000, 8, 402-410.

Hancock, R. E.; Rozek, A. FEMS Microbiol Lett 2002, 206, 143-149.

Hancock, R. E.; Sahl, H. G. Nat Biotechnol 2006, 24, 1551-1557.

Harrison, P. L.; Abdel-Rahman, M. A.; Miller, K.; Strong, P. N. Toxicon 2014, 88, 115-137.

Hartmann, L.; Hafele, S.; Peschka-Suss, R.; Antonietti, M.; Borner, H. G. Macromolecules 2007, 40, 7771-7776.

Hartmann, L.; Krause, E.; Antonietti, M.; Borner, H. G. Biomacromolecules 2006, 7, 1239-1244.

Heitz, F.; Morris, M. C.; Divita, G. Brit J Pharmacol 2009, 157, 195-206.

Hennig, A.; Gabriel, G. J.; Tew, G. N.; Matile, S. J Am Chem Soc 2008, 130, 10338-10344.

Hill, D. J.; Mio, M. J.; Prince, R. B.; Hughes, T. S.; Moore, J. S. Chem Rev 2001, 101, 3893-4012.

Horne, W. S.; Gellman, S. H. Acc Chem Res 2008, 41, 1399-1408.

Huang, K.; Voss, B.; Kumar, D.; Hamm, H. E.; Harth, E. Bioconjug Chem 2007, 18, 403-409.

Huang, Y. W.; Lee, H. J.; Tolliver, L. M.; Aronstam, R. S. Biomed Res Int 2015, 2015, 834079.

Iczkowski, K. A.; Omara-Opyene, A. L.; Klosel, R. Mol Biotechnol 2004, 28, 97-103.

Ilker, M. F.; Nusslein, K.; Tew, G. N.; Coughlin, E. B. J Am Chem Soc 2004, 126, 15870-15875.

Ishitsuka, Y.; Arnt, L.; Majewski, J.; Frey, S.; Ratajczek, M.; Kjaer, K.; Tew, G. N.; Lee, K. Y. J Am Chem Soc 2006, 128, 13123-13129.

Ivanov, A. I. Methods Mol Biol 2008, 440, 15-33.

Jackson, A. L.; Burchard, J.; Schelter, J.; Chau, B. N.; Cleary, M.; Lim, L.; Linsley, P. S. RNA 2006, 12, 1179-1187.

Jackson, A. L.; Linsley, P. S. Nat Rev Drug Discov 2010, 9, 57-67.

Jayatunga, M. K.; Thompson, S.; Hamilton, A. D. Bioorg Med Chem Lett 2014, 24, 717-724.

Jeffrey, G. A.; Saenger, W. Hydrogen Bonding in Biological Structures; Springer-Verlag: Berlin, 1991.

John Haynes, W.; Zhou, X. L.; Su, Z. W.; Loukin, S. H.; Saimi, Y.; Kung, C. FEBS Lett. 2008, 582, 1514-1518.

Johnston, S. A.; Qu, B. X.; McGuire, M.; Stemke-Hale, K.; Sykes, K. Developments in biologicals 2000, 104, 3-8.

Joliot, A.; Pernelle, C.; Deagostinibazin, H.; Prochiantz, A. Proc. Natl. Acad. Sci. U. S. A. 1991, 88, 1864-1868.

Joliot, A.; Prochiantz, A. Nat Cell Biol 2004, 6, 189-196.

Jones, T. V.; Blatchly, R. A.; Tew, G. N. Org Lett 2003, 5, 3297-3299.

Jones, T. V.; Slutsky, M. M.; Tew, G. N. N J Chem 2008, 32, 676-679.

Juliano, R.; Alam, M. R.; Dixit, V.; Kang, H. Nucleic Acids Res 2008, 36, 4158-4171.

Katayama, S.; Hirose, H.; Takayama, K.; Nakase, I.; Futaki, S. J Control Release 2011, 149, 29-35.

Killian, J. A.; von Heijne, G. Trends Biochem. Sci. 2000, 25, 429-434.

Kim, J.; Lee, S. H.; Choe, J.; Park, T. G. J Gene Med 2009, 11, 804-812.

Kim, S. H.; Jeong, J. H.; Kim, T. I.; Kim, S. W.; Bull, D. A. Mol Pharm 2009, 6, 718-726.

Kim, S. H.; Jeong, J. H.; Ou, M.; Yockman, J. W.; Kim, S. W.; Bull, D. A. Biomaterials 2008, 29, 4439-4446.

Kim, T. I.; Kim, S. W. React Funct Polym 2011, 71, 344-349.

Kim, T. I.; Lee, M.; Kim, S. W. Biomaterials 2010, 31, 1798-1804.

Kim, T. I.; Ou, M.; Lee, M.; Kim, S. W. Biomaterials 2009, 30, 658-664.

Kolonko, E. M.; Kiessling, L. L. J Am Chem Soc 2008, 130, 5626-5627.

Kolonko, E. M.; Pontrello, J. K.; Mangold, S. L.; Kiessling, L. L. J Am Chem Soc 2009, 131, 7327-7333.

Kuroda, K.; Caputo, G. A. Wiley Interdiscip Rev Nanomed Nanobiotechnol 2013, 5, 49-66.

Kuroda, K.; Caputo, G. A. WIREs Nanomed. Nanobiotechnol. 2013, 5, 49-66.

Kurzawa, L.; Pellerano, M.; Morris, M. C. Biochim Biophys Acta 2010, 1798, 2274-2285.

Laddy, D. J.; Weiner, D. B. International reviews of immunology 2006, 25, 99-123.

Lai, W.; Chang, C. H.; Farber, D. L. J. Immunol. Methods 2003, 282, 93-102.

Lemeshko, V. V. Arch Biochem Biophys 2014, 545, 167-178.

Li, J. M.; Zhang, W.; Su, H.; Wang, Y. Y.; Tan, C. P.; Ji, L. N.; Mao, Z. W. International journal of nanomedicine 2015, 10, 3147-3162.

Li, W.; Tailhades, J.; O'Brien-Simpson, N. M.; Separovic, F.; Otvos, L., Jr.; Hossain, M. A.; Wade, J. D. Amino Acids 2014, 46, 2287-2294.

Liechty, W. B.; Kryscio, D. R.; Slaughter, B. V.; Peppas, N. A. Annu Rev Chem Biomol 2010, 1, 149-173.

Lienkamp, K.; Kumar, K. N.; Som, A.; Nusslein, K.; Tew, G. N. Chem Eur J 2009, 15, 11710-11714.

Lienkamp, K.; Madkour, A. E.; Kumar, K. N.; Nusslein, K.; Tew, G. N. Chem Eur J 2009, 15, 11715-11722.

Lin, C.; Blaauboer, C. J.; Timoneda, M. M.; Lok, M. C.; van Steenbergen, M.; Hennink, W. E.; Zhong, Z.; Feijen, J.; Engbersen, J. F. J Control Release 2008, 126, 166-174.

Lin, C.; Zhong, Z.; Lok, M. C.; Jiang, X.; Hennink, W. E.; Feijen, J.; Engbersen, J. F. Bioconjug Chem 2007, 18, 138-145.

Lindgren, M.; Hallbrink, M.; Elmquist, A.; Soomets, U.; Gallet, X.; Brasseur, R.; Zorko, M.; Langel, U. Eur J Neurosci 2000, 12, 48-48.

Lindgren, M.; Langel, U. Cell-Penetrating Peptides: Methods and Protocols 2011, 683, 3-19.

Lindgren, M.; Langel, U. Methods Mol Biol 2011, 683, 3-19.

Lindgren, M.; Rosenthal-Aizman, K.; Saar, K.; Eiriksdottir, E.; Jiang, Y.; Sassian, M.; Ostlund, P.; Hallbrink, M.; Langel, U. Biochem Pharmacol 2006, 71, 416-425.

Lorenzer, C.; Dirin, M.; Winkler, A. M.; Baumann, V.; Winkler, J. J Control Release 2015, 203, 1-15.

Love, J. A.; Morgan, J. P.; Trnka, T. M.; Grubbs, R. H. Angew Chem Int Ed Engl 2002, 41, 4035-4037.

Luedtke, N. W.; Baker, T. J.; Goodman, M.; Tor, Y. J Am Chem Soc 2000, 122, 12035-12036.

Luedtke, N. W.; Carmichael, P.; Tor, Y. J Am Chem Soc 2003, 125, 12374-12375.

Lundberg, M.; Wikstrom, S.; Johansson, M. Mol Ther 2003, 8, 143-150.

Luo, D.; Saltzman, W. M. Nat. Biotechnol. 2000, 18, 33-37.

Macia, E.; Ehrlich, M.; Massol, R.; Boucrot, E.; Brunner, C.; Kirchhausen, T. Dev Cell 2006, 10, 839-850.

Madani, F.; Lindberg, S.; Langel, U.; Futaki, S.; Graslund, A. J Biophys 2011, 2011, 414729.

Madkour, A. E.; Dabkowski, J. M.; Nusslein, K.; Tew, G. N. Langmuir 2009, 25, 1060-1067.

Maiolo, J. R.; Ferrer, M.; Ottinger, E. A. Biochim Biophys Acta 2005, 1712, 161-172.

Maiti, K. K.; Jeon, O. Y.; Lee, W. S.; Chung, S. K. Chemistry 2007, 13, 762-775.

Maiti, K. K.; Jeon, O. Y.; Lee, W. S.; Kim, D. C.; Kim, K. T.; Takeuchi, T.; Futaki, S.; Chung, S. K. Angew Chem Int Ed Engl 2006, 45, 2907-2912.

Maiti, K. K.; Lee, W. S.; Takeuchi, T.; Watkins, C.; Fretz, M.; Kim, D. C.; Futaki, S.; Jones, A.; Kim, K. T.; Chung, S. K. Angew Chem Int Ed Engl 2007, 46, 5880-5884.

Manceur, A.; Wu, A.; Audet, J. Anal Biochem 2007, 364, 51-59.

Mangoni, M. L.; Shai, Y. Cell Mol Life Sci 2011, 68, 2267-2280.

Mantei, A.; Rutz, S.; Janke, M.; Kirchhoff, D.; Jung, U.; Patzel, V.; Vogel, U.; Rudel, T.; Andreou, I.; Weber, M.; Scheffold, A. Eur J Immunol 2008, 38, 2616-262.

Marodon, G.; Mouly, E.; Blair, E. J.; Frisen, C.; Lemoine, F. M.; Klatzmann, D. Blood 2003, 101, 3416-3423.

Martinek, T. A.; Fulop, F. Chem Soc Rev 2012, 41, 687-702.

McManus, M. T.; Haines, B. B.; Dillon, C. P.; Whitehurst, C. E.; van Parijs, L.; Chen, J.; Sharp, P. A. J Immunol 2002, 169, 5754-5760.

Meerak, J.; Wanichwecharungruang, S. P.; Palaga, T. Vaccine 2013, 31, 784-790.

Meister, G.; Tuschl, T. Nature 2004, 431, 343-349.

Mello, C. C.; Conte, D. Nature 2004, 431, 338-342.

Mishra, A.; Lai, G. H.; Schmidt, N. W.; Sun, V. Z.; Rodriguez, A. R.; Tong, R.; Tang, L.; Cheng, J.; Deming, T. J.; Kamei, D. T.; Wong, G. C. Proc. Natl. Acad. Sci. U. S. A. 2011, 108, 16883-16888.

Mitchell, D. J.; Kim, D. T.; Steinman, L.; Fathman, C. G.; Rothbard, J. B. J Pept Res 2000, 56, 318-325.

Moazed, D.; Noller, H. F. Nature 1987, 327, 389-394.

Morris, M. C.; Depollier, J.; Mery, J.; Heitz, F.; Divita, G. Nat Biotechnol 2001, 19, 1173-1176.

Morris, M. C.; Deshayes, S.; Heitz, F.; Divita, G. Biol Cell 2008, 100, 201-217.

Morris, M. C.; Vidal, P.; Chaloin, L.; Heitz, F.; Divita, G. Nucleic Acids Res 1997, 25, 2730-2736.

Moulton, H. M.; Moulton, J. D. Drug Discov Today 2004, 9, 870.

Nanjappan, P.; Czarnik, A. W. J. Org. Chem. 1986, 51, 2851-2853.

Nguyen, L. T.; Haney, E. F.; Vogel, H. J. Trends Biotechnol 2011, 29, 464-472.

Nishihara, M.; Perret, F.; Takeuchi, T.; Futaki, S.; Lazar, A. N.; Coleman, A. W.; Sakai, N.; Matile, S. Org Biomol Chem 2005, 3, 1659-1669.

Oehlke, J.; Scheller, A.; Wiesner, B.; Krause, E.; Beyermann, M.; Klauschenz, E.; Melzig, M.; Bienert, M. BBA-Biomembranes 1998, 1414, 127-139.

Ohkuma, S.; Poole, B. Proc Natl Acad Sci U S A 1978, 75, 3327-3331.

Oliveira, M. D.; Franco, O. L.; Nascimento, J. M.; de Melo, C. P.; Andrade, C. A. Curr Protein Pept Sci 2013, 14, 543-555.

Opalinska, J. B.; Gewirtz, A. M. Nat Rev Drug Discov 2002, 1, 503-514.

Orner, B. P.; Ernst, J. T.; Hamilton, A. D. J Am Chem Soc 2001, 123, 5382-5383.

Osborne, B. A.; Minter, L. M. Nature Reviews Immunology 2007, 7, 64-75.

Ou, M.; Kim, T. I.; Yockman, J. W.; Borden, B. A.; Bull, D. A.; Kim, S. W. J Control Release 2010, 142, 61-69.

Ou, M.; Wang, X. L.; Xu, R.; Chang, C. W.; Bull, D. A.; Kim, S. W. Bioconjug Chem 2008, 19, 626-633.

Pae, J.; Saalik, P.; Liivamagi, L.; Lubenets, D.; Arukuusk, P.; Langel, U.; Pooga, M. J Control Release 2014, 192, 103-113.

Park, T. G.; Jeong, J. H.; Kim, S. W. Adv Drug Deliv Rev 2006, 58, 467-486.

Patel, L. N.; Zaro, J. L.; Shen, W. C. Pharm Res 2007, 24, 1977-1992.

Pellagatti, A.; Dolatshad, H.; Valletta, S.; Boultwood, J. Archives of toxicology 2015, 89, 1023-1034.

Perret, F.; Nishihara, M.; Takeuchi, T.; Futaki, S.; Lazar, A. N.; Coleman, A. W.; Sakai, N.; Matile, S. J Am Chem Soc 2005, 127, 1114-1115.

Persengiev, S. P.; Zhu, X.; Green, M. R. RNA 2004, 10, 12-18.

Polyansky, A. A.; Chugunov, A. O.; Vassilevski, A. A.; Grishin, E. V.; Efremov, R. G. Curr Protein Pept Sci 2012, 13, 644-657.

Pooga, M.; Hallbrink, M.; Zorko, M.; Langel, U. FASEB J 1998, 12, 67-77.

Porter, E. A.; Weisblum, B.; Gellman, S. H. J Am Chem Soc 2002, 124, 7324-7330.

Pu, J.; Frescas, D.; Zhang, B.; Feng, J. Experimental biology and medicine 2015, 240, 1065-1070.

Ramakrishna, S.; Kwaku Dad, A. B.; Beloor, J.; Gopalappa, R.; Lee, S. K.; Kim, H. Genome research 2014, 24, 1020-1027.

Rennie, J.; Arnt, L.; Tang, H.; Nusslein, K.; Tew, G. N. J Ind Microbiol Biotechnol 2005, 32, 296-300.

Richard, J. P.; Melikov, K.; Vives, E.; Ramos, C.; Verbeure, B.; Gait, M. J.; Chernomordik, L. V.; Lebleu, B. J Biol Chem 2003, 278, 585-590.

Riordan, S. M.; Heruth, D. P.; Zhang, L. Q.; Ye, S. Q. Cell & bioscience 2015, 5, 33.

Rodal, S. K.; Skretting, G.; Garred, O.; Vilhardt, F.; van Deurs, B.; Sandvig, K. Mol Biol Cell 1999, 10, 961-974.

Rotem, S.; Mor, A. Biochim Biophys Acta 2009, 1788, 1582-1592.

Rothbard, J. B.; Kreider, E.; Vandeusen, C. L.; Wright, L.; Wylie, B. L.; Wender, P. A. J Med Chem 2002, 45, 3612-3618.

Rutz, S.; Scheffold, A. Arthritis Res. Ther. 2004, 6, 78-85.

Sakai, N.; Futaki, S.; Matile, S. Soft Matter 2006, 2, 636-641.

Sakai, N.; Matile, S. J Am Chem Soc 2003, 125, 14348-14356.

Sakai, N.; Takeuchi, T.; Futaki, S.; Matile, S. Chembiochem 2005, 6, 114-122.

Samson, F.; Donoso, J. A.; Heller-Bettinger, I.; Watson, D.; Himes, R. H. J Pharmacol Exp Ther 1979, 208, 411-417.

Sandgren, S.; Cheng, F.; Belting, M. J Biol Chem 2002, 277, 38877-38883.

Saraogi, I.; Hamilton, A. D. Chem Soc Rev 2009, 38, 1726-1743.

Schmid, S. L.; Carter, L. L. J Cell Biol 1990, 111, 2307-2318.

Schmidt, N. W.; Lis, M.; Zhao, K.; Lai, G. H.; Alexandrova, A. N.; Tew, G. N.; Wong, G. C. J Am Chem Soc 2012, 134, 19207-19216.

Schmidt, N. W.; Lis, M.; Zhao, K.; Lai, G. H.; Alexandrova, A. N.; Tew, G. N.; Wong, G. C. J. Am. Chem. Soc. 2012, 134, 19207-19216.

Schmidt, N. W.; Mishra, A.; Lai, G. H.; Davis, M.; Sanders, L. K.; Tran, D.; Garcia, A.;

Tai, K. P.; McCray, P. B.; Ouellette, A. J.; Selsted, M. E.; Wong, G. C. J Am Chem Soc 2011, 133, 6720-6727.

Schmidt, N. W.; Tai, K. P.; Kamdar, K.; Mishra, A.; Lai, G. H.; Zhao, K.; Ouellette, A. J.; Wong, G. C. J Biol Chem 2012, 287, 21866-21872.

Scholz, C.; Wagner, E. J Control Rel 2012, 161, 554-565.

Schottel, B. L.; Chifotides, H. T.; Dunbar, K. R. Chem. Soc. Rev. 2008, 37, 68-83.

Schrock, R. R.; Hoveyda, A. H. Angew Chem Int Ed Engl 2003, 42, 4592-4633.

Schwab, P.; France, M. B.; Ziller, J. W.; Grubbs, R. H. Angew Chem Int Ed Engl 1995, 34, 2039-2041.

Schwarze, S. R.; Ho, A.; Vocero-Akbani, A.; Dowdy, S. F. Science 1999, 285, 1569-1572.

Scocchi, M.; Tossi, A.; Gennaro, R. Cell Mol Life Sci 2011, 68, 2317-2330.

Scott, R. W.; DeGrado, W. F.; Tew, G. N. Curr Opin Biotechnol 2008, 19, 620-627.

Seebach, D.; Beck, A. K.; Bierbaum, D. J. Chem Biodivers 2004, 1, 1111-1239.

Semizarov, D.; Frost, L.; Sarthy, A.; Kroeger, P.; Halbert, D. N.; Fesik, S. W. Proc. Natl. Acad. Sci. U. S. A. 2003, 100, 6347-6352.

Sgolastra, F.; deRonde, B. M.; Sarapas, J. M.; Som, A.; Tew, G. N. Acc Chem Res 2013.

Sgolastra, F.; Minter, L. M.; Osborne, B. A.; Tew, G. N. Biomacromolecules 2014, 15, 812-820.

Shai, Y. Biopolymers 2002, 66, 236-248.

Shai, Y.; Makovitzky, A.; Avrahami, D. Curr Protein Pept Sci 2006, 7, 479-486.

Shoichet, M. S. Macromolecules 2010, 43, 581-591.

Sieczkarski, S. B.; Whittaker, G. R. J Gen Virol 2002, 83, 1535-1545.

Silverstein, S. C.; Steinman, R. M.; Cohn, Z. A. Annu Rev Biochem 1977, 46, 669-722.

Simeoni, F.; Arvai, A.; Bello, P.; Gondeau, C.; Hopfner, K. P.; Neyroz, P.; Heitz, F.; Tainer, J.; Divita, G. Biochemistry 2005, 44, 11997-12008.

Simeoni, F.; Morris, M. C.; Heitz, F.; Divita, G. Nucleic Acids Res 2003, 31, 2717-2724.

Singh, R.; Czekelius, C.; Schrock, R. R. Macromolecules 2006, 39, 1316-1317.

Siprashvili, Z.; Reuter, J. A.; Khavari, P. A. Mol Ther 2004, 9, 721-728.

Slutsky, M. M.; Phillip, J. S.; Tew, G. N. N J Chem 2008, 32, 670-675.

Smith, D.; Pentzer, E. B.; Nguyen, S. T. Polym Rev 2007, 47, 419-459.

Snyder, E. L.; Dowdy, S. F. Pharm Res 2004, 21, 389-393.

Som, A.; Navasa, N.; Percher, A.; Scott, R. W.; Tew, G. N.; Anguita, J. Clin Vaccine Immunol 2012, 19, 1784-1791.

Som, A.; Reuter, A.; Tew, G. N. Angew Chem Int Ed Engl 2012, 51, 980-983.

Som, A.; Tezgel, A. O.; Gabriel, G. J.; Tew, G. N. Angew Chem Int Ed Engl 2011, 50, 6147-6150.

Som, A.; Vemparala, S.; Ivanov, I.; Tew, G. N. Biopolymers 2008, 90, 83-93.

Soomets, U.; Lindgren, M.; Gallet, X.; Hallbrink, M.; Elmquist, A.; Balaspiri, L.; Zorko, M.; Pooga, M.; Brasseur, R.; Langel, U. BBA-Biomembranes 2000, 1467, 165-176.

Stanzl, E. G.; Trantow, B. M.; Vargas, J. R.; Wender, P. A. Acc Chem Res 2013, 46, 2944-2954.

Stigers, K. D.; Soth, M. J.; Nowick, J. S. Curr Opin Chem Biol 1999, 3, 714-723.

Strandberg, E.; Morein, S.; Rijkers, D. T.; Liskamp, R. M.; van der Wel, P. C.; Killian, J. A. Biochemistry 2002, 41, 7190-7198.

Strong, L. E.; Kiessling, L. L. J Am Chem Soc 1999, 121, 6193-6196.

Sun, T. M.; Du, J. Z.; Yao, Y. D.; Mao, C. Q.; Dou, S.; Huang, S. Y.; Zhang, P. Z.; Leong, K. W.; Song, E. W.; Wang, J. ACS nano 2011, 5, 1483-1494.

Suzuki, T.; Futaki, S.; Niwa, M.; Tanaka, S.; Ueda, K.; Sugiura, Y. The Journal of biological chemistry 2002, 277, 2437-2443.

Tabujew, I.; Freidel, C.; Krieg, B.; Helm, M.; Koynov, K.; Mullen, K.; Peneva, K. Macromol Rapid Commun 2014, 35, 1191-1197.

Takahashi, H.; Palermo, E. F.; Yasuhara, K.; Caputo, G. A.; Kuroda, K. Macromol Biosci 2013, 13, 1285-1299.

Takeuchi, T.; Kosuge, M.; Tadokoro, A.; Sugiura, Y.; Nishi, M.; Kawata, M.; Sakai, N.; Matile, S.; Futaki, S. ACS Chem Biol 2006, 1, 299-303.

Tang, H. Y.; Yin, L. C.; Kim, K. H.; Cheng, J. J. Chem. Sci. 2013, 4, 3839-3844.

Tew, G. N.; Scott, R. W.; Klein, M. L.; Degrado, W. F. Acc Chem Res 2010, 43, 30-39.

Tezgel, A. O.; Gonzalez-Perez, G.; Telfer, J. C.; Osborne, B. A.; Minter, L. M.; Tew, G. N. Mol Ther 2013, 21, 201-209.

Tezgel, A. O.; Jacobs, P.; Telfer, J. C.; Tew, G. N. Submitted 2015.

Tezgel, A. O.; Telfer, J. C.; Tew, G. N. Biomacromolecules 2011, 12, 3078-3083.

Thaker, H. D.; Cankaya, A.; Scott, R. W.; Tew, G. N. ACS Med Chem Lett 2013, 4, 481-485.

Thaker, H. D.; Sgolastra, F.; Clements, D.; Scott, R. W.; Tew, G. N. J Med Chem 2011, 54, 2241-2254.

Thaker, H. D.; Som, A.; Ayaz, F.; Lui, D. H.; Pan, W. X.; Scott, R. W.; Anguita, J.; Tew, G. N. J Am Chem Soc 2012, 134, 11088-11091.

Thomas, M.; Klibanov, A. M. Appl Microbiol Biot 2003, 62, 27-34.

Thoren, P. E.; Persson, D.; Isakson, P.; Goksor, M.; Onfelt, A.; Norden, B. Biochem. Biophys. Res. Commun. 2003, 307, 100-107.

Trabulo, S.; Cardoso, A. L.; Mano, M.; Pedroso de Lima, M. Pharmaceuticals 2010, 3, 961-993.

Treat, N. J.; Smith, D.; Teng, C.; Flores, J. D.; Abel, B. A.; York, A. W.; Huang, F.; McCormick, C. L. ACS Macro Lett 2012, 1, 100-104.

Trnka, T. M.; Grubbs, R. H. Acc Chem Res 2001, 34, 18-29.

Umezawa, N.; Gelman, M. A.; Haigis, M. C.; Raines, R. T.; Gellman, S. H. J Am Chem Soc 2002, 124, 368-369.

Vader, P.; van der Aa, L. J.; Storm, G.; Schiffelers, R. M.; Engbersen, J. F. Curr Top Med Chem 2012, 12, 108-119.

Vasquez, R. J.; Howell, B.; Yvon, A. M.; Wadsworth, P.; Cassimeris, L. Mol Biol Cell 1997, 8, 973-985.

Vercauteren, D.; Vandenbroucke, R. E.; Jones, A. T.; Rejman, J.; Demeester, J.; De Smedt, S. C.; Sanders, N. N.; Braeckmans, K. Mol Ther 2010, 18, 561-569.

Vicentini, F. T. M. D.; Borgheti-Cardoso, L. N.; Depieri, L. V.; Mano, D. D.; Abelha, T. F.; Petrilli, R.; Bentley, M. V. L. B. Pharm Res 2013, 30, 915-931.

Vives, E.; Brodin, P.; Lebleu, B. J Biol Chem 1997, 272, 16010-16017.

Vriens, K.; Cammue, B. P.; Thevissen, K. Molecules 2014, 19, 12280-12303.

Wang, L. H.; Rothberg, K. G.; Anderson, R. G. J Cell Biol 1993, 123, 1107-1117.

Wei, W.; Lv, P. P.; Chen, X. M.; Yue, Z. G.; Fu, Q.; Liu, S. Y.; Yue, H.; Ma, G. H. Biomaterials 2013, 34, 3912-3923.

Weiser, P. T.; Chang, C. Y.; McDonnell, D. P.; Hanson, R. N. Bioorg Med Chem 2014, 22, 917-926.

Wender, P. A.; Galliher, W. C.; Goun, E. A.; Jones, L. R.; Pillow, T. H. Adv Drug Deliv Rev 2008, 60, 452-472.

Wender, P. A.; Huttner, M. A.; Staveness, D.; Vargas, J. R.; Xu, A. F. Mol Pharm 2015, 12, 742-750.

Wender, P. A.; Kreider, E.; Pelkey, E. T.; Rothbard, J.; Vandeusen, C. L. Org Lett 2005, 7, 4815-4818.

Wender, P. A.; Mitchell, D. J.; Pattabiraman, K.; Pelkey, E. T.; Steinman, L. Rothbard, J. B. Proc Natl Acad Sci U S A 2000, 97, 13003-13008.

Wender, P. A.; Rothbard, J. B.; Jessop, T. C.; Kreider, E. L.; Wylie, B. L. J Am Chem Soc 2002, 124, 13382-13383.

White, S. H.; Wimley, W. C. Annu Rev Biophys Biomol Struct 1999, 28, 319-365.

Whitehead, K. A.; Langer, R.; Anderson, D. G. Nat Rev Drug Discov 2009, 8, 129-138.

Wibo, M.; Poole, B. J Cell Biol 1974, 63, 430-440.

Wilmes, M.; Sahl, H. G. Int J Med Microbiol 2014, 304, 93-99.

Wimley, W. C.; White, S. H. Nat. Struct. Biol. 1996, 3, 842-848.

Wolf, Y.; Pritz, S.; Abes, S.; Bienert, M.; Lebleu, B.; Oehlke, J. Biochemistry 2006, 45, 14944-14954.

Wolff, J. A.; Malone, R. W.; Williams, P.; Chong, W.; Acsadi, G.; Jani, A.; Felgner, P. L. Science 1990, 247, 1465-1468.

Wymann, M. P.; Bulgarelli-Leva, G.; Zvelebil, M. J.; Pirola, L.; Vanhaesebroeck, B.; Waterfield, M. D.; Panayotou, G. Mol Cell Biol 1996, 16, 1722-1733.

Yang, L.; Gordon, V. D.; Trinkle, D. R.; Schmidt, N. W.; Davis, M. A.; DeVries, C.; Som, A.; Cronan, J. E., Jr.; Tew, G. N.; Wong, G. C. Proc Natl Acad Sci U S A 2008, 105, 20595-20600.

Yau, W. M.; Wimley, W. C.; Gawrisch, K.; White, S. H. Biochemistry 1998, 37, 14713-14718.

Yeaman, M. R.; Yount, N. Y. Pharmacol Rev 2003, 55, 27-55.

Yezid, H.; Konate, K.; Debaisieux, S.; Bonhoure, A.; Beaumelle, B. The Journal of biological chemistry 2009, 284, 22736-22746.

Yin, L. C.; Tang, H. Y.; Kim, K. H.; Zheng, N.; Song, Z. Y.; Gabrielson, N. P.; Lu, H.; Cheng, J. J. Angew. Chem., Int. Ed. Engl. 2013, 52, 9182-9186.

Zaro, J. L.; Shen, W. C. Exp. Cell. Res. 2005, 307, 164-173.

Zasloff, M. Nature 2002, 415, 389-395.

Zatsepin, T. S.; Turner, J. J.; Oretskaya, T. S.; Gait, M. J. Curr Pharm Des 2005, 11, 3639-3654.

Zhang, Y. F.; Lu, H. Z.; LiWang, P.; Sili, U.; Templeton, N. S. Mol Ther 2003, 8, 629-636.

Zhou, P.; Wang, M.; Du, L.; Fisher, G. W.; Waggoner, A.; Ly, D. H. J Am Chem Soc 2003, 125, 6878-6879.

Ziegler, A. Adv Drug Deliv Rev 2008, 60, 580-597.

Zuris, J. A.; Thompson, D. B.; Shu, Y.; Guilinger, J. P.; Bessen, J. L.; Hu, J. H.; Maeder, M. L.; Joung, J. K.; Chen, Z. Y.; Liu, D. R. Nat Biotechnol 2015, 33, 73-80.